MONASH University

INVESTIGATING THE ROLE OF CD45 IN THE PATHOGENESIS AND DISEASE PROGRESSION OF MULTIPLE MYELOMA

Wing Yu MAN

BSc (Hons)

A thesis submitted for the degree of Doctor of Philosophy at

Monash University in 2019

Australian Centre for Blood Disease

Department of Clinical Haematology

Faculty of Medicine, Nursing and Health Sciences

COPYRIGHT NOTICE

ABSTRACT

Multiple myeloma (MM) is a plasma cell malignancy that manifests continuous cell dissemination to multiple bone marrow (BM) niches and extramedullary sites. However, the molecular mechanisms behind this phenomenon remain elusive. CD45, a receptor tyrosine phosphatase, is an important regulator for T-cell and B-cell signalling pathways. The loss of CD45 expression has been correlated with earlier disease progression and inferior treatment outcomes in MM. It has been shown that $CD45^-$ murine MM cells have lower homing capacity, remain longer in peripheral blood circulation and induce higher tumour load *in vivo*. Further *in vitro* investigations suggest that $CD45^-$ cells have impaired chemotaxis towards BM and lower expression of extracellular matrix proteases than $CD45^+$ cells. All these observations suggest that $CD45^-$ phenotype is associated with a more metastatic disease. This project aimed to investigate the biological role of CD45 in MM and the underlying mechanisms accounting for the differences between CD45 phenotypes.

Previous studies have been limited to using $CD45^+$ and $CD45^-$ myeloma cell lines, however, the genetic heterogeneity among the cell lines confounded the interpretation of CD45 expression-related differences. Therefore, there is a need to establish a new approach to study CD45. The first part of this study aimed to employ the CRISPR/Cas9 genome editing to establish CD45 knockout ($CD45^{KO}$) cells from $CD45^+$ human myeloma cell lines (HMCLs). The loss of extracellular and intracellular expression of CD45 and the genomic sequence were evaluated.

Src family kinases (SFKs) are the main downstream targets of CD45. $CD45^{KO}$ cells showed SFK inactivation as compared to CD45 wild-type ($CD45^{WT}$) cells, confirming the loss of CD45 phosphatase activity in these cells. Although both phenotypes shared similar proliferation profiles in various liquid culture conditions, $CD45^{KO}$ cells were less clonogenic in semi-solid culture. The loss of CD45 expression also did not impact on the two important cytokine signalling pathways, interleukin-6 (IL-6) and insulin-like growth factor-1 (IGF-1). The differentially expressed genes identified by RNA sequencing were significantly

enriched in the GO annotations and KEGG pathways related to cell mobility, angiogenesis and tumour progression, highlighting the potential role of CD45 in these areas.

Given the reported differential *in vivo* homing potential in murine MM cells and our results in the transcriptional changes in cell mobility-related pathways, the last part of this study interrogated the homing process of $CD45^{WT}$ and $CD45^{KO}$ cells. Consistently, we demonstrated a significant reduction in homing capacity towards BM stromal cells in $CD45^{KO}$ cells. We also demonstrated that a SFK-binding kinase, proline-rich kinase (Pyk2), was inactivated in $CD45^{KO}$ cells. Treatment of $CD45^{WT}$ cells with a SFK inhibitor (saracatinib) and a Pyk2 inhibitor (PF573228) replicated the reduced homing capacity suggesting their roles in homing. Finally, we showed that $CD45^{KO}$ cells displayed delayed engraftment but higher metastatic potential *in vivo*.

This thesis has demonstrated the distinct characteristics of $CD45^{WT}$ and $CD45^{KO}$ cells. We proposed that the impaired homing potential in CD45 void cells was due to the disruption in the CD45/SFKs/Pyk2 signalling cascade. Our findings suggested that CD45 may represent a biomarker for metastatic progression of MM.

DECLARATION

This thesis contains no material which has been accepted for the award of any other degree or diploma at any university or equivalent institution and that, to the best of my knowledge and belief, this thesis contains no material previously published or written by another person, except where due reference is made in the text of the thesis.

Signature:

Print Name:

Wing Yu MAN

Date: 28/7/2019

PUBLICATIONS AND CONFERENCE ABSTRACTS DURING ENROLMENT

(In chronological order)

Poster presentation: **Wing Yu Man**, Tiffany Khong, Sridurga Mithraprabhu, Andrew Spencer. Unraveling CD45 in multiple myeloma through CRISPR/Cas9 gene editing. HAA 2017: The Combined Annual Scientific Meeting of the HSANZ, ANZSBT and THANZ — Sydney, New South Wales, Australia

Oral presentation: **Wing Yu Man**, Tiffany Khong, Andrew Spencer. The critical role of CD45/SFK in cell migration in multiple myeloma. 9th Annual ASMR VIC Student Research Symposium — Melbourne, Victoria, Australia

Poster presentation: **Wing Yu Man**, Tiffany Khong, Andrew Spencer. The critical role of CD45/SFK in cell migration in multiple myeloma. Alfred Health Week Research Poster Display 2018 — Melbourne, Victoria, Australia

Oral presentation: **Wing Yu Man**, Tiffany Khong, Andrew Spencer. CRISPR-Cas9 mediated CD45 knockout inactivates Src family kinases and impairs cell migration in multiple myeloma. 2nd National Myeloma Workshop — Yarra Valley, Victoria, Australia

Oral presentation: **Wing Yu Man**, Tiffany Khong, Andrew Spencer. Beyond a marker: a novel role of CD45 in myeloma metastasis. BLOOD 2018: The Combined Annual Scientific Meeting of the HSANZ, ANZSBT and THANZ — Brisbane, Queensland, Australia

Poster presentation: **Wing Yu Man**, Tiffany Khong, Andrew Spencer. CRISPR-Cas9 Mediated CD45 Knockout Inactivates Src Family Kinases and Impairs Cell Migration in Multiple Myeloma. American Society of Hematology Annual Meeting 2018 — San Diego, California, USA

ACKNOWLEDGEMENTS

I would like to express my sincere gratitude to everyone who has supported me along the way and make this work possible.

First, I would like to thank my supervisors, Professor Andrew Spencer and Dr Tiffany Khong for giving me this incredible opportunity. Thank you for your guidance, encouragement and support throughout my PhD. You have shown me the world where science and clinic meet and shaped me into a better researcher. For that, I am forever grateful. I would also like to thank Dr Ioanna Savvidou for her research ideas and technical support, and Dr Maoshan Chen for his help in bioinformatics.

To all the present and past members of Myeloma Research Group, thank you all for your support over the last few years. Special thanks to Ms Sophie Whish for her help in animal works and proofreading. I could not imagine doing animal works without you!

There are many members of the Australian Centre for Blood Diseases who I would like to thank for the support and making my time enjoyable, especially to Maria, Ethan, Steven, Mitch and Jacklyn, for sharing the excitement and frustration of PhD life.

Finally, I would like to thank my family for their support and patience. Most importantly, I would like to thank my partner, Heath for his endless love and support. Thank you for always being there for me especially during the stressful times.

To my father.

CONTENTS

LIST OF TABLES

LIST OF FIGURES

LIST OF ABBREVIATIONS AND ACRONYMS

°C	degree Celsius
AKT	protein kinase B
AKTi	AKT inhibitor
BD	Becton Dickinson
bFGF	basic fibroblast growth factor
BM	bone marrow
BMME	bone marrow microenvironment
BMSC	bone marrow stromal cell
bp	base pair
BSA	bovine serum albumin
CAM-DR	cell-adhesion mediated drug resistance
CCND1	cyclin D1
cDNA	complementary deoxyribonucleic acid
CFSE	carboxyfluorescein diacetate succinimidyl ester
CO_2	carbon dioxide
CRISPR	clustered regularly interspaced short palindromic repeats
CST	Cell Signaling Technologies
CXCR	chemokine CXC motif receptor
CXCL	CXC motif chemokine
DMSO	dimethyl sulfoxide
DNA	deoxyribonucleic acid
ECL	enhanced chemiluminescence
EDTA	ethylenediaminetetraacetic acid
EMT	epithelial mesenchymal transition
ERK	extracellular signal-related kinase
FACS	fluorescence activated cell sorting
FCS	foetal calf serum
FDR	false discovery rate
FGF	fibroblast growth factor
FGFR	fibroblast growth factor receptor
FITC	fluorescence isothiocyanate
FN	fibronectin

gRNA	guide ribonucleic acid
HDAC	histone deacetylase
HDACi	HDAC inhibitor
HDR	homology-directed repair
HGF	hepactocyte growth factor
HMCL	human myeloma cell line
HRP	horseradish peroxidase
hr	hour
HSP	heat shock protein
ICAM	intercellular adhesion molecule
Ig	immunoglobulin
IGF-1	insulin-like growth factor-1
IGF-1R	IGF-1 receptor
IL	interleukin
IL-6R	IL-6 receptor
IMiDs	immunomodulatory drugs
JAK	Janus kinase
kDa	kilo Dalton
KO	knockout
LFA	lymphocyte function-associated antigen 1
MAPK	mitogen-activated protein kinase
MEK	mitogen-activated protein kinase kinase
MEKi	MEK inhibitor
MFI	mean fluorescence intensity
MGUS	monoclonal gammopathy of undetermined significance
min	minute
ml	millilitre
MM	multiple myeloma
MNC	mononuclear cell
mRNA	messenger ribonucleic acid
NF-κB	nuclear factor-kappa B
ng	nanogram
NHEJ	nonhomologous end-joining
NMD	nonsense-mediated mRNA decay

PAGE	polyacrylamide gel electrophoresis
PAM	protospacer-adjacent motif
PB	peripheral blood
PBS	phosphate buffered saline
PCR	polymerase chain reaction
PE	phycoerythrin
PFA	paraformaldehyde
PI	propidium iodide
PI3K	phosphatidylinositol-3 kinase
PTC	premature termination codon
PTP	protein tyrosine phosphatase
PVDF	polyvinylidene fluoride
qRT-PCR	quantitative reverse transcription PCR
RANK	receptor activator of nuclear kappa B
RIPA	radioimmunoprecipitation
RNA	ribonucleic acid
rpm	revolutions per minute
SDF-1	stromal derived factor-1
SDS	sodium dodecyl sulphate
SEM	standard error of means
SFK	Src family kinase
STAT	signal transducer and activator of transcription
TBST	Tris buffered saline with 0.1% Tween-20
TGF-β	transforming growth factor beta
TNF-α	tumour necrosis factor-alpha
U	unit
V	volt
VCAM-1	vascular adhesion molecule-1
VEGF	vascular endothelial growth factor
VLA	very late activating antigen
WT	wild-type

LIST OF APPENDICES

CHAPTER 1:
INTRODUCTION

1.1 Overview

Multiple myeloma (MM) is an incurable haematological malignancy characterised by the uncontrolled growth of plasma cells in the bone marrow (BM). In the last 10 years, the introduction of novel therapeutics has significantly improved patients' quality of life and overall survival, however, the 5-year relative survival is still below the average of all cancers. The presence of multiple bone lesions at diagnosis suggests that there is a continuous cell dissemination even at the early stage of the disease. As this is a determining step in the disease establishment and metastasis, tremendous efforts have been spent on understanding this process. CD45 has been correlated to BM homing and disease outcome in MM.

CD45 is a transmembrane phosphatase expressed on a number of tissues and nucleated haemopoietic cells. It is indispensable in T cell and B cell signalling by directly interacting with the downstream signalling molecules, particularly Src family kinases (SFKs) and Janus kinases (JAKs). CD45 negative MM cells have lower homing capacity towards BM in murine models and are more resistant to pharmacological inhibitions *in vitro* than the CD45 positive counterparts. More strikingly, CD45 expression decreases along disease progression and is correlated with disease outcome. However, the underlying mechanisms are not well understood.

This chapter summarises the current knowledge of MM and CD45, and the rationale of this study.

1.2 Multiple myeloma

MM is a B cell malignancy characterised by the clonal proliferation of the terminally differentiated plasma cells in BM. The uncontrolled growth of these antibody-secreting plasma cells results in abnormal accumulation of non-functional monoclonal immunoglobulins (paraproteins/M-proteins) in both blood and urine[1]. Common clinical manifestations include anaemia, bone fractures and renal failure. MM displays remarkably complicated genetic variations which make it very difficult to target therapeutically. Despite the recent development in novel therapeutics, the 5-year relative survival at diagnosis is only 48.5%, nearly 20% below the average of all cancers in Australia[2], and the disease is incurable.

1.2.1 Epidemiology of multiple myeloma

MM accounts for 0.9% of all newly diagnosed cancers and 13% of all blood cancers worldwide[3]. In Australia, about 1600 new cases were diagnosed in 2013 and the prevalence is expected to rise in line with the ageing population[2]. The incidence rate in men is 1.3-1.6 times higher than in women[2,4]. MM is most commonly diagnosed among people of older age: about 30% of new cases are of 65-74 years old and the median age is around 69 years old[4]. The incidence rate for those younger than 35 years old is extremely low, about 0.5%[4]. Notably, MM has strong ethnic disparities in incidence and mortality rate. MM and its premalignant state monoclonal gammopathy of undetermined significance (MGUS) are 2-3 fold more common among individuals of African background than other races[4,5]. Although the differences in socioeconomic and access-to-care may contribute to the ethnic disparities, the undetermined intrinsic genetic and biological differences are more likely to explain these observations.

1.2.2 Stages of Multiple Myeloma

The disease is characterised by the abnormal proliferation of plasma cells in the BM and a high level of M-proteins/paraproteins in the blood or urine[6]. Common

pathologies include hyper**c**alcemia, **r**enal failure, **a**naemia and lytic **b**one lesions ('CRAB')[7]. One-third of myeloma patients may suffer from hypercalcemia induced by tumour-promoted osteolysis[8]. Renal failure is caused by the accumulation and precipitation of paraproteins resulting in renal obstruction while anaemia is resulted from the loss of erythropoietin[9].

MM is defined into four distinct stages as illustrated in Figure 1-1. Prior to progressing into a symptomatic disease, MM occurs as two premalignant stages: MGUS and smouldering/asymptomatic multiple myeloma (SMM), which have no detectable end-organ damage. MGUS has a prevalence of around 3% for those of age over 50. The prevalence increases with age and is affected by race, sex, family history, immunosuppression and toxin exposure[10,11]. These two stages are distinguished by the different levels of monoclonal protein in serum or urine and clonal plasma cells in the bone marrow. About 15-59% of patients with MGUS or SMM progress into symptomatic MM[9]. However, the mechanisms of the disease stage transition are still unknown. In symptomatic stage, malignant myeloma cells expand continuously and cause severe organ impairment, such as bone fractures and renal failure (the 'CRAB' features).

MM is highly dependent on BM microenvironment (BMME), yet the involvement of extramedullary locations is often presented, that includes solitary plasmacytoma of bone, extramedullary plasmacytoma and PCL. Solitary plasmacytoma of bone is relatively rare and occurs in only 3-5% of patients but with 50% chance of evolving into overt MM. Common symptoms are pain at the site of skeletal lesion, severe back pain, spinal cord compression or pathological fractures. On the other hand, extramedullary plasmacytoma can develop in any organs, such as respiratory tract, bladder, breasts and thyroid. It is often curable with tumourcidal radiation (40-50Gy) and only 15% patients with solidary extramedullary plasmacytomas go on to develop symptomatic MM. PCL is defined as over $2x10^9$/L or 20% plasma cell count in the peripheral blood. About 60% of PCL patients are primary type – with no prior diagnosed MM; whereas secondary PCL is transformed from pre-existed MM. Primary PCL patients are generally younger, have a higher incidence of hepatosplenomegaly and lymphadenopathy, and longer survival[1]. Detailed diagnostic criteria for

MM[1,12,13] are listed in Table 1-1.

Although the above diagnostic criteria sufficiently define the disease stages, there is a need to have a better classification to identify risk groups and disease outcome so that patient treatment can be optimised. As such, in 2005, the International Staging System (ISS) was introduced based on the clinical data from over 10000 patients internationally. ISS stratified patients into three stages: stage I, serum β_2-microglobulin <3.5mg/L and serum albumin ≥3.5g/L (median survival 62 months); stage II, neither stage I nor stage III (median survival 44 months); and stage III, serum β_2-microglobulin ≥5.5mg/L (median survival 29 months)[14]. With more reports showing the importance of other prognostic factors, such as serum lactase dehydrogenase (LDH)[15,16], and chromosomal abnormalities (CA) detected by interphase fluorescent in situ hybridization (FISH)[17,18], a revised ISS (R-ISS) was published in 2015 to incorporate these factors. The R-ISS has an improved power to stratify patients into subgroups to provide more personalised therapies. Details of ISS and R-ISS are listed in Table 1-2.

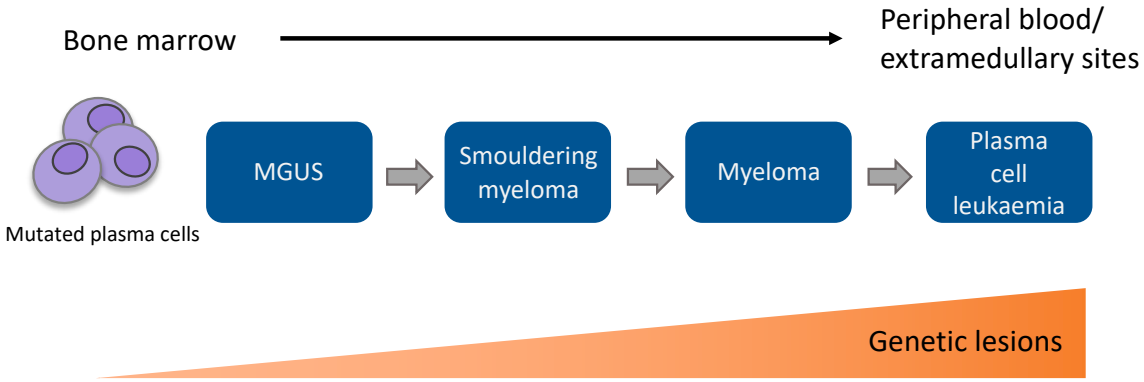

Figure 1-1: Pathogenesis of multiple myeloma.

Myeloma is defined into 4 disease stages, of which MGUS, smouldering myeloma and symptomatic myeloma are predominately located in the BM; only at the late stage of disease myeloma cells can egress to extramedullary sites. As the disease progresses, myeloma cells accumulate and acquire genetic alterations giving rise to tumour diversity. Adapted from G. Morgan et al[19].

Table 1-1: Diagnostic criteria for different stages of multiple myeloma.

Disease stages	Diagnostic criteria
Monoclonal gammopathy with undetermined significance (MGUS)	• clonal plasma cells in BM: <10% • M-protein in serum at myeloma levels: <30 g/L • No related organ or tissue impairment end-organ damage or bone lesions (CRAB) or myeloma-related symptoms
Smouldering/ asymptomatic multiple myeloma (SMM)	• clonal plasma cells in BM: 10-60% and/or M-protein in serum at myeloma levels: >30 g/L • No related organ or tissue impairment end-organ damage or bone lesions (CRAB) or myeloma-related symptoms
Symptomatic/active multiple myeloma	• clonal plasma cells in BM: >10% or biopsy-proven bony or extramedullary plasmacytoma • clonal plasma cells in BM ≥60% or involved:uninvolved serum free light chain ratio ≥100 or or related organ or tissue impairment heavy chain disease (CRAB) or >1 focal lesions on MRI studies
Extramedullary plasmacytoma	• Biopsy proven solidary lesion of bone or soft tissue with evidence of clonal plasma cells • clonal plasma cells in BM <10% • Normal bone marrow and skeletal survey • No related organ or tissue impairment end-organ damage or bone lesions (CRAB)
Plasma cell leukaemia (PCL)	• Peripheral blood absolute plasma cell count >$2x10^9$/L or >20% in peripheral blood differential white cell count • Primary PCL: no prior MM diagnosis • Secondary PCL: leukaemic transformation of previously recognised MM

Table 1-2: Standard risk factors and R-ISS for MM.

Prognostic factor		**Criteria**
ISS stage	I	serum β_2-microglobulin <3.5mg/L and serum albumin ≥3.5g/L
	II	Not ISS stage I or III
	III	serum β_2-microglobulin ≥5.5mg/L
CA by iFISH	High risk	Presence of del(17p) and/or translocation t(4;14) and/or translocation t(14;16)
	Standard risk	No high-risk CA
LDH	Normal	Serum LDH<the upper limit of normal
	High	Serum LDH>the upper limit of normal
R-ISS stage	I	ISS stage I and standard-risk CA by iFISH and normal LDH
	II	Not R-ISS stage I or III
	III	ISS stage III and either high-risk CA by iFISH or evevated LDH

1.2.3 Cytogenetics of multiple myeloma

MM is a highly complex and heterogeneous disease with various genetic aberrations that can be further classified by different combination of gains and losses of whole chromosomes, nonrandom chromosomal translocations and point mutations. Epigenetic changes including DNA methylation[20–24], histone modifications[25–28] and microRNAs[29,30] have also been identified.

Based on their chromosomal abnormalities MM can be subdivided into two groups: hyperdiploid and nonhyperdiploid. The hyperdiploid karyotype is found in approximately 55-60% of primary tumours and is characterized by the additional chromosomes to a total number of 48-74 and trisomies of odd-numbered chromosomes[31]. The nonhyperdiploid karyotype comprises of the remaining cases including hypodiploid, near-diploid, pseudodiploid and near-tetraploid[18,31,32]. Notably, majority of patients retain the same ploidy status throughout disease progression[33] and hyperdiploid patients generally have better outcomes than non-hyperdiploid patients[18] except a subset of hyperdiploid patients presenting additional gains on 1q and/or losses of chromosome 13. Genes located at these chromosomes are inevitably altered, such as loss of tumour-suppressor gene *TP53* due to loss of the short arm of chromosome 17.

Apart from gains and losses of whole chromosomes, chromosomal translocations are also commonly found in MM. The most frequent translocation is the IgH locus at 14q32.3 representing around 50% cases; while the remaining are the IgL locus at 2p12,κ and 22q11,λ[34,35]. These translocation events result in juxtaposition of various genes to a strong Ig enhancer that dysregulates their expression. Cyclin D1 and D3 are overexpressed in 15-25% of patients due to the translocations of t(11;14)(q13;q32) and t(6;14)(p21;q32) respectively[36,37]; multiple myeloma set domain (MMSET, or Wolf-Hirschhorn syndrome candidate 1 gene, WHSC1) and fibroblast growth factor receptor 3 (FGFR3) are dysregulated in t(4;14)(p16.3;q32)[38], and MAF and MAFB transcription factor family are affected by t(14;16)(q32;q23) and t(14;20)(q32;q11)[39,40].

Several tumour suppressor genes in MM are frequently mutated, including *TP53, PTEN, CDKN2A, CDKN2C, NRAS, KRAS, BRAF* and *MYC*[19]. Of these genes, the *RAS* family is often mutated: at least one *RAS* mutation is found in 43% patient samples using whole-exome sequencing[41] and more strikingly in 69% of liquid biopsy samples using the OnTarget Mutation Detection platform[42].

The altered gene expression from these chromosomal rearrangement and secondary mutation events changes MM tumour cells behaviour and survival, for instance, *MAF* promotes cell proliferation and adhesion to bone marrow stromal cells (BMSC)[40]. Identifying these genetic events not only provides prognostic information but also allows targeted therapy.

1.2.4 BM microenvironment

MM is a tumour of terminally differentiated plasma cells that home to bone marrow and greatly depend on bone marrow microenvironment (BMME) for growth and survival. BMME consists of extracellular matrix proteins and various types of cells (Figure 1-2). BM cells secrete a variety of chemokines, such as interleukin-6 (IL-6), insulin-like growth factor 1 (IGF-1), vascular endothelial growth factor (VEGF), fibroblast growth factor (FGF), stromal cell-derived factor 1 (SDF-1) and tumour necrosis factor-α (TNFα) to facilitate cell-cell interaction and proliferation. These components are arranged into a well-balanced niche to support survival, growth and differentiation of the diverse lineages of blood cells as well as malignant cells. This balance constantly changes and evolves with the disease progression in MM.

1.2.4.1 Extracellular matrix

The extracellular matrix is the most abundant component in the BMME. It includes mainly fibronectin, collagen type I and IV, laminin, osteopontin, heparin sulfate, chondroitin sulfate and hyaluronan[43,44]. MM cells express various adhesion molecules which some of them interact with the components of the extracellular matrix. Some examples are β1-integrins bind to laminin and fibronectin[45]; syndecan-1 (CD138) binds to collegen-1[46]; and CD44 interacts

with hyaluronan[47]. These interactions contribute to the adhesion, migration and drug resistance of MM cells.

J. Damiano et al. demonstrated that MM cell lines expressing both VLA-4 and VLA-5 developed resistance towards doxorubicin and melphalan when they were pre-adhered to fibronectin but not in suspension[48]. This cell adhesion-mediated drug resistance (CAM-DR) was possibly a result of perturbation of cell cycle as fibronectin-adhered MM cells expressed a higher level of $p27^{kip1}$ and arrested in G1 phase[49]. Since most of cytotoxic drugs target proliferating cells, the fibronectin-adhered MM cells were not affected. One of the possible mediator in CAM-DR could be the nuclear factor-kappa B (NF-κB) family as the same group further showed that fibronectin adhesion repressed the expression of 469 genes and some of these genes were regulated by the NF-κB family[50]. This is also supported by the fact that activation of NF-κB pathway decreased the susceptibility of MM cells to cytotoxic drugs by inhibiting apoptosis. Although the precise mechanism is yet to be resolved, targeting CAM-DR offers a potential therapeutic strategy to overcome drug resistance.

1.2.4.2 Cellular compartment

Other than the extracellular matrix, cells in the BMME, such as haemopoietic stem cells, immune cells, erythrocytes, BMSCs, bone marrow endothelial cells, osteoclasts and osteoblasts[43], play an important role in regulating the proliferation, differentiation and survival of MM cells.

BMSCs are vital for growth and survival of both normal plasma cells and MM cells. In fact, feeder layers of BMSCs are indispensable for *in vitro* culture of primary MM cells[51]. The interaction between BMSCs and MM cells is initiated by the bidirectional chemokine signals, which then activate signalling pathways to induce expression and secretion of adhesion molecules, such as VLA-2 to VLA-6, CD44v9, CD21, CD56 (NCAM) and LFA-1[52–54], to reinforce adhesion. The adhesion of MM cells to BMSCs induces IL-6 secretion through NF-κB pathway. It then strongly increases CD44 expression, creating an amplification loop to intensify MM-stimulatory signals[55,56]. Other soluble factors released from MM

cells, including tumour necrosis factor-α (TNF-α)[57], transforming growth factor-β (TGF-β)[58], basic fibroblast growth factor (bFGF)[59] and VEGF[60], can also trigger IL-6 secretion.

The interaction between MM cells, osteoclasts and osteoblasts manoeuvres the balance of bone remodelling. Bone tissue is constantly resorbed by osteoclasts (osteolysis) and deposited by osteoblasts (osteogenesis). In MM, however, this balance inclines to osteolysis. About 80% of MM patients experience pathological fracture over the course of their disease and 90% of them have bone lesions[61]. MM supports osteoclast differentiation by activating the receptor activator of nuclear kappa B (RANK) which induces osteoclast formation from its precursor, enhances osteolysis and inhibits osteoblast formation[62]. RANK is expressed on both osteoclasts and osteoblasts, while its ligand RANKL is expressed on BMSCs, osteoblasts and MM cells[63]. Although normal BMSCs express RANKL, they prevent excessive osteoclast activation by expressing osteoprotegrin (OPG) to antagonise RANKL[64]. On the other hand, the binding of α4β1 integrin on MM cells to vascular cell adhesion molecule-1 (VCAM1) on BMSCs significantly upregulates RANKL and downregulates OPG expression[63,65,66]. Alongside with BMSCs, osteoclasts secrete several growth factors including IL-6 to induce MM cells proliferation, stimulate osteoclastogenesis and increase bone resorption[67].

1.2.4.3 Soluble factors

IL-6 is one of the most important MM growth factor produced by BMSCs. Other than paracrine production, it is also secreted by MM cells themselves in an autocrine way[68–71]. The importance of IL-6 to MM is reflected in the correlation between IL-6/IL-6 receptor (IL-6R) and disease progression: high IL-6/IL-6R level is detected in patients with relapse and primary refractory disease[71–73]. Multiple studies have also shown that inactivation of IL-6 by RNA interference or neutralizing monoclonal antibody significantly inhibited MM cell proliferation[74–76]. The binding of IL-6 to IL-6R activates three signalling pathways in MM: JAK/signal transducer and activator of transcription 3 (JAK/STAT3) pathway, phosphatidylinositol-3 kinase (PI3K) pathway and Ras/mitogen-activated protein

kinase (Ras/MAPK) pathway. Activation of these pathways not only triggers MM cells proliferation but also protects cells from apoptosis[71,77–82].

IGF-1 is another critical growth factor which supports the proliferation of both IL-6-dependent and -independent MM cells, inhibits drug-induced apoptosis, and mediates survival in serum-free culture medium[83–87]. It is secreted by many tissues and secretory sites, such as BMSCs, liver and cartilaginous cells[88]. Similar to IL-6, IGF-1 stimulation activates both Ras/MAPK and PI-3K pathway[89]. In addition, IGF-1 activates NF-κB pathway and decreases sensitivity to Apo2 ligand/TNF-related apoptosis inducing ligand (Apo2L-TRAIL) of MM cells, thereby overcoming cytotoxic drugs-induced apoptosis[89–91].

Other important soluble factors, such as interleukin family[92–95], Wnt family[96], Jagged family[97–101], VEGF[60,102] and fibroblast growth factor 2/basis FGF (FGF2/bFGF)[59,103], are also produced by MM cells and BMSCs. VEGF is associated with angiogenesis by inducing neovascularization in solid tumours to promote tumour growth, invasion and metastasis (reviewed by G. McMahon[104] and P. Carmeliet[105]). It contributes to the increase in micro vessel density in the BM of MM patients[106,107]. VEGF triggers MM cell growth via the Raf-1-MEK-1-ERK pathway and induces migration via a protein kinase C (PKC)-dependent ERK-independent pathway. Inhibition of PKC has been shown to attenuate the migration potential of MM cell lines and patient plasma leukaemia cells *in vitro*[102]. In addition, activation of NOTCH pathway by its ligands, Jagged family, is involved in the acquisition of chemotherapy resistance[97,98,100]. All these data provide the rationale to target these important growth factors as a novel therapeutic strategy.

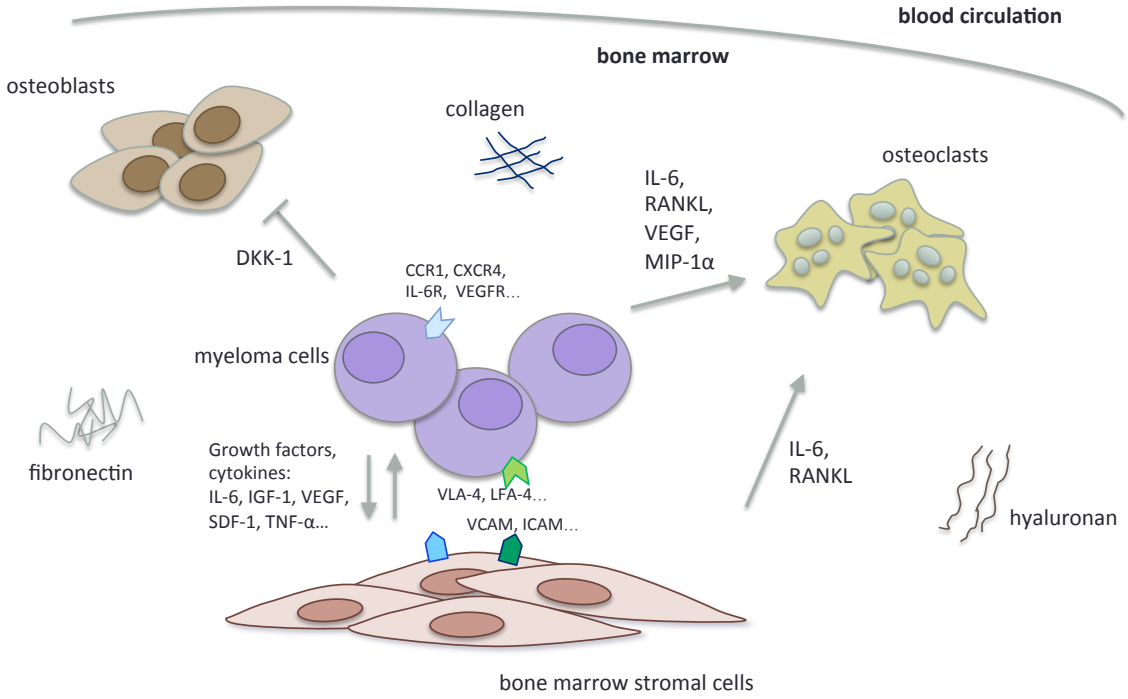

Figure 1-2: Interaction between MM and BMME.

BMME is made up of extracellular matrix and cellular compartment. The extracellular matrix consists of fibronectin, collagen, hyaluronan and other structural elements. MM cells express multiple adhesion molecules that bind to these components, anchoring themselves to BM. The interaction between extracellular matrix and MM also contribute to cell proliferation and CAM-DR. Most of these components of extracellular matrix are produced by BMSCs. The interactions between BMSCs and MM are mediated by the bidirectional paracrine signals. BMSCs secrete different growth factors and cytokine to support MM proliferation and upregulate adhesion molecules expression. In turn, MM cells secrete certain growth factors to stimulate BMSC growth. In normal physiological conditions, bone tissue is constantly resorbed by osteoclasts and rebuilt by osteoblasts. In MM, however, this balance is switched to osteolysis, resulting in bone lesion in patients. MM cells induce osteoclastogenesis and enhance osteolytic properties. On the other hand, MM cells inhibit osteoblast differentiation from their progenitors.

1.2.5 Metastasis in myeloma

Metastasis is the leading cause of mortality in cancers. Although it is not generally used to describe the dissemination of haematological malignancies, increasing evidence has shown that MM shares similar characteristics of metastasis with solid tumours in order to spread throughout BM. The presence of multiple myelomatous lesions throughout the axial and appendicular skeleton at diagnosis is a compelling evidence that myeloma cells are capable of continuous spreading from the original tumour site to multiple BM niches even at the early stage of the disease. Indeed, a small number of MM cells can be detected in the peripheral circulation throughout the disease progression[108,109]. MM cells returning to BM is known as the 'homing process' and it is a critical step in disease dissemination. Together with other mutations that allow MM cells to survive beyond BM niches, aberrant homing process could induce metastasis to other organs and plasma cell leukemia.

1.2.5.1 Epithelial-mesenchymal transition

In solid tumours, the process of metastasis involves multiple steps known as the invasion-metastasis cascade[110,111]. This cascade includes (1) local invasion of primary tumour cells into surrounding tissues; (2) intravasation of these cells into the circulatory system and survival in peripheral circulation; (3) arrest and extravasation through vascular walls into the parenchyma of distant tissues; (4) formation of micrometastatic colonies in this parenchyma; (5) the subsequent proliferation of microscopic colonies into overt, clinically detectable metastatic lesions and lastly (6) colonising in the new sites. Tumour cells hijack one of the most important cellular transformation, epithelial-mesenchymal transition (EMT) to equip themselves with the ability to leave the primary site and relocate to distant sites. EMT is an essential developmental programme for embryogenesis and healing epithelial tissues[112]. During this transition, several transcriptional factors, such as Snail, Slug, Twist and ZEB1 and ZEB2, are activated[113], leading to the inhibition of epithelial cadherin (E-cadherin)[114,115]. E-cadherin is a key cell-to-cell adhesion molecule that forms adherent junctions to bind cells to each other. Accompanying the downregulation of E-cadherin is the upregulation

or de novo expression of neural cadherin (N-cadherin), resulting in loss of epithelial cell-cell adhesive junctions and apical-basal cell polarity. This 'cadherin switching' is the hallmark of EMT which subsequently initiates tumour cell mobility and invasion[116,117].

The upregulation of N-cadherin has been reported in a subpopulation of MM patients harbouring the high risk t(4;14)(p16;q32) translocation involving MMSET[118,119]. Knockdown of N-cadherin in MM cell lines attenuated the BM homing, resulting in higher levels of circulating cells in blood *in vivo*. However, neither blocking nor knockdown of N-cadherin changed transendothelial migration towards SDF-1 in Transwell migration assays[118]. Further investigation by Mrozik et al. showed that the knockdown of N-cadherin reduced murine MM cell adhesion to BM endothelial cells but not the transendothelial migration[120]. These results suggest the homing defect seen in the N-cadherin knockdown is due to the decrease in endothelial cell adhesion, highlighting the potential role of N-cadherin in MM cell homing process.

1.2.5.2 Initiation of MM metastasis

Hypoxia has been shown to initiate EMT by mediating hypoxia inducible factor-1 (HIF-1)-activated TWIST[121]. Recent studies have also suggested that hypoxia can regulate each step of metastasis[121]. In MM, A. Azab et al. demonstrated that hypoxia activated the EMT-related machinery, decreased the expression of E-cadherin, decreased the adhesion of MM cells to the BM and enhanced the egress of MM cells to the circulation[122]. Due to the hypoxic nature of BM (with approximately 1-2% oxygen)[121], MM cells could be encouraged to activate EMT. In addition, MM cells may enhance cell mobilisation by disrupting the SDF-1-CXCR4 axis (more details in 1.2.5.5). This can be achieved by decreasing the concentration of endogenous SDF-1 or stimulating the protease-mediated inactivation of SDF-1 in BM[123].

1.2.5.3 Circulation of MM cells in peripheral blood

The next step of metastasis is the circulation of cancer cells in the peripheral

blood (PB). Circulating tumour cells are particularly vulnerable at this stage due to the lack of adhesion to the extracellular matrix and endothelial cells, leading to anoikis. In addition, they are subjected to immune surveillance, notably by NK cells for rapid elimination; and shear stress in the circulation[111]. To avoid anoikis and immune surveillance, circulating tumour cells attach themselves to platelets through tissue factor and/or L- and P-selectins to form microemboli or microthrombi that carry them to the target organs[121].

The presence of circulating plasma cells is evident in 50-70% of MM patients at diagnosis[124,125] and up to 92% at relapse[108]. High levels of circulating plasma cells have been associated with poor survival in both newly diagnosed and relapse/refractory MM, as well as a higher risk of malignant transformation from MGUS and smouldering MM to symptomatic MM[124–127]. Recent advanced flow cytometry and gene sequencing technology take advantage of these circulating MM cells to detect and identify special markers and gene mutations in the circulating MM cells which are also present in the BM counterparts, paving a way for a less invasive mutation screening[124,125].

1.2.5.4 Preferential homing to BM

The dissemination of MM cells from the post-germinal centre origin to BM requires a highly selective homing process. This selective homing to BM of MM cells has been demonstrated in murine model: the intravenously injected 5T2MM and 5T33MM cells migrated preferentially to the BM, the spleen and the liver *in vivo*, but only survived within the BM[128,129]. In addition to MM, other metastatic solid tumours also preferentially home to the BM. Approximately 65-75% of breast and prostate cancer patients with advanced metastatic disease develop bone metastasis; this is also observed in 60% of thyroid; 30-40% of lung; 40% of bladder and 20-25% of renal cell carcinoma[130]. This preferential trafficking to BM is believed to be in relation to the haemopoietically active red bone marrow[131]. The growth factors and cytokines in the BM make it a favourable place for tumour cell proliferation.

The ability of MM cells homing to the BM and spreading to other sites is similar

to leukocytes trafficking as a part of the immune system. In normal physiological conditions, lymphocytes migrate from blood to particular tissues and specific microenvironments during immune surveillance[132]. This is a multi-step process and is tightly regulated by adhesion and migration pathways. First, the cells adhere and crawl along the endothelium, and express appropriate receptors for external chemoattractants for firm adhesion. Then, the cells penetrate through the subendothelial membrane by degrading the basement membrane with the secreted proteolytic enzymes, such as metalloproteinases (MMPs) and collagenases. The MMPs are also involved in cleaving cell surface receptors and chemokine and cytokine inactivation[133].

The extravasation of circulating tumour cells into extravascular tissues depends on the interactions between locally produced chemoattractants, including extracellular matrix proteins, chemokines and growth factors, and the corresponding cell surface receptors. These interactions then invoke a multistep adhesion cascade similar to normal leukocytes. This implicates that MM cells must be equipped with appropriate cell surface molecules and receptors to facilitate the binding to and traversing through the endothelium. These molecules/receptors include VLA-4 and CD44, which interact with VCAM-1 and hyaluronan expressed on BM endothelium respectively[47,52,134,135]. Once the circulating MM cells adhere to the endothelium, SDF-1 produced by the BMSCs activates CXCR4 signalling pathway, leading to the transmigration of MM cells into the BM vascular niche. Other chemokines and integrins, including LFA-1, VLA-5, and activation of MMP-9, also trigger multiple complex signalling cascades, inducing adhesion and migration[136–138].

Besides the SDF-1/CXCR4 axis, it is believed that many other chemotactic signals play a role in enhancing MM cell migration. MM cells express functional chemokine receptors that mediate migration *in vitro*. Some of the examples are C-C chemokine receptor type 1 (CCR1), CCR2, CCR3 and CCR5 [139–143]. These receptors interact with macrophage inflammatory protein-1α (MIP-1α, ligand for CCR1 and CCR5) and monocyte chemotactic proteins (MCP-1, MCP-2 and MCP-3, ligands for CCR2) as shown in the *in vitro* MM cell migration assays. MCP-1 to 3 are detectable in the BMSCs isolated from MM patients[140].

Interestingly, MCP-1 secretion by MM cells can be stimulated by IL-6 in BM. MCP-1 can also activate MM cells through MAPK signalling which is associated with MM cell proliferation. This indicates paracrine secretion of IL-6 not only stimulates MM cell growth but also induces autocrine MCP-1 production, resulting in growth stimulation and enhanced chemoattraction[144].

Transmigration through the BM endothelium and the subendothelial basement membrane requires proteolytic degradation of the latter. Human myeloma cell lines (HMCLs), primary tumour cells and murine MM cell lines were shown to constitutively produce MMP9 and able to transmigrate through the reconstituted basement membrane[145–147]. BM endothelial cells upregulate MMP9 expression upon the stimulation of different growth factors such as HGF[145]. The unique BMME provides a perfect niche for MM and other cancer cells.

1.2.5.5 SDF-1/CXCR4 axis in MM migration

The most studied factors for cell trafficking are the CXCR4/SDF-1 axis, IGF-1, and the intracellular regulators downstream of CXCR4, such as Rho and Rac[139,148,149]. SDF-1, also known as C-X-C motif chemokine 12 (CXCL12), is constitutively produced by BMSCs and many other organs; while its receptor, CXCR4, is expressed on the surfaces of normal cells, such as haemopoietic stem cells and T and B lymphocytes, and on malignant cells including breast cancer cells and lymphoid malignancies[139,141,150,151]. SDF-1 induces B-lineage progenitor cells proliferation and B-cell maturation[152].

SDF-1 also promotes proliferation, induces migration and protects against dexamethasone-induced apoptosis in MM[153]. It has been shown that SDF-1 induces the phosphorylation of MAPK as well as Akt and its downstream target Bad, and activating NF-κB pathway in a time-dependent manner in both MM cell lines and primary MM cells[153]. Additionally, it induces IL-6 and VEGF secretion to promote cell growth[153], and up-regulates VLA-4-mediated cell adhesion to fibronectin and VCAM-1[135,154] in MM cells. SDF-1 promotes MM cell invasion across the basement membranes and type I collagen gels by upregulating MMP9 and MMP14 activity *in vitro*[155].

CXCR4, on the other hand, is the sole receptor of SDF-1. The binding of SDF-1 to CXCR4 triggers the dimerisation and internalisation of the receptor[156]. Recent data have suggested that CXCR4 is required to be included in lipid rafts for efficient signal transduction[156]. CXCR4 regulates both homing and mobilisation of MM cells. The addition of a CXCR4 inhibitor, AMD3100 (Plerixafor), disrupts the interaction between MM cells and BM, thereby inhibiting MM cells homing to the BM *in vivo*[148]. It is also used for autologous and allogeneic stem cell mobilisation in the clinic[157]. In short, the SDF-1-CXCR4 axis plays a pivotal role in regulating migration and adhesion of MM cells.

1.2.6 Therapies

Despite the fact that MM remains incurable, the introduction of novel therapeutics in the last 20 years has considerably improved the overall survival and patients' quality of life. Currently treatment is offered when patients have developed symptomatic MM. In Australia, the first-line treatment for newly diagnosed and transplant-eligible patients is bortezomib-based induction therapy followed by autologous stem cell transplantation (ASCT). Eligibility for ASCT is determined by age (upper limit of around 70-75 years), comorbidities and frailty[158]. Transplant-ineligible patients can be treated with bortezomib in combination with cyclophosphamide and dexamethasone[159], or lenalidomide in combination with dexamethasone[160], depending on the risk factors and disease stage[6,161]. Consolidation and maintenance therapy are also given following the first-line therapy. In the case of relapse after ASCT, a second ASCT is given to patients who relapse >12 months after the first ASCT. Patients who relapse within 12 months of the ASCT are preferably treated with new regimens.

1.2.6.1 Proteasome inhibitors

Bortezomib is a first-in-class proteasome inhibitor that blocks the action of 26S proteasome[162], leading to the accumulation of misfolded proteins and apoptosis in MM cells. It has also been shown to promote apoptosis in osteoclasts and induce osteoblast differentiation[163,164], thereby reducing bone resorption. Bortezomib is often coupled with dexamethasone and an addition agent in the

induction therapy for newly diagnosed, transplant-eligible patients[165]. With the introduction of bortezomib in the early 2000s, overall survival of MM patients has been remarkably improved[166]. Since then new generations of proteasome inhibitors, including carfilzomib and ixazomib, are developed and proved to be effective in relapsed/refractory patients who may have received several lines of therapy and/or been unresponsive to bortezomib[167–169].

1.2.6.2 Immunomodulatory drugs

As mentioned in 1.2.4, MM has an intricate relationship with BMME and that would be sensible to therapeutically target this relationship. Thalidomide was synthesised in 1954 and indicated to treat morning sickness in the first trimester of gestation; but due to the reports of congenital malformations, it was banned in the 1960s. Further studies revealed that thalidomide has an immunomodulating effect by affecting macrophages, B cells and T cells; it also decreases TNF-α synthesis, and more importantly affects IL-6 level and angiogenesis[170,171]. It is then introduced to treat relapsed/refractory MM[172–175]. New thalidomide analogues lenalidomide and pomalidomide have been developed for the purpose of reducing side effects and improving potency. This second-generation of immunomodulatory drugs (IMiDs) not only directly induce cell cycle arrest and apoptosis in MM cells, but also disrupts the interaction between MM cells and BMME (reviewed by V. Kotla et al.[176]). IMiDs sensitise MM cells to both bortezomib and dexamethasone, and promote immune defence mechanisms, making them invaluable for induction therapy[177]. Recently cereblon (CRBN) has been identified as the primary molecular target of IMiDs[178–180]. Silencing CRBN resulted in reduction in MM cell viability and strong resistance to lenalidomide and pomalidomide[181]. Research on the mechanisms of IMiDs and CRBN is actively in progress.

1.2.6.3 Monoclonal antibodies

Monoclonal antibodies, which stimulate immune response against target cells, has provided an alternative approach for the treatment of MM. Daratumumab is an anti-CD38 antibody for the treatment of MM. Despite the concern of targeting

CD38 – a transmembrane glycoprotein widely expressed in haemopoietic cells, neuronal cells, skeletal muscle cells and highly expressed in MM cells, preclinical studies showed that daratumumab induces cytotoxicity in MM cells by complement-mediated cytotoxicity, antibody-dependent cellular cytotoxicity and antibody-dependent cellular phagocytosis[182,183]. Initial clinical trials have demonstrated the efficacy of daratumumab monotherapy in heavily pre-treated relapse or refractory patients[184,185]. Currently multiple clinical trials are open to evaluate the efficacy of combining daratumumab with other anti-myeloma agents[186–188]. Elotuzumab is another humanised IgG1 monoclonal antibody targeting signalling lymphocytic activation molecule F7 (SLAMF7) and is used in combination with lenalidomide/pomalidomide and dexamethasone for patients received prior therapies[189,190]. Rituximab (anti-CD20), BI-505 (anti-ICAM1), MDX-1097 (anti-kappa light chain) and indatuximab ravtansine (anti-CD138 conjugated to cytotoxic maytansinoid) are the other emerging monoclonal antibodies for treating MM. These antibodies are in the pre-clinical and early phase of clinical studies[191–194].

1.2.6.4 Other inhibitors

Histone deacetylase inhibitors (HDACi), such as vorinostat, SAHA and panobinostat, have an anti-proliferative and a cytotoxic effect on MM cells. They also overcome the resistance to the novel anti-MM agents and the protection by IL-6 and BMSCs *in vitro*[195,196]. Panobinostat is the first FDA-approved HDACi to treat patients with relapse MM in combination with bortezomib and dexamethasone. In a phase III clinical trial, the combination of panobinostat, bortezomib and dexamethasone had significantly prolonged the progression-free survival than the placebo, bortezomib and dexamethasone group[197]. Other inhibitors targeting heat shock protein 90 (Hsp90), Akt, MEK, etc, have shown encouraging results *in vitro*[198,199], further studies are required to elucidate their efficacy in real life situations.

1.3 CD45

CD45, also known as leukocyte common antigen (LCA) or T200, is a transmembrane protein tyrosine phosphatase (PTP) encoded by *PTPRC* gene (1q31-32). It comprises up to 10% of the cell surface area in all nucleated haemopoietic cells and their precursors, making it one of the most abundant cell surface glycoproteins[200]. In humans, mutations in *PTPRC* gene and abnormalities in the expression of CD45 splice variants are known to cause severe-combined immunodeficiency (SCID)[201–203] and T cell acute lymphoblastic leukaemia (T-ALL)[204].

1.3.1 CD45 Structure

CD45 is a highly glycosylated transmembrane protein tyrosine phosphatase (PTP) comprising up to 10% of cell surface of nucleated leukocytes[200]. It consists of a large variable extracellular region, a single transmembrane domain and a large cytoplasmic region (Figure 1-3). CD45 has multiple isoforms with variable N-terminal in the extracellular region due to alternate splicing of exons 4-6. The alternate splicing can produce eight isoforms of CD45, of which only five have been detected in humans at protein level (exon 4: RA, exon 5: RB, exon 6: RC, exon 4-6: RABC, lacking 4-6: RO)[205,206]. Although mRNA studies have evident the alternate splicing of exon 7, 8 and 10 in murine cell lines, the corresponding protein expression has not been observed[207,208]. This variable region provides multiple sites for o-linked glycosylation; as a result, these isoforms are substantially different in molecular weight, ranging from 180kDa (CD45RO) to 240kDa (CD45RABC), shape and negative charge. The remaining of the extracellular region includes a cysteine-rich region and three fibronectin type III repeats[209].

The cytoplasmic portion of CD45, which is highly conserved across all species, consists of two tandem PTP domains, D1 and D2, and a C-terminal tail. Only the membrane-proximal D1 has phosphatase activity[210]. A. Weiss et al. demonstrated that the introduction of a chimeric molecule consisting of the

epidermal growth factor receptor (EGFR) extracellular and transmembrane domains fused to the cytoplasmic region of CD45 was able to restore T cell receptor (TCR) activity in a CD45-deficient cell[211], indicating that the cytoplasmic region of CD45 is essential for signal transduction. Using the same chimeric molecule in a CD45-deficient model, they further characterized the function of D1 and D2 by replacing the catalytic cysteine to serine in either or both domains. Point mutations in D1 and D1+D2 abolished the phosphatase activity of the chimera completely whereas mutation in D2 retained similar phosphatase activity to the wild-type molecule *in vitro* and *in vivo*. One of the hallmarks of TCR engagement is the induction of phosphorylation. As predicted, mutations in D1 and D1+D2 failed to induce phosphorylation upon stimulation, while mutation in D2 reproduced a similar effect as the wild-type chimera[212]. It appears that the membrane-proximal D1 alone was sufficient to regulate signal transduction and D2 was redundant. However, *in vitro* translated cytoplasmic CD45 lacking D2 existed as a dimer, was less thermostable and only retained approximately only one-third of phosphatase activity as full-length cytoplasmic CD45. The dimerization was not observed in the full-length cytoplasmic CD45, indicating a potential intramolecular interaction between D1 and D2. D2 lacks the catalytic activity but it is essential for stability and optimal activity of cytoplasmic CD45[213–215].

1.3.2 CD45 isoforms

Multiple isoforms of CD45 are expressed depending on the subpopulation of leukocytes, activation and differentiation stages[208,216,217]. Such pattern is highly conserved across different species[209,218,219]. For instance, during thymocyte differentiation from the immature form, $CD3^{-}CD4^{-}CD8^{-}$, to the mature form, $CD4^{+}CD8^{+}$, expression of CD45RO increased; whereas expression of RB, RC and especially RA declined[220,221]. The expression pattern of CD45 isoforms is less extensively analysed in B cells. Generally, both immature and mature B cell express RABC predominately; in activated B cells, CD45 expression switches to the lower molecular weight isoforms RA, RB and RC[222]. Increasing expression of lower molecular weight isoforms was also observed in myeloid lineages, but not in erythroid differentiation[217].

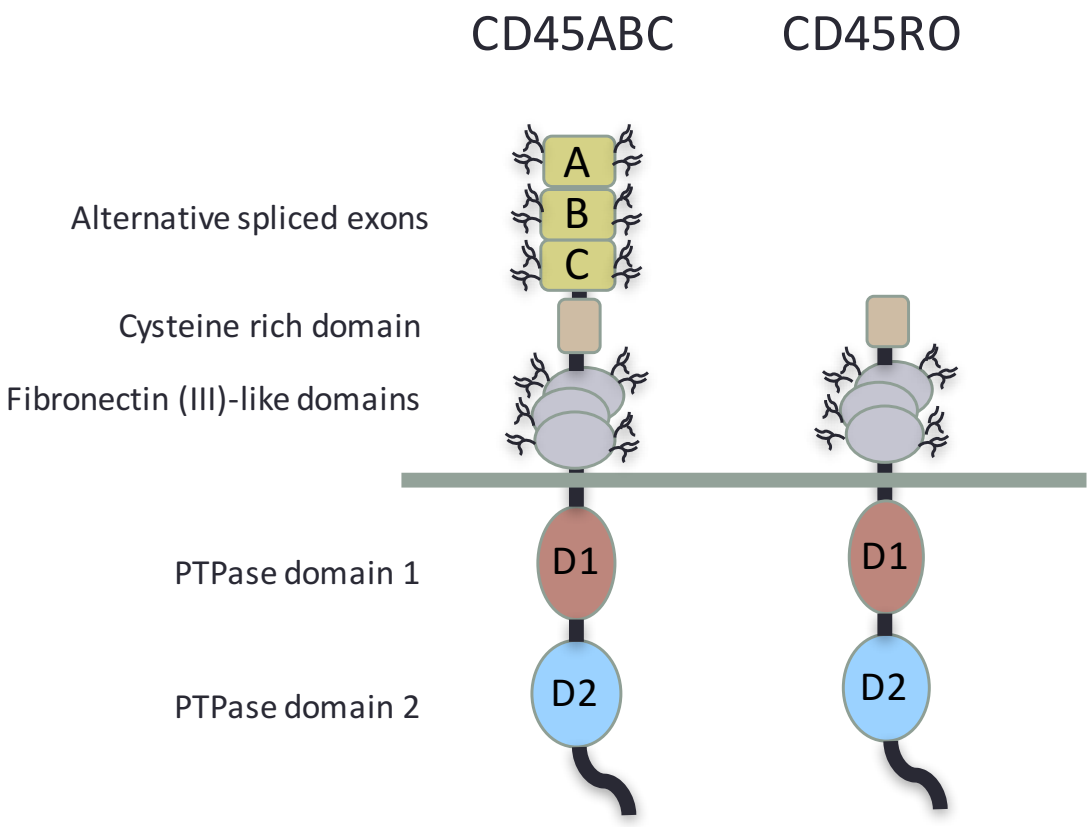

Figure 1-3: Structure of CD45.

CD45 consists of a large extracellular region, a single transmembrane domain and a large cytoplasmic region. The extracellular region includes a variable region which provides multiple sites for o-linked glycosylation, a cysteine-rich region and three fibronectin type III repeats. The cytoplasmic portion of CD45 consists of two tandem PTP domains, D1 and D2, and a C-terminal tail. Only the membrane-proximal D1 has phosphatase activity. Alternative splicing of exons results in multiple isoforms of CD45 (exon 4: CD45RA, exon 5: CD45RB, exon 6: CD45RC). High molecular weight isoform CD45ABC (220kDa) and low molecular isoform CD45RO (180kDa) are shown.

1.3.3 CD45 in T and B cell development

Considering that CD45 is widely expressed in haemopoietic lineages and switches isoforms during cell differentiation and activation, it is not surprising that CD45 influences T cell and B cell development. It has been shown that loss of CD45 remarkably reduced the number of total and mature T cells in the spleen of transgenic $CD45^{-/-}$ mice by 5-fold and 10-fold respectively compared with the wild-type mice. The thymocyte development and differentiation were also impaired. Furthermore, the number of splenic B cells was doubled in the $CD45^{-/-}$ mice due to the accumulation of immature B cells[223]. Overexpression of either CD45RO and RB was sufficient to restore the thymocyte development and T cell functions in the periphery of $CD45^{-/-}$ mice; yet neither the isoform restored the peripheral B cell maturation and activation[224]. These data suggest that CD45 is indispensable for both T cell and B cell development and its isoforms are engaged in different circumstances. Functions of other isoforms are yet to be explored.

1.3.4 CD45 in T and B cell receptor signalling

The antigen specific receptors on T cells and B cells are complexes composing of receptor proteins and clonally variable antigen binding chains: α and β chains in T cells, heavy and light immunoglobulin chains in B cells; as well as other accessory molecules including CD4, CD8, tyrosine kinases and phosphatases. Together, these molecules orchestrate the signal transduction from ligand-receptor to other signalling molecules via a series of phosphorylation and dephosphorylation within the complex, which ultimately activates transcription factors to modulate gene expression. The initial event of intracellular signal transduction is the phosphorylation of the immunoreceptor tyrosine-based activation motifs (ITAMs) located in the cytoplasmic portion of accessory chains by Src family kinases (SFKs). In T cells, two of the SFKs: Lck, which is constitutively associated with the cytoplasmic domain of CD4 and CD8; and Fyn, are responsible for this phosphorylation[225–227]. Subsequently, a second protein tyrosine kinase, ZAP-70, is rapidly recruited to the phosphorylated ITAMs to activate the downstream signalling pathways. B cell signalling is

transmitted in a similar manner. Blk, Fyn and Lyn of SFKs phosphorylate ITAMs and hence facilitate the association of ITAMs with Syk family kinases[228].

CD45 acts on the upstream of T and B cell signalling pathways in which it modulates the activity of SFKs by dephosphorylating the inhibitory site in SFKs (further discussion in 1.3.5.1). Recent studies have revealed an additional regulatory mechanism by CD45 in T cell signalling. High-resolution imaging showed that upon stimulation T cells developed small, dynamically regulated clusters containing receptor and accessory proteins within the plasma membrane[229–231]. CD45 is excluded from the cluster, possibly due to the large, highly glycosylated extracellular domain. Thus, kinases are favoured over phosphatases in the cluster, leading to TCR phosphorylation[232].

1.3.5 CD45 regulated pathways

1.3.5.1 Dual role of CD45 on SFK

The most well established function of CD45 is its regulation on the non-receptor protein tyrosine kinases, SFKs[233,234]. SFKs play a key role in cell proliferation, differentiation, migration, morphology and survival, and more importantly in TCR and BCR signalling. The nine family members, Src, Lyn, Lck, Hck, Blk, Fgr, Yes, Fyn and Frk, are expressed across different cell types, for example, the predominant forms in T cells are Lck and Fyn and in B cells are Lyn and Blk[235]. The activity of SFKs is controlled by the phosphorylation and dephosphorylation of an activating tyrosine residue in the kinase domain and an inhibitory tyrosine in the C-terminus respectively. In dormant state, the phosphorylation at tyrosine 527 (Y527, referring to Src amino acid sequence) facilitates the intramolecular binding of SH2 and kinase domain thereby inhibiting its catalytic activity. CD45 removes the inhibitory phosphorylation at Y527, releasing the catalytic loop from the intramolecular binding. Subsequently, the kinase domain undergoes autophosphorylation at Y416, promoting the catalytic activity of SFKs[236–239] (Figure 1-4).

Complicating this model is that CD45 can also downregulate SFK activity. C.

Burns et al. demonstrated the activity of Lck and Fyn was elevated paradoxically in three CD45-deficient murine lymphoma T-cell lines, in spite of the hyperphosphorylation of Lck at the inhibitory Y505. Phosphorylation of other tyrosine residues was also increased, but at a lesser extent[240]. CD45 can directly dephosphorylate Lck Y394 *in vitro*, either in the form of derived peptide or native conformation[210,212]. Similar observation was found in CD45 negative immature B cells in which Lyn was constitutively active and its positive and negative regulatory sites (Y397 and Y508 respectively) were dephosphorylated by CD45[241]. Moreover, loss of CD45 expression in murine macrophage dysregulated integrin-mediated adhesion and led to an increase in activity of Hck and Lyn[233]. Therefore, the regulation of SFK activity by CD45 is a much more complex and dynamic process that CD45 has dual functions on SFK: it positively and negatively regulates SFK in a cell-type specific and context-dependent manner.

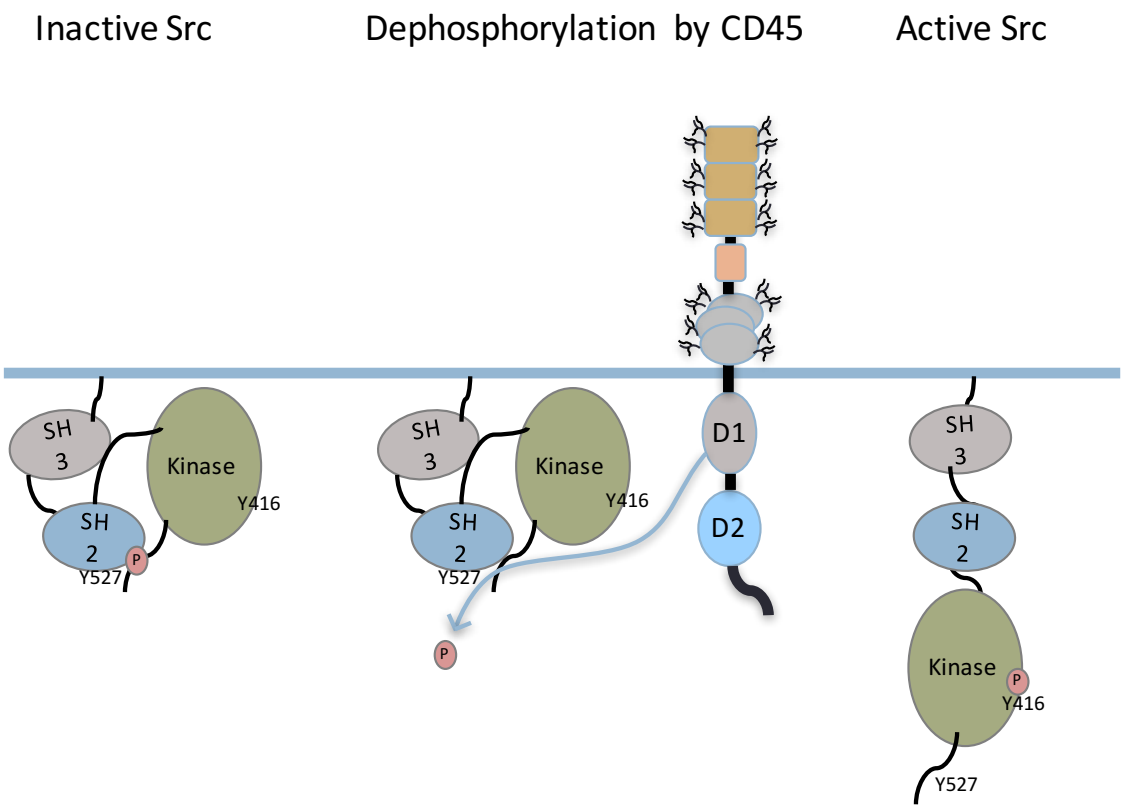

Figure 1-4: Structure of Src in basal and active conformation.

Under basal condition, Src is stabilised by the binding of phosphorylated Y527 to its SH2 domain and SH2-kinase linker to SH3 domain (left panel). These intramolecular interactions are disrupted upon the dephosphorylation of Y527 by CD45, leading to conformational changes in the kinase domain (middle panel). The kinase can then autophosphorylate Y416 in the activation loop and hence facilitates access of substrate to the catalytic site (right panel).

1.3.5.2 CD45 as a negative regulator of JAK in cytokine signalling pathway

CD45 is expressed in all nucleated haemopoietic cells at all stages of development, indicating that CD45 functions are not restricted to TCR and BCR signalling pathways. J. Irie-Sadaki et al. investigated the possible functions of CD45 in other cell types and were first to demonstrate that CD45 suppresses JAK and negatively regulates the cytokine pathway. They showed that the isolated IL-3-dependent bone-marrow-derived mast cells from $CD45^{-/-}$ mice exhibited significant enhanced JAK2, STAT3 and STAT5 phosphorylation upon IL-3 stimulation[242]. Similar results were also obtained from COS cells, Jurkat T cells, freshly isolated murine thymocytes and macrophages in which interferon-α (IFN-α) induced stronger activation of JAK1 and Tyk2 in CD45-deficient cells than the wild-type counterparts. Furthermore, *in vitro* phosphatase assay revealed that recombinant CD45 can directly dephosphorylate all four JAK family members, JAK1, JAK2, JAK3 and Tyk2, at their activating tyrosine residues[242,243]. In fact, hyperphosphorylations on Y1022 and Y1023 of JAK1, Y1007 and Y1008 of JAK2, and Y1054 and Y1055 of Tyk2 were detected upon IL-3 stimulation in CD45-deficient mast cells[242]. These results reinforce the concept that CD45 regulates JAK in cytokine signalling.

JAK family has four members: JAK1, JAK2, JAK3 and TYK2. Unlike most of the tyrosine kinases, JAK has two kinase domains, JH1 and JH2. Only JH1 has functional kinase activity while JH2 lacks the essential residues for catalytic activity and nucleotide binding[244]. Studies have demonstrated that the deletion of JH2 increased JAK2 and JAK3 kinase activity and cytokine-independent STAT activation, indicating that JH2 suppresses JAKs and cytokine signalling[245–247]. The other domains, FERM (4.1, ezrin, radixin, moesin) and SH2, function as receptor association and phosphotyrosine binding domains. In general, the binding of cytokines to their corresponding receptors induces receptor dimerisation and JAKs recruitment. JAKs then undergo autophosphorylation or phosphorylation by other tyrosine kinases and subsequently phosphorylate STATs. The active STATs dimerise and translocate into nucleus to initiate or repress target gene promoters[248–250].

SFKs can also directly activate STATs (reviewed by C. Silvia[251]), as such, CD45 mediates cytokine signalling through different kinases.

Given that JAK/STAT pathway is important in regulating cytokine-dependent gene expression, cell survival and differentiation (reviewed by S. Baker et al.[252], K. Shuai et al.[253]), altered CD45 expression may induce changes in cell differentiation patterns and/or survival in response to cytokine stimulation. J. Irie-Sadaki et al. demonstrated that the number of erythropoietin (EPO)-induced erythroid colonies and IL-3-induced neutrophil/macrophage myeloid colonies were greater in the BM progenitors isolated from the $CD45^{-/-}$ than the wild-type mice[242]. In addition, suppression of picornavirus Coxsackievirus B3 replication by IFN-α was more efficient in CD45-deficient background both *in vitro* and *in vivo*[242]. These data suggest that CD45 plays a role in cytokine-dependent cell differentiation and IFN-α regulated viral infections.

1.3.6 CD45 and diseases

Although the links between CD45 and diseases are debatable, several diseases have been reported to have higher rates of altered CD45 expression or mutations. Loss of CD45 expression has been reported in 13% of patients with acute lymphoblastic leukaemia[254], Hodgkin's lymphoma[255] and MM cells[256]. An overexpression of CD45 was also observed in lamina propia B lymphocytes and PB mononuclear cells (MNCs) from patients suffering Crohn's disease in a small study[257]. A C77G point mutation in exon 4 of human CD45 appears at a low rate, around 3.5% in healthy individual; but at a much higher rate in patients with multiple sclerosis, around 6.8%[257]; 7.4% in systemic sclerosis, 4% in systemic lupus erythematosous[258] and 3.6% in hepatitis C[259,260]. In addition, C77G carriers with ovarian cancer had a weak beneficial effect in the form of a less aggressive disease. However it had no impact on patients' survival outcome[261]. In spite of these observations, the role of CD45 in the pathogenesis of these diseases have not been established.

1.3.7 CD45 as a therapeutic target

The concept of therapeutic modulation of CD45 function has been explored in organ transplantation, treatment of autoimmune disease and microglial activation-associated Alzheimer's disease by using selective phosphatase inhibitors and isoform-specific CD45 antibodies. CD45 antibody therapy has been employed for myeloablation for BM transplantation[262], to prevent allogeneic and xenogeneic heart and kidney transplant rejection in animal models[263,264]. Microglial activation, which plays a significant role in the pathophysiology of Alzheimer disease and Parkinson's disease, was reduced by cross-linking CD45 in murine primary culture microglia in some studies[265,266].

Modulating CD45 functions can also be beneficial in haematological malignancies due to the wide expression of CD45. A phase I study demonstrated that a radioisotope-labelled CD45 antibody could be used for delivering selective radiation to haemopoietic tissues in stem cell transplantation while sparing non-targeted organs in patients with advanced acute leukemia and myelodysplastic syndrome. In this study, seven out of 25 patients survived disease-free for 15-89 months[267,268]. A similar strategy was also applied to acute myeloid leukaemia and acute lymphatic leukaemia patients and showed encouraging results[269].

Other than targeting the extracellular component of CD45, tremendous efforts have been made to develop inhibitors specific to CD45 phosphatase domain while avoiding the inhibition of other tyrosine phosphatases[270,271]. Compound 211, an allosteric non-competitive small molecule inhibitor for CD45, has over 100-fold selectivity over six other related tyrosine phosphatases. It has been shown to suppress T cell receptor signalling by preventing the dephosphorylation of Lck at Y505 in primary T cells *in vitro*, and delay the growth and metastasis of established lymphoid tumours *in vivo*[272,273].

Targeting CD45 in diseases may seem appealing at a glance, however, due to its wide expression in tissues and being a phosphatase, selective inhibition of CD45 remains extremely challenging. Future studies are deemed to address the specificity and safety concern over the use of CD45 as a therapeutic target.

1.4 The role of CD45 in myeloma

As mentioned before, CD45 is commonly expressed on nucleated haemopoietic cells, and malignant MM cells are no exception. For the last 20 years, the role of CD45 in MM has been explored in different aspects. It has been suggested that CD45 is correlated to disease and treatment outcome, however relevant mechanistic study is very limited. This section discusses the role of CD45 in MM and addresses any unresolved questions.

1.4.1 CD45 expression in normal plasma cells and myeloma

Normal plasma cells are heterogeneous in morphology, life span, origin, final residing site and the class of antibodies which they secreted. Upon stimulation, naïve B cells or memory B cells differentiate into plasmablasts which then leave the germinal centres (lymph nodes and spleen) to blood circulation and migrate to BM for terminal differentiation into long-lived antibody secreting plasma cells. To characterise plasma cells, C. Pellat-Deceunynck et al.[274] examined plasma cells generated *in vitro* as well as isolated from the tonsils, peripheral blood, and BM of healthy donors and MM patients. They showed that normal plasma cells from tonsil and blood expressed high levels of CD45 and were highly proliferative, whereas those from BM were heterogeneous for CD45. The $CD45^{bright}$ cells (65% of total) were more proliferative than the $CD45^{low}$ cells (BrdU labelling index of 22% vs 4%). They also observed a gradual decrease in CD45 expression – from bright to dim – during memory B cell differentiation into pre-plasma cell *in vitro*. Similarly, consistent with another study[275] MM cells were heterogeneous for CD45 expression and proliferation was restricted to the $CD45^{bright}$ compartment (BrdU labelling index of 9% vs 2%). However, unlike healthy BM plasma cells, only 20% of the MM cells were $CD45^{bright}$ and the CD45 expression was frequently negative in MM patients. The heterogeneity of CD45 was also observed in circulating MM cells[276] and HMCLs[277]. The authors concluded that CD45 expression is correlated with maturity of both normal and malignant plasma cells which high CD45 expression represents the highly proliferative immature plasma cells and vice versa. Surprisingly, even though

$CD45^+$ cells are more proliferative, they only account for a small portion of tumour cells. Whether the $CD45^+$ cells are more apoptotic or some of them lose CD45 expression, has not been addressed so far.

To date it is still unclear how exactly MM cells lose some but not all CD45 expression. However, it is possible to manipulate CD45 expression in some MM cells by the addition of IL-6. The idea of IL-6 being able to change CD45 expression is based on the observation that $CD45^+$ cell lines are quite often IL-6-dependent while $CD45^-$ cell lines are IL-6-independent[277]. In two separate studies, the addition of IL-6 into culture media induced CD45 expression in $CD45^-$ cells: LP-1 and sorted $CD45^-$ U266 cells but not KMS-5[277,278]. Moreover, the withdrawal of IL-6 converted $CD45^+$ U266 cells into $CD45^-$ gradually suggesting that U266 can reversibly change CD45 expression depending on the presence of IL-6. As mentioned in 1.2.4.3, IL-6 is an important growth factor of MM and the binding of IL-6 to its receptor activates JAK/STAT3, PI3K and MAPK pathways. IL-6 activates both STAT3 and MAPK pathways in both $CD45^+$ and $CD45^-$ cells, however, IL-6-induced proliferation has been observed only in $CD45^+$ cells and required SFK activity[277,279]. Further investigation on how IL-6 induces CD45 expression would be very useful in deciphering the molecular mechanisms of CD45 expression regulation in MM.

1.4.2 Correlation of CD45 expression and drug sensitivity

Other than the differences in proliferation and response to IL-6 stimulation, $CD45^+$ and $CD45^-$ cells exhibit different sensitivities towards inhibitors and cellular stresses. Given that PI3K/Akt pathway is involved in MM cells proliferation, G. Descamps et al. examined the impact of CD45 on the pathway activation. They demonstrated that CD45 expression suppressed the magnitude and duration of IGF-1-induced PI3K/Akt proliferating signalling. While inhibition of PI3K by wortmannin promoted growth inhibition in $CD45^-$ HMCLs characterised by G_1 arrest but not in $CD45^+$ HMCLs[278]. In addition, $CD45^-$ cells were more sensitive to the inhibition of IGF-1 signalling by an anti-IGF1R monoclonal antibody[280]. Taken together, IGF-1-induced PI3K signalling could

be essential for $CD45^-$ phenotype.

On the other hand, targeting the JAK/STAT3 signalling pathway with a JAK2 inhibitor TG101209, both HMCLs and patients cells showed decline in proliferation with or without the presence of BMSC, and increase in apoptosis in a dose- and time-dependent manner[281]. Interestingly, such effect was more pronounced in the $CD45^+$ portion of U266. The addition of PI3K/Akt inhibitors augmented the cytotoxicity effect of TG101209 in two $CD45^-$ HMCLs, MM1S and OPM2. However, the authors neither explained the preferential cytotoxicity for $CD45^+$ cells nor tested the combination of TG101209 and PI3K/Akt inhibitors on $CD45^+$ cells. One could speculate that it was due to the dependence of IL-6 for proliferation in $CD45^+$ cells: targeting its downstream pathway JAK/STAT3 could lead to catastrophic effects on these cells.

Hsp90 is a chaperone protein that regulates a wide range of processes, such as stress regulation, protein folding, DNA repair and immune response[282]. Inhibition of Hsp90 has been shown to suppress PI3K/Akt/mTOR signalling in Burkitt Lymphoma[283] and JAK/STAT signalling in Hodgkin lymphoma[284]. In MM, inhibition of Hsp90 induced more profound effect on $CD45^+$ cells with activated JAK/STAT while sparing the $CD45^-$ cells[285]. Among the $CD45^+$ HMCLs tested, those with higher PI3K/Atk were relatively more sensitive to Hsp90 inhibition. As mentioned in 1.4.1, IL-6 can induce CD45 expression in the $CD45^-$ HMCL LP-1. Only the IL-6-induced $CD45^+$ portion of LP-1 became sensitive to Hsp90 inhibitor but not the $CD45^-$ portion despite the activation of JAK/STAT by IL-6 in both portions. This suggests that both CD45 expression as well as the JAK/STAT signalling determine the sensitivity to Hsp90 inhibition.

The above studies implicate that CD45 expression depicts the dependence on either JAK/STAT3 or PI3K/Akt pathways. Targeting both pathways could be a reasonable approach in MM treatments.

1.4.3 CD45 and cell migration

Homing to BM is a critical, yet selective step in MM dissemination, as discussed

in 1.2.5.4. Using a murine model that closely resembled human MM, K. Asosingh et al.[286] showed that $CD45^+$ and $CD45^-$ 5T murine MM cells had different homing kinetics *in vivo*. In their model, 5T2MM and 5T33MM cells spontaneously derived from C57BL/KalwRij mice were separated into $CD45^+$ and $CD45^-$ portions and injected into naïve mice intravenously. The homing of $CD45^-$ cells was significantly lower than $CD45^+$ in both 5T2MM and 5T33MM, and more $CD45^-$ cells remained in blood circulation. Both CD45 populations migrated to the livers and spleens. In addition, although both CD45 populations induced disease, mice inoculated with $CD45^-$ 5TMM cells had a higher tumour load and serum paraprotein concentration. Further *in vitro* experiments suggested that the $CD45^-$ portion had impaired chemotaxis towards BM endothelial cell conditioned medium, BMSC conditioned medium and basement membrane component laminin-1. Moreover, the $CD45^-$ cells had low expression of extracellular matrix proteases including matrix metalloproteinase-9 (MMP9) and urokinase type plasminogen activator (uPA)[287]. These results show that $CD45^+$ and $CD45^-$ populations have differential *in vitro* migratory and invasive capacities which explains the differential *in vivo* BM homing.

Apart from MM, the role of CD45 in migration has been observed in BM MNCs and thymocytes. The migration of BM MNC and thymocytes from $CD45^{-/-}$ mice in response to SDF-1 was significantly lower compared to their CD45 wild-type counterparts [288,289]. Both $CD45^-$ BM and PB MNCs secreted lower levels of MMP9 as seen in the $CD45^-$ 5TMM cells mentioned above. These BM MNCs demonstrated higher expression levels of activated β1 integrin, leading to an increased adhesion capacity to fibronectin, which may explain their reduced mobility. CD45 has also been associated with macrophage adhesion. However, in the context of macrophage, the absence of CD45 expression led to defects in adhesion: $CD45^{-/-}$ BM macrophages were unable to maintain integrin-mediated adhesion, these cells spread more rapidly and detached after a period of time, such behaviour was not observed in $CD45^{+/+}$ macrophages[233]. Mechanistic studies suggested that the defects in adhesion of $CD45^-$ macrophages was due to the decreased level of a cytoskeletal-associated protein paxillin by focal adhesion kinases, FAK and Pyk2 (proline-rich tyrosine kinase)[290]. These

kinases are directly phosphorylated and activated by SFKs[291,292], indicating that CD45 regulates cell adhesion through SFKs and FAKs. A similar phenomenon was also observed in T lymphoma cell BW5147 stimulated with CD44, in which Pyk2 activation was induced by the enhanced SFKs activity in the absence of CD45[293,294]. Table 1-3 summarises CD45 expression and cell behaviour in different cell types.

It is clear that CD45 regulates cell adhesion and migration through SFKs which directly regulates Pyk2, but the role of CD45 in SFKs activation is complicated. As mentioned in 1.3.5.1, CD45 can dephosphorylate both inhibitory and activating tyrosine residues on SFKs in a cell type-specific and context-dependent manner. Although SFKs were activated in the $CD45^-$ cells in the studies mentioned above, SFKs were, in fact, activated in only $CD45^+$ but not $CD45^-$ MM cells[295]. The correlation of SFKs activity and MM homing has not been addressed so far but from the differential homing properties between $CD45^+$ and $CD45^-$ cells, one could postulate that CD45 expression has an indispensable role in MM homing and potentially in disease dissemination.

Table 1-3: Correlation of CD45 and adhesion and migration.

Cell types	Adhesion		Migration to BM or chemoattractant		SFKs or FAKs activity	
	$CD45^+$	$CD45^-$	$CD45^+$	$CD45^-$	$CD45^+$	$CD45^-$
MM[286,287]	/	/	++	+	/	/
thymocytes[289]	/	/	++	+	/	/
BM/PB MNCs[288]	+	++	++	+	+	++ (Src)
macrophages[233,290]	++	++ (but easy to detach)	/	/	+	++ (Hck and Lyn; FAK and Pyk2)
T lymphoma cells[293,294]	round cell spreading	elongated cell spreading	/	/	+	++ (SFKs/Lck; Pyk2)

1.4.4 Correlation of CD45 expression and clinical manifestations

Normal plasma cells change from a highly proliferative $CD45^+$ to a nearly quiescent $CD45^-$ phenotype during maturation, and malignant plasma cells are no exception. Such phenotypic changes of MM cells during disease progression was examined in 5T2MM murine model in which MM was divided into quiescent, intermediate and end stage according to the serum paraprotein level. About 77% of MM cells expressed CD45 at the quiescent stage, corresponding to an immature and less proliferative yet invasive and apoptosis-resistant phenotype. As the disease progressed, only 34% of cells were $CD45^+$ at the intermediate stage and this was further decreased to 14% at the end stage, corresponding to a mature, highly proliferative but less invasive and less apoptosis-resistant phenotype[296]. These results contradict other studies which showed that the $CD45^+$ cells were proliferative but not the $CD45^-$ cells (see 1.4.1). The difference between these studies is the consideration of disease stages. It is possible that $CD45^-$ cells evolve and adapt better to the changing BMME than $CD45^+$ cells at the advanced disease stage. Nevertheless, the 5T2MM murine model demonstrates the gradual loss of CD45 expression during disease progression.

Indeed, this concept applies to human MM. The proportion of $CD45^+$ BM plasma cells was higher among patients with early disease, MGUS or smouldering MM, compared to those with advanced, symptomatic or relapsed MM[297]. More importantly, CD45 expression is closely related to overall survival. P. Moreau et al. showed that patients lacking CD45 expression at diagnosis had significantly shorter overall survival than patients with CD45 expression (median not reached vs 42 months), despite the fact that both cohorts received high-dose therapy and had similar disease characteristics and burden. The $CD45^-$ cohort did not respond to further therapy and had shorter overall survival after relapse[298]. The same trend was observed by S. Kumar et al. who showed that $CD45^-$ newly diagnosed and relapsed patients tended to have shorter overall survival than $CD45^+$ patients (median 18 vs 39 months, p-value=0.07). The

presence of lytic bone lesions and high-grade angiogenesis in $CD45^-$ patients, which were less commonly observed in $CD45^+$ patients, might contribute to the poor prognosis[297].

More recently, similar studies were conducted with advanced flow cytometry techniques and gating strategies, but showed counterintuitive results: the presence of $CD45^+$ plasma cells may represent a more aggressive disease and be associated with shorter overall survival[299,300]. W. Gonsalves et al.[299] pointed out that the difference in flow cytometry techniques; patient cohorts receiving conventional versus novel therapeutics; and the difference in defining patients into $CD45^+$ and $CD45^-$ cohorts; could contribute to the discrepancy. More specifically, patients were defined as $CD45^+$ when all the plasma cells expressed CD45 in the P. Moreau et al. study compared to >20% plasma cells expressed CD45 in the S. Kumar et al. and W. Gonsalves et al. studies. It should be noted that patients often present variable CD45 expression in their plasma cells: $CD45^-$, $CD45^{dim}$ but positive, and $CD45^+$. Additionally, S. Kumar et al. included both newly diagnosed and replased patients while the other two studies focused on newly diagnosed patients only. These factors complicate the definition of patient cohorts and the interpretation of results, especially when the CD45 cohorts might not be mutually exclusive in these studies. Interestingly, although both P. Moreau et al. and W. Gonsalves et al. showed that the $CD45^-$ cohort had increased incidence of chromosomal translocations t(4;14) and t(14;16) (which are associated with poor prognosis[301]), it had better prognosis compared to the $CD45^+$ cohort.

These studies have proven CD45 expression carries a valuable prognostic value in disease outcome, however, it has yet to be properly defined. Given that CD45 expression is correlated with disease progression, drug sensitivity and BM homing, further investigation in the biology of CD45 in MM would be undoubtedly beneficial in optimising therapeutic regimens and predicting treatment outcomes.

1.5 Hypotheses and aims of thesis

The role of variable CD45 expression during MM disease progression is poorly understood. Using U266, a HMCL with distinct $CD45^+$ and $CD45^-$ populations, our group has found that the sorted $CD45^+$ U266 cells exhibit higher proliferative rates, greater clonogenic potential and a higher level of active Lyn (phosphorylated at Y397); while the $CD45^-$ U266 cells have higher NF-κB and Notch activity and epithelial-mesenchymal transition (EMT) activation. In addition, the two populations show distinct oncogene and tumour suppressor gene profiles. However, the exact mechanisms accounting for these observations remain unknown. In this project, the overall aim is to address the biological role of CD45 in MM.

Based on the previous studies, there are two hypotheses in this project. Firstly, $CD45^-$ phenotype could represent a more advanced or aggressive disease in MM. This is evident in patients with advanced disease having a higher percentage of $CD45^-$ BM plasma cells and $CD45^-$ patients having shorter overall survival (see 1.4.4). In addition, in the murine model, CD45 expression was lost gradually as disease progressed. $CD45^-$ MM cell lines were also less sensitive to certain inhibitors (see 1.4.2). Secondly, $CD45^-$ phenotype can also represent a more metastatic disease. This is based on the fact that $CD45^-$ murine cells showed lower homing capacity, longer circulation in peripheral blood and induced higher tumour load in mice (see 1.4.3). Our own data has shown EMT activation in $CD45^-$ U266 cells.

Previous *in vitro* studies compared $CD45^+$/$CD45^-$ HMCLs or U266 cells to identify the biological differences between these two populations; however, the genetic heterogeneity among the HMCLs confounded the interpretation of CD45 expression-related differences. Conventional gene disruption methods, such as RNA interference, had limited success in reducing CD45 expression due to its huge gene size and multiple transcripts. Thus, better tools should be employed to manipulate CD45 expression for further investigation. Given the correlation between disease progression and CD45 expression, as well as the distinct

characteristics of the HMCLs, there is a need to establish a new model to investigate the role of CD45 in MM and identify the underlying mechanisms involved.

This project has 3 aims:

1. To generate CD45 knockout ($CD45^{KO}$) cell lines by genetic manipulation using the CRISPR/Cas9 system. These $CD45^{KO}$ cells will be the tools for subsequent biological studies.
2. To characterise the biological and molecular differences between $CD45^{+}$ (CD45 wild-type, $CD45^{WT}$) and $CD45^{-}$ ($CD45^{KO}$) cell populations *in vitro*; and whether these observations are in concordance with previous studies.
3. To investigate the role of CD45 in MM development in murine models. Immunodeficient NSG mice will be injected with the $CD45^{WT}$ and $CD45^{KO}$ cells intravenously and intratibially to mimic the disease development in humans.

CHAPTER 2:
MATERIALS AND METHODS

2.1 Tissue culture

2.1.1 Cell lines

2.1.1.1 Human myeloma cell lines

HMCLs JJN3, LP-1, MOLP-8, OPM2, L363 and EJM were obtained from Deutsche Sammlung von Mikroorganismen und Zelkulturen (Braunschweig, Germany). NCI-H929, RPMI-8226, MM1.S, MM1.R, and U266 were obtained from the American Type Culture Collection (Virginia, USA). KMM-1 were obtained from Japanese Collection of Research Bioresources Cell Bank (Osaka, Japan). KMS11, KMS12BM, KMS12PE, KMS18, KMS26, KMS28BM, KMS28PE, KMS34 were a kind gift from Dr. Takemi Otsuki, Kawasaki Medical School, Japan. ANBL-6, OCI-MY1 and XG-1 cell lines were a kind gift from the Winthrop P. Rockefeller Cancer Institute (Arkansas, USA).

TK1 to TK10 were derived from BM aspirates or PB from new diagnosed, relapsed or refractory MM patients (following written informed consent with approval from the Alfred Hospital Research and Ethics Committee).

2.1.1.2 Human stromal cell lines

Human stromal cell line HS5 from healthy donor was acquired from the American Type Culture Collection.

2.1.2 Culture conditions

2.1.2.1 Serum-containing culture conditions

Cells grown under normal condition were cultured in complete medium containing RPMI1640 medium (Gibco, Thermo Fisher Scientific, Victoria, Australia) supplemented with 10% heat inactivated foetal calf serum (FCS) (Lonza, Victoria, Australia), 2mM L-glutamine, 100U/ml penicillin and 100µg/ml streptomycin (Gibco), in a humidified incubator, 5% CO_2 at 37°C. All HMCLs,

primary cells and stromal cells were cultured in complete medium unless otherwise specified.

TK1 to TK10 were cultured in complete medium with 10% HS5 conditioned medium. The HS5 conditioned medium was obtained by culturing HS5 to 70-80% confluent, replacing with fresh complete medium. Supernatant were collected after 16-18hr and passed through a sterile 0.22μm filter.

ANBL-6 and XG-1 (IL-6-dependent HMCLs) were cultured in complete medium supplemented with 2-5ng/ml IL-6 as required.

2.1.2.2 Serum-free culture conditions

In the case of starving HMCLs, cells were removed from the normal culture medium, washed with sterile PBS twice and resuspended in RPMI1640 medium supplemented with 2mM L-glutamine, 100U/ml penicillin and 100μg/ml streptomycin at a density of $2x10^5$ cells/ml for 16-18hr.

2.1.2.3 Glutamine-free conditions

Cells were removed from the normal culture medium, washed with sterile PBS twice and resuspended in RPMI1640 medium supplemented with 10% dialyzed FCS, 100U/ml penicillin and 100μg/ml streptomycin at a density of $2x10^5$ cells/ml. Dialyzed FCS was prepared by dialyzing 50ml of FCS against 2L of PBS using a membrane with a molecular cut-off of 3,500 molecular weight cutoff. PBS was changed every 12hr for 72hr.

2.1.2.4 Cell passaging

Confluent suspension cells were mixed by gentle pipetting and semi-adherent cells were dislodged by gentle tapping the flask or scrapping with a cell scraper. Depending on the cell proliferation rate, approximately 1ml of cell suspension was added into a new flask with 15ml of fresh complete medium and returned to the incubator.

For adherent cells (stromal cells), existing medium was decanted in a 1% bleach solution. Cells were rinsed with sterile PBS twice to remove remaining medium. Cells were then incubated with 2ml of TrypLE™ Express Enzyme (Gibco) for 5-10min. Disassociated cells were pelleted by centrifugation at 1000rpm for 5min. Supernatant was decanted, and the pellet was resuspended in 10ml fresh complete medium. Approximately 1ml of cell suspension was added into a new flask with 15ml of fresh complete medium and returned to the incubator.

2.1.2.5 Cryopreservation

Cells were collected and pelleted as described in Section 2.1.2.4. Supernatant was decanted, and the pellet was resuspended in complete medium supplemented with 10% dimethyl sulfoxide (DMSO) (Sigma-Aldrich, New South Wales, Australia) at a density of $1x10^6$ cells/ml. The resuspended cells were transferred into cryovials and stored in freezing containers in -80°C overnight before long-term storage in liquid nitrogen.

2.2 Transactivation assays

2.2.1 CRISPR/Cas9 plasmids

The plasmids for generating CD45 (*PTPRC*) knockout cells were based on a lentiviral vector LentiCRISPRv2 (GenScript Biotech, New Jersey, USA) developed by Dr. F. Zhang's lab[302]. This vector contains both the *Streptococcus pyogenes* Cas9 nuclease and the single guide RNA (gRNA) scaffold. The specific gRNA sequences targeting PTPRC (5'- TTAATATTAGATGTGCCACC -3') was selected from Genome-scale CRISPR Knock-Out (GeCKO) v2.0 library[302,303].

2.2.1.1 gRNA sequence cloning

The selected gRNA sequence was cloned into the lentiviral vector pLentiCRISPR_v2 as described by Dr. F. Zhang's lab[302,303]. In brief, 2

oligonucleotides were synthesised with 5' or 3' overhangs for each gRNA as follows:

5'-CACCGNNNNNNNNNNNNNNNNNNN-3' and

3'CNNNNNNNNNNNNNNNNNNNCAAA-5',

where N represents the gRNA sequence. Each pair of oligonucleotides were phosphorylated and annealed with T4 polunucleotide kinase (New England Biolabs, Massachusetts, United States), which was then ligated into *Bsm*BI digested pLentiCRISPR_v2. The resulting plasmid was transformed in Stbl3 bacteria (Invitrogen, Thermo Fisher Scientific). The plasmid was subjected to Sanger sequencing (Micromon, Moash University) to ensure correct gRNA sequence in the vector.

2.2.2 Luciferase reporter plasmid

The plasmid containing GFP and luciferase (Luc) gene was a kind gift from Associate Professor Marco Herold (Walter and Eliza Hall Institute, Melbourne, Australia). It was introduced into HMCLs for *in vivo* imaging.

2.2.3 Lentivirus production

The vector containing gene of interest (transfer plasmid) and three packaging plasmids (pRSV, pMDL, pVSVG) were transiently transfected into HEK293T cells using Lipofectamine 2000 reagents (Invitrogen). HEK293T cells were seeded at a density of $5x10^6$ cells/10ml in a 10cm plate the day before transfection. On the day of transfection, the existing medium was replaced with 5ml pre-warmed DMEM without FCS and antibiotics. The transfection mixture containing 1ml Opti-MEM (Invitrogen), 10µg transfer plasmid, 5µg pMDL, 2.5µg pRSV, 3µg pVSVG and 30µl Lipofectamine 2000 were incubated at RT for 20min before adding into HEK293T cells. After 16-20hr, medium was replaced with fresh DMEM with 10% FCS and antibiotics. Supernatant containing lentiviral particles was collected after 48 and 72hr of transfection and filtered through a 0.45µm sterile syringe filter. It was then aliquoted and stored in -80°C.

2.2.4 Lentivirus infection of target cells

Cells were seeded in 24-well plates at $3x10^5$ cells/ml in RPMI1640 medium supplemented with 20% FCS and double the amount of cytokines (if applicable). Polybrene (Sigma-Aldrich) was added to cells at a concentration of 16μg/ml which was then incubated in 37°C humidified incubator for 15min. Lentiviral supernatant was added to cells at 1:1 ratio and spun at 32°C at 2500rpm for 60-90min, after that, cells were placed back into 37°C humidified incubator. Cells were washed with pre-warmed PBS twice and cultured in complete medium with 500ng/ml puromycin (Sigma-Aldrich) to select infected cells until control (un-infected) cell died completely.

2.3 Gene silencing assay

SMARTpool ON-TARGETplus LYN and FYN siRNAs (Dharmacon, Colorado, USA), and Universal Negative Control #1 (scramble siRNA) (Sigma-Aldrich) were transfected into targeted cells with RNAiMAX reagent (Invitrogen) according to the manufacturer's protocol.

2.4 Cell-based assays

2.4.1 Proliferation assays

Cell proliferation was measured by Trypan Blue (Sigma-Aldrich) staining. Cells were seeded at a density of $2x10^5$ cells/ml in different culture media. At the indicated time-points, cells were gently mixed to ensure even distribution and a small amount of cells were taken out for Trypan Blue staining. Stained cells were applied to haemocytometer and counted under an inverted microscope.

2.4.2 Cell mobility assays

2.4.2.1 CFSE staining

Carboxyfluorescein succinimidyl ester (CFSE) staining was performed to

differentiate cell populations. In short, BMSCs were trypsinised and counted before being washed in sterile PBS. Cells were resuspended at a density of $1x10^6$ cells/ml in 0.5% FCS-PBS and stained with 200nM CFSE (Invitrogen) for 10min with frequent vortexing. The free dye was removed by adding 5 times the staining volume of complete medium and spun at 1000rpm. Cells were then resuspended in complete medium and seeded into tissue culture plates as described in experiments.

2.4.2.2 Homing assay

The homing capacity of MM cells towards BMSCs was assessed by modified Boyden chamber assay. HS5 or patient-derived BMSCs were labelled with CFSE (as per 2.4.2.1) and seeded into a 24-well plate at a density of $2x10^5$ cells/ml for overnight incubation. Transwell inserts with 5μm pore size (Corning, Victoria, Australia) were carefully placed into the wells of the plate and 100μl MM cells at $2x10^6$ cells/ml were loaded into the inserts. After 4hr incubation at 37°C, the inserts were discarded, and contents of the wells (cells and media) were collected. Samples were stained with CD138-PE and analysed on a flow cytometer immediately. The $CFSE^-$ $CD138^+$ population represented the MM cells homed to BMSCs. The ability of MM cells digesting extracellular matrix was assessed by a similar fashion but with 8μm pore size Transwell inserts pre-coated with Matrigel and MM cells were incubated for 24hr. For drug treatment, MM cells were pre-treated with indicated concentrations of saracatinib and/or PF-473228 (Selleck Chemicals, Victoria, Australia) for 1hr before loading into the Transwell inserts.

2.4.2.3 Adhesion assay

The adhesion capacity of MM cells to BMSCs was assessed in a similar fashion to the homing assay (2.4.2.2) but without Transwell inserts. CFSE-labelled BMSCs (as per 2.4.2.1) were seeded in a 24-well plate and allowed to established overnight. MM cells were added into the wells directly and cultured for 2hr. The contents of the wells were collected and stained with CD138-PE

before being analysed on a flow cytometer.

2.4.3 Colony-forming assay

Five hundred cells were plated in Methocult media (StemCell Technologies, Victoria, Australia) supplemented with 25% FCS and IMDM (Invitrogen) in duplicated 60mm plates according to manufacturer's protocol. Cells were cultured in a 37°C, 5% CO_2 humidified atmosphere for 12 days. Photographs of colonies and number of colonies were assessed using an inverted microscope equipped with a colour camera. Cells from the entire plate were recovered by resuspending and washing in 2% FCS/IMDM, and counted by Trypan Blue staining.

2.5 Flow cytometry

2.5.1 Surface staining

Approximately 2-5x10^5 cells were harvested and washed in 0.5% FCS-PBS (FACS buffer) twice, then resuspended in 100µl FACS buffer. Antibodies were added into cell suspension and incubated for 20min at 4°C in dark. Cells were then washed twice and resuspended in 300µl FACS buffer and analysed on a flow cytometer immediately. For multi-colour staining, single colour isotype controls were used for colour compensation.

2.5.2 Intracellular staining

Harvested cells were washed in PBS and fixed in ice-cold 2% paraformaldehyde (PFA) in PBS for 20min at 4°C. PFA was then washed off with PBS and the cells were resuspended in permeablisation buffer (0.1% saponin, 1% FCS in PBS) with antibodies and incubated for 30min at RT in the dark. After washing with FACS buffer twice, the cells were ready for analysis.

2.5.3 Flow cytometry reagents

Table 2-1: Flow cytometry antibodies used in this study.

Antibody	Conjugate	Specificity	Catalogue number	Supplier
CD45	FITC	CD45	555482	BD Pharmingen
CD138	PE	CD138 (syndecan-1)	552026	
CD38	PE	CD38	555460	
CD19	FITC	CD19	555412	
CD20	PE	CD20	347677	
CD184	PE	CXCR4	555974	
CD126	PE	IL-6 receptor α	551850	
CD221	PE	IGF-1 receptor α	555999	
IgG1	FITC/PE	Mouse IgG1 isotype control	555748/555749	
IgG2bκ	FITC/PE	Mouse IgG2bκ isotype control	555742/555743	

2.5.4 Cell cycle analysis

Harvested cells were washed in PBS and fixed in 1mL of ice-cold 70% ethanol, added dropwise whilst vortexing. Samples were stored in -20°C for 24hr and then centrifuged and washed twice with PBS to remove the remaining ethanol. Cells were resuspended in 200µl propidium iodide (PI)/RNase solution (BD) and incubated at RT for 15min, followed by acquisition.

2.5.5 Acquisition and analysis

Flow cytometry samples were analysed on a FACSCalibur (BD) with Cell Quest software or LSR-Fortessa with FACS DiVA software. The acquired data was analysed using FlowJo (Treestar, Oregon, USA).

2.6 Gene expression analysis

2.6.1 RNA extraction

Total RNA was isolated using the RNeasy extraction kit (Qiagen, Hilden, Germany) according to manufacturer's instructions. In brief, harvested cells were lysed in Buffer RLT with sufficient pipetting for complete homogenisation and then 70% ethanol was added to the lysate facilitate RNA binding to the silica membrane of the spin column. The mixture was loaded into the spin column followed by centrifugation for 15 seconds at 13,000rpm. The spin column membrane was washed with Buffer RW1. Next, On-Column DNase digestion was performed with the RNase-free DNase Set (Qiagen) to remove genomic DNA: DNase I and Buffer RDD were added directly to the spin column membrane and incubated at room temperature for 15 minutes. The membrane was washed with Buffer RW1 followed by Buffer RPE twice. RNA was eluted with RNase-free water, quantified (as per 2.6.2) and converted into complementary DNA (cDNA) (as per 2.6.3) immediately.

2.6.2 RNA quantification

RNA quantity and quality were determined by ratios of 260/280nm and 260/230nm using the Nanodrop1000 (Thermo Fisher). Samples with any ratio below 1.9 were discarded.

2.6.3 cDNA synthesis by reverse transcription

cDNA was synthesed using SuperScript III Reverse Transcriptase First Strand Synthesis System (Invitrogen) according to manufacturer's instructions and stored in -20°C until use.

2.6.4 Quantitative mRNA analysis

Quantitative real-time PCR (qRT-PCR) was used to measure gene expression

and validate RNA sequencing results. Each reaction was performed in three technical and biological replicates. A reaction mixture contained 1X SYBR PCR Master Mix (Applied Biosystems, Thermo Fisher), 500nM each of forward and reverse primers for target genes and 10-20ng/µl template cDNA was loaded into a 384-well plate. The reaction was performed using a Light Cycler 480 (Roche, Basel, Switzerland) at 95°C for 10min, 50 cycles of amplification at 95°C for 30 seconds, 60°C for 15 seconds and 72°C for 15 seconds. Amplified products were verified by melting curve analysis. Relative gene expression was analysed using the $2^{-\Delta\Delta Ct}$ method and housekeeping gene *ACTB*.

2.6.5 Genomic DNA isolation

Genomic DNA was isolated using DNeasy Blood Tissue Kit (Qiagen) as per manufacturer's instructions.

2.6.6 PCR

Each reaction contained ~100ng template DNA, 0.5µM forward and reverse primers, 3% DMSO and Phusion High-Fidelity PCR Master Mix (New England Biolabs) and loaded into a PCR tube. The reaction was performed using a thermos cycler (Bio-Rad, Hercules, CI, USA) at 98°C for 30 seconds, 35 cycles of amplification at 98°C for 10 seconds, 45-72°C for 20 seconds and 72°C for 15-30 seconds. The PCR products were sent for Sanger sequencing (Micromon, Monash University).

2.6.7 Primer sequences

Table 2-2: Primers used in qRT-PCR and PCR.

Gene	Accession number	Forward primer	Reverse primer
ACTB	NM_001101	GACAGGATGCAGAAGGAGATTACT	TGATCCACATCTGCTGGAAGGT
ITGAL	NM_002209	CCAGAGAAGACAGTTGGGGT	TGACTTGGCTGGGGACTAAG
CXCR4	NM_001008540	CTGGCCTTCATCAGTCTGGA	TCATCTGCCTCACTGACGTT
ADAM19	NM_033274	GCATCGTTTCCCAGGACTTC	AGCTAATCATCCCTCCAGCC
PTPRC	ENSG00000081237	TAGCCTAGACTTTGCTCTCATGG	AAAGAAAGCTTGCAGACAATCAC

2.6.8 RNA sequencing

Total RNA was extracted and quantified as per 2.6.1 and 2.6.2. RNA aliquots (5-10µg) was stored in GenTegra tubes (Custom Science, Australia) which stabilise RNA at ambient temperature and transferred to Novogene Technology Co. Ltd. (Beijing, China) for RNA sequencing. Raw data was cleaned by removing low quality reads and reads with adaptors, followed by aligning the clean reads to the human reference genome (GRCh37). Then, gene expression was profiled using HTSeq v0.6.1[304] and normalised using FPKM (fragments per kilobase of transcript per million mapped reads) method. After lowly expressed genes were filtered, differential expressed genes (DEGs) were determined using edgeR[305]. Significantly regulated genes were identified using a cut-off of $\log_2$ fold-change (log2FC)>1 or <-1, p-value<0.05 and false discovery rate (FDR)<0.05. Functional annotation for the DEGs, including Gene ontology (GO) and Kyoto Encyclopaedia of Genes and Genomes (KEGG) enrichment pathway analysis was performed by using the DAVID Bioinformatics Resources 6.8[306,307]. Triplicates were performed for each sample in the RNA sequencing,

2.7 Protein expression analysis

2.7.1 Preparation of whole cell lysates

Cell pellets were resuspended with whole cell lysis buffer containing radioimmunoprecipitation assay (RIPA) buffer (150mM NaCl, 1% Nonidet P-40, 0.1% sodium deoxycholate, 25mM Tris) with cOmplete™ Mini Protease Inhibitor Cocktail (Roche), and PhosStop (Roche) and incubated on ice for 30min with occasional vortexing. Lysed cells were spun at 15000rpm for 15min at 4°C and the supernatant (cell lysate) was carefully transferred into a new tube and kept on ice followed by protein quantification (as per 2.7.2) immediately.

2.7.2 Protein quantification

Total protein concentration of cell lysates was determined by utilising the Pierce™ BCA Protein Assay kit (Thermo Fisher Scientific) according to the

manufacturer's protocol. Absorbance at 563nm was measured by Multiskan™ FC Microplate Photometer (Thermo Fisher Scientific). Appropriate amount of cell lysate was mixed with 5X sample buffer and incubated at 100°C for 5min.

2.7.3 Immunoprecipitation

Harvested cells were lysed in IP lysis buffer (Pierce, Thermo Fisher Scientific) supplemented with PhosSTOP and cOmplete EDTA-free protease inhibitor cocktail (Roche, Basel, Switzerland). Protein lysate was prepared and quantified as described previously, and then incubated with an anti-Pyk2 antibody overnight in 4°C on rotation. Protein-antibody complex was pulled down by Dynabead protein G (Thermo Fisher Scientific) and analysed by western blotting.

2.7.4 Western blotting

Pre-stained Precision Plus Protein Standards (Bio-Rad) and 40-100μg of each protein samples were loaded into a 10-15% SDS-PAGE gel. Proteins were separated by electrophoresis using Protein Gel System (Bio-Rad) at 100-120V for 1.5hr and transferred onto Immobilon-P Polyvinylidene Fluoride (PVDF) membranes (Millipore, Massachusetts, USA) using the Mini Trans-Blot electrophoretic transfer system (Bio-Rad) at 100V at 4°C for 90min. The membranes were then blocked with 4% bovine serum albumin (BSA) or skim milk in Tris-buffered saline-0.1% Tween-20 (TBST) for 30min at RT with gentle rocking. After 30min, the blocking buffer was decanted, and the membranes were incubated with primary antibody diluted in 4% BSA-TBST overnight at 4°C. Following primary antibody incubation, the membranes were washed with TBST 3 times for 10min each. Appropriated secondary antibody conjugated with horseradish peroxidase (HRP) was diluted in TBST and added to the membranes for 2hr at RT. The membranes were then washed with TBST 3 times for 10min each and ready for visualisation.

The membranes were incubated with SuperSignal™ West Pico PLUS Chemiluminescent Substrate (Thermo Fisher Scientific) followed by exposing to

X-ray film (AGFA, Victoria, Australia) and developed using a 100-plus film developer (All-Pro Imaging, New York, USA).

2.7.4.1 Primary and secondary antibodies

Table 2-3: Primary and secondary antibodies used for Western blotting.

Antibody	Catalogue number	Supplier
Phosphor-Akt (S473)	9271	Cell Signalling Technologies (CST)
Akt	9272	CST
Phosphor-STAT3 (Y705)	9145	CST
STAT3	12640	CST
Phosphor-Src (Y416)	2101	CST
Lyn	2796	CST
Lyn (LYN-01)	628102	Biolegend
Fyn	MA1-19331	Thermo Fisher Scientific
Phosphor-Pyk2 (Y580)	44634G	Thermo Fisher Scientific
Phosphor-Pyk2 (Y402)	44618G	Thermo Fisher Scientific
Pyk2	3480	CST
β-actin-HRP	12262	CST
α-tubulin	T9026	Sigma-Aldrich
CD45 (D9M8I)	13917	CST
CD45 (HI30)	304002	Biolegend
Swine anti-rabbit Ig HRP	P0217	Dako (Victoria, Australia)
Rabbit anti-mosue Ig HRP	P0260	Dako

2.8 Microscopy

2.8.1 Immunofluorescent microscopy

Harvested cells were washed in PBS and fixed in ice-cold 2% PFA in PBS for 20min at 4°C. PFA was then washed off with PBS and the cells were resuspended in permeablisation buffer (0.1% saponin, 1% FCS in PBS)

incubated for 30min at RT. After washing with PBS, cells were resuspended in permeablisation buffer with primary antibody for 1hr at RT. Cells were then washed again with PBS and resuspended in permeablisation buffer with secondary antibody for 1hr at RT in the dark. To visualise the nuclei, cells were washed with PBS and resuspended in permablisation buffer with 4',6-diamidino-2-phenylindole (DAPI) for 20min at RT in the dark. After washing with PBS twice, cells were ready for imaging.

All immunofluorescent images were acquired on a confocal microscope Nikon A1r Plus si (Tokyo, Japan) and analysed on ImageJ (FIJI image analysis software, USA).

Table 2-4: Antibodies used for immunofluorescence.

Antibody	Catalogue number	Supplier
CD45 (D9M8I)	13917	CST
CD45 (HI30)	304002	Biolegend
Goat anti-Mouse IgG Alexa Fluor 488	A11029	Invitrogen
Goat anti-Rabbit IgG Alexa Fluor 546	A11010	Invitrogen
DAPI	D1306	Invitrogen

2.9 In vivo experiments

OCI-MY1 $CD45^{WT}$ (vector) and $CD45^{KO}$ (C9) cells were transduced with the plasmid FUL2tG-GFP-Luc to express GFP and luciferase as per 2.2.4. GFP-expressing cells were sorted by flow cytometry. NOD.scid $IL2Rg^{-/-}$ (NSG) mice were purchased from Monash Animal Research Platform (Victoria, Australia). GFP^{+} Luc^{+} cells were injected into the tail vein (intravenous injection, $2x10^5$ cells/100µL) or the right tibia (intratibial injection, $1x10^5$ cells/10µL, under anaesthesia) of 4-6-week-old mice. Tumour growth was monitored weekly by bioluminescence. In brief, mice were given 125mg/kg of luciferin via intraperitoneal injection and anaesthetised with inhalational isoflurane. Imaging

was performed using the IVIS Spectrum In Vivo Imaging System (Perkin Elmer, Glen Waverley, Victoria, Australia). Animal studies were approved by Alfred Research Alliance Animal Ethics Committee, Alfred Hospital, Melbourne, Australia).

Mouse tissues were collected immediately after CO_2 euthanasia. For flow cytometry analysis, the tissues were mashed and passed through a 35µm cell strainer to remove large debris. The cells were then incubated in red blood cell lysis buffer (155mM NH_4Cl, 12mM $NaHCO_3$, 0.1mM EDTA) for 5 minutes followed by 3 washes of FACS buffer. The cells were analysed on a FACSCalibur (BD) as per 2.5.5.

2.10 Statistical analysis

All statistical analyses were performed on GraphPad Prism 7 software (California, USA). Statistical significance was determined with Student t-test, one-way ANOVA or two-way ANOVA as described in the individual experiment.

CHAPTER 3:

ESTABLISHING CRISPR/CAS9-MEDIATED CD45 KNOCKOUT MODELS IN HMCLS

3.1 Introduction

For the past two decades, many laboratories had investigated the role of CD45 in MM following the prognostic significance finding that plasma cells lacking surface CD45 is often associated with poor overall survival and inferior disease[297,298]. There is no general consensus that CD45 is a major player in patient survival or treatment-related outcomes; however, it could potentially be a surrogate for a more aggressive phenotype. This is because of insufficient mechanistic approaches available to confirm this hypothesis. Studies involving CD45 primarily rely on variable expressions among MM cell lines; characterised as $CD45^{-}$, $CD45^{intermediate}$ and/or $CD45^{+}$. The advantage of this method is cell line availability; however, MM is a heterogeneous disease with complex cytogenetics further obscuring the experimental outcome. For example, in the Hsp90 inhibitor study[285], the authors suggested the $CD45^{+}$ cell lines (AMO-1 and INA-1) were more sensitive than the $CD45^{-}$ cell lines (LP-1 and OPM-2) but AMO-1 and INA-1 harbour t(12;14) and t(11;14) respectively whilst LP-1 and OPM-2 harbour t(4;14) (cytogenetics obtained from keatslab.org). The difference in sensitivity could be due to their diverse cytogenetic background, not to mention other molecular heterogeneities. Our laboratory and other groups tried to overcome the heterogeneity issue by flow sorting U266 which expresses both CD45 phenotypes[281] but the sorted cells either regained or lost CD45 with time resulting in a cell line emerging with both populations of CD45 (Cindy Lin thesis 2013). G. Descamps et al. and H. Lin et al. demonstrated CD45 expression can also be induced in an HMCL (LP-1) with IL-6[278,285], a cytokine vital in MM, but IL-6 is well-known and has been proven to involve in different signalling pathways (1.2.4.3); thus it is not applicable in all experimental procedures, especially *in vivo* studies.

In order to avoid the inter-cell line heterogeneity, manipulating CD45 expression in one cell line would be the best option. Overexpression of CD45 has been proven to be highly challenging due to its large molecular mass (180-240kDa), multiple alternative splice isoforms, numerous post-translational modifications and location in the cell. An ectopic expression of CD45 had been achieved in T cells by fusing the intracellular domain of CD45 to the extracellular and

transmembrane domains of EGFR[211]. Although this chimeric model showed CD45 phosphatase activity, it did not fully represent a functional CD45. Other techniques, such as short-hairpin RNA (shRNA)[308] which manipulates post-translational genes by silencing target gene expression, and short-interfering RNA (siRNA) (Figure 3-1) which specifically target particular mRNA for degradation can be applied; however, by using these methods some functional mRNA or proteins can remain expressed, further complicating the interpretation of results. A complete abrogation of CD45 expression is therefore required for this study.

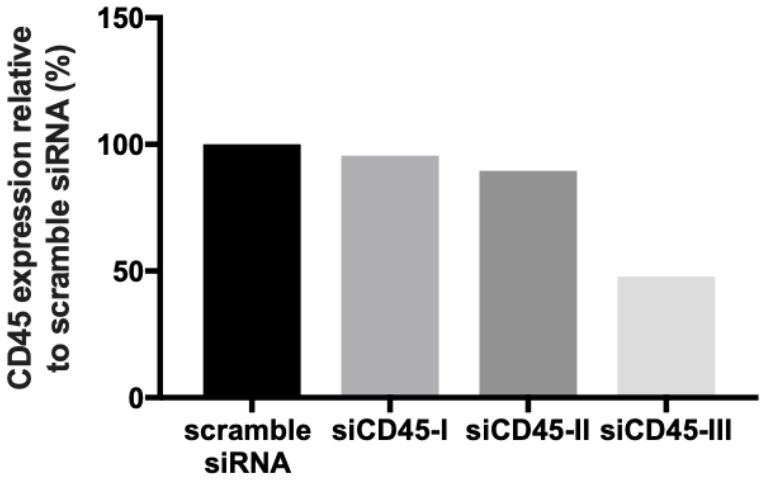

Figure 3-1: Silencing CD45 by siRNA transfection.

CD45 expression of OCI-MY1 cells transfected with 3 different siRNAs (10nM) for 72hr was analysed by flow cytometry and normalised to scramble siRNA control (n=1).

Since the introduction of CRISPR/Cas9 technology in 2012, genome editing in eukaryotic cells has been revolutionised, providing a precise, efficient and simple method alternative to the traditional techniques. The CRISPR (clustered regularly interspaced short palindromic repeats) system is an adaptive immune system of microbes that eliminates invading viruses by recording and targeting their DNA sequences[309,310]. Distinct CRISPR loci have been sequenced from different organisms and divided into 2 classes, 5 types and 16 subtypes[311,312]. Of which, only Class 2 has been adapted for genome editing. Unlike other genetic editing methods, such as zinc finger nucleases (ZFNs) and transcription activator-like effector nucleases (TALENs)[313,314], CRISPR does not require a unique nuclease-pair for every genomic target. Instead, it utilises a short customised guide RNA (gRNA) and a CRISPR-associated endonuclease (Cas9) to create a double-stranded break (DSB) in DNA which then activates DNA repair pathways and thereby introduces various mutations into the genome[315]. Due to its simplicity and high adaptability, CRISPR/Cas9 has become a popular technology for genome editing and potential gene therapy for human diseases.

The two components of the Class 2 system, Cas9 and the gRNA specific to the targeted sequence, can be introduced into (as a small particle[316]) or expressed in (lentiviral transduction[317], plasmid DNA transfection[318]) cells or organisms for genome editing. The gRNA consists of a CRISPR RNA (crRNA) and a fixed trans-activating crRNA (tracrRNA). The 20 nucleotides of the 5' end of the gRNA are specific and immediately adjacent to the 5' end of a protospacer-adjacent motif (PAM) of the target sequence. The gRNA directs Cas9 to the target site and if the gRNA shares sufficient homology with the target sequence[319], Cas9 cleaves both strands of DNA at 3-4 base pairs (bp) upstream of the PAM sequence.

The resulting DSB can be repaired by either DNA repair pathways: the nonhomologous end-joining (NHEJ) and the homology-directed repair (HDR) pathway. The predominant NHEJ pathway repairs the DSB by joining the broken ends and it operates throughout all phases of cell cycle[320]. Although it is efficient, it is prone to errors. The resulting insertion/deletion mutations (indels)

lead to in-frame amino acid mutations or disruption of the reading frame, resulting in a non-functional target gene. On the other hand, the HDR pathway uses the undamaged sister chromatid as a template to repair the DSB in an error-free manner[321]. It can be used to introduce specific mutations when a donor sequence is incorporated with the Cas9/gRNA complex, however, it occurs at a much lower rate than NHEJ (Figure 3-2).

In order to study the functions of CD45 in MM, we first established $CD45^{KO}$ cells using CRISPR/Cas9 genome editing, thereby avoiding the inter-cell line heterogeneity. The $CD45^{KO}$ and the respective $CD45^{WT}$ cells would be the basis for the subsequent biological studies.

The work described in this chapter aimed to:

1. Identify suitable HMCLs for CRISPR/Cas9 editing;
2. Generate $CD45^{KO}$ cells;
3. Evaluate CD45 expression and gene sequence in the $CD45^{KO}$ cells.

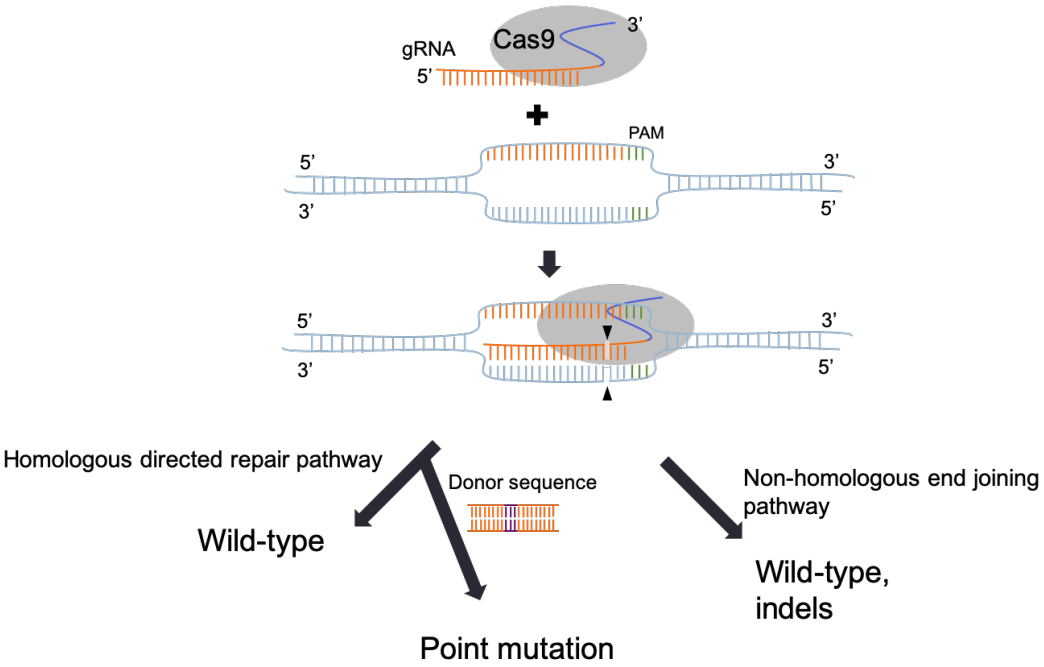

Figure 3-2: CRISPR/Cas9 working principle.

The Cas9/gRNA complex is introduced or expressed in the cells of interest. The gRNA directs Cas9 to the target site where they share high homology. Cas9 cleaves both strands of DNA at 3-4bp upstream of the PAM sequence. DSB triggers DNA repair pathways: NHEJ results in loss-of-function mutations, while HDR results in point mutations when a donor sequence is supplied.

3.2 Results

3.2.1 Evaluation of CD45 expression in HMCLs

In order to select suitable HMCLs for CRISPR/Cas9 genome editing, CD45 expression of 34 HMCLs was first evaluated by flow cytometry. Of these HMCLs, 10 were propagated from primary tumours in our lab, namely TK1 to TK10. The percentage of CD45 positive cells in each HMCLs was first assessed. Twenty HMCLs had below 34.7% (mean value; standard deviation, SD=39.2%) of $CD45^+$ cells; five HMCLs had between 34.7% to 73.9% (between mean and mean + 1SD) of $CD45^+$ cells and nine HMCLs had above 73.9% of $CD45^+$ cells. The mean fluorescence intensity (MFI) of $CD45^+$ cells in HMCLs with above 34.7% of $CD45^+$ cells were further analysed. These cells showed different levels of MFI as shown in Figure 3-3. Representative plots were shown in Appendix 1. MM cells in patients often display two distinctive CD45 populations (bimodal expression)[274,297–299]; however, such phenomenon was not observed in HMCLs, except in U266 (Appendix 1).

Based on this analysis, five HMCLs with a high percentage of CD45 expressing cells (above 73.9%): OCI-MY1, XG1, TK1 and TK2, were selected for CRISPR/Cas9 genome editing and further studies.

3.2.2 LentiCRISPRv2 system

A lentiviral vector, pLentiCRISPRv2, containing both the Cas9 and gRNA scafflold[302] was used to generate $CD45^{KO}$ cells. It simultaneously delivers these two elements into any cell types, without the need to generate cell lines that express Cas9 first. This plasmid also contains puromycin for cell selection. Figure 3-4A shows the simplified map of pLentiCRISPRv2.

The gRNA sequence against CD45 gene *PTPRC* (5'-TTAATATTAGATGTGCCACC-3') was selected from Genome-scale CRISPR Knock-Out (GeCKO) pooled library version 2[302], which targets the end of exon 9 encoding the first fibronectin(III)-like domain common to all isoforms (Figure

3-4B). The gRNA was subjected to Cas-OFFinder, a publicly available online algorithm to identify potential off-target sites[322]. All the potential off-target sites require at a minimum of 3bp mismatches, one RNA bulge and 1bp mismatch, or one DNA bulges and 1bp mismatch. These sites are located either in the non-coding regions of the genome or *PTPRC* itself as listed in Table 3-1. This analysis suggests this gRNA is highly specific to *PTPRC*.

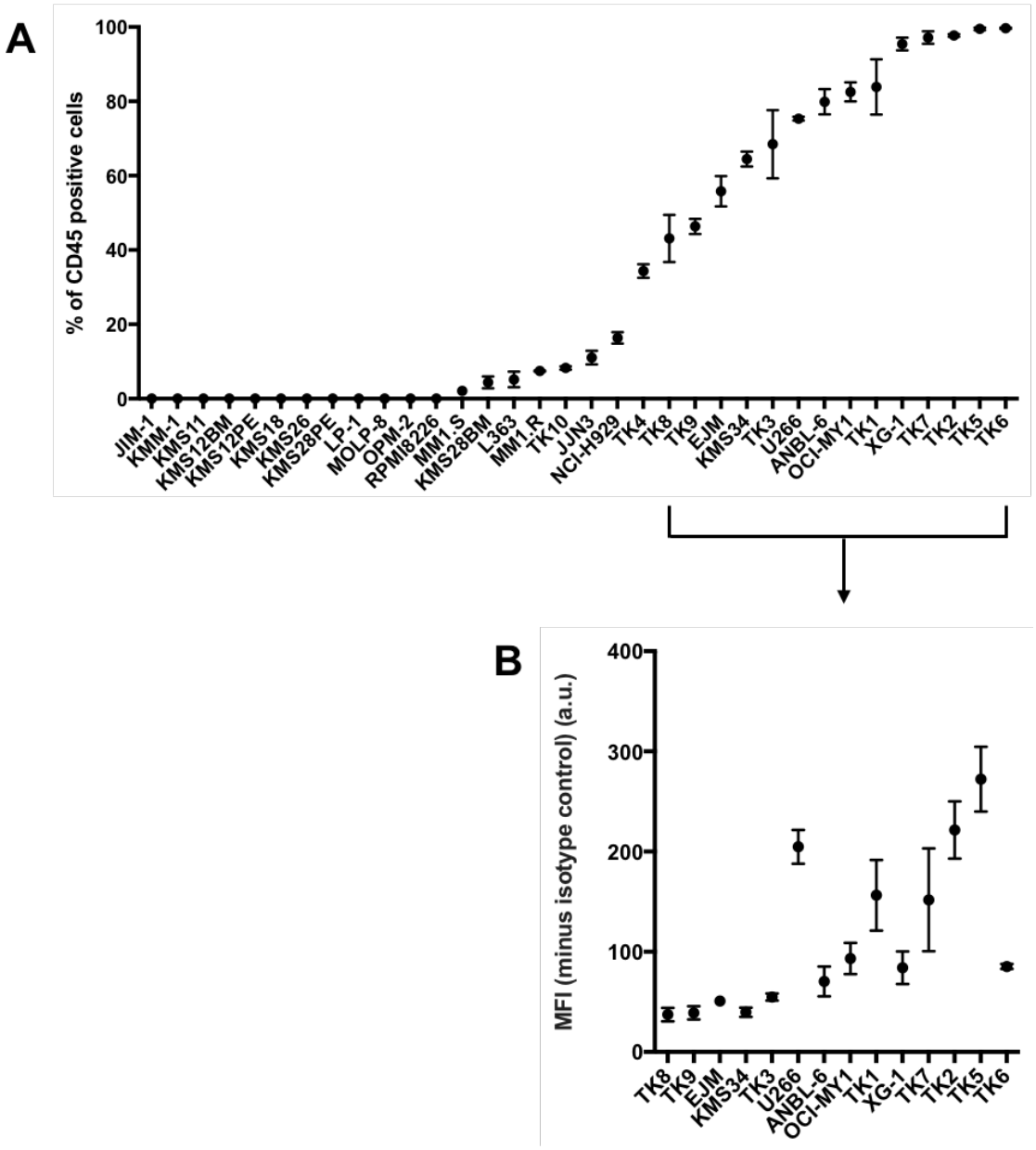

Figure 3-3: CD45 expression in HMCLs.

CD45 expression was analysed in 34 HMCLs by flow cytometry. **(A)** The percentage of $CD45^+$ cells in each cell lines. **(B)** MFI of $CD45^+$ cells in HMCLs with >34.7% $CD45^+$ cells. Mean values ±SEM are plot (n=3).

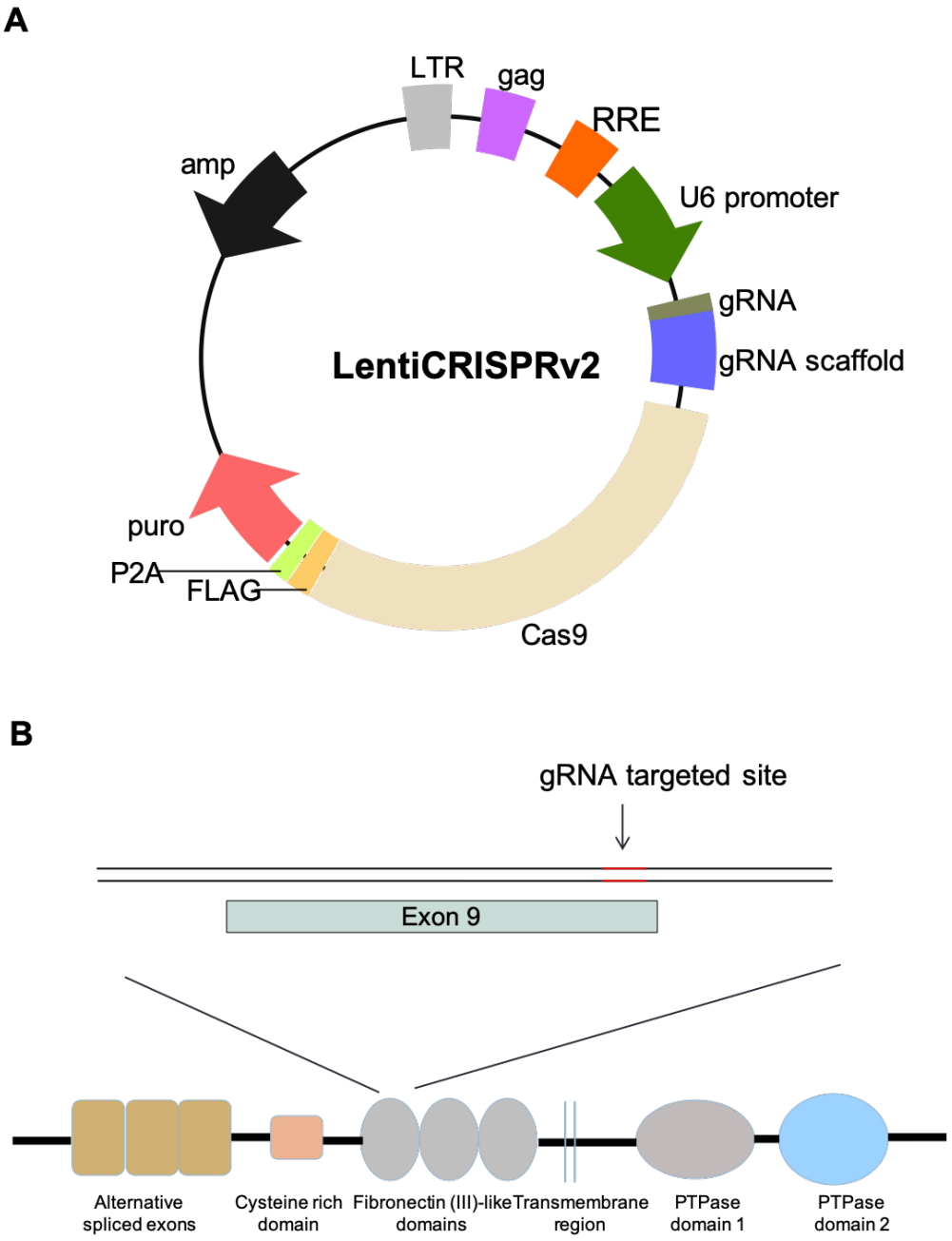

Figure 3-4: LentiCRISPRv2 system for generating CD45^{KO} cells.

(A) Simplified map of pLentiCRISPRv2: LentiCRISPRv2 is a single vector contains Cas9, a gRNA and a puromycin selection marker. FLAG: FLAG tag; P2A: 2A self-cleaving peptide; puro: puromycin selection marker; amp: ampicillin selection marker; LTR: long terminal repeat; gag: group-specific antigen; RRE: rev response element. **(B)** Schematic diagram illustrating gRNA targeted region of PTPRC: The gRNA targets exon 9 which encodes the first fibronectin (III)-like domain in the extracellular region of CD45.

Table 3-1: Potential off-target sites.

(small letter: mismatched nucleotide; 'N': any nucleotides, '-': bulge site)

Chromosome position	gRNA sequence	DNA sequence	Number of mismatches	Bulge type	Bulge size	Encoding gene
chr1: 186792803	TTAATATTAGATGTGCCACCNGG	TTAATATTAGATaTtCtACCAGG	3	/	0	/
chr13: 53271277	TTAATATTAGATGTGCCACCNGG	TTAATATTAcATGTGCCAtgTGG	3	/	0	/
chr2: 7310014	TTAATATTAGATGTGCCACCNGG	TTAtTgTaAGATGTGCCACCAGG	3	/	0	/
chr2: 41737093	TTAATATTAGATGTGCCACCNGG	TTAAaATcAGATGTGtCACCAGG	3	/	0	/
chr15: 69325433	TTAATATTAGATGTGCCACCNGG	TTAcTATTAGATGTGCCgCgTGG	3	/	0	/
chr6: 159855052	TTAATATTAGATGTGCCACCNGG	TTAATcTTAGATGaGCtACCAGG	3	/	0	/
chr20: 45240467	TTAATATTAGATGTGCCACCNGG	TTAATATTAtATGTGCtACaTGG	3	/	0	/
chr1: 198706931	TTAATATTAGATGTGCCACCNGG	T-AATATTAGATGTGCCACCAGG	0	RNA	1	PTPRC
chr7: 121485013	TTAATATTAGATGTGCCACCNGG	TTAA-ATTAGATGTGCCACtTGG	1	RNA	1	/

chr5: 135956342	TTAATATTAGATGTGCCACCNGG	TTAATATTAGATGaG-CACCTGG	1	RNA	1	/
chr5: 135956342	TTAATATTAGATGTGCCACCNGG	TTAATATTAGATGaGC-ACCTGG	1	RNA	1	/
chr1: 198706931	TTAATATTAGATGTGCCACCNGG	Ta-ATATTAGATGTGCCACCAGG	1	RNA	1	PTPRC
chr1: 198706931	TTAATATTAGATGTGCCACCNGG	TaA-TATTAGATGTGCCACCAGG	1	RNA	1	PTPRC
chr10: 57482749	TTAATATTAGATGTGCCACCNGG	TTAcT-TTAGATGTGCCACCTGG	1	RNA	1	/
chr1: 198706929	TT-AATATTAGATGTGCCACCNGG	aTTAATATTAGATGTGCCACCAGG	1	DNA	1	PTPRC
chr: 198706929	T-TAATATTAGATGTGCCACCNGG	aTTAATATTAGATGTGCCACCAGG	1	DNA	1	PTPRC

3.2.3 Generation of CD45 knockout cells

The selected HMCLs were transduced with lentiviral particles containing pLentiCRISPRv2 as described in 2.2, and puromycin was added to enrich transduced cells. $CD45^{KO}$ polyclonal populations from each HMCL were then sorted by flow cytometry. The resulting $CD45^{KO}$ polyclonal populations lost CD45 surface expression stably (Figure 3-5A).

CD45 is a transmembrane protein with the phosphatase domains located in the cytoplasm. Expression analysis and cell sorting by far were done by staining the cells with an anti-CD45 antibody (clone: HI30) recognising the extracellular region proximal to the cell membrane. Thus, only cells without extracellular CD45 had been isolated from flow cytometry sorting. It is crucial to evaluate the cytoplasmic CD45 expression in these sorted cells to ensure complete abrogation.

Another anti-CD45 antibody (clone: C9M8I) recognizing the PTP D2 portion of CD45 was employed to evaluate the cytoplasmic CD45 expression. The $CD45^{KO}$ polyclonal populations from the five HMCLs showed moderate cytoplasmic CD45 expression although at a lower level than the vector control cells (Figure 3-5B). As expected, the truncated form of CD45 had lower molecular weight than the full-length CD45, ranging from 100-150kDa as shown in the immunoblotting analysis (Figure 3-6). The presence of multiple bands suggests there were multiple forms of truncated cytoplasmic CD45. Interestingly, the localisation of the residual cytoplasmic CD45 was different from the full-length CD45: a small portion of was dispersed in the cytoplasm instead of concentrated on the cell membrane (Figure 3-7).

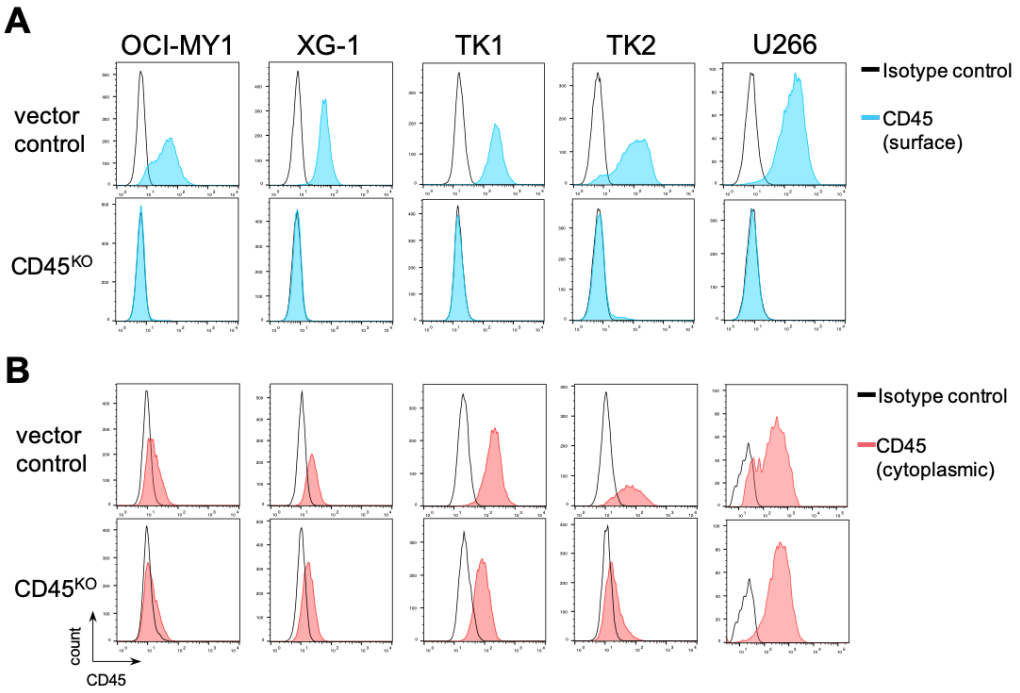

Figure 3-5: CD45 expression of sorted polyclonal CD45^{KO} cells.

Flow cytometry analysis of **(A)** CD45 surface expression (blue histogram) and **(B)** cytoplasmic expression (red histogram) of vector control cells and the corresponding sorted transduced cells of OCI-MY1, XG-1, TK1, TK2 and U266. Isotype control is indicated by the open black histogram.

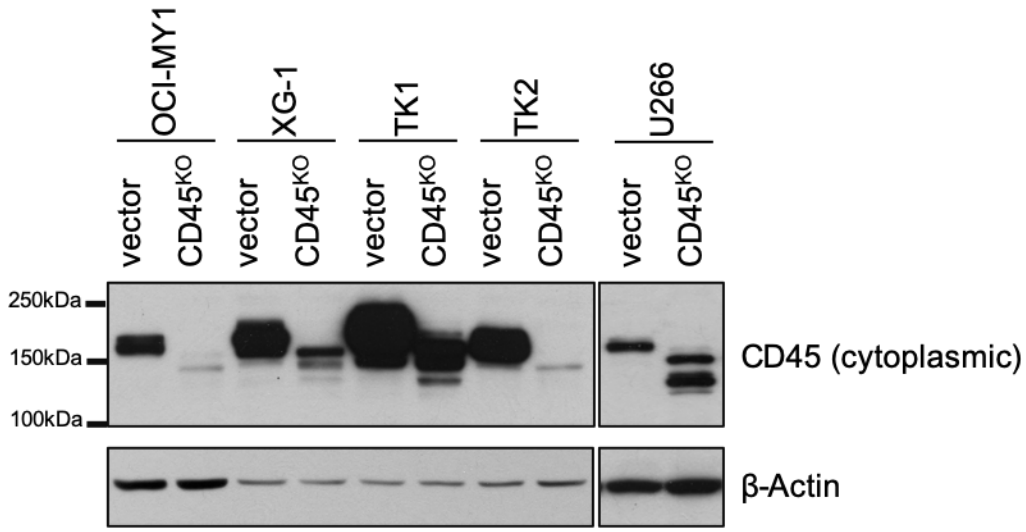

Figure 3-6: Expression of cytoplasmic CD45 in the sorted polyclonal CD45^{KO} cells.

Immunoblotting analysis showed the truncated cytoplasmic CD45 in the sorted polyclonal CD45^{KO} cells.

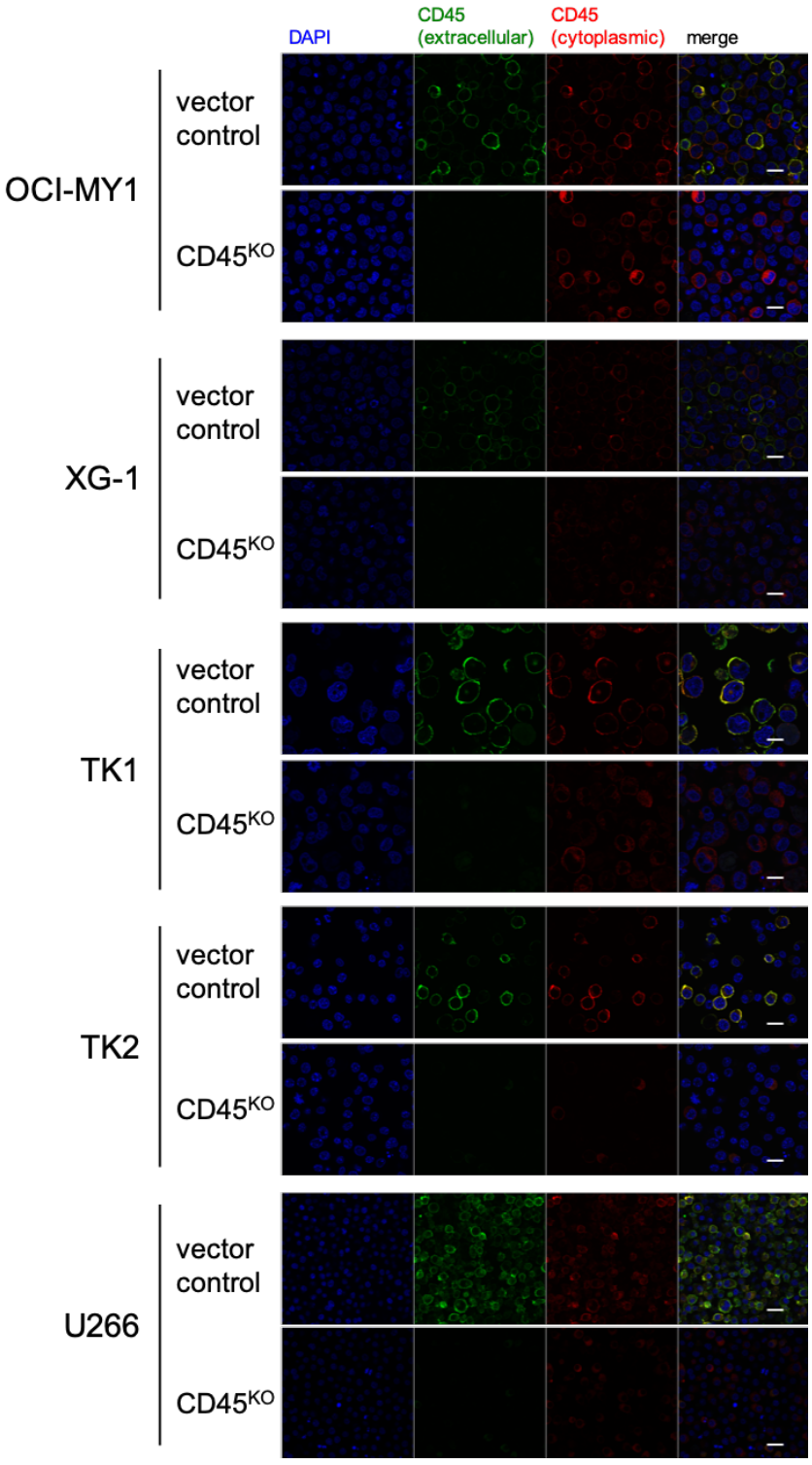

Figure 3-7: Expression and localisation of extracellular and cytoplasmic CD45 in vector control and CD45^{KO} cells.

Vector control and corresponding CD45^{KO} cells were stained with antibodies recognising extracellular or cytoplasmic CD45 and imaged by confocal microscopy. Scale bar represents 20μm.

3.2.4 Isolation of monoclonal populations of CD45^{KO} cells

Although the sorted polyclonal CD45^{KO} cells did not express extracellular CD45, there was a considerable amount of cytoplasmic CD45 detectable in these cells. It has been shown that in CD45-deficient T cells the expression of cytoplasmic portion alone was able to restore TCR signalling[211] (detailed description in 1.3.1), suggesting that the phosphatase activity was retained without the presence of extracellular CD45. To avoid any residual phosphatase activity in the CD45^{KO} models, further isolation was performed by sorting single cells into each well of 96-well plates. Expression of CD45 in each monoclonal population was re-evaluated by flow cytometry and immunofluorescence. About 100-300 clones of each cell lines were screened. Monoclonal cell populations that do not express any part of CD45 were identified and expanded for further studies.

CD45 void cells from OCI-MY1 (clone A11, C9, 3C9, D8 and E8), XG-1 (clone D5 and F5), TK2 (clones G2 and G3) and U266 (clone B4 and F9) were isolated and the complete loss of CD45 (both extracellular and cytoplasmic) expression was confirmed by confocal microscopy (Figure 3-8) and immunoblotting (Figure 3-9). TK1 was unable to expand from a single cell, thereby excluded from further studies.

3.2.5 Sanger sequencing of CD45^{KO} cells

The loss of CD45 expression was due to the errors in the cell's endogenous DNA repair process induced by Cas9 cleaving, creating indels and mismatches within the gene. In order to identify the genomic sequence of the resulting alleles in the selected CD45^{KO} clones, the targeted exon 9 region was amplified by PCR and sequenced directly by Sanger sequencing. The resulting sequence was then analysed by CRISP-ID to de-convolute the overlapping spectra from the different alleles[323].

The CD45^{KO} cells showed different degrees of editing: only OCI-MY1 C9, TK2 C2 and TK2 G3 were homozygous with 1bp deleted or inserted; while the others were heterozygous with multiple indels and mismatches. Interestingly,

three alleles were resolved from OCI-MY1 A11, OCI-MY1 3C9, OCI-MY1 6E8, XG-1 D5, XG-1 F5 and U266 B4 (Figure 3-10). This could be possibly due to the continuous cleaving by the stable expression of Cas9 in these cells, giving rise to additional alleles even after single cell isolation. Additionally, these cells may have chromosomal abnormalities involving the amplification of 1q31, in which *PTPRC* gene is located, resulting in additional copies of *PTPRC*. The resolved sequences are listed in Appendix 2.

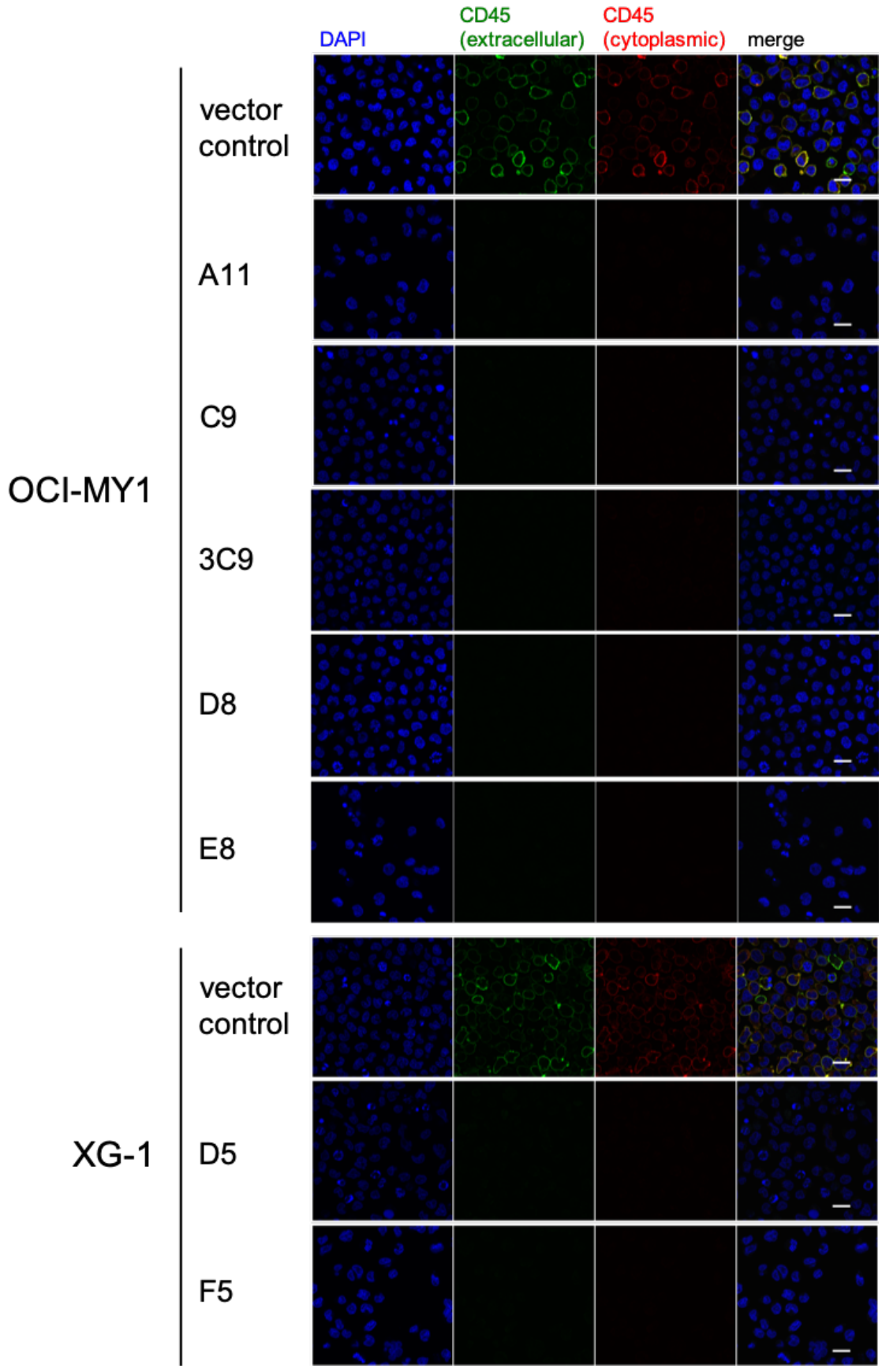
DAPI
CD45 (extracellular)
CD45 (cytoplasmic)
merge
OCI-MY1
vector control
A11
C9
3C9
D8
E8
XG-1
vector control
D5
F5

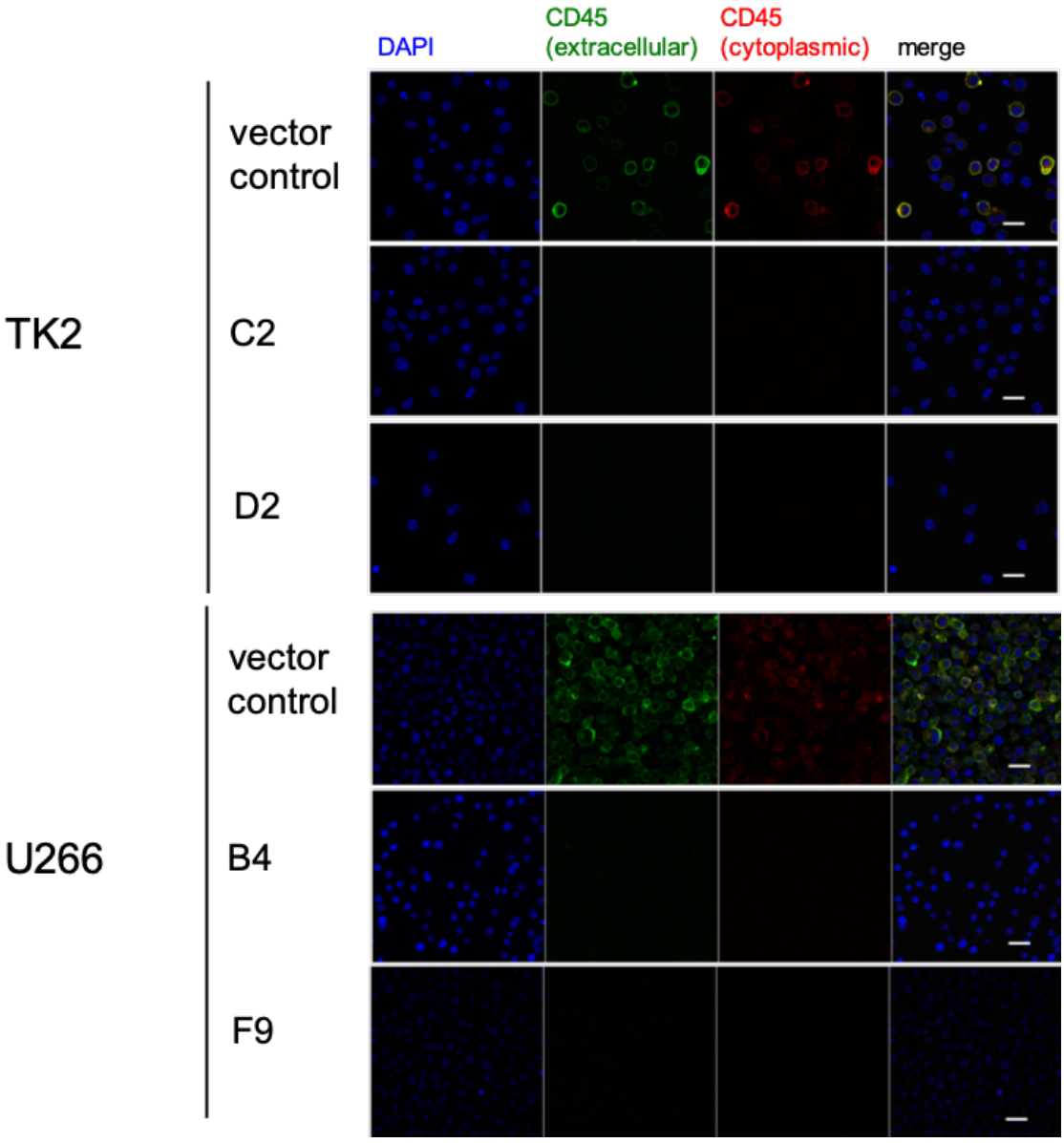

Figure 3-8: Expression of extracellular and cytoplasmic CD45 in vector control and monoclonal CD45^{KO} cells.

Vector control and corresponding monoclonal CD45^{KO} cells from OCI-MY1, XG-1, TK2 and U266 were stained with antibodies recognising extracellular or cytoplasmic CD45 and imaged by confocal microscopy. Scale bar represents 20μm.

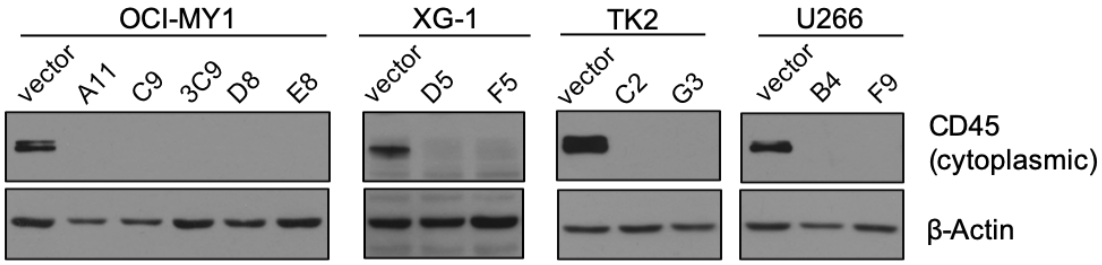

Figure 3-9: Immunoblotting of cytoplasmic CD45 expression in vector control and monoclonal CD45^{KO} cells.

Cytoplasmic CD45 expression was assessed using an anti-CD45 antibody (clone: C9M8I) specific to PTP D2.

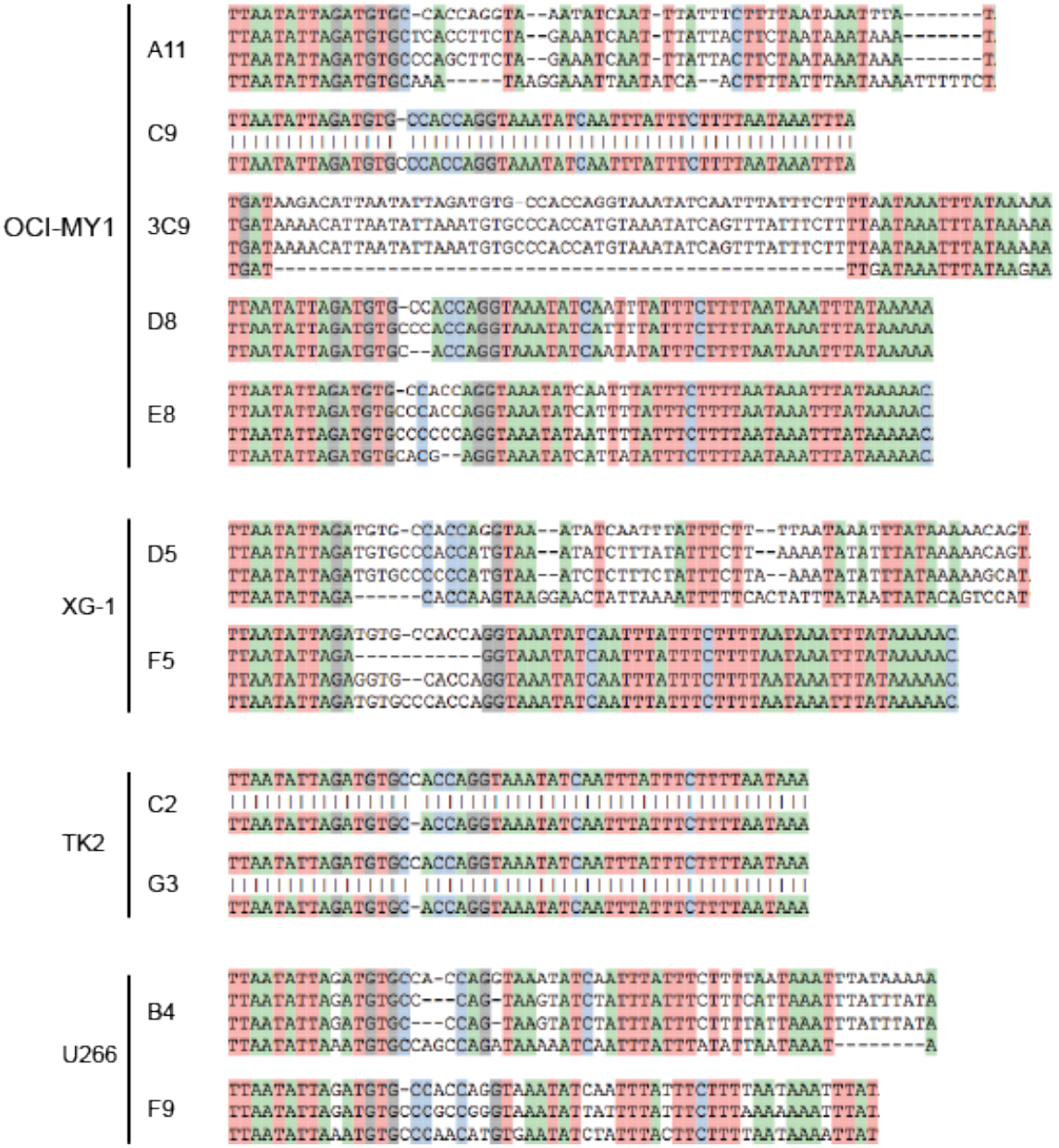

Figure 3-10: Snapshots of genomic sequence around the gRNA-targeted site of CD45^{KO} cells.

The targeted genomic region was amplified by PCR and sequenced directly by Sanger sequencing. The resulting sequence was then analysed by CRISP-ID. The top row of each clone represents the reference sequence and the remaining row(s) represent the resolved allele sequence(s).

3.3 Discussion

The work in this chapter described the establishment of $CD45^{KO}$ models using CRISPR/Cas9 genome editing. The differences in disease outcome, *in vivo* and *in vitro* homing, and drug sensitivities between $CD45^{+}$ and $CD45^{-}$ phenotypes warrant further investigation in the biological roles of CD45 in MM. Previous studies relied on the heterogeneous CD45 expression between cell lines, in which the underlying cytogenetics complicated the analysis and interpretation of results. CRISPR/Cas9 genome editing introduces permanent changes into the genome, providing a stable model for biological studies.

CD45 is commonly expressed on the surface of haemopoietic cells. Depending on the cell type, activation and differentiation stages, CD45 is expressed as different isoforms at different levels[208,216,217]. Normal plasma cells isolated from tonsil and peripheral blood express high level of CD45 whereas those from BM are heterogeneous for CD45[274]. CD45 expression is frequently lost in MM: about 20% of MM cells are $CD45^{bright}$ and 80% are $CD45^{low/negative}$ [274]. In this chapter, CD45 expression was first analysed in a panel of 34 HMCLs. Consistent with previous reports, the majority of HMCLs showed low to moderate levels of CD45 expression; only 9/34 (26.5%) HMCLs had more than 73.9% (mean value + 1SD) of $CD45^{+}$ cells. MM cells are known for their chromosomal abnormality and the amplification of 1q, in which CD45 gene is located, has been reported[324]. Future studies should perform karyotyping to identify any 1q gain in these HMCLs. Based on the result above, five HMCLs were selected for CRISPR/Cas9 genome editing for this project.

The lentiviral vector utilised possesses both Cas9 and gRNA capable of infecting both dividing and non-dividing cells[325], providing an efficient way to transduce cells, especially HMCLs which are grouped under the difficult-to-transduce cells. Cas9 and gRNA were integrated into the genome and stably expressed in the selected HMCLs. Although the puromycin selection and flow cytometry sorting successfully isolated '$CD45^{-}$ cells', it was out of our expectation that these cells retained cytoplasmic CD45 expression. The working mechanism of CRISPR/Cas9-mediated gene knockout relies on the indels and

frameshifts near the DSB, thereby generating a premature termination codon (PTC). The corresponding truncated mRNA with the PTC is then recognised and degraded by the nonsense-mediated mRNA decay (NMD) pathway in a translation-dependent manner[326]. However, the efficiency of NMD depends on the position of the PTC in the transcript and the sequence around the PTC. Some truncated transcripts are able to evade the NMD pathway and translated into truncated proteins, in this case, the truncated cytoplasmic CD45. From the immunoblotting analysis, the cytoplasmic CD45 appeared in multiple sizes, suggesting that there were multiple truncated transcripts present in the sorted cells. These truncated forms of CD45 were mislocalised in the cells: instead of localising on the plasma membrane, they were also found in the cytoplasm, as shown in the immunofluorescent images. We speculated that the loss of extracellular domain prevented the truncated protein from orientating and attaching to the plasma membrane.

The catalytic activity of CD45 has been shown to be independent of its extracellular domain; PTP D1 alone is sufficient for signal transduction[213,327]. In addition to isolating complete $CD45^{KO}$ cells, we had isolated cells with only cytoplasmic CD45 expression from OCI-MY1. Indeed, these cells (clone A8 and B5) preserved CD45 phosphatase activity of activating SFK as was seen in the vector control cells (Figure 3-11). This demonstrated the importance of examining both extracellular and cytoplasmic expression in CD45 studies. Further analysis of six other $CD45^{-}$ HMCLs showed no cytoplasmic CD45 expression in these cells, suggesting that the observed truncated forms of CD45 was the result of genome editing (Figure 3-12). Additional strategies should be employed to validate the efficiency of gene editing, especially those involving large genes, as residual protein expression could potentially be functional or act as dominant negative.

CRISP-ID, a web-based application, was used to characterise the sequences of $CD45^{KO}$ clones directly from Sanger sequencing of PCR products around the gRNA-targeted site. This method avoids the labourious conventional method which requires cloning the PCR products into a vector for bacterial single colony sequencing. Next generation sequencing can be applied for this purpose;

however, it is often limited by the short read-lengths and the generation of unique tags for multiplexing. CRISP-ID analysis revealed the heterogeneous genotypes of these cells. While three $CD45^{KO}$ clones were homozygous with 1bp deleted or inserted, other clones were heterozygous with multiple indels and mismatches. Some clones also showed three alleles in the analysis suggesting the possibility of 1q31 amplification in these cells and the stable expression of Cas9 creating additional cleavages even after the initial NHEJ and single cell isolation. The new generation of CRISPR/Cas9 plasmids is able to avoid the additional cleaving by incorporating an inducible expression system to control the expression of Cas9[328]. Alternatively, a ribonucleoprotein complex consists of the recombinant Cas9 protein and a targeting gRNA can be directly introduced into cells of interest by electroporation or cationic lipid-mediated method[316,329,330]. Nevertheless, the established $CD45^{KO}$ clones did not show any CD45 expression.

In summary, $CD45^{KO}$ cells have been successfully established from four HMCLs using the contemporary CRISPR/Cas9 genome editing. Both extracellular and cytoplasmic CD45 expression, and genomic sequences in these cells were evaluated. These $CD45^{KO}$ cells served as the basis of the subsequent investigations in this study.

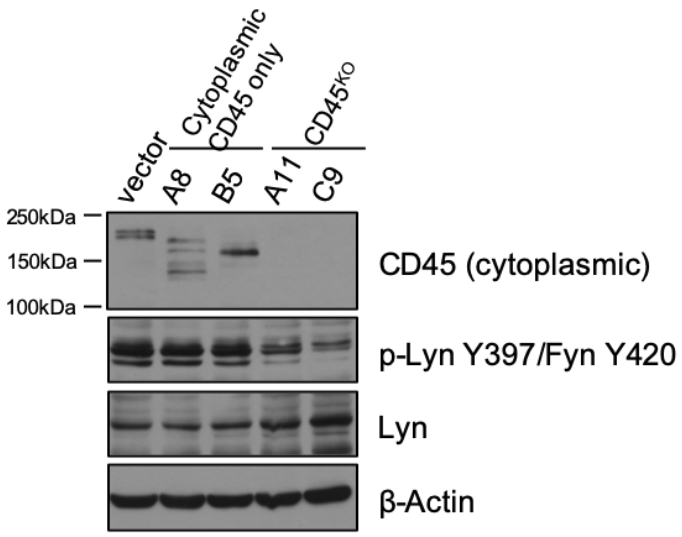

Figure 3-11: SFK activity in CD45^{cytoplasmic} and CD45^{KO} cells.

Lyn and Fyn retained similar phosphorylation levels at the respective activation sites, Y397 and Y420, in CD45^{cytoplasmic} OCI-MY1cells (A8 and B5).

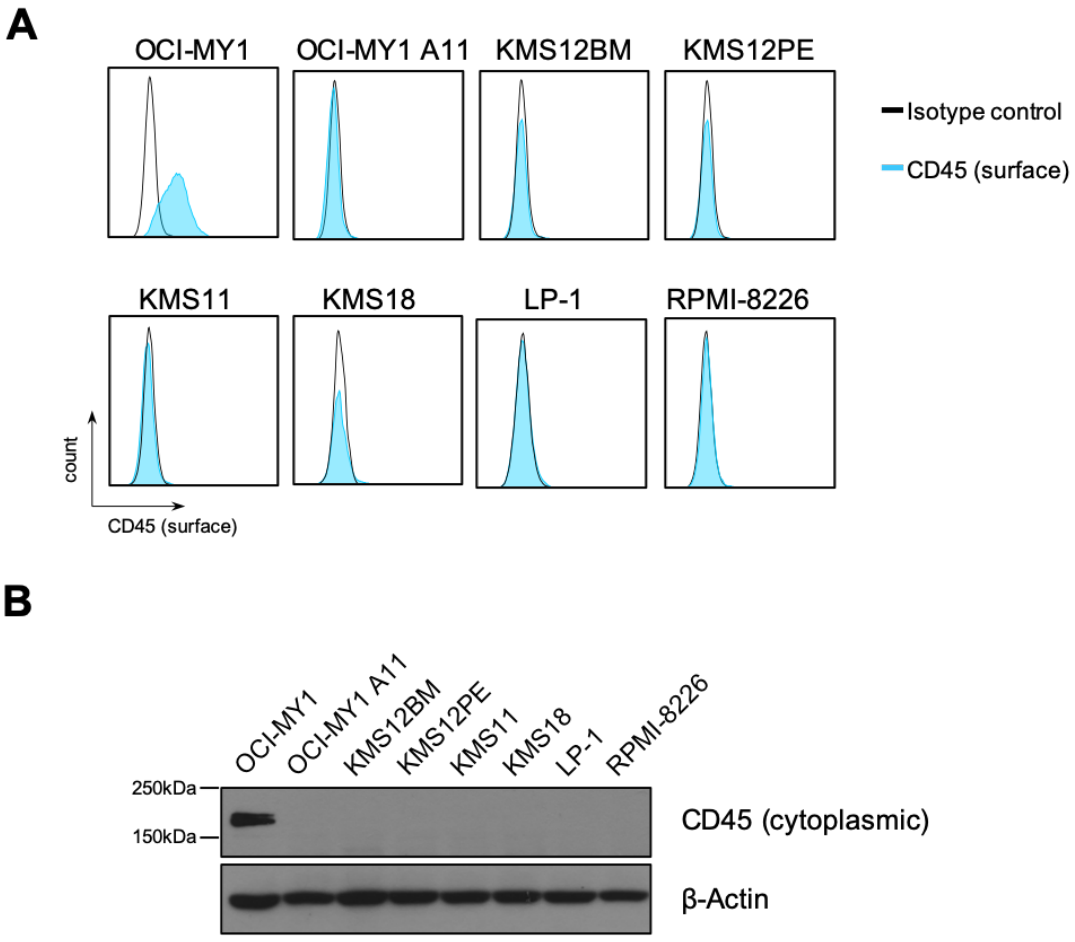

Figure 3-12: CD45 expression in CD45⁻ HMCLs.

(A) Extracellular and **(B)** cytoplasmic CD45 expression in CD45⁻ HMCLs. OCI-MY1 and OCI-MY1 A11 were positive and negative controls respectively.

CHAPTER 4:

CHARACTERISING THE BIOLOGICAL DIFFERENCES BETWEEN $CD45^{WT}$ AND $CD45^{KO}$ POPULATIONS

4.1 Introduction

As previously discussed in 1.4, studies have suggested that CD45 plays a role in MM pathogenesis. MM is traditionally regarded as $CD45^{-}$, and we have shown that the majority of HMCLs are $CD45^{-}$ or express low levels of CD45 in a panel of 34 HMCLs (see 3.2.1), yet a small portion of MM cells is $CD45^{+}$. The association of $CD45^{-}$ phenotype with poor overall survival and inferior disease had prompted the investigation on the role of CD45 in MM, particularly in cell proliferation, drug sensitivity and BM homing. However, as previously discussed, the genetic heterogeneity between HMCLs has obscured the interpretation of results. In this chapter, we aimed to use the CRISPR/Cas9-mediated $CD45^{KO}$ models generated in Chapter 3 to characterise the biological differences between the $CD45^{WT}$ and $CD45^{KO}$ cells.

Chapter 3 has demonstrated the loss of both extracellular and intracellular CD45 expression and identified the sequence of $CD45^{KO}$ cells. Here we assessed the phosphatase function of CD45, if any, in the $CD45^{KO}$ cells by evaluating SFK activity. SFKs are a group of highly conserved tyrosine kinases that share very similar but not identical functions. These kinases also have different tissue distributions. As mentioned in 1.3.5.1, CD45 regulates SFK activity by dephosphorylating the activating and inhibitory tyrosine residues, Y416 at the kinase domain and Y527 at the C-terminal respectively (referring to Src amino acid sequence). CD45 removes the inhibitory phosphorylation at Y527, disrupting the intra-molecular binding; the kinase then undergoes autophosphorylation at Y416 and becomes activated. We postulated that with the loss of CD45, SFKs remained phosphorylated at the inhibitory site and could not be activated in the $CD45^{KO}$ cells.

C. Pellat-Deceunynck et al. demonstrated that normal plasma cells from tonsil and peripheral blood displayed a homogeneous $CD45^{bright}$ phenotype and were highly proliferative; whereas BM plasma cells were heterogeneous for CD45 expression and the proliferation was restricted to the $CD45^{bright}$ compartment[274]. Similarly, MM is heterogeneous for CD45 expression as in normal BM plasma cells and only a small portion of MM cells are $CD45^{bright}$ and proliferating[274]. To

understand the role of CD45 on MM proliferation, the proliferation rates of $CD45^{WT}$ and $CD45^{KO}$ cells were investigated in different culture conditions including glutamine-free, serum-free, the addition of IL-6, IGF-1 and HS5 conditioned medium. These conditions were designed to mimic the BMME and nutrient-deprived situations. Based on our hypothesis that $CD45^{-}$ phenotype represents a more advanced or aggressive disease, $CD45^{KO}$ cells could potentially have survival advantages in nutrient-deprived situations over the $CD45^{WT}$ cells.

Using the models established in Chapter 3, the work described in this chapter aimed to:

1. Evaluate the role of CD45 in SFKs in MM cells;
2. Compare the proliferation rates between $CD45^{WT}$ and $CD45^{KO}$ cells under different conditions;
3. Evaluate the clonogenic potential of $CD45^{WT}$ and $CD45^{KO}$ cells;
4. Examine the cytokine-mediated signalling pathways in $CD45^{WT}$ and $CD45^{KO}$ cells;
5. Identify transcriptional changes induced by the loss of CD45.

4.2 Results

4.2.1 Inactivation of Src family kinases in $CD45^{KO}$ cells

CD45 regulates SFK activity through dephosphorylating the critical phosphorylation sites[234,240,241]. The SFK activity in the $CD45^{KO}$ cells was examined by immunoblotting with an antibody recognising the phosphorylation at the activating site Y416. Since SFKs share high homology, this antibody also cross-reacts with Lyn, Fyn, Yes, Lck and Hck (manufacturer data sheet), of which Lyn and Fyn were predominately expressed in OCI-MY1, XG-1, TK2 and U266 (unpublished RNA sequencing data). Another antibody that recognises phosphorylated Lyn at Y507 (analogous to Src Y527) was used to represent the inhibitory phosphorylation of SFKs.

Higher level of phosphorylation at the inhibitory site (represented by Lyn Y507) was detected in the $CD45^{KO}$ clones from OCI-MY1 and TK2, although not all reached statistical significance. More importantly, all clones had significantly lower level of phosphorylation (>50% less than vector) at the activating sites, represented by Lyn Y397/Fyn Y420, indicating that Lyn and Fyn were inactivated in the $CD45^{KO}$ cells (Figure 4-1). This result confirms the loss of CD45 phosphatase activity in the $CD45^{KO}$ cells.

4.2.2 Cell proliferation in liquid culture

Given that CD45 expression is correlated with MM cell proliferation, the proliferation rate of $CD45^{WT}$ and $CD45^{KO}$ OCI-MY1, XG-1, TK2 and U266 cells was compared. Under normal culture condition (complete medium, as described in 2.1.2.1) both $CD45^{WT}$ and $CD45^{KO}$ cells proliferated consistently over the period of 48hr, except for TK2, in which a slower proliferation rate was observed at 48hr for the $CD45^{KO}$ clones D3 (p-value=0.0102) and G3 (p-value=0.0154) (Figure 4-2 solid lines).

The proliferation rate was also assessed in the glutamine-free medium. Glutamine is a nonessential amino acid and is the second most abundant

nutrient after glucose in blood circulation. Tumour cells, but not their healthy counterparts, often display cellular metabolic reprogramming in order to utilise glutamine as an alternative energy source to sustain tumour growth when glucose is insufficient. MM patients display a specific metabolomic profile in which serum glutamine level is significantly lower than the healthy controls, suggesting that glutamine is highly metabolised in MM cells. Here we explored the role of CD45 in the glutamine-deprived situation.

As expected, glutamine-free medium reduced cell proliferation compared with complete medium. Although OCI-MY1 cells showed a slower proliferation in the first 24hr, the number of cells at 48hr dropped below that at 24hr, suggesting that OCI-MY1 not only failed to proliferate, but some cells also committed cell death (Figure 4-2A dotted lines). In the glutamine-free medium, only U266 $CD45^{KO}$ clone F9 showed a higher proliferation rate (p-value=0.0358) at 48hr than U266 $CD45^{WT}$ vector cells, however, there was no significant difference in the proliferation between $CD45^{WT}$ and $CD45^{KO}$ cells in other cell lines (Figure 4-2 dotted lines).

The proliferation rate was further investigated in other culture conditions. OCI-MY1 cells were exposed to different conditions: complete medium; serum-free medium (no FCS); complete medium supplemented with 10ng/mL IL-6, 100ng/mL IGF-1 or 20% HS5 conditioned medium, for an extended period of time. Both $CD45^{WT}$ and $CD45^{KO}$ cells grew steadily in the normal culture condition (Figure 4-3A). OCI-MY1 cells were able to proliferate at a slower rate in the serum-free condition but then committed cell death beyond 72hr. There was a slight difference in proliferation however overall it did not reach statistical significance (Figure 4-3B). Both $CD45^{WT}$ and $CD45^{KO}$ cells also grew steadily in the addition of HS5 conditioned medium, IL-6 or IGF-1 (Figure 4-3C-E). No significant difference in proliferation was observed between $CD45^{WT}$ and $CD45^{KO}$ cells under these conditions.

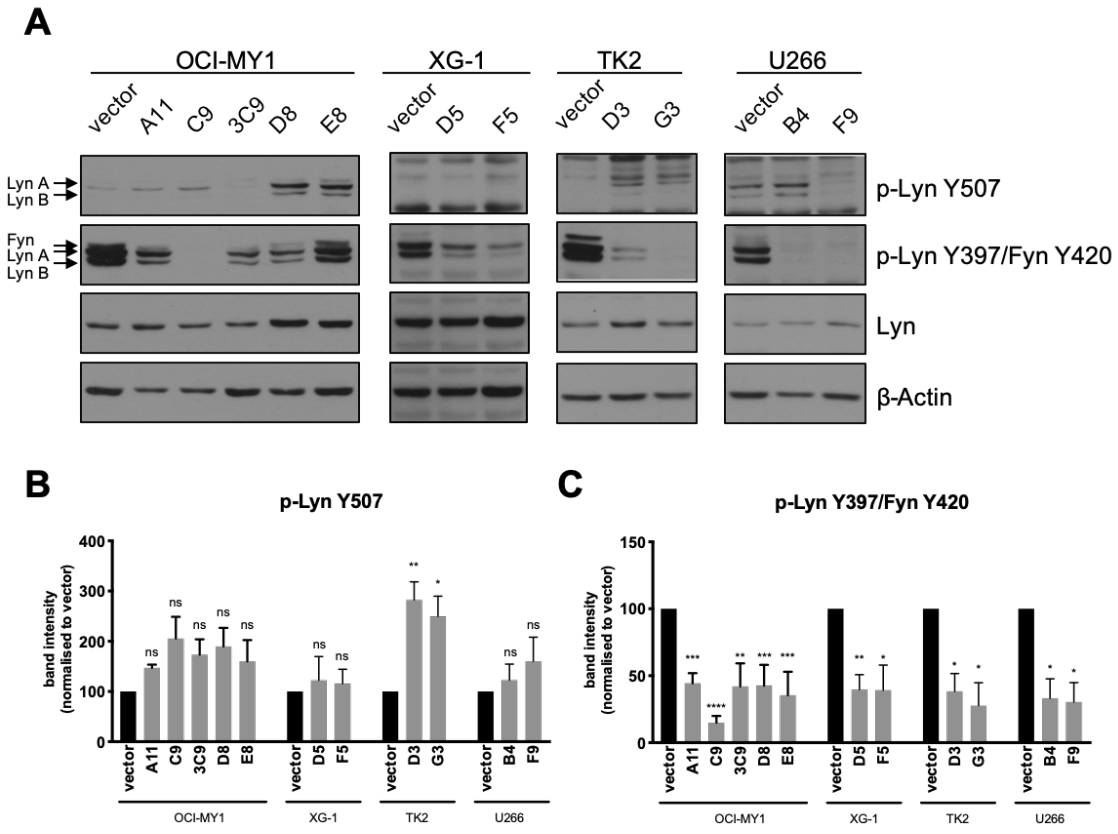

Figure 4-1: SFK activity in CD45^{WT} and CD45^{KO} cells.

SFK activity in CD45^{WT} (vector) and CD45^{KO} cells of OCI-MY1, XG-1, TK2 and U266 was assessed by immunoblotting. **(A)** The inhibitory phosphorylation (p-Lyn Y507, the arrows indicate the two isoforms of Lyn: Lyn A and Lyn B) in CD45^{KO} cells was higher than that in CD45^{WT} cells; while the activating phosphorylation (p-Lyn Y397/Fyn Y420) was significantly lower in the CD45^{KO} cells. **(B-C)** Quantification of p-Lyn Y507 and p-Lyn Y397/Fyn Y420 was performed by densitometry and normalised to total Lyn expression and the corresponding vector control. All values represent mean±SEM, n=3-4. Statistical significance was analysed using one-way ANOVA with Dunnett's multiple comparisons test, **** = p<0.0001, *** = p<0.001, ** = p<0.01, * = p<0.05 and ns=not significant.

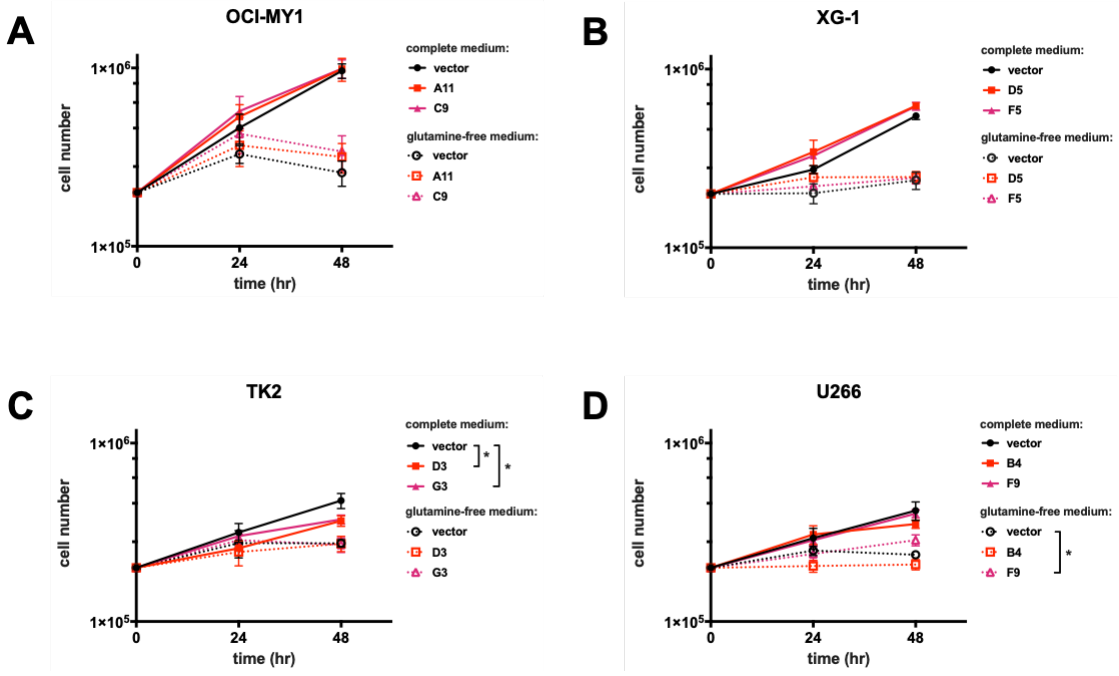

Figure 4-2: Proliferation rate of OCI-MY1, XG-1, TK2 and U266 for 48hr.

$CD45^{WT}$ and $CD45^{KO}$ cells **(A)** OCI-MY1, **(B)** XG-1, **(C)** TK2 and **(D)** U266 were cultured in complete medium (solid lines) and glutamine-free medium (dotted line) for 48hr. Cell counting was performed at 24hr and 48hr. Mean of three independent experiments ± SEM is plotted. Significance was determined by using two-way ANOVA with Dunnett's multiple comparisons test. (∗ = $p<0.05$)

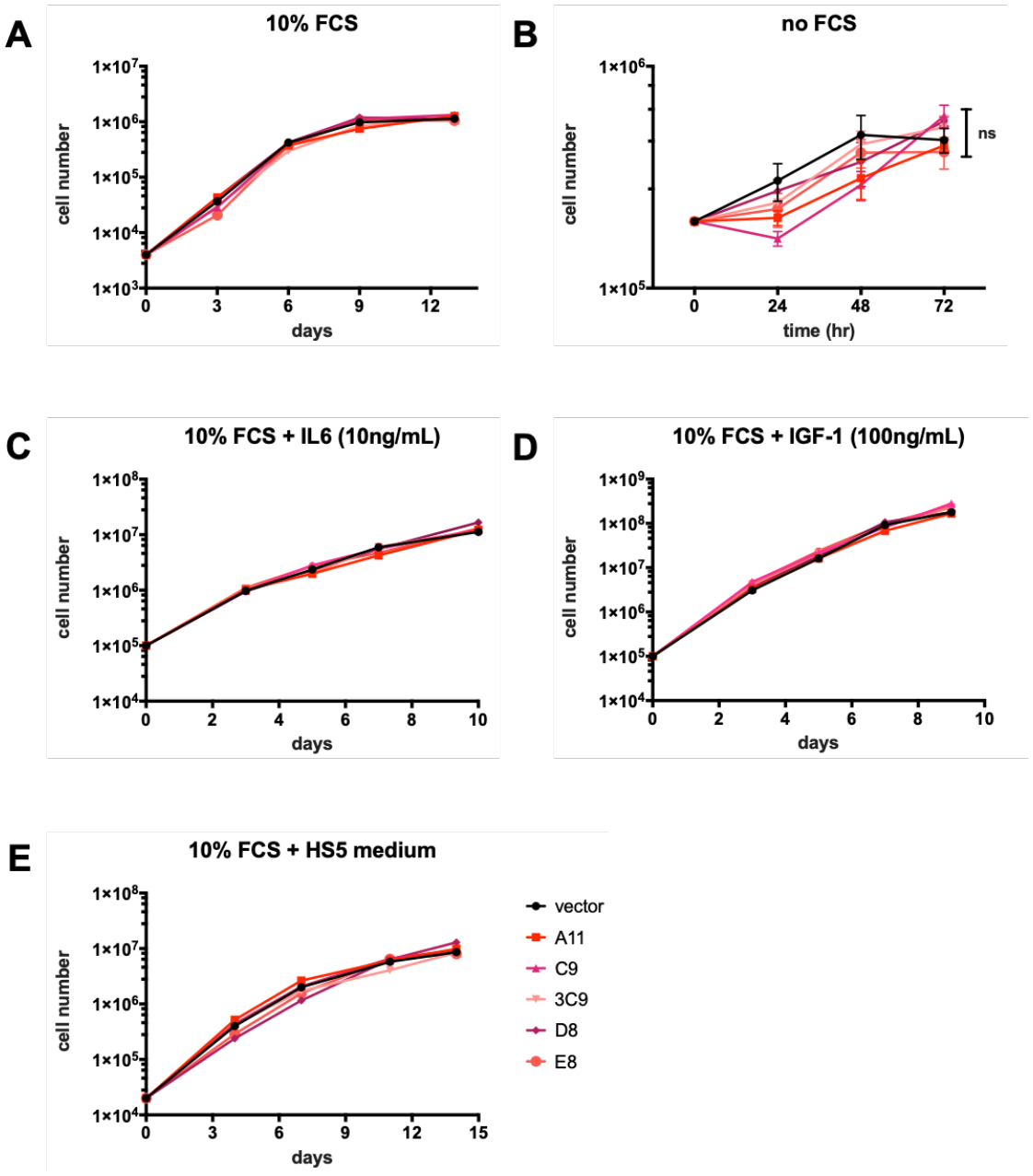

Figure 4-3: Proliferation rate of OCI-MY1 at different culture conditions.

OCI-MY1 cells were cultured in **(A)** complete medium, **(B)** serum-free medium, **(C)** complete medium supplemented with 10ng/mL IL-6, **(D)** complete medium supplemented with 100ng/mL IGF-1 and **(E)** complete medium supplemented with 20% HS5 conditioned medium for 3-15 days. Mean of three independent experiments ± SEM is plotted in **(B)**. Significance was determined by using two-way ANOVA with Tukey's multiple comparisons test (ns=not significant).

4.2.3 Clonogenic potential of $CD45^{KO}$ cells

The clonogenic potential of OCI-MY1 $CD45^{WT}$ and $CD45^{KO}$ cells were compared in the methylcellulose-based semi-solid culture condition. $CD45^{WT}$ cells yielded 96±6 colonies/500 cells plated, whereas $CD45^{KO}$ cells yielded 15-69 colonies (p-value=0.0039-0.0478). The colonies showed very different morphology: $CD45^{WT}$ cell colonies were larger and contained more cells (Figure 4-4). As such, the number of cells recovered from the $CD45^{WT}$ cell plates was higher than the $CD45^{KO}$ cell plates.

Generally, MM cells have the phenotypic signature of long-lived plasma cells – $CD19^{-}$ $CD20^{-}$ $CD38^{+}$ $CD138^{+}$. However, it has been shown that a small population of MM cells resembled a similar phenotype to the clonogenic $CD138^{-}$ B cells and these cells were capable of forming colonies both *in vitro* and *in vivo*[331,332]. Therefore, we analysed the expression of common B cell antigens on OCI-MY1 cells by flow cytometry. Consistent with the plasma cell phenotype, both $CD45^{WT}$ and $CD45^{KO}$ cells were $CD19^{-}$ $CD20^{-}$ $CD38^{+}$ $CD138^{+}$ (Figure 4-5).

4.2.4 Cell cycle profile of $CD45^{KO}$ cells

The cell cycle progression of $CD45^{WT}$ and $CD45^{KO}$ cells in complete medium at 48hr was analysed by flow cytometry. $CD45^{WT}$ and $CD45^{KO}$ OCI-MY1, XG-1 and U266 cells shared similar cell cycle profiles (Figure 4-6A, B and D), whereas $CD45^{KO}$ TK2 cells (clone D3 and G3) showed higher proportions of cells arrested in G_0/G_1 and lower proportions of cells entered G_2/M compared to $CD45^{WT}$ TK2 (vector) cells (Figure 4-6C). This difference in cell cycle profile of TK2 is consistent with the lower proliferation rate observed in Figure 4-2C at 48hr.

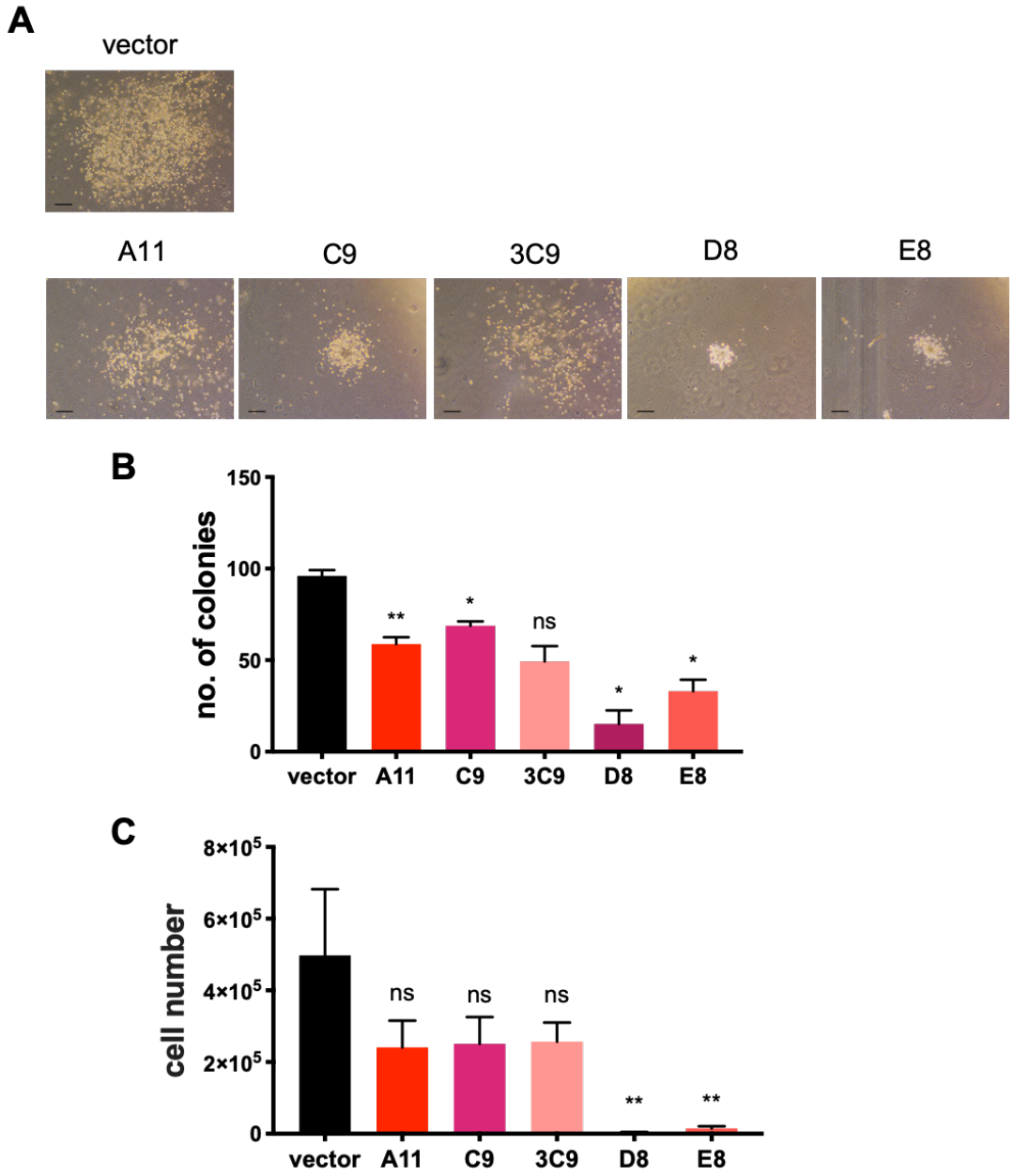

Figure 4-4: Clonogenic potential of CD45^{WT} and CD45^{KO} OCI-MY1 cells.

(A) Representative images of cells cultured in the methylcellulose-based semi-solid medium for 11 days. Scale bar=200μm. **(B)** The number of colonies was counted under an inverted microscope. **(C)** Cells from each plate were resuspended and counted. Mean value of technical duplicates from three independent experiments ±SEM is plotted. Statistical significance was determined by one-way ANOVA with Dunnett's multiple comparisons test where ∗∗ = $p<0.01$, ∗ = $p<0.05$ and ns=not significant.

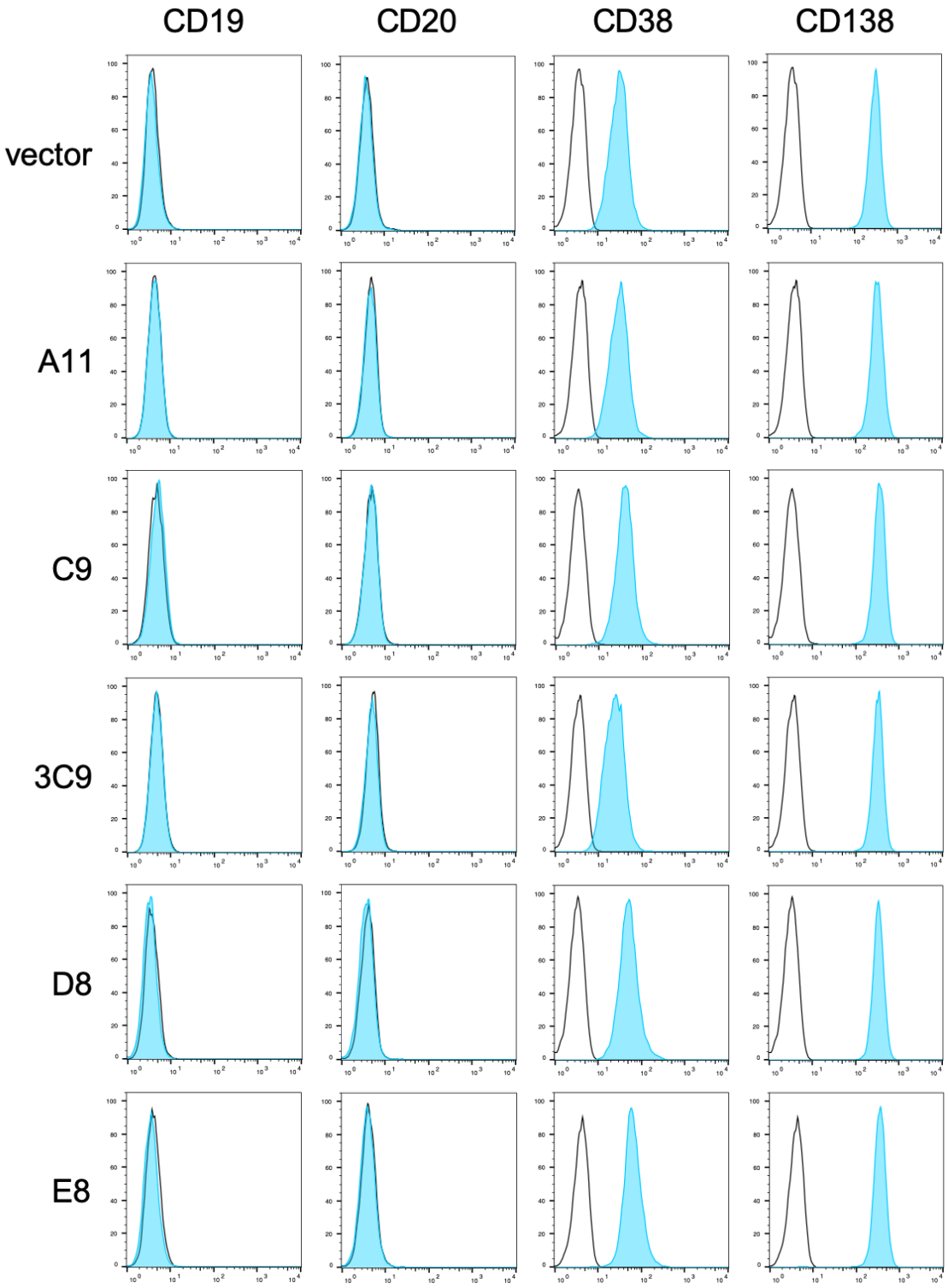

Figure 4-5: Expression of B cell antigens on OCI-MY1 cells.

Expression of CD19, CD20, CD38 and CD138 (blue histograms) on $CD45^{WT}$ and $CD45^{KO}$ OCI-MY1 cells was evaluated by flow cytometry (n=1). Isotype control is represented by an open black histogram.

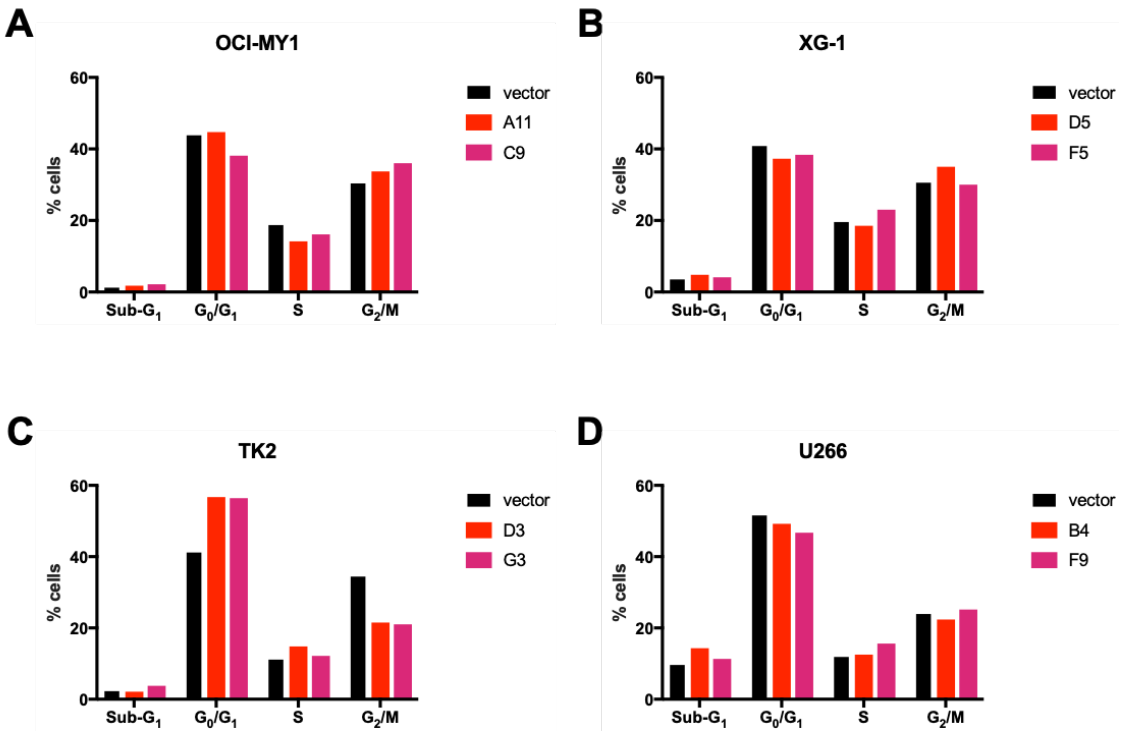

Figure 4-6: Cell cycle profiles of OCI-MY1, XG-1, TK2 and U266.

Cell cycle analysis of $CD45^{WT}$ (black bar) and $CD45^{KO}$ (red and pink bars) cells of **(A)** OCI-MY1, **(B)** XG-1, **(C)** TK2 and **(D)** U266 at 48hr (n=1).

4.2.5 The effect of loss of CD45 on signalling

To determine the effect of the loss of CD45 on cell signalling, OCI-MY1 cells (vector, C9, D8 and E8) were cultured with the addition of 10ng/mL IL-6 and 100ng/mL IGF-1. The level of activation of SFKs, STAT3 and AKT was then assessed by immunoblotting (Figure 4-7A-B). Both $CD45^{WT}$ and $CD45^{KO}$ cells showed a similar level of STAT3 activation upon IL-6 stimulation, except E8, which showed a slightly lower level of STAT3 activation at 60min. The level of SFK activation remained lower in $CD45^{KO}$ cells as shown in 4.2.1. No apparent change in SFK activation was induced by IL-6. On the other hand, IGF-1-stimulated AKT activation was observed in both $CD45^{WT}$ and $CD45^{KO}$ cells, especially at 60min. Similar to IL-6, IGF-1 did not activate SFK. Additionally, the expression level of IL-6R and IGF-1R were analysed by flow cytometry (Figure 4-7C). Two of the $CD45^{KO}$ clones expressed lower levels of IL-6R compared to $CD45^{WT}$ cells, which may account for the decreased p-STAT3 level in response to IL-6 in these cells. The expression of IGF-1R was comparable in both CD45 phenotypes.

4.2.6 The effect of loss of CD45 on autophagy

Autophagy is a catabolic process whereby dysfunctional cellular components are enclosed in double-membraned autophagosomes and subjected to lysosomal degradation into useful amino acids, nucleotides and fatty acids[333]. This process is upregulated in cancer cells in order to cope with stress and nutrient deprivation. Inhibiting autophagy in cancer cells decreases cell proliferation and even leads to cell death. Chloroquine (CQ) and its derivative hydroxychloroquine (HCQ) inhibit autophagy by blocking the fusion of autophagosomes and lysosomes as well as their degradation[334], and have been used in clinical trials for cancer therapies.

OCI-MY1 cells were treated with 20μM and 40μM CQ and cell counting was performed at 24hr. Both $CD45^{WT}$ and $CD45^{KO}$ cells showed significantly lower cell proliferation at 40μM compared to untreated cells (compared to untreated: vector=78.28%, p-value=0.0055; A11=78.93%, p-value=0.067; and

C9=64.63%, p-value=0.0001) (Figure 4-8A). The expression of cytosolic microtubule-associated protein 1A/1B-light chain 3 (LC3-I) and its phosphatidylethanolamine conjugate LC3-II, which is recruited to autophagosomal membranes, was analysed by immunoblotting. Dose-dependent induction and accumulation of LC3-II were observed. The turnover of LC3II, as represented by the ratio of LC3-II:LC3-I was listed under the band (Figure 4-8B). No significant difference in response to autophagy inhibition was observed between $CD45^{WT}$ and $CD45^{KO}$ cells.

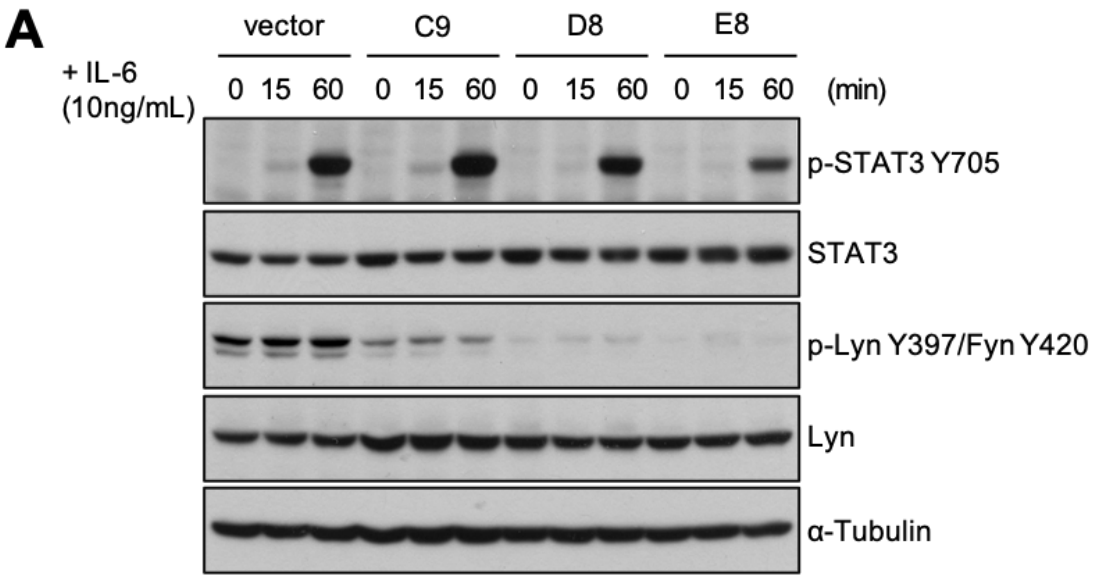
A
vector
C9
D8
E8
+ IL-6
(10ng/mL)
0 15 60 0 15 60 0 15 60 0 15 60
(min)
p-STAT3 Y705
STAT3
p-Lyn Y397/Fyn Y420
Lyn
α-Tubulin

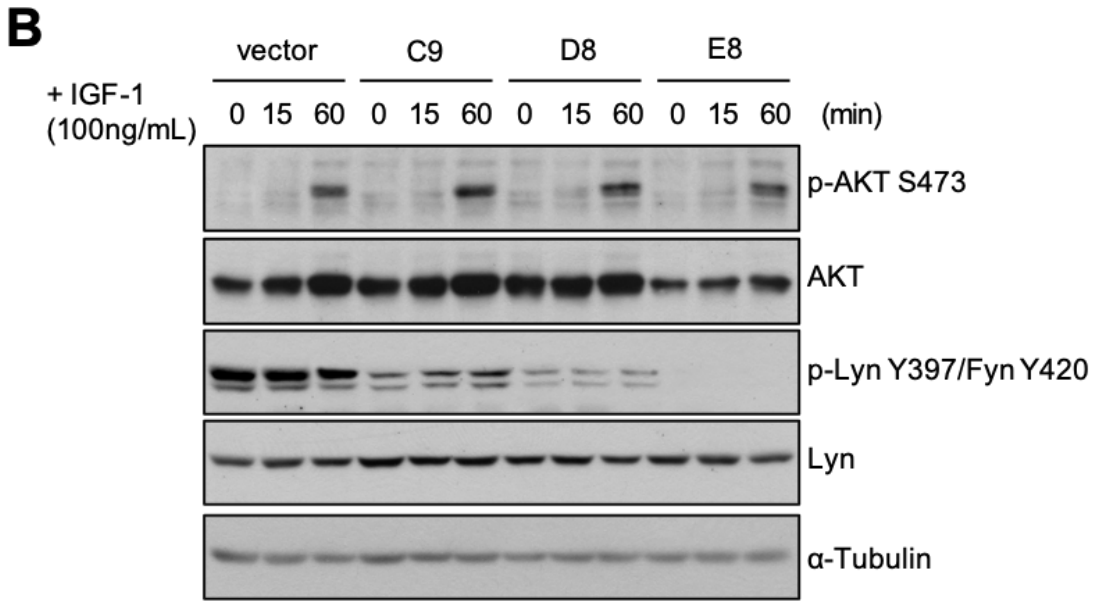
B
vector
C9
D8
E8
+ IGF-1
(100ng/mL)
0 15 60 0 15 60 0 15 60 0 15 60
(min)
p-AKT S473
AKT
p-Lyn Y397/Fyn Y420
Lyn
α-Tubulin

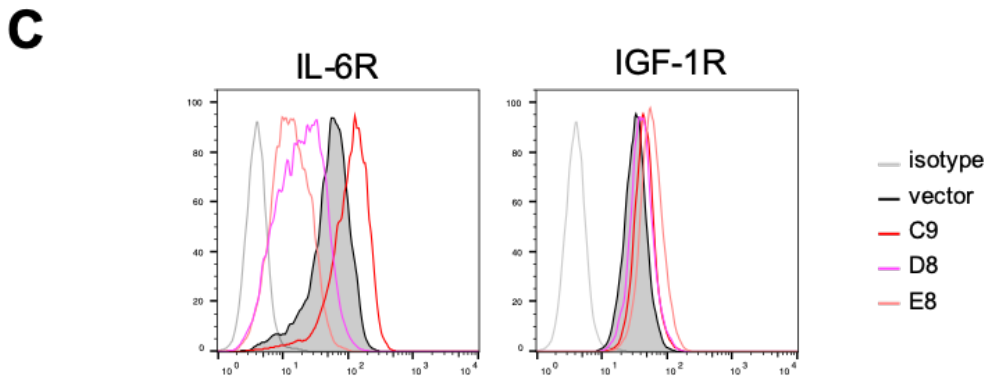
C
IL-6R
IGF-1R
isotype
vector
C9
D8
E8

Figure 4-7: Cell signalling upon cytokine stimulation.

Overnight serum-starved OCI-MY1 cells were treated with **(A)** 10ng/mL IL-6 and **(B)** 100ng/mL IGF-1 for 15 and 60min. The activation of STAT3, AKT and SFK was analysed by immunoblotting. **(C)** IL-6R and IGF-1R expression were analysed by flow cytometry (n=2).

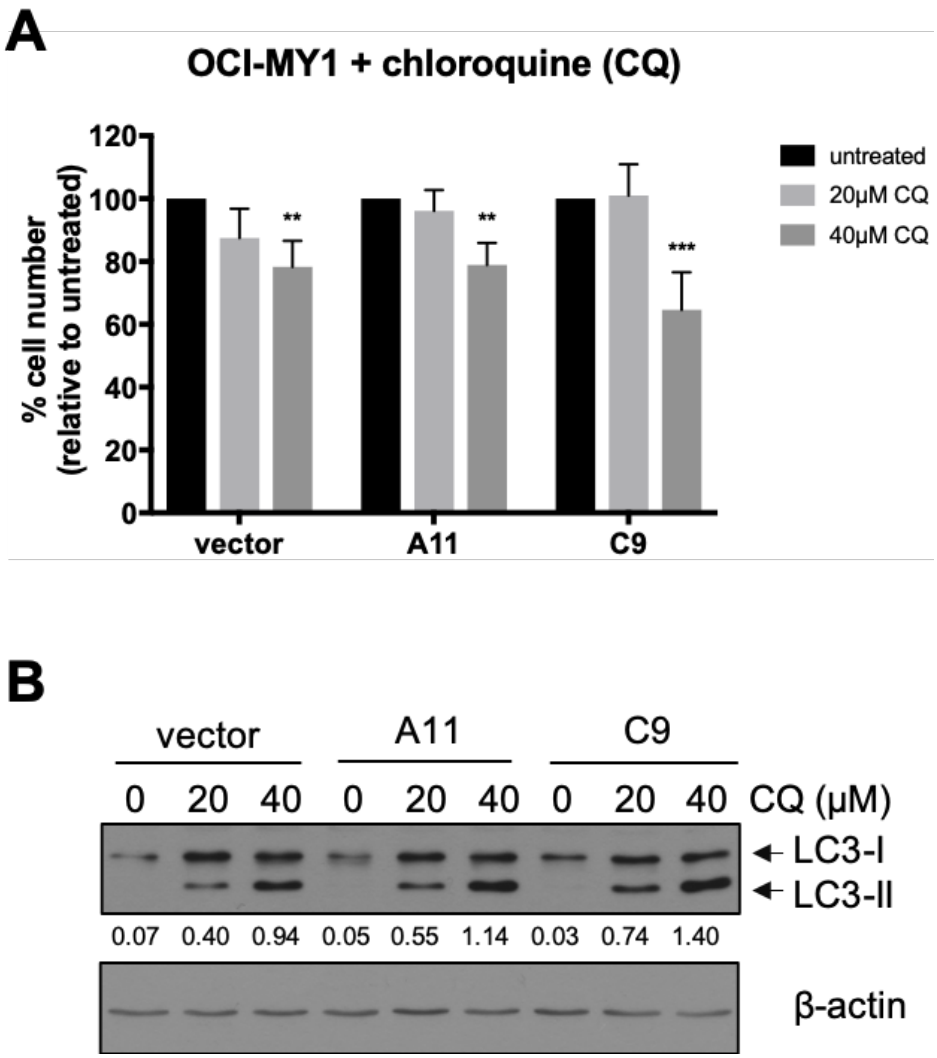

Figure 4-8: Inhibition of autophagy in OCI-MY1 cells.

(A) $CD45^{WT}$ and $CD45^{KO}$ OCI-MY1 cells were treated with 20μM and 40μM CQ for 24hr. Cell number was normalised to untreated control. Mean±SEM of three independent experiments is shown. Significance was determined by using 2-way ANOVA with Dunnett's multiple comparisons test (∗∗∗ = $p<0.001$ and ∗∗ = $p<0.01$). **(B)** Expression of LC3-I and LC3-II was analysed by immunoblotting. The turnover of LC3-II was represented by the ratio of LC3-II:LC3-I.

4.2.7 Transcriptional changes induced by the loss of CD45

To investigate the transcriptome changes induced by the loss of CD45 expression, RNA-sequencing was performed on $CD45^{WT}$ (vector) and $CD45^{KO}$ (C9) OCI-MY1 cells from three biological replicates. Compared to vector control cells, 195 genes were differentially expressed, of which 139 genes were downregulated and 56 genes were upregulated (fold-change>$\log_2$ 1 and false discovery rate, FDR<0.05). The overall changes in gene expression are presented in a volcano plot in Figure 4-9A and the complete list of dysregulated genes is in Appendix 3. As expected, the loss of CD45 from OCI-MY1 cells resulted in a notable decrease in CD45 gene expression (*PTPRC,* log2FC=4.04, FDR=8.18E-18). The gene read aligned to the *PTPRC* gene was visualised in Integrative Genomics Viewer (IGV, Broad Institute, USA) and all 33 exons of *PTPRC* were covered. Figure 4-9B shows the snapshot of the read counts of exon 8-12.

Next, to determine the biological role of CD45 in MM cells, GO annotation analysis and KEGG pathway analysis were performed on the significantly differentially expressed genes using the DAVID Bioinformatics Resources 6.8. A total of 42 GO annotations (modified Fisher Exact P-value, EASE score<0.05) were identified, including 26 biological processes, 11 cellular components and five molecular functions (Figure 4-10). Among these annotations, three GO terms were found to be related to cell mobility, such as cell-matrix adhesion (*BCL2L11, EMP2, FERMT2* and *ITGAL*), focal adhesion (*WASF1, DPP4, FERMT2, FLNB, FHL1, MME, PARVB, PLAUR, PTPRC, RHOB* and *RPL13A*) and cytoskeleton (*CDC42EP5, WASF1, WIPI1, ADD2, FERMT2, GAS2L1, PARVB* and *SEPT2*). KEGG enrichment pathway analysis revealed 11 dysregulated pathways in $CD45^{KO}$ cells (Figure 4-11) including genes related to proteoglycans in cancer (*CCND1, CDKN1A, FLNB, HBEGF, PIK3R3, PLAUR and PRKCB*) and ErbB signalling pathway (*JUN, CDKN1A, HBEGF, PIK3R3, PRKCB and STAT5A*), which take part in cell migration, angiogenesis and tumour progression. The transcriptome analysis has highlighted the role of CD45 in cell mobility and inspired further investigation.

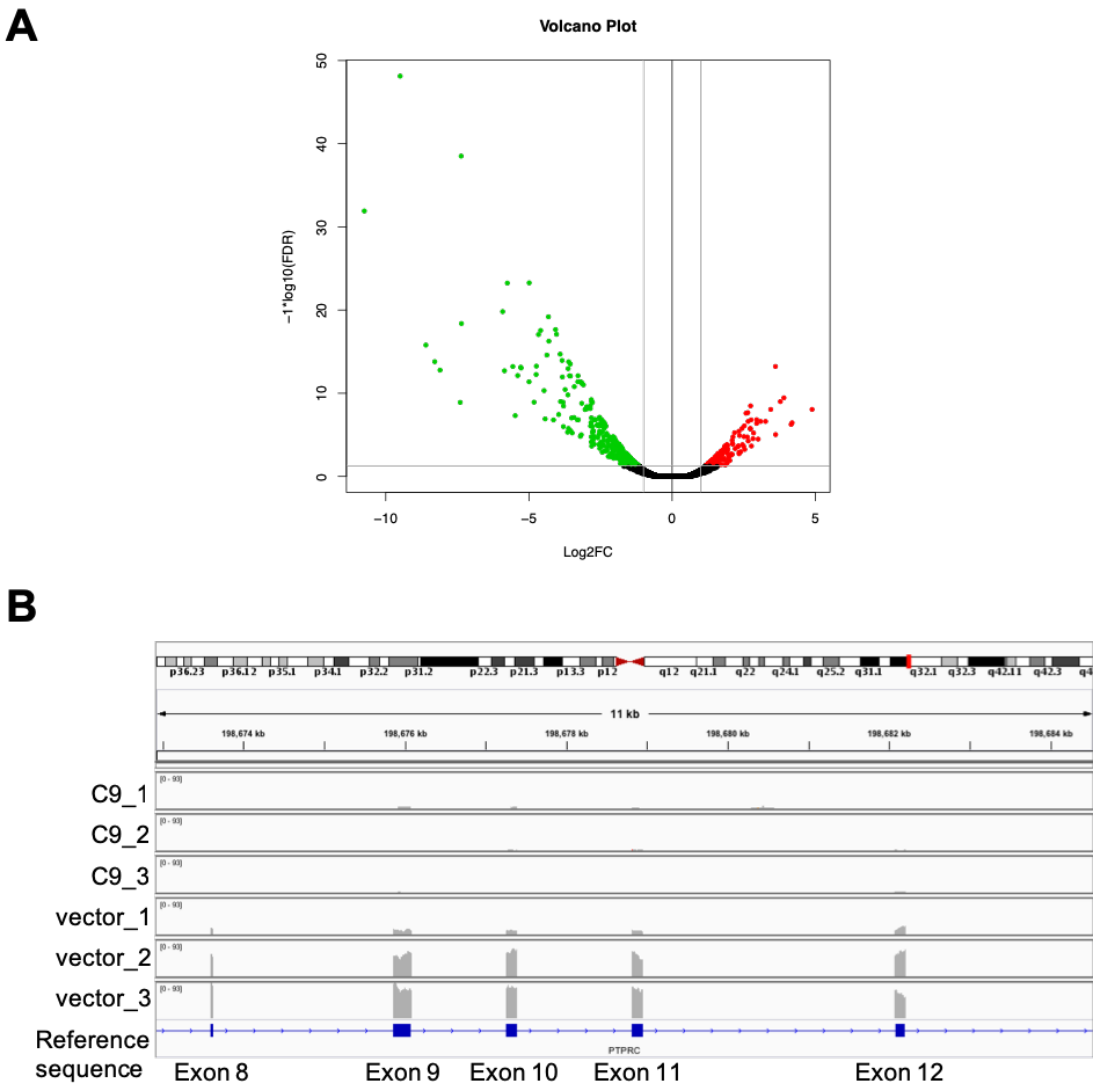

Figure 4-9: Differentially expressed genes in CD45^{KO} OCI-MY1 cells (C9) identified by RNA-sequencing using edgeR.

(A) Differentially expressed genes between CD45^{WT} (vector) and CD45^{KO} (C9) OCI-MY1 cells were plotted against the significance of difference in volcano plot. Red dots indicate the upregulated genes with log2FC >1 and FDR<0.05; while green dots indicate the downregulated genes with log2FC <-1 and FDR<0.05. **(B)** Snapshot of read alignment of exon 8-12 of *PTPRC* in the three biological replicates of vector and C9 in IGV.

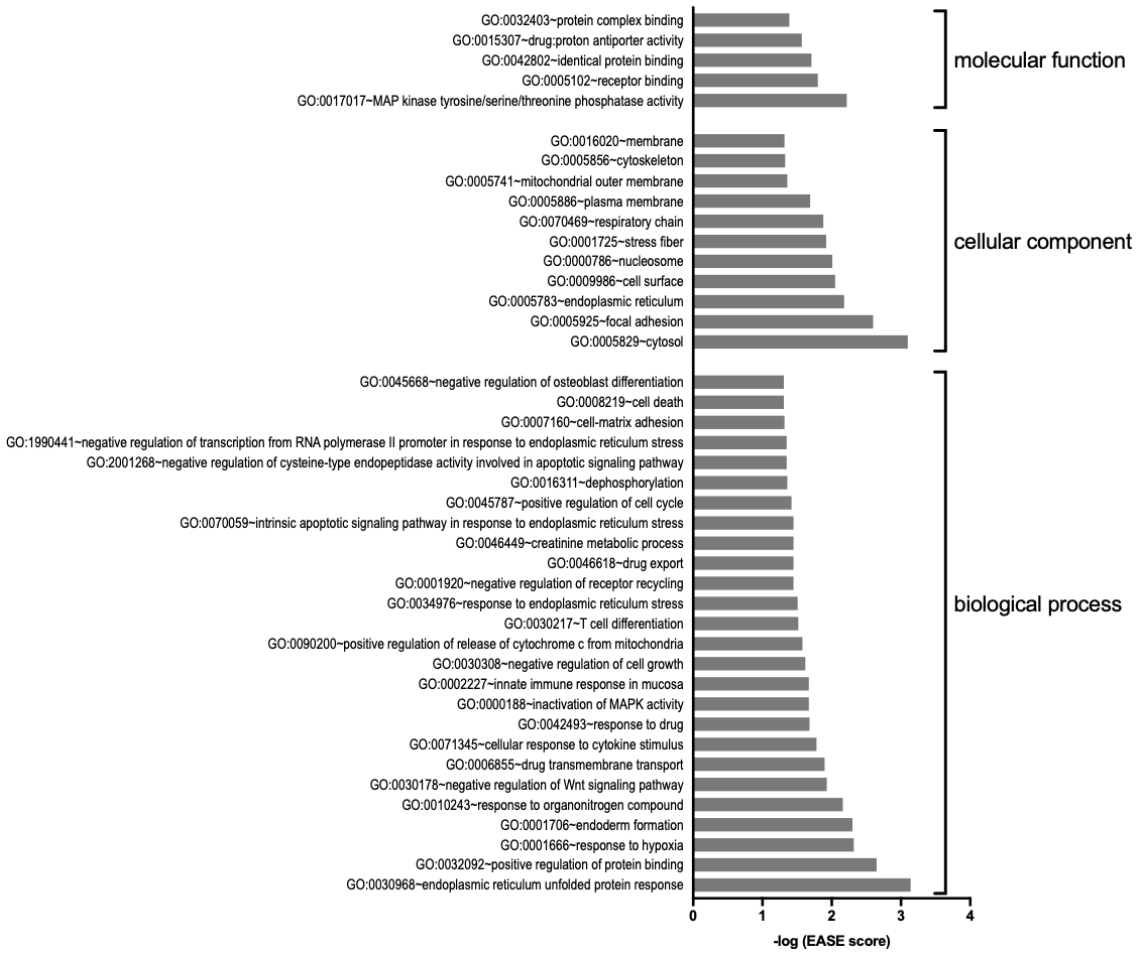

Figure 4-10: Gene ontology (GO) analysis.

DAVID functional annotation clustering analysis of differentially expressed genes in CD45^{KO} OCI-MY1 cells. GO terms with modified Fisher Exact p-value (EASE score) <0.05 are plotted.

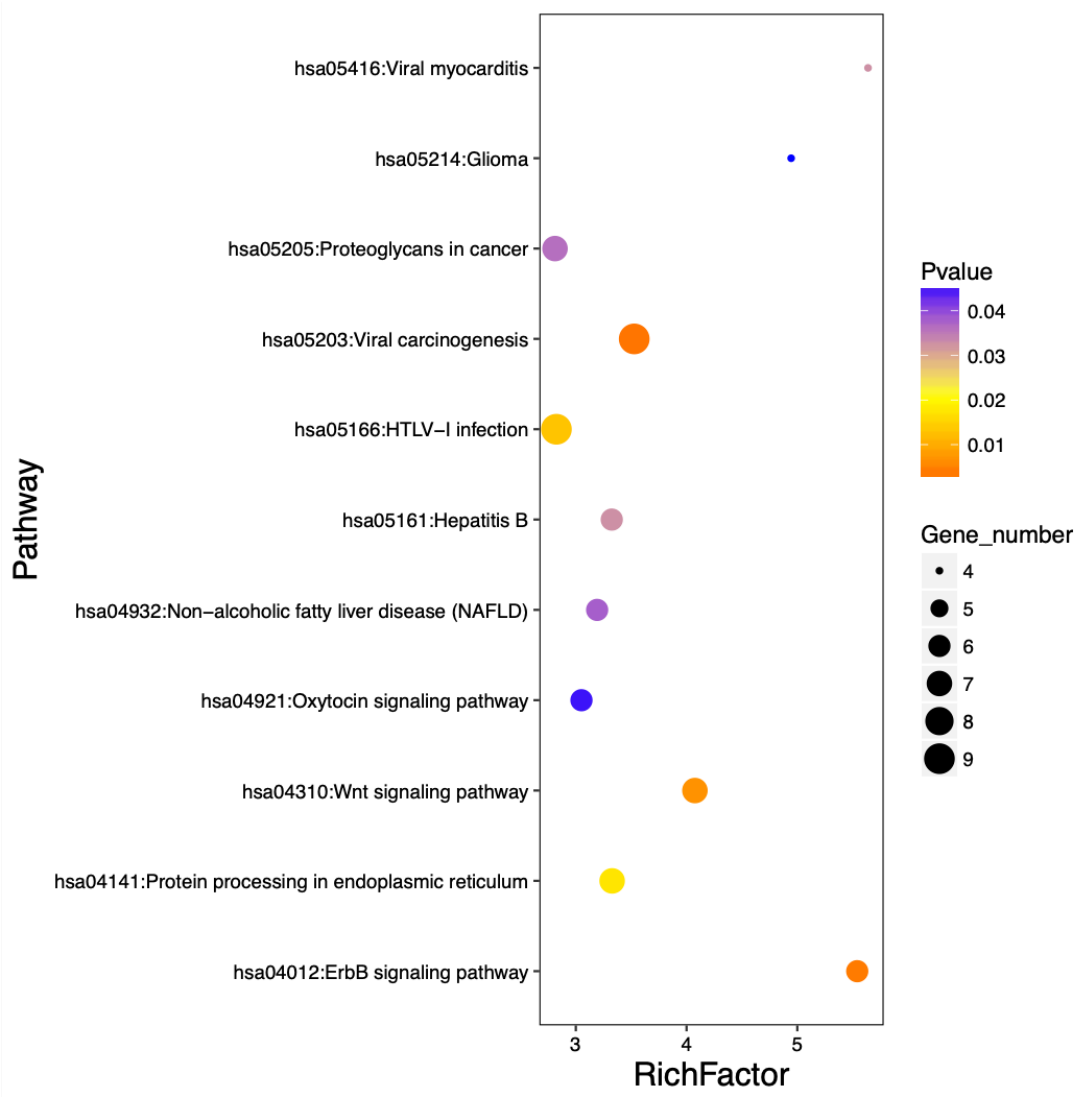

Figure 4-11: KEGG pathway analysis of differentially expressed genes.

Bubble chart shows the enrichment of differentially expressed genes identified in $CD45^{KO}$ cells in signalling pathways. Size and colour of the bubbles represent the amount of differentially expressed genes and the corresponding significance enriched in the pathway respectively. The x-axis represents the rich factor (fold enrichment) of input genes to the background genes.

4.3 Discussion

In this Chapter, we aimed to identify the biological differences between $CD45^{WT}$ and $CD45^{KO}$ cells focusing on their level of SFK activity, proliferation under different culture conditions and transcriptional changes.

The best-characterised function of CD45 is its regulation on SFK activity. Studies have shown that CD45 dephosphorylates both the inhibitory and activating phosphorylation on SFKs in a cell type and context-dependent manner (1.3.5.1 and reviewed by J. Penninger et al.[335]). Here we demonstrated that CD45 plays a positive regulatory role in MM by using our $CD45^{KO}$ models: all the $CD45^{KO}$ cells from 4 HMCLs exhibited lower SFK activity compared to $CD45^{WT}$ cells. This result recapitulates the SFK activation in $CD45^{+}$ but not $CD45^{-}$ HMCLs in another study[295]. Surprisingly, despite the fact that SFKs govern many important pathways especially in cell proliferation and survival, only $CD45^{KO}$ TK2 cells showed slower proliferation than their counterparts while other HMCLs retained similar proliferation rates and cell cycle profiles. This also contradicts previous studies showing $CD45^{-}$ cells were less proliferative. One possible explanation is that these $CD45^{KO}$ cells upregulated alternative pathway(s) to maintain cell growth and survival. However, we did not observe a significant difference in STAT3 and AKT activation upon IL-6 and IGF-1 stimulation respectively in $CD45^{WT}$ and $CD45^{KO}$ cells, suggesting the loss of CD45 expression did not impact on PI3K/Akt and JAK/STAT3 but on other pathways. The introduction of Cas9 and gRNA may disrupt the genome stability, resulting in the reduced proliferation of $CD45^{KO}$ TK2 cells at 48hr.

The proliferation and survival of $CD45^{KO}$ cells were further investigated in the nutrient-deprived and cytokine-supplemented conditions. We hypothesised that $CD45^{KO}$, but not $CD45^{WT}$ cells, would be more tolerant to unfavourable environments and thrive with the addition of growth factors thereby leading to a more aggressive disease. We investigated cell proliferation in the absence of glutamine or FCS, and in the inhibition of autophagy. FCS contains a variety of growth factors and is an indispensable component of the tissue culture medium. Surprisingly, both $CD45^{WT}$ and $CD45^{KO}$ OCI-MY1 cells were able to survive and

proliferate without FCS for a period of 72hr. We did observe a subtle variation between these two phenotypes: $CD45^{KO}$ cells proliferated slower than $CD45^{WT}$ cells in the initial 48hr but then proliferated at a similar rate until 72hr. Unfortunately, we were unable to verify whether $CD45^{KO}$ cells were more capable in adapting to the serum-free condition due to the cell death in both populations after 72hr.

The requirement of glutamine in cancer cell proliferation was first described by H. Eagle[336]. Despite the fact that glutamine is a non-essential amino acid and can be synthesised from glucose, cancer cells have exhibited 'glutamine addition' in tissue culture: they cannot survive without the presence of exogenous glutamine. Not only do cancer cells acquire exogenous glutamine at a higher rate than normal cells, but they also metabolise glutamine into α-ketoglutarate which then enters Krebs cycle to generate ATP, or other components for amino acid, nucleotide and fatty acid production (reviewed by B. Altman et al.[337]). As a result, targeting glutamine metabolic machinery has emerged as a new strategy for cancer therapy[338].

A body of evidence has shown the importance of glutamine in MM. For example, a study comparing the metabolomic profiles between MM patients and healthy individuals using nuclear magnetic resonance spectroscopy revealed that MM patients had lower serum levels of glutamine, highlighting the high demand for glutamine of MM cells. Indeed, both HMCLs and primary MM cells express a high level of glutaminase, which catalyses the hydrolysis of glutamine, but a low level of glutamine synthetase[339]. Inhibiting glutaminase or incubating MM cells in low glutamine medium reduces cell viability[339,340]. Although targeting glutamine metabolism is limited by the off-target effect and toxicity[337], it has been shown to sensitise MM cells to the BCL-2 inhibitor venetoclax[341], thus, providing an alternative anti-myeloma therapy while sparing the less glutamine-demanding normal cells.

Similarly, autophagy is a highly conserved cellular process that is particularly upregulated in cancer cells. It regulates the degradation of dysfunctional components into useful amino acids, nucleotides and fatty acids in response to the nutrient-deprived extracellular milieu[342]. Cancer cells upregulate this

process to supply themselves with additional nutrients for the rapid local and distal expansion[343], therefore inhibiting autophagy has also become an appealing target in cancer therapy.

Both glutamine and autophagy are important for MM, yet the role of CD45 in MM metabolism has not been reported. To this end, we utilised glutamine-free medium and CQ to examine the proliferation of $CD45^{WT}$ and $CD45^{KO}$ cells. As we predicted, deprivation of glutamine and inhibition of autophagy led to a slower growth rate, however, no apparent difference was observed between $CD45^{WT}$ and $CD45^{KO}$ cells (except one $CD45^{KO}$ U266 clones) under the described conditions. As we hypothesised that $CD45^{-}$ phenotype represents a more metastatic disease and a study showed circulating MM cells had lower CD45 expression compared to the paired BM MM cells (although it did not reach statistical significance)[124], this seemingly contradicted our previous finding that extramedullary MM cells have a higher level of autophagy[344]. One of the drawbacks of these *in vitro* experiments is the short incubation time. These genetically modified cells have never been exposed to these environments and could take a longer time to rewire the metabolic machinery. We anticipate that using *in vivo* models would be more representative for this purpose; however, this is beyond the scope of this study.

MM is remarkably dependent on the BMME for proliferation, differentiation and survival (details in 1.2.4). HS5 is a BMSC line and like other BMSCs, HS5 secretes a variety of soluble factors. The response of $CD45^{WT}$ and $CD45^{KO}$ cells to the addition of HS5 conditioned medium and two specific cytokines in BMME, IL-6 and IGF-1, was compared. M. Mahmoud et al. demonstrated IL-6 induced a positive proliferative response in $CD45^{+}$ HMCLs (ILKM-2, ILKM-3, flow cytometry-sorted $CD45^{+}$ U266) but not in $CD45^{-}$ HMCLs (KMS-5 and flow cytometry-sorted $CD45^{-}$ U266), and this required CD45 phosphatase activity[277] and SFK activity[295]. Similarly, IGF-1 is another vital cytokine that induces an anti-apoptotic and a proliferative effect on MM. Although no solid evidence has been found on the correlation of IGF-1-induced proliferation and CD45 expression, the magnitude of induced AKT activation was indeed related to CD45[89,278]. Unlike the previous studies suggested, we demonstrated that our

$CD45^{WT}$ and $CD45^{KO}$ cells share similar proliferation profile and activation of STAT3 and AKT upon the IL-6 and IGF-1 stimulation, indicating that CD45 does not correlate to IL-6 and IGF-1 pathways.

The proliferation of these cells was also studied in the methylcellulose-based semi-solid culture. Traditionally, this assay is used to assess the ability of haemopoietic stem cells to proliferate and differentiate into colonies – colony formation unit. In the context of myeloma, MM stem cells have the ability to propagate indefinitely and initiate overt disease; however, the phenotypic characterisation of these cells is yet to be elucidated due to the discrepancy between studies[345]. For example, D. Kim et al. showed that the $CD19^{-}CD45^{low/-}CD38^{high}/CD138^{+}$ plasma cells but not the $CD19^{+}/CD45^{high}CD38^{high}/CD138^{+}$ were enriched with MM-initiating cells[346]; however, another study pointed out that $CD138^{-}$ cells were more clonogenic both *in vitro* and *in vivo*[331]. CD45 is generally weakly expressed on MM cells. Only a small $CD45^{+}$ compartment has been found in patients and represents the proliferating population, suggesting that $CD45^{+}$ could be more clonogenic. Another study showed that $CD45^{-}$ primary MM cells (with $CD138^{-}/CD34^{-}$ background) produced less colonies[331]. Consistently, we showed $CD45^{KO}$ cells yielded much fewer colonies than $CD45^{WT}$ cells. Further analysis on cell surface antigens confirmed the difference in clonogenic potential was due to the loss of CD45 but not CD19, CD20, CD38 or CD138 expression.

RNA sequencing identified that CD45 (gene symbol: *PTPRC*) was among the 139 genes significantly downregulated in the $CD45^{KO}$ cells compared to the $CD45^{WT}$ cells. The number of dysregulated genes identified was relatively small considering SFKs; the key regulators for signal transduction; were mostly inactivated in the $CD45^{KO}$ cells. We suspect that the residual SFK activity was able to drive the downstream transcription factor activities. Nevertheless, GO analysis revealed that the differentially expressed genes were significantly enriched in annotations related to cell mobility, such as focal adhesion (GO:0005925) and cell-matrix adhesion (GO: 0007160). Moreover, KEGG pathway analysis showed the differentially expressed genes enriched in the pathways of ‘proteoglycans in cancer’ (hsa05205) and ‘ErbB signalling pathway’

(hsa04012). Both pathways contribute to cell mobility, angiogenesis and tumour progression highlighting the potential role of CD45 in these areas.

In summary, this chapter interrogated the biological differences between $CD45^{WT}$ and $CD45^{KO}$ cells. We have shown that SFKs are inactivated in the $CD45^{KO}$ populations; however, no apparent difference in cell proliferation is found in nutrient-deprived or enriched conditions. The $CD45^{KO}$ cells are less clonogenic than the $CD45^{WT}$ counterparts. More importantly, our transcriptional analysis revealed that the biological processes and pathways related to cell mobility are dysregulated, supporting our hypothesis that CD45 expression correlates to MM metastatic progression. These results warrant further investigation with respect to the role of CD45 in MM cell homing and dissemination.

CHAPTER 5:
THE ROLE OF CD45 IN MYELOMA CELL HOMING AND DISSEMINATION

5.1 Introduction

The homing of dysregulated plasma cells from the post-germinal centres to multiple BM niches is one of the hallmarks of MM pathogenesis. Whilst this homing process marks the initiation of the disease, the presence of circulating MM cells in all disease stages suggests it takes place throughout the disease progression[108,125–127]. Aberrations in this homing process including chemotactic response to BM soluble factors, adhesion to BM endothelium and digestion of endothelial membrane, have been implicated in enhancing the metastatic progression in MM.

CD45 has demonstrated an important role in MM homing. As mentioned in 1.4.3, the $CD45^-$ subsets of 5T murine cells, 5T2MM and 5T33MM, homed significantly less than the $CD45^+$ subsets *in vivo*. The invasive capacity of $CD45^-$ cells towards synthetic basement membrane was also impaired in this model[287,289,290]. Our group has previously shown that the sorted $CD45^-$ U266 cells have lower homing potential towards BMSCs than the $CD45^+$ U266 cells[347]. Consistent with these established data, the transcriptome analysis on $CD45^{WT}$ and $CD45^{KO}$ cells in Chapter 4 has identified that biological processes and pathways related to cell adhesion and mobility are dysregulated in $CD45^{KO}$ cells. Despite all these observations, the molecular mechanisms of MM homing remain elusive.

Many studies have correlated SFK expression and activity to cancer progression and metastasis in solid tumours, such as colon, pancreatic and breast cancers[348], yet the evidence of SFK regulating MM homing has been very limited. Previous studies of SFK in MM primarily focused on the SFK-related signalling pathways[349], proliferation[295] and osteolytic bone disease[350]. Recently, a study has reported that suppressing Src activity can further attenuate the production of VEGF and *in vivo* angiogenesis in checkpoint kinase-1 (Chk1) inhibitor-treated MM cells[351], rationalising further investigation on the potential role of SFK in metastasis. Additionally, CD45 has also been shown to interact with focal adhesion kinases, FAK and Pyk2, through SFKs in macrophages, T cells and non-haemopoietic cells (e.g. HeLa, HEK293T)[290–294].

Of these kinases, Pyk2 has been correlated to MM progression[352–354]. Overexpression of Pyk2 is detected in MGUS, SMM and MM patients, and associated with poor survival *in vivo*[353]. The regulation of Pyk2 activity requires active Src to phosphorylate Pyk2 at Y402 which facilitates the binding of Src to Pyk2, Src further phosphorylates Pyk2 at Y579/580 for full activation[291]. With low SFK activity, $CD45^{KO}$ cells could also have low Pyk2 activity.

Given the differential *in vivo* homing kinetics between CD45 phenotypes in other studies, the growth of $CD45^{WT}$ and $CD45^{KO}$ cells in NSG mice were compared. Cells were introduced into mice intravenously or intratibially. Intravenous injection assesses the homing of MM cells to BM niches while intratibial injection represents the early stage of the disease which MM cells are mostly confined in the BM. We postulated that the loss of CD45 expression could potentially drive the metastatic progression through the dysregulated homing process, resulting in poor disease outcome. To investigate the role of CD45 in MM homing, this chapter was designed to

1. Evaluate the homing potential in $CD45^{WT}$ and $CD45^{KO}$ cells *in vitro*;
2. Identify the molecular mechanism(s) in the homing process;
3. Evaluate the homing and metastatic potentials of $CD45^{WT}$ and $CD45^{KO}$ cells *in vivo.*

5.2 Results

5.2.1 Homing and adhesion potential towards BMSCs

The homing potential towards BMSCs, HS5, of $CD45^{WT}$ and $CD45^{KO}$ cells was determined by using modified Boyden chamber assays as described in 2.4.2.2. XG-1, U266 and TK2 did not migrate under any conditions used in this study, precluding the evaluation of the effects of CD45 on cell mobility in these HMCLs, we therefore focused on OCI-MY1 $CD45^{WT}$ vector cells and 3 $CD45^{KO}$ clones. In OCI-MY1 cells, the loss of CD45 expression strikingly reduced the homing potential: down to 38.4%, 10.3% and 9.1% (all p-values <0.0001) in $CD45^{KO}$ cells C9, D8 and E8 respectively as compared to $CD45^{WT}$ (vector) cells (Figure 5-1A). The addition of a layer of Matrigel to Transwell inserts further reduced the homing potential (C9: 23%, p-value=0.0003; D8: 4.7%, p-value<0.0001 and E8: 3.3%, p-value<0.0001) suggesting the ability of digesting extracellular matrix in $CD45^{KO}$ cells was also impaired (Figure 5-1B).

Our transcriptome analysis identified cell adhesion was one of the differences between $CD45^{WT}$ and $CD45^{KO}$ cells; thus the adhesive capacity of $CD45^{WT}$ and $CD45^{KO}$ OCI-MY1 cells to BMSCs, HS5, was assessed. Surprisingly, while a substantial difference in homing potential was found between $CD45^{WT}$ and $CD45^{KO}$ cells, no difference in adhesion was observed (Figure 5-1C).

5.2.2 Expression of adhesion and extracellular matrix metalloprotease molecules

Using the RNA sequencing data from 4.2.7, the gene expressions of adhesion molecules and extracellular matrix proteases in $CD45^{WT}$ (vector) and $CD45^{KO}$ (C9) OCI-MY1 cells were compared (Table 5-1). Among the adhesion molecules, only *ITGAL* was significantly downregulated (log2FC=1.79, FDR<0.05) in $CD45^{KO}$ cells, while other genes were only slightly dysregulated but not statistically significant. Furthermore, two extracellular matrix protease genes, *ADAM19* and *MMP17*, were significantly decreased in $CD45^{KO}$ cells

(FDR<0.05). Three other genes (*MMP11*, *MMP14*, and *MMP25*) related to the extracellular matrix protease were also downregulated by more than 2-fold in spite of not reaching statistical significance. The expression of C-X-C motif chemokine ligands and receptors was also examined. Only *CXCR4* expression was significantly increased (log2FC=2.58, FDR<0.05) whereas other genes were barely expressed and with FDR=1 (data not shown).

The expression levels of the above genes were validated by qRT-PCR. Consistent with our RNA sequencing analysis, *ITGAL* and *ADAM19* were downregulated whereas *CXCR4* was upregulated significantly in all $CD45^{KO}$ cells (Figure 5-2). However, we could not detect *MMP17* using qRT-PCR.

The protein expression of CXCR4 was also analysed by flow cytometry. Consistent with gene expression analysis, CXCR4 expression was increased in $CD45^{KO}$ clone C9 and, to a lesser extent, clone D8 and E8 (Figure 5-2). It is surprising that the majority of adhesion molecules and extracellular matrix proteases remained at similar expression levels in $CD45^{KO}$ cells, suggesting that there are other regulatory machinery contributing to the drastic difference in homing potential between the two CD45 phenotypes.

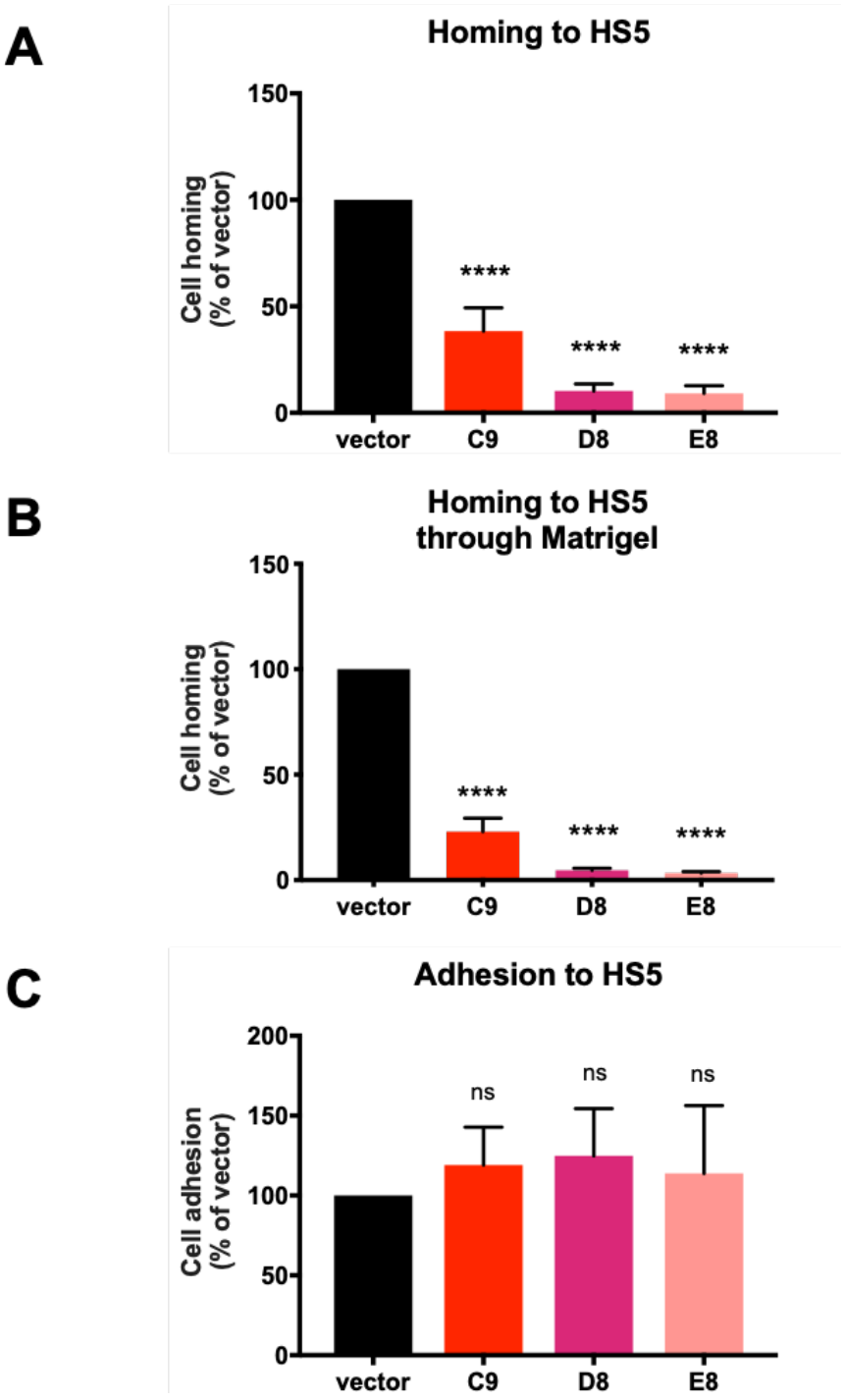

Figure 5-1: Homing and adhesion potential in OCI-MY1.

Homing potential towards **(A)** HS5 and **(B)** HS5 through Matrigel were examined by modified Boyden chamber assay. Adhesion capacity **(C)** was examined by direct incubation with HS5. All values represent mean±SEM, n=3-4. Statistical significance was analysed using one-way ANOVA with Dunnett's multiple comparisons test where **** = $p<0.0001$ and ns=not significant.

Table 5-1: Gene expression of adhesion and protease molecules.

Genes	Log2 FC	p-value	FDR	Significance
Adhesion molecules				
CADM1	-0.6921091	0.06637824	0.54810116	no
ICAM1	0.74807797	0.07690664	0.59509766	no
ITGA3	-0.5888212	0.11898419	0.74591787	no
ITGA7	-0.6730828	0.11300845	0.73070608	no
ITGAL	-1.7899081	3.95E-06	0.00025403	yes
ITGAV	0.46768101	0.22049527	0.94431322	no
ITGB7	-0.5173618	0.16783091	0.86195802	no
Proteolytic enzymes				
ADAM19	-2.3507335	3.82E-09	5.26E-07	yes
ADAM8	-0.8090787	0.03338258	0.37132321	no
MMP11	-1.3704528	0.00339087	0.07290369	no
MMP14	-1.0461759	0.02917897	0.34339517	no
MMP16	-0.7564834	0.04913587	0.46006135	no
MMP17	-2.0021393	2.30E-06	0.00016376	yes
MMP25	-1.3978745	0.00273138	0.06194663	no
Chemokine receptor				
CXCR4	2.57947421	1.31E-10	2.54E-08	yes

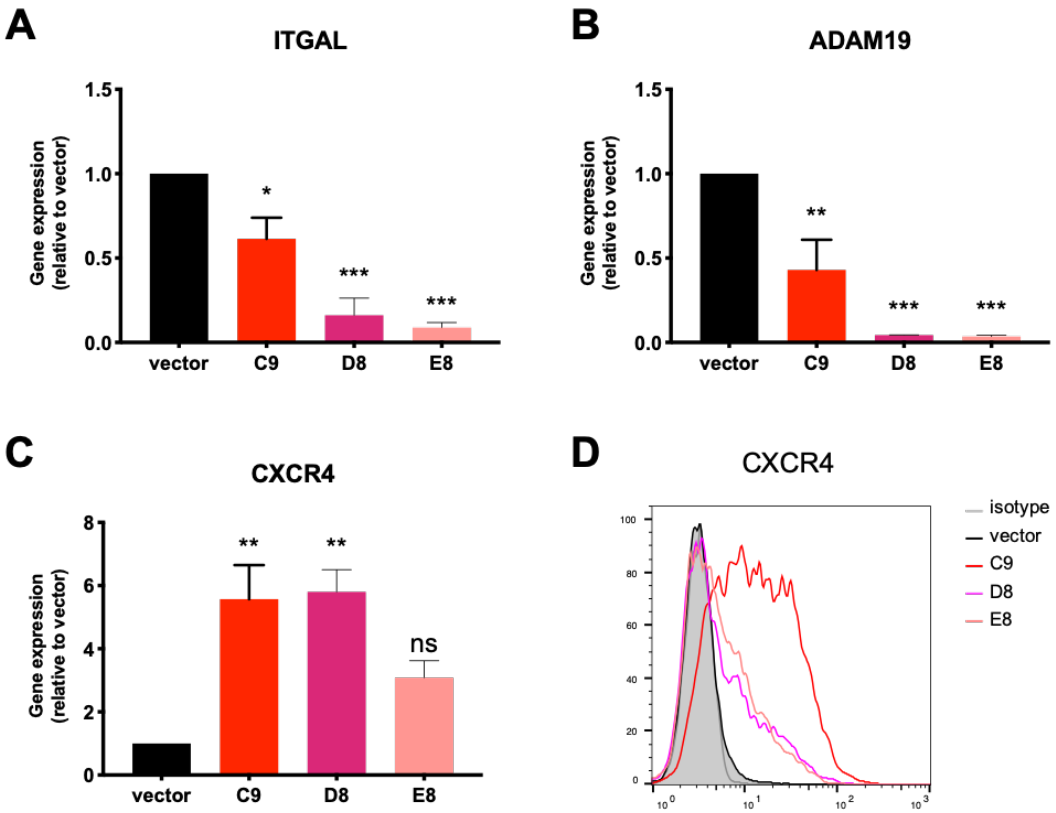

Figure 5-2: Expression of ITGAL, ADAM19 and CXCR4.

Gene expression of **(A)** *ITGAL*, **(B)** *ADAM19* and **(C)** *CXCR4* was identified by qRT-PCR. All values represent mean±SEM, n=3. Statistical significance was analysed using one-way ANOVA with Dunnett's multiple comparisons test where *** = $p<0.001$, ** = $p<0.01$, * = $p<0.05$ and ns=not significant. **(D)** Protein expression of CXCR4 was analysed by flow cytometry. Grey: isotype control; black: vector; red: C9; purple: D8 and pink: E8.

5.2.3 Pyk2 inactivation in CD45^{KO} cells

FAK (gene symbol: *PTK2*) and Pyk2 (gene symbol: *PTK2B*) have been shown to interact with SFKs[293,355]. To investigate their role in MM, the gene expression of *PTK2* and *PTK2B* in OCI-MY1 cells was first analysed. Figure 5-3A shows *PTK2B* was expressed more than *PTK2* by >1300-fold, indicating that Pyk2 is the predominant form of focal adhesion kinase in OCI-MY1 cells. The gene expression of *PTK2B* was comparable in CD45^{WT} (vector) and CD45^{KO} (C9) cells (Figure 5-3B). Next, to demonstrate the interaction between SFKs and Pyk2 in MM cells, cell lysates from CD45^{WT} (vector) and CD45^{KO} (C9) OCI-MY1 cells were immunoprecipitated with an anti-Pyk2 antibody and the resulting immunocomplexes were analysed by immunoblotting (Figure 5-3C). Lyn and Fyn were co-immunoprecipitated with Pyk2 in both CD45^{WT} and CD45^{KO} cells indicating the presence of molecular interaction between Lyn and Fyn with Pyk2 in MM cells regardless of CD45 expression.

Pyk2 activity was then analysed in CD45^{WT} and CD45^{KO} cells. As shown in Figure 5-3D, Pyk2 was slightly less phosphorylated at Y402 in CD45^{KO} cells as compared to CD45^{WT} cells, while the phosphorylation at Y580 was remarkably reduced, especially in clone D8 and E8 (C9: 31.3%, p-value=0.0209; D8: 1.77%, p-value<0.0001; and E8=3.22%, p-value<0.0001; Figure 5-3E). This result suggested that other than the inactivation of SFKs shown in 4.2.1, Pyk2 was also inactivated in CD45^{KO} cells.

5.2.4 Requirement of SFK and Pyk2 activity for MM cell homing

Since both SFKs and Pyk2 are implicated in cell mobility in many cancers and were inactivated in CD45^{KO} cells, the correlation between these two kinases and MM cell homing was investigated. Saracatinib is a selective inhibitor against Src and other SFKs including Lyn and Fyn. As shown in Figure 5-4A, saracatinib inhibited SFKs activity in CD45^{WT} (vector) OCI-MY1 cells in a dose-dependent manner following a 1-hr treatment. Another inhibitor, PF573228, was used to inhibit Pyk2 activity. Similarly, PF573228 inhibited Pyk2 activity in a

dose-dependent manner (Figure 5-4B). $CD45^{WT}$ (vector) OCI-MY1 cells were pre-treated with saracatinib and/or PF375228 for 1hr and subjected to homing assay. Inhibition of SFKs or Pyk2 reduced the homing potential significantly, down to 54.9% (p-value=0.0005) and 38.7% (p-value=0.0009) respectively compared to control; while no significant difference was observed between these two inhibitor-treated cells. Interestingly, combining both inhibitors only further reduced the homing potential to 27.4% (p-value=0.0002) and was not significantly different from the single drug treatments. In addition, treating $CD45^{KO}$ (C9) cells with saracatinib or PF573228 did not further reduce the homing potential, indicating that CD45 mediates homing potential through SFKs and Pyk2.

To differentiate which SFK – Lyn or Fyn – was responsible for homing, $CD45^{WT}$ (vector) OCI-MY1 cells were transfected with siRNA against Lyn or Fyn and subsequently subjected to homing assay. The siRNAs reduced the expression of Lyn and Fyn as shown by immunoblotting (Figure 5-5A). Silencing either Lyn or Fyn by siRNA reduced the homing potential of $CD45^{WT}$ cells to 76.7% (p-value=0.0179) and 55.36% (p-value=0.0028) respectively as compared to control siRNA transfected cells (Figure 5-5B). No significant difference in homing potential was observed between LYN and FYN siRNA transfected cells.

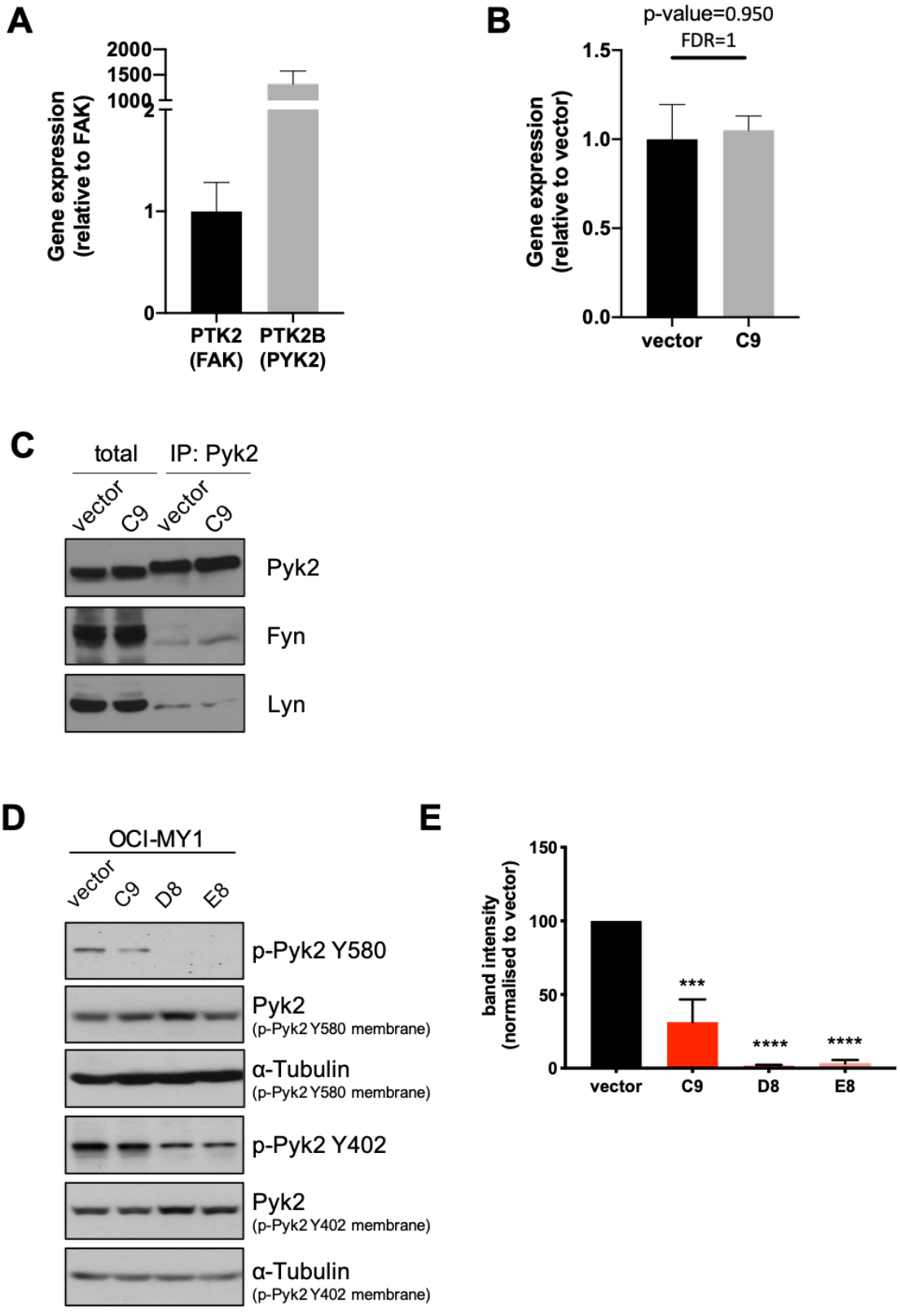
A
Gene expression (relative to FAK)
2000
1500
1000
2
1
0
PTK2 (FAK)
PTK2B (PYK2)
B
p-value=0.950
FDR=1
Gene expression (relative to vector)
1.5
1.0
0.5
0.0
vector
C9
C
total
IP: Pyk2
vector
C9
vector
C9
Pyk2
Fyn
Lyn
D
OCI-MY1
vector
C9
D8
E8
p-Pyk2 Y580
Pyk2
(p-Pyk2 Y580 membrane)
α-Tubulin
(p-Pyk2 Y580 membrane)
p-Pyk2 Y402
Pyk2
(p-Pyk2 Y402 membrane)
α-Tubulin
(p-Pyk2 Y402 membrane)
E
band intensity (normalised to vector)
150
100
50
0
***
****
****
vector
C9
D8
E8

Figure 5-3: Pyk2 inactivation in CD45^{KO} cells.

(A) *In silico* analysis on relative gene expression of *PTK2B* and *PTK2* (normalised to *PTK2)* in OCI-MY1 cells. **(B)** Relative gene expression of *PTK2B* in CD45^{WT} (vector) and CD45^{KO} (C9) OCI-MY1 cells. **(C)** Pyk2 was immunoprecipitated from OCI-MY1 CD45^{WT} (vector) and CD45^{KO} (C9) cell lysates and probed for Fyn and Lyn. Total lysates were loaded for comparison. **(D)** Representative images of phosphorylation of Pyk2 at Y580 and Y402. **(E)** Quantification of p-Pyk2 Y580 was performed by densitometry and normalised to total Pyk2 expression and the vector control. All values represent mean±SEM, n=3. Statistical significance was analysed using one-way ANOVA with Dunnett's multiple comparisons test where ∗∗∗∗ = $p<0.0001$ and ∗∗∗ = $p<0.001$.

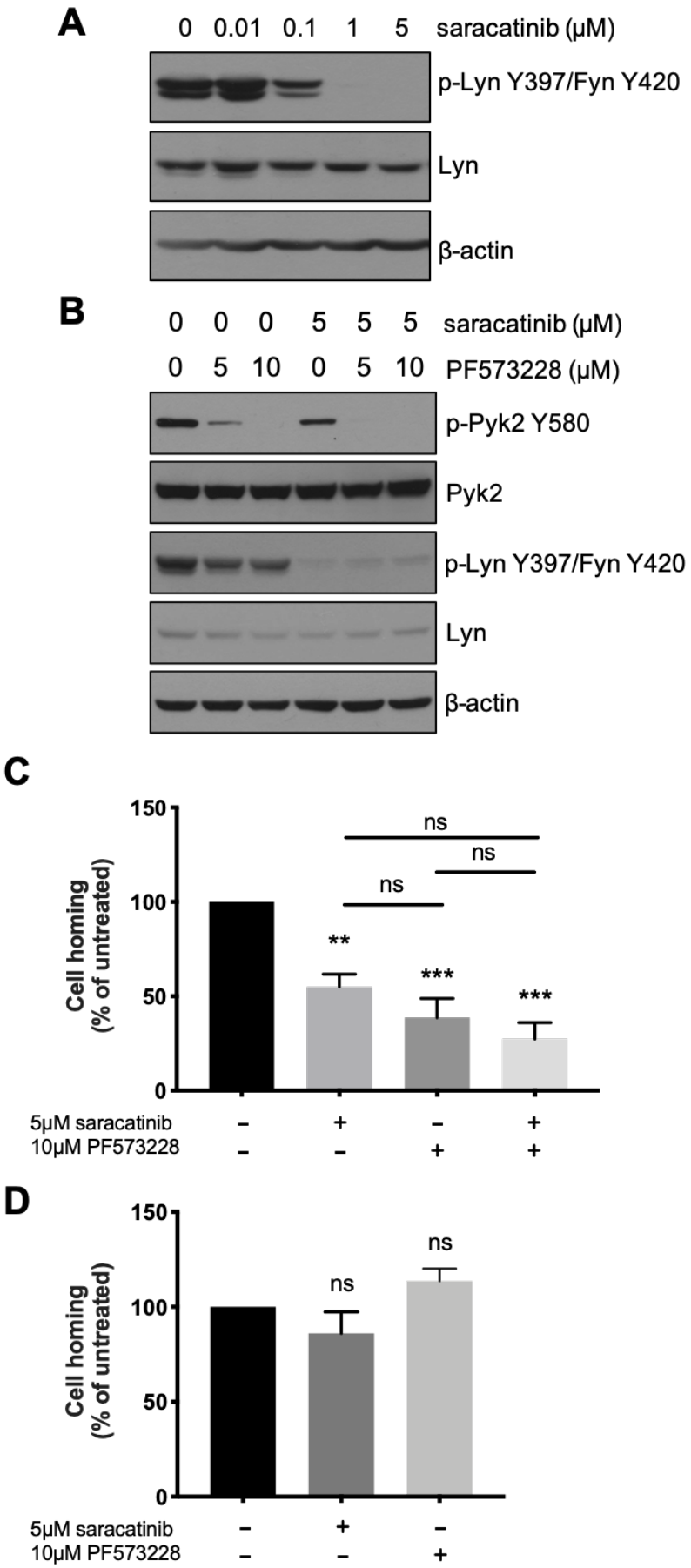
A
0 0.01 0.1 1 5 saracatinib (μM)
p-Lyn Y397/Fyn Y420
Lyn
β-actin
B
0 0 0 5 5 5 saracatinib (μM)
0 5 10 0 5 10 PF573228 (μM)
p-Pyk2 Y580
Pyk2
p-Lyn Y397/Fyn Y420
Lyn
β-actin
C
Cell homing (% of untreated)
150
100
50
0
ns
ns
ns
**
***
***
5μM saracatinib – + – +
10μM PF573228 – – + +
D
Cell homing (% of untreated)
150
100
50
0
ns
ns
5μM saracatinib – + –
10μM PF573228 – – +

Figure 5-4: Pharmacological inhibition of SFK and Pyk2 reduced homing potential in CD45^{WT} cells.

(A) CD45^{WT} (vector) OCI-MY1 cells were incubated with 0.01, 0.1, 1 and 5μM saracatinib for 1hr and the activity of SFK was assessed by immunoblotting. **(B)** CD45^{WT} (vector) OCI-MY1 cells were treated with the indicated concentrations of saracatinib and/or PF573228 for 1hr, followed by immunoblotting analysis with β-actin as the loading control. **(C)** CD45^{WT} (vector) and **(D)** CD45^{KO} (C9) OCI-MY1 cells were pre-treated with 5μM saracatinib and/or 10μM PF573228 for 1hr before assessing the homing potential by modified Boyden chamber assay. All values represent mean±SEM, n=3. Statistical significance was analysed using one-way ANOVA with Tukey's multiple comparisons test for **(C)** or Dunnett's multiple comparisons test for **(D)** where ∗∗∗ = $p<0.001$, ∗∗ = $p<0.01$ and ns = not significant.

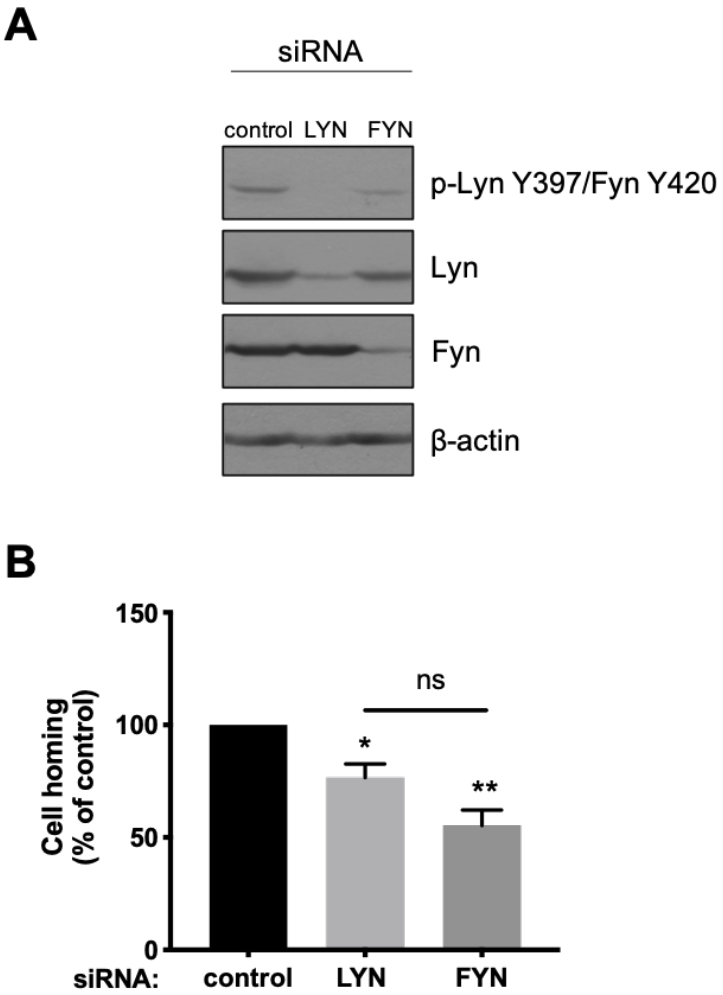

Figure 5-5: Reduction in homing potential by silencing Lyn and Fyn.

(A) $CD45^{WT}$ (vector) OCI-MY1 cells were transfected with 20nM siRNA targeting LYN or FYN for 72hr. The downregulation of Lyn and Fyn expression was verified by immunoblotting with β-actin as loading control. **(B)** Silencing either Lyn or Fyn reduced the homing potential of $CD45^{WT}$ (vector) OCI-MY1 cells as compared to control siRNA transfected cells. All values represent mean±SEM, n=3. Statistical significance was analysed using one-way ANOVA with Tukey's multiple comparisons test where ∗∗ = $p<0.01$, ∗ = $p<0.05$ and ns = not significant.

5.2.5 Delayed engraftment of CD45^{KO} cells *in vivo*

To translate the *in vitro* difference in homing potential into a physiological setting, we examined the tumour progression in mouse xenograft models. GFP^{+} Luc^{+} CD45^{WT} (vector) and CD45^{KO} (C9) OCI-MY1 cells were injected intravenously into NSG mice (n=6 per group) and the tumour development was monitored weekly by bioluminescence for 35 days. Disease was evident 7 days after injection in 5/6 of the CD45^{WT} cell-bearing mice but only in 3/6 of the CD45^{KO} cell-bearing mice (Figure 5-6A), suggesting that the loss of CD45 expression impaired the *in vivo* engraftment. The CD45^{WT} cell-bearing mice also appeared to have higher tumour burden. All mice showed detectable disease 14 days after injection and the tumours continued to develop exponentially throughout the course of the experiment. Higher tumour burden was detected among the CD45^{WT} cell-bearing mice at the end-point, as shown in both bioluminescence (Figure 5-6B) and serum β-2-microglobulin level (Figure 5-6C) in spite of not reaching statistical significance (p-value=0.1248).

5.2.6 Higher metastatic potential of CD45^{KO} cells *in vivo*

To further investigate the role of CD45 in disease progression *in vivo*, we performed a pilot study using the intratibial injection method. Direct inoculation of MM cells into the BM allows better representation of the clinical manifestations of early MM. GFP^{+} Luc^{+} CD45^{WT} (vector) and CD45^{KO} (C9) OCI-MY1 cells were injected into the tibial cavity of NSG mice (n=5 per group). Similar to the intravenous injection study, CD45^{WT} cells engrafted more efficiently than CD45^{KO} cells: all five mice injected with CD45^{WT} cells established detectable disease seven days after injection compared to only two mice with CD45^{KO} cells (Figure 5-7A). The average time taken for engraftment was seven days in the CD45^{WT} group compared to 15.4 days in the CD45^{KO} group (p-value=0.0125). Although CD45^{KO} cells required a longer time to engraft, these cells metastasised to other areas much earlier than CD45^{WT} cells. Metastasis was observed in 4/5 of the CD45^{KO} cell-injected mice an average of 29 days after injection whereas 3/5 of the CD45^{WT} cell-injected mice

developed metastasis 30 days after engraftment. The difference in the time of metastasis was more pronounced if the time of engraftment was considered: 23 days from engraftment for $CD45^{WT}$ cells compared to 16.75 days for $CD45^{KO}$ cells (Figure 5-7C-F). Moreover, from the bioluminescence images and visual inspection during autopsies, we observed that $CD45^{KO}$ cells induced a wider spread of disease. Other than kidneys, spleens and preputial glands, $CD45^{KO}$ cells were also found in salivary glands and the intrascapular region (Figure 5-7G). These results indicate that the loss of CD45 expression promotes the metastatic potential of MM.

5.2.7 Heterogenous CD45 expression in the $CD45^{WT}$ cell-recipient mice

Given that metastatic disease was also detected in the $CD45^{WT}$ cell-injected mice but only at the latter stage of disease in our intratibial injection experiment (5.2.6), we speculated that $CD45^{WT}$ cells underwent clonal evolution along the disease progression. To test this notion, the right tibiae of NSG mice (n=5) were inoculated with GFP^+ Luc^+ $CD45^{WT}$ (vector) OCI-MY1 cells. Upon the mice reaching the terminal stage, GFP^+ cells from the BM and other organs commonly involved in MM were isolated and phenotyped for CD45 expression (Figure 5-8A). Other than the right tibiae, GFP^+ cells were also detected in the BM from the left tibiae and femurs (3/5), peripheral blood (2/5), livers (3/5), spleens (3/5) and lungs (1/5). Although the injected cells consisted of over 95% of $CD45^+$ cells, the detected MM cells in the BM as well as in the different organs demonstrated heterogeneous CD45 expression profiles. Specifically, in mice #2 and #3, only 31.7% and 57.7% of detected cells in the tumour or BM isolated from the right tibiae and femurs expressed CD45. Interestingly, although the tumour on the right leg of mouse #4 contained 95.3% of $CD45^+$ cells, other organs including peripheral blood, spleen and liver, had much lower percentages of $CD45^+$ cells (25.7-60.6%). The percentages of GFP^+ OCI-MY1 cells from different organs expressing CD45 are shown in Figure 5-8B.

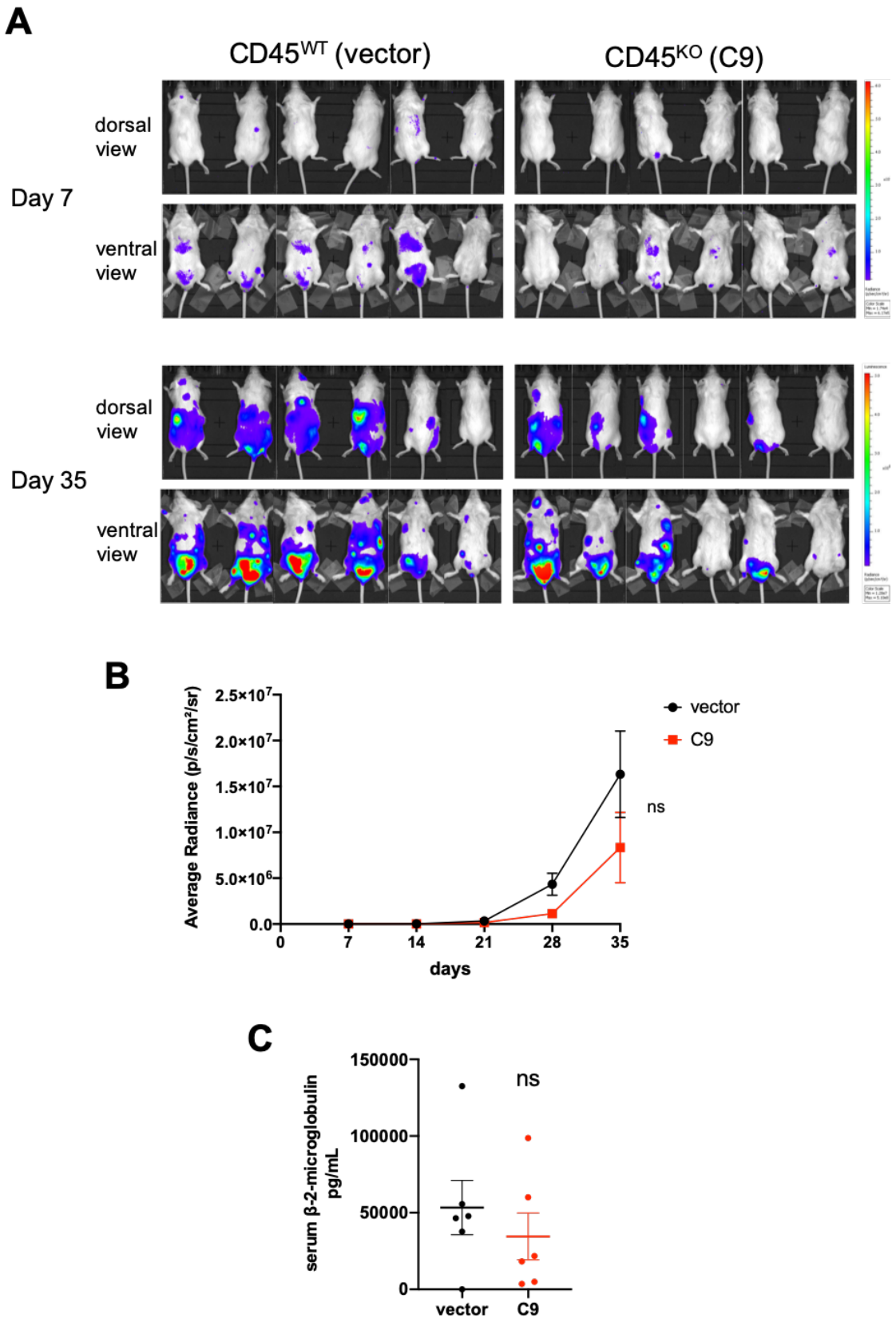
A
CD45WT (vector)
CD45KO (C9)
dorsal view
ventral view
Day 7
Day 35
B
Average Radiance (p/s/cm²/sr)
2.5×10⁷
2.0×10⁷
1.5×10⁷
1.0×10⁷
5.0×10⁶
0.0
0
7
14
21
28
35
days
vector
C9
ns
C
serum β-2-microglobulin pg/mL
150000
100000
50000
0
vector
C9
ns

Figure 5-6: Delayed engraftment of $CD45^{KO}$ cells in NSG mice.

$CD45^{WT}$ (vector) and $CD45^{KO}$ (C9) OCI-MY1 cells were injected intravenously into NSG mice (n=6/group). Tumour growth was monitored by bioluminescence imaging weekly. **(A)** Bioluminescence images of dorsal and ventral view of Day 7 and 35 were shown. Colour scales of radiance were set at $1.74x10^4$ to $6.17x10^5$ for Day 7 and $1.28x10^7$ to $5.18x10^8$ (photons/second/cm^2/steradian) for Day 35. Higher tumour burden as in **(B)** radiance and **(C)** serum β-2-microglobulin was observed in $CD45^{WT}$ group. All values represent mean±SEM, n=6.

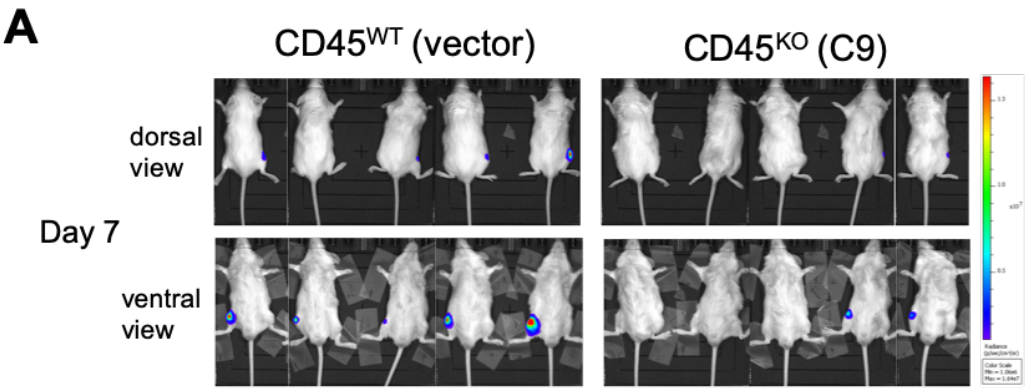

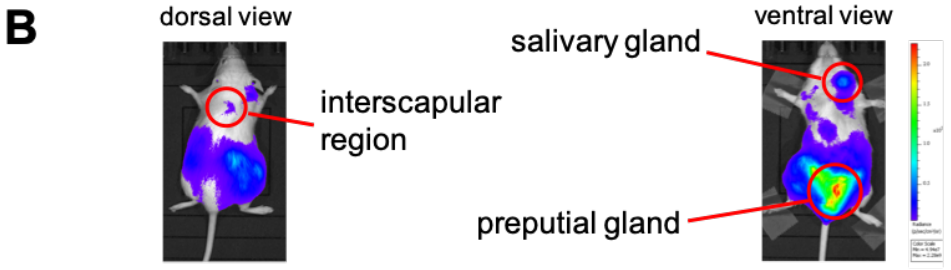

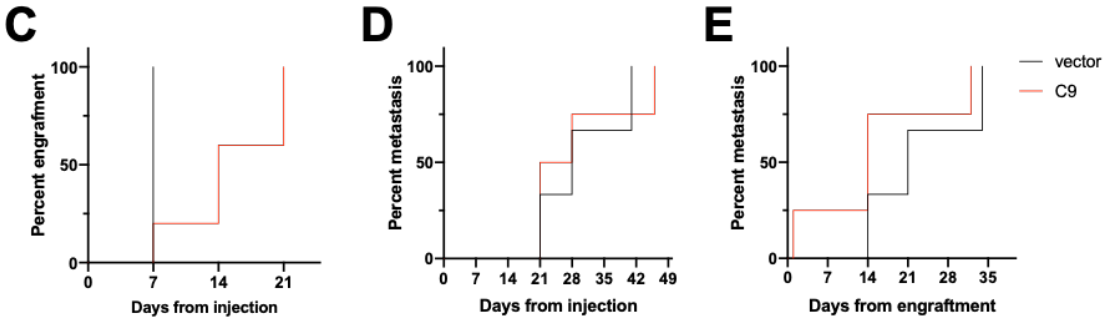

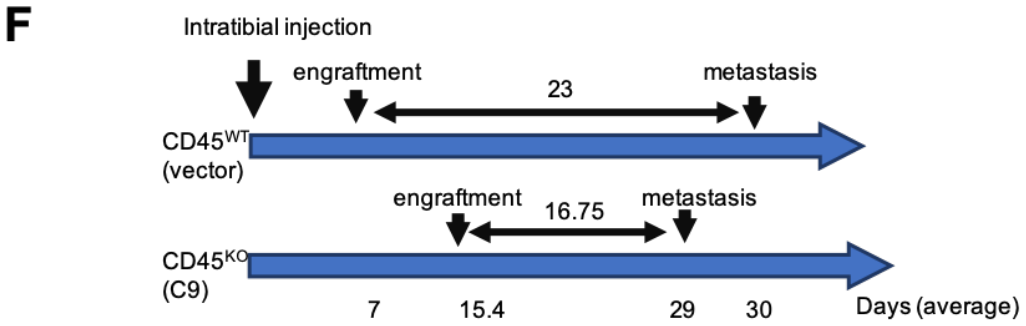

G

Group	Days to engraft (mean±SEM)	Days to develop metastasis from injection (mean±SEM)	Days to develop metastasis from engraftment (mean±SEM)	Metastatic sites
CD45^{WT} (vector) (n=5)	7 ± 0	30 ± 5.859	23 ± 5.859	Kidneys (1/3) spleen (2/3) preputial glands (2/3)
CD45^{KO} (C9) (n=5)	15. ± 4 2.619	29 ± 5.902	16.75 ± 5.344	Kidneys (2/4) spleen (2/4) preputial glands (3/4) salivary glands (1/4) interscapular region (1/4)

Figure 5-7: Higher metastatic potential of $CD45^{KO}$ cells in NSG mice.

(A) Bioluminescence images of dorsal and ventral view of mice 7 days after intratibial injection of $CD45^{WT}$ (vector) and $CD45^{KO}$ (C9) OCI-MY1 cells. Colour scale of radiance was set at $5.03x10^5$ to $1.64x10^7$ (photons/second/cm^2/steradian). **(B)** Representative bioluminescence images of dorsal and ventral view of a $CD45^{KO}$ cell inoculated mouse on Day 41. Red circles indicate the metastatic sites: preputial gland, salivary gland and the interscapular region. Colour scale of radiance were set at $4.94x10^7$ to $2.28x10^9$ (photons/second/cm^2/steradian). **(C)** Cumulative incidence curve of engraftment. **(D)** Cumulative incidence curve of metastasis from injection. **(E)** Cumulative incidence curve of metastasis from engraftment. **(F)** Schematic timeline shows the time of engraftment and metastasis (not to scale). **(G)** Table summarises the days taken for engraftment and metastasis.

A

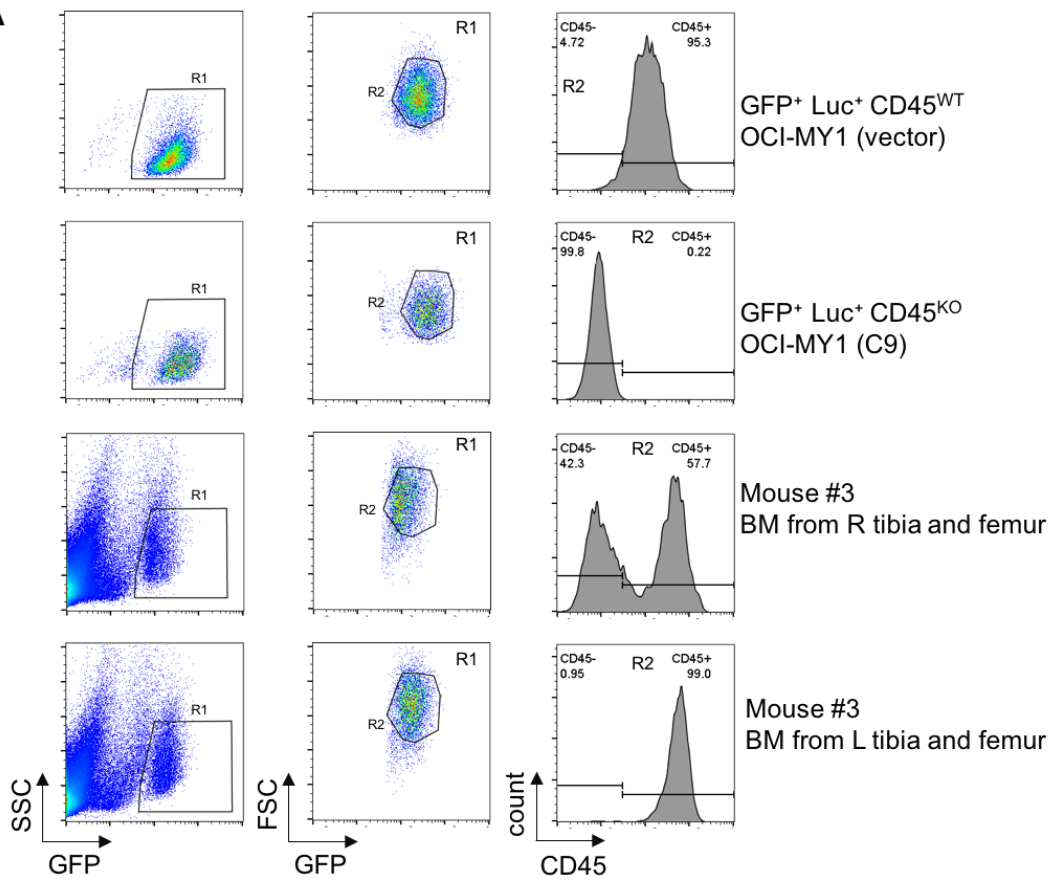

B

Mouse #	tumour on R leg	BM from L tibia and femur	PB	liver	spleen	lung
1	86.9%	100.0%	n.d.	92.7%	99.4%	n.d.
2	31.7%	n.d.	n.d.	78.4%	n.d.	n.d.
3	* 57.7%	99.0%	77.1%	88.6%	99.6%	n.d.
4	95.3%	80.0%	25.7%	n.d.	60.6%	33.4%
5	69.6%	n.d.	n.d.	n.d.	n.d.	n.d.

Figure 5-8: Expression of CD45 on MM cells isolated from CD45^{WT} cell-bearing mice.

(A) GFP$^+$ Luc$^+$ CD45^{WT} OCI-MY1 cells from different organs were identified by SSC^{low} GFP$^+$ (R1) and FSC$^{mid-high}$ GFP$^+$ (R2) in flow cytometry analysis. GFP$^+$ Luc$^+$ CD45^{WT} and CD45^{KO} (C9) OCI-MY1 in tissue culture were used as controls (top 2 panels). BM from the right (R) and left (L) tibiae and femurs of mouse #3 were shown as examples (bottom 2 panels). **(B)** Table summarises the percentages of GFP$^+$ CD45^{WT} OCI-MY1 cells from different organs expressing CD45. (* no visible tumour, BM was analysed; n.d.=not detected)

5.3 Discussion

MM is a unique haematological malignancy that is generally located in the BM and highly dependent on the BMME for proliferation and survival. The presence of circulating MM cells and multiple BM lesions even at the early stage of the disease suggest that MM cells are capable of extravasating into blood circulation and homing to new BM niches. This homing process is highly selective as has been demonstrated in the 5T mouse model by K. Asosingh et al.[286]. Although the authors concluded that $CD45^-$ cells had impaired homing and invasive capacity[287], the underlying molecular mechanisms remained largely unknown. Further investigation of this phenomenon was hindered by the inter-cell line heterogeneity. We have overcome this issue by using our $CD45^{KO}$ models. The subsequent transcriptome analysis (4.2.7) suggests that the biological processes related to cell adhesion and mobility are dysregulated in the absence of CD45 expression, corroborating the role of CD45 in MM cell mobility. This Chapter investigated the *in vitro* homing potential of $CD45^{WT}$ and $CD45^{KO}$ cells and its mechanisms, as well as its implication in mouse models.

As mentioned in 1.2.5.4, the homing process requires MM cells to first adhere to the endothelium and then penetrate through the subendothelial membrane by degrading the basement membrane. By using BMSCs as the chemoattractant, the homing potential and the adhesion capacity of $CD45^{WT}$ and $CD45^{KO}$ cells were first compared. The reduction in homing potential of $CD45^{KO}$ cells not only recapitulates the differential *in vitro* homing between $CD45^+$ and $CD45^-$ murine MM cells[287] but also justifies the validity of our CRISPR/Cas9-mediated KO models. We assessed the ability of MM cells digesting extracellular matrix by using Matrigel-coated Transwell inserts. Matrigel is a mixture of extracellular proteins including laminin, collagen and other protein growth factors, and is often used to resemble the basement membrane and extracellular matrix environment[356]. The addition of Matrigel further reduced the homing potential of $CD45^{KO}$ cells by nearly 50%, suggesting their inability in digesting basement membrane and low invasive capacity.

Unexpectedly, no significant difference in adhesion to BMSCs was observed

between $CD45^{WT}$ and $CD45^{KO}$ cells despite the substantial difference in homing as well as the dysregulation in gene expression associated with the GO annotation 'focal adhesion'. It could be possible that the adhesion of MM cells to HS5 reached a plateau at the end of the experiment. Future studies should repeat the adhesion experiment with earlier timepoints to confirm these findings. Additionally, the lack of difference in adhesion could be explained by the minimal changes in the gene expression of adhesion molecules. We showed that *ITGAL* was the only one among the cell surface adhesion molecules downregulated. *ITGAL* encodes the integrin alpha L chain, also known as CD11a or lymphocyte function-associated antigen 1 (LFA-1), which plays an important role in leukocyte adhesion and migration via the interaction with its ligand ICAMs[357]. It has been shown that blocking either CD11a or ICAM-1 impaired the T cell migration in thymic medulla[358]. Moreover, circulating MM cells have demonstrated a lower CD11a expression than their BM counterparts[124], indicating that CD11a could also participate in the MM homing process. However, we believe that cell adhesion is a far more complicated process that requires the interactions between multiple ligands and receptors, it cannot simply be altered by the dysregulation of *ITGAL* per se. Of note, the decreased protein expression of CD11a has also been reported in primary $CD45^{+}$ MM cells[297]. Future studies should investigate the protein expression of CD11a in $CD45^{WT}$ and $CD45^{KO}$ MM cells as well as their adhesion to ICAM-expressing cells, such as BMSCs.

In addition to adhesion molecules, we analysed the gene expression of proteolytic enzymes, chemokine ligands and receptors, and found that *ADAM19* and *MMP17* were downregulated whereas CXCR4 were upregulated (p-value and FDR<0.05). ADAM19 (a disintegrin and metalloprotease 19) and MMP17 are transmembrane proteases which involve in various tumour invasion and metastasis processes[133,359]. Although very little is known about the functions of these two particular proteases, their family members, such as ADAM10, ADAM17[360] and MMP9 are correlated with aggressive diseases. Of note, the downregulation of MMP9 has been observed in $CD45^{-}$ 5T murine MM cells, as mentioned in 1.4.3. The upregulation of CXCR4 in $CD45^{KO}$ cells, however, appears to contradict with previous publications – the increase in CXCR4

expression generally favours the migration of haemopoietic cells, either healthy or malignant, to the BM[151,361,362]. Indeed, BMSCs secrete high levels of CXCR4 ligand, SDF-1, to attract haemopoietic cells; and CXCR4 antagonists have been used in mobilising stem cells for leukemia and MM treatment[149,362]. SDF-1 is also secreted by other organs, such as liver, kidney and central nervous system[151]. High expression of CXCR4 has been paradoxically correlated to extramedullary disease in childhood acute lymphoblastic leukemia[363]. In MM cells, overexpression of CXCR4 has been shown to favour the cell dissemination from bone to liver rather than bone to bone[364]. Furthermore, an elevated CXCR4 protein expression was evident in PB MM cells compared to the matched BM MM cells in patient samples in 2 separate studies[124,365]. These results indicate that the increase in CXCR4 expression does not always guarantee an increase in BM homing; instead it could promote extramedullary progression.

Apart from the inactivation of SFKs (4.2.1), $CD45^{KO}$ cells also exhibited Pyk2 inactivation as determined by the phosphorylation level at the activating tyrosine residues. It has been shown in the literature that Pyk2 autophosphorylates at Y402 to provide a docking site for SFKs; the binding of SKFs further phosphorylates Pyk2 at Y402 and Y580[291]. In support of this, we were able to detect the interaction between Pyk2 and Lyn/Fyn in both $CD45^{WT}$ and $CD45^{KO}$ cells by immunoprecipitation, and the phosphorylation levels of Pyk2 at Y402 and Y580 were lower in $CD45^{KO}$ cells (which also had low SFK activity). We also observed a slight decrease in phosphorylation of Pyk2 under SFK inhibition and vice versa in $CD45^{WT}$ cells, further suggesting their reciprocal relationship. Pyk2 overexpression has been reported in all stages of MM and correlated to disease progression[353]. Although we did not see any difference in Pyk2 expression between the CD45 phenotypes, we demonstrated the activating phosphorylation of Pyk2 was abolished by the loss of CD45 expression, in part via SFKs.

The downregulation of both SFKs and Pyk2 provided us a sound rationale to investigate their correlation to the homing process, given their role in cell migration and invasion[348,366]. Treatment of $CD45^{WT}$ cells with either saracatinib

or PF573228 replicated the reduced homing potential observed in $CD45^{KO}$ cells, while the combined treatment did not exert any synergistic effect on the homing potential. We proposed that CD45 mediated the homing potential through SFKs and Pyk2. This concept is supported by the lack of effect of saracatinib and PF573228 on $CD45^{KO}$ (C9) cells, in which SFK and Pyk2 are already inactivated. Our loss-of-function study demonstrated that both Lyn and Fyn were involved in the homing process which is not to our surprise as both kinases have been implicated in cell migration in other cancers[367,368].

To translate our *in vitro* findings into *in vivo* settings, we introduced $CD45^{WT}$ and $CD45^{KO}$ cells intravenously and intratibially into NSG mice and compared the tumour development. Intravenous injection is perhaps the most commonly used technique for *in vivo* haemopoietic studies. However, as MM cells are predominately residing in the BM, this technique does not truly reproduce the human disease development in mice; it can only represent the late stage of the disease at which MM cells extravasate into blood circulation. On the other hand, intratibial injection directly introduces the cells of interest into the BM cavity and is more suitable to study the interaction between target cells and BMME. We demonstrated that the loss of CD45 expression hindered the tumour engraftment and development in the intravenous injection model. This result concurs with our *in vitro* findings that $CD45^{KO}$ cells had reduced homing potential. Such delay in engraftment could be explained by the Pyk2 inactivation in $CD45^{KO}$ cells as similar observations were reported in a study showing that Pyk2 silencing delayed MM tumour growth in a mouse xenograft model with intravenous injection[353]. Although there is no direct evidence backing the correlation between SFKs and tumour engraftment, the inhibition of SFKs by saracatinib has shown anti-tumour effect *in vivo* in other cancers[369–371], indicating that the SFK inactivation in $CD45^{KO}$ cells may also contribute to the decreased tumour growth.

Similarly, delayed engraftment also occurred in the intratibial injection model. $CD45^{KO}$ cells took double the time to establish detectable disease in mice in spite of the direct BM inoculation. This observation is consistent with the slow proliferation in the methylcellulose-based semi-solid culture as we

demonstrated previously (4.2.3). More importantly, the $CD45^{KO}$ cell-bearing mice developed metastatic disease much earlier than their counterparts regardless of the time of injection or engraftment. In addition to spleens, kidneys and preputial glands, $CD45^{KO}$ cells were found in the salivary glands and the interscapular region. We speculate that the growth factors produced by salivary glands and the proximity of salivary glands to lymph nodes attracted MM cells[372]. Moreover, the intercapular region in rodents is the home of brown adipose tissues, which carry a large amount of lipids and glucose for thermoregulation and produce a variety of cytokines including IL-6[373]. These conditions provide a perfect niche for malignant cell growth and in our case $CD45^{KO}$ cells. However, our speculations remain unexplored.

We further analysed the expression of CD45 in the MM cells isolated from the $CD45^{WT}$ cell-bearing mice and showed the heterogenous CD45 expression in different organs and even at the injected site. We postulate that the $CD45^{WT}$ cells in mice underwent *in vivo* differentiation from $CD45^{+}$ into $CD45^{-}$. Similar *in vivo* differentiation had been reported by K. Asosingh et al. who showed that a proportion of $CD45^{+}$ cells differentiated into $CD45^{-}$ cells and vice versa in the 5TMM murine MM models[286]. They also demonstrated the gradual loss of CD45 expression during disease progression in mice[296]. We were able to show a similar phenomenon with human MM cells. This shift of $CD45^{+}$ to $CD45^{-}$ phenotype can also be explained by the outgrowth of the small population of $CD45^{-}$ cells (<5%) in the $CD45^{WT}$ OCI-MY1 cells. Although the two CD45 phenotypes did not show any significant difference in proliferation *in vitro* (4.2.2), the complicated microenvironment in different organs *in vivo* may provide the perfect niche for $CD45^{-}$ cells. This differentiation or shift in CD45 expression could be a part of clonal evolution of MM cells (reviewed by G. Morgan et al.[19]). It could also be explained by the exposure of microenvironment stimuli, such as hypoxia, growth factors and BMSCs, which might contribute to the CD45 plasticity of these cells (see 1.4.1). We believe that losing CD45 expression might provide survival advantages and metastatic capacity. Unfortunately, we did not see a clear migratory pattern in the detected $CD45^{-}$ cells. Due to the small number of mice used, we could not perform statistical analysis on the intravenous and intratibial studies. Nevertheless, we

provided the evidence that $CD45^{KO}$ cells have lower BM homing but higher metastatic capacity than $CD45^{WT}$ cells, as well as the differentiation and shift of $CD45^{+}$ cells into $CD45^{-}$ cells *in vivo.*

In conclusion, this Chapter demonstrates that the loss of CD45 expression reduces the BM homing potential but not the adhesion capacity of MM cells. We also established the mechanism of this phenomenon: CD45 has a novel role in Pyk2 activation and that Pyk2 together with SFK activity are required for MM homing. The difference in BM homing can be translated into murine models in which $CD45^{KO}$ cells display delayed engraftment but higher metastatic potential. We also demonstrated the *in vivo* differentiation of $CD45^{+}$ cells into $CD45^{-}$ cells. Taken together, we provided the evidence that $CD45^{-}$ phenotype represents a more metastatic disease and further investigations on preventing metastasis in $CD45^{-}$ patients are highly anticipated.

CHAPTER 6:
GENERAL DISCUSSION

6.1 Summary of key findings

MM is an incurable plasma cell dyscrasia predominantly located in the BM. The homing of MM cells from the post-germinal centres to BM is regarded as the fundamental step to develop a symptomatic disease, as such immense efforts have been spent on addressing the regulation of this homing process. MM cells are known for their variable CD45 phenotypes of which $CD45^-$ cells have lower homing potential and induce higher tumour burden in mouse models[286]. Further investigations suggest $CD45^-$ cells have impaired chemotaxis towards BM and lower expression of extracellular matrix proteases than $CD45^+$ cells, resulting in the differential *in vivo* homing[287]. $CD45^+$ cells have also been characterised as more proliferative and sensitive to treatment[274,275,281,285]. In fact, CD45 expression carries a significant prognostic value in disease outcome. Patients with $CD45^-$ phenotype have been associated with shorter overall survival and poor response to the conventional treatments[297,298], but the more recent studies suggest the opposite[299,300]. These contradictory observations emphasise the need to properly define the role of CD45 in MM.

This project was designed to investigate the biological role of CD45 in MM and the underlying mechanisms accounting for the differences between the CD45 phenotypes. We hypothesised that firstly, $CD45^-$ phenotype represents a more advanced or aggressive disease in MM, and secondly, $CD45^-$ phenotype represents a more metastatic disease. Given that MM cell lines possess diverse cytogenetic backgrounds, we employed genome-editing technology to modify CD45 expression for this study, thereby avoiding the inter-cell line heterogeneity.

Chapter 3 aimed to establish $CD45^{KO}$ models using CRISPR/Cas9 genome editing. We first evaluated CD45 expression in a panel of 34 HMCLs and showed that the majority of HMCLs carry $CD45^-$ phenotype as suggested in previous reports. We selected 5 HMCLs with high percentages of CD45 expressing cells (above 73.9%) for genome editing by introducing Cas9 and a gRNA specific to CD45. It is interesting that some cells expressed the cytoplasmic portion of CD45 despite the loss of expression of the extracellular

portion. We then isolated the monoclonal populations of $CD45^{KO}$ cells and confirmed the complete loss of CD45 expression by immunoblotting, immunofluorescence and flow cytometry. These $CD45^{KO}$ cells and their respective $CD45^{WT}$ vector control cells were the basis for the subsequent characterisation and functional studies.

Chapter 4 focused on identifying the biological differences between $CD45^{WT}$ and $CD45^{KO}$ cells, particularly in SFK activity, proliferation under different culture conditions and transcriptional differences. We first compared the activity of the well-established CD45 downstream target, SFKs. All $CD45^{KO}$ cells exhibited lower SFK activity as determined by the reduced phosphorylation at the activating tyrosine residue, confirming the loss of CD45 phosphatase activity in these cells. We hypothesised that $CD45^{KO}$ cells would have proliferation and survival advantage in different culture conditions so as to contribute to an aggressive disease. However, we did not observe any significant changes in proliferation in all the liquid culture conditions tested, except for TK2 in the complete medium and U266 in the glutamine-free medium. Moreover, we investigated the two key cytokine signalling pathways, IL-6 and IGF-1, as well as the level of autophagy in $CD45^{KO}$ cells, and we did not find any significant differences in these pathways. Whilst very little difference was found in the liquid culture conditions, $CD45^{KO}$ cells were less clonogenic and less proliferative than $CD45^{WT}$ cells in the methylcellulose-based semi-solid culture. Unlike other studies suggested, $CD45^{WT}$ and $CD45^{KO}$ cells shared the same phenotypic signature with mature plasma cells ($CD19^{-}$ $CD20^{-}$ $CD38^{+}$ $CD138^{+}$) regardless of their difference in clonogenic potential. Our transcriptome analysis not only confirmed the loss of CD45 gene expression but also revealed that the differentially expressed genes were significantly enriched in the GO annotations related to cell mobility, such as focal adhesion (GO: 0005925) and cell-matrix adhesion (GO: 0007160). Additionally, KEGG pathway analysis showed the differentially expressed genes enriched in the pathways of ‘proteoglycans in cancer’ (hsa05205) and ‘ErbB signalling pathway’ (hsa04012). Both pathways contribute to cell mobility, angiogenesis and tumour progression, highlighting the potential role of CD45 in these areas.

Given the reported differential *in vivo* homing potential in murine MM cells and our results in the transcriptional changes in cell mobility-related pathways, we interrogated the homing process of $CD45^{WT}$ and $CD45^{KO}$ cells in Chapter 5. We demonstrated that $CD45^{KO}$ cells had substantially lower homing potential towards BMSCs and impaired invasive capacity through the extracellular matrix. These observations agree with previous studies[287]. Extensive analysis of gene expression of adhesion molecules, extracellular matrix proteases and chemokine receptors identified the dysregulation of *ITGAL, MMP17*, *ADAM19*, and *CXCR4*. We also demonstrated that Pyk2 was inactivated in $CD45^{KO}$ cells and it was partially due to the inactivation of SFKs. More importantly, we provided the first evidence that CD45 mediated the homing process through SFKs and Pyk2 from our loss-of-function studies. Furthermore, we adopted the intravenous and intratibial injection approaches to reproduce the different stages of human disease development in mice. We showed that the tumour engraftment in NSG mice was hindered by the loss of CD45 expression, as suggested by the reduced *in vitro* homing potential. The tumour growth in $CD45^{KO}$ cell-bearing mice was also slower than the $CD45^{WT}$ cell-bearing mice. Notably, $CD45^{KO}$ cells induced earlier metastasis and wider spread of disease. We observed additional metastatic sites in the $CD45^{KO}$ cell-inoculated mice but not in the $CD45^{WT}$ cell-inoculated mice. We also demonstrated the *in vivo* differentiation of $CD45^{+}$ cells into $CD45^{-}$cells.

Together, these results support our hypothesis that $CD45^{-}$ phenotype represents a more metastatic disease. This thesis provides valuable insights into the biological differences between CD45 phenotypes and the role of CD45 in MM progression.

6.2 CD45 as a phosphatase

Although the functions of CD45 in T and B cells have been well-established, the characterisation of CD45 in MM is fairly limited. CD45 has been overlooked and simply used as a cell surface marker in MM until the discovery of differential homing potential and proliferation between CD45 phenotypes. In this study, we demonstrated that CD45 functions as a protein tyrosine phosphatase to mediate

other kinases, particularly SFKs and Pyk2. This phosphatase activity is independent of the extracellular domain as suggested in a recombinant CD45 protein study[213]. It is interesting to note that we discovered a relatively small number of differentially expressed genes as opposed to other transcriptome analyses. This implies that CD45 exerts very few effects on gene transcription. Instead, we found striking differences in SFKs and Pyk2 phosphorylation while their gene and protein expression remained unchanged. Our finding suggests that genomics and perhaps proteomics may not suffice for CD45 study. Future studies should focus on the use of phosphoproteomics to identify other potential direct and indirect targets of CD45. Additionally, this technique can be applied to the characterisation of CD45-mediated signalling pathways in cell lines and patient samples[374].

6.3 CD45/SFKs/Pyk2 signalling cascade in MM homing

Previous mechanistic study on the role of CD45 in MM homing suggested that $CD45^-$ cells had impaired chemotaxis towards BM and had low expression of extracellular matrix proteases[287]. This study is the first to show a CD45/SFKs/Pyk2 signalling cascade that regulates the MM homing process (Figure 6-1). CD45 dephosphorylates the inhibitory tyrosine site of SFKs leading to the autophosphorylation at the kinase domain. The fully activated SFKs then bind to and activate Pyk2 in order to conduct the homing signalling. It should be noted that, although SFKs and Pyk2 are known to cross-activate, inhibition of SFKs by saracatinib only slightly reduced Pyk2 activity, suggesting that SFKs are not the sole activators of Pyk2 in MM. We postulate that Pyk2 is either directly activated by CD45 in a similar fashion to SFKs – possessing an inhibitory and an activating site; or by an unknown protein that is sensitive to CD45. Indeed, FAK, another focal adhesion kinase that is functionally and structurally related to Pyk2, has been shown to share a similar autoinhibition mechanism with SFKs. The activation of FAK requires the displacement of FERM domain from the kinase domain followed by the autophosphorylation at Y397 (Y402 in Pyk2) and the binding of Src to phosphorylate additional sites[375].

Although the authors did not characterise this displacement, it is tempting to speculate that CD45 is involved in this process. Future studies dissecting the molecular interaction between CD45 and Pyk2 will be valuable in understanding the functions of CD45 in this aspect and designing strategies to target this cascade.

In this study, although we presented the CD45/SFKs/Pyk2 cascade in MM homing, we did not touch on the downstream targets that led to cell mobility. There is a large body of evidence indicating that the Src-FAK complex mediates cell mobility through a series of the phosphorylation events on p130Cas and paxillin[292,376–378]. In general, the binding of Src to FAK facilitates FAK to bind to p130Cas and phosphorylates p130Cas at multiple sites, which in turn promotes the binding of p130Cas to the Crk adaptor protein leading to Rac activation for cell migration[379,380]. At the meantime, Src-FAK complex phosphorylates paxillin to promote the binding of Crk to paxillin[381]. We believe that due to the structural and functional similarity of Src and FAK with their respective family members, Lyn/Fyn and Pyk2 may operate in a similar manner in our case. Indeed, it has been shown that Pyk2 knockdown inhibited the phosphorylation of paxillin and Src in MM cells[353]. Future studies should validate the interactions between the CD45/SFKs/Pyk2 cascade and their potential downstream targets, p130Cas and paxillin.

Additionally, we used BMSCs, HS5, as the source of chemoattractants but not a specific chemokine for our homing assays. Our previous study has shown that HS5 secretes a variety of cytokines and growth factors, such as SDF-1, GM-CSF, IL-6, IL-8, MCP1-3 and VEGF (Katherine Monaghan thesis, 2011). Future experiments should also identify the specific chemokines that trigger CD45 signalling and the homing process.

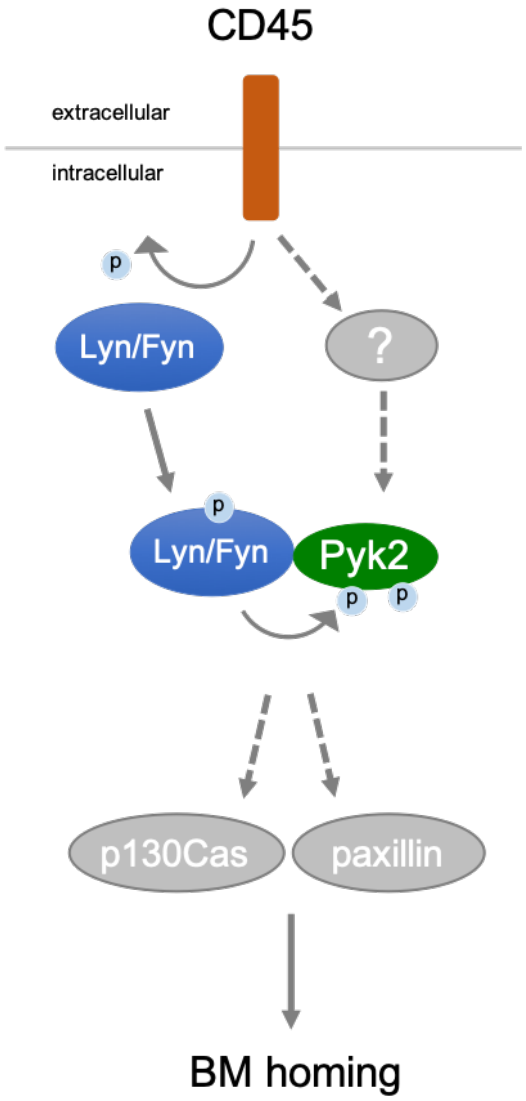

Figure 6-1: Proposed CD45/SFKs/Pyk2 cascade in BM homing.

CD45 activates SFKs (Lyn and Fyn in this study) by removing the inhibitory phosphorylation upon stimulation. The SFKs then bind to and activate Pyk2. Pyk2 may also be activated by other molecules that are sensitive to CD45. We believe that the resulting SFKs/Pyk2 complex further promotes the activation of p130Cas and paxillin, leading to BM homing.

6.4 CD45⁻ phenotype: good or bad?

The association between CD45⁻ phenotype and poor prognosis may be controversial, but we cannot ignore the role of CD45 in MM progression. As W. Gonsalves et al. suggested, these studies were greatly affected by the definition of patient cohorts, flow cytometry techniques and the different therapies given. The introduction of novel therapeutics has tremendously changed the treatment regimens in MM over the past decade. These therapeutics may exert distinct effects on CD45⁺ and CD45⁻ cells compared with the conventional therapies, as a result, defining the association between CD45 and prognosis is overly complicated and challenging (details in 1.4.4).

Further complicating this matter is that from our preliminary *in vivo* studies, although CD45⁻ cells displayed slower engraftment and proliferation, these cells appeared to metastasise earlier and to more sites than CD45⁺ cells. These results suggest that MM patients with CD45⁻ phenotype may have a less progressive disease but have a higher chance of developing extramedullary disease. This finding aligns to the clinical observation that patients with high-grade angiogenesis had lower mean percentage of CD45⁺ plasma cells[297]. It would be worthwhile to incorporate the incidence of extramedullary disease into the future studies on the clinical significance of CD45.

The presence of extramedullary disease at diagnosis has been associated with shorter overall survival in patients receiving conventional therapy[382,383]. Although the CD45 status of extramedullary disease is relatively unclear, there is a case of expression transition from CD45$^{dim/+}$ in the BM aspirate to CD45⁻ in the abdominal extramedullary mass[384]. Moreover, CD45 expression is downregulated in the circulating MM cells[124] and a high level of circulating MM cells has also been associated with disease progression and shorter overall survival[125–127]. These results support our hypotheses that CD45⁻ phenotype represents an aggressive and metastatic disease. Interestingly, the frequency of extramedullary disease is higher in patients treated with the novel agent thalidomide despite a good response in the BM[385,386]. Bortezomib, on the other hand, has shown efficacy in treating extramedullary disease[387,388]. It would be

interesting to compare the sensitivity of $CD45^{+}$ and $CD45^{-}$ cells to different anti-MM agents. Taken together, we believe that CD45 is associated with extramedullary disease progression and future studies should investigate the potential role of CD45 as a biomarker for extramedullary disease.

6.5 Future directions

As mentioned previously, there are several areas of this study that require further investigation. Whilst we have presented a novel CD45/SFKs/Pyk2 signalling cascade in the MM homing process, other signalling molecules may also be involved. Future studies should search for other CD45 and SFKs/Pyk2 downstream targets utilising phosphoproteomics, as we have shown that gene expression profiling was insufficient in the current circumstances. To further confirm the specificity of this signalling pathway in the homing process, rescue experiments should be performed by overexpressing the intracellular portion of CD45 (which has the phosphatase activity) in the $CD45^{KO}$ cells. This is because overexpressing the full-length CD45 is technically challenging. Alternatively, overexpression or activation of SFKs and Pyk2 can be applied to restore the homing potential in the $CD45^{KO}$ cells. The involvement of p130Cas and paxillin in our proposed signalling pathway should also be explored. Given the promising anti-tumour effect of SFKs and FAK inhibitions in other solid tumours, future *in vivo* studies should investigate the efficacy of SFK inhibitor and Pyk2 inhibitor whether they have any clinical impacts in MM.

6.6 Conclusion

This thesis has established the role of CD45 in disease progression in MM by using the CRISPR/Cas9-mediated knockout models. In particular, we have demonstrated that $CD45^{WT}$ and $CD45^{KO}$ cells share similar proliferation profiles in various liquid culture conditions but $CD45^{KO}$ cells are less clonogenic in the methylcellulose-based semi-solid culture. Importantly, we have shown $CD45^{KO}$ cells have impaired homing potential *in vitro* and *in vivo*, and we propose that this is due to the disruption in the CD45/SFKs/Pyk2 signalling cascade. We

have also shown the higher metastatic potential of $CD45^{KO}$ cells and the differentiation of $CD45^{+}$ to $CD45^{-}$ phenotype *in vivo*. Our findings demonstrate the distinct characteristics of $CD45^{+}$ and $CD45^{-}$ cells and provide rationale for further investigation in the mechanisms of CD45-mediated disease progression and dissemination. Better understanding of these processes would be highly beneficial in optimising the treatment regimens. We propose that the loss of CD45 expression represents extramedullary progression and CD45 could be a biomarker in MM stratification.

REFERENCES

1. International Myeloma Working Group. Criteria for the classification of monoclonal gammopathies, multiple myeloma and related disorders: a report of the International Myeloma Working Group. *Br. J. Haematol.* **121**, 749–757 (2003).

2. Australian Institute of Health and Welfare & Australian Institute of Health and Welfare 2017. *Cancer in Australia 2017*. *Cancer in Australia 2017* (2017).

3. Bray, F. *et al.* Global cancer statistics 2018: GLOBOCAN estimates of incidence and mortality worldwide for 36 cancers in 185 countries. *CA. Cancer J. Clin.* **68**, 394–424 (2018).

4. Noone AM, Howlader N, Krapcho M, Miller D, Brest A, Yu M, Ruhl J, Tatalovich Z, Mariotto A, Lewis DR, Chen HS, Feuer EJ, C. K. (eds). *Cancer Statistics Review, 1975-2015*.

5. Weiss, B. M. Multiethnic myeloma. *Blood* **121**, 3062–3064 (2013).

6. Fairfield, H., Falank, C., Avery, L. & Reagan, M. R. Multiple myeloma in the marrow: pathogenesis and treatments. *Ann. N. Y. Acad. Sci.* **1364**, 32–51 (2016).

7. Talley, P. J., Chantry, A. D. & Buckle, C. H. Genetics in myeloma: Genetic technologies and their application to screening approaches in myeloma. *Br. Med. Bull.* **113**, 15–30 (2015).

8. Oyajobi, B. O. Multiple myeloma/hypercalcemia. *Arthritis Res. Ther.* **9**, S4 (2007).

9. Baris, D., Brown, L. M., Andreotti, G. & Devesa, S. S. Epidemiology of Multiple Myeloma. in *Neoplastic Diseases of the Blood* **76**, 547–563 (Springer New York, 2013).

10. Kyle, R. A. *et al.* Prevalence of Monoclonal Gammopathy of Undetermined Significance. *N. Engl. J. Med.* **354**, 1362–1369 (2006).

11. Therneau, T. M. *et al.* Incidence of monoclonal gammopathy of

undetermined significance and estimation of duration before first clinical recognition. *Mayo Clin. Proc.* **87**, 1071–9 (2012).

12. Rajkumar, S. V. *et al.* International Myeloma Working Group updated criteria for the diagnosis of multiple myeloma. *Lancet Oncol.* **15**, e538–e548 (2014).

13. Rajkumar, S. V. Multiple myeloma: 2018 update on diagnosis, risk-stratification, and. *Am. J. Hematol.* **93**, 1091–1110 (2018).

14. Sonneveld, P. *et al.* International Staging System for Multiple Myeloma. *J. Clin. Oncol.* **23**, 3412–3420 (2005).

15. Terpos, E. *et al.* High serum lactate dehydrogenase adds prognostic value to the international myeloma staging system even in the era of novel agents. *Eur. J. Haematol.* **85**, 114–9 (2010).

16. Dimopoulos, M. A., Barlogie, B., Smith, T. L. & Alexanian, R. High serum lactate dehydrogenase level as a marker for drug resistance and short survival in multiple myeloma. *Ann. Intern. Med.* **115**, 931–5 (1991).

17. Ross, F. M. *et al.* Report from the European Myeloma Network on interphase FISH in multiple myeloma and related disorders. *Haematologica* **97**, 1272–1277 (2012).

18. Fonseca, R. *et al.* International Myeloma Working Group molecular classification of multiple myeloma: Spotlight review. *Leukemia* **23**, 2210–2221 (2009).

19. Morgan, G. J., Walker, B. a & Davies, F. E. The genetic architecture of multiple myeloma. *Nat. Rev. Cancer* **12**, 335–48 (2012).

20. Chim, C.-S., Liang, R., Leung, M.-H., Yip, S.-F. & Kwong, Y.-L. Aberrant gene promoter methylation marking disease progression in multiple myeloma. *Leukemia* **20**, 1190–1192 (2006).

21. Gonzalez-Paz, N. *et al.* Tumor suppressor p16 methylation in multiple myeloma: biological and clinical implications. *Blood* **109**, 1228–32 (2007).

22. Walker, B. A. *et al.* Aberrant global methylation patterns affect the molecular pathogenesis and prognosis of multiple myeloma. *Blood* **117**, 553–62 (2011).

23. Agirre, X. *et al.* Whole-epigenome analysis in multiple myeloma reveals DNA hypermethylation of B cell-specific enhancers. *Genome Res.* **25**, 478–87 (2015).

24. Sive, J. I. *et al.* Global hypomethylation in myeloma is associated with poor prognosis. *Br. J. Haematol.* **172**, 473–475 (2016).

25. Mitsiades, C. S. *et al.* Transcriptional signature of histone deacetylase inhibition in multiple myeloma: biological and clinical implications. *Proc. Natl. Acad. Sci. U. S. A.* **101**, 540–5 (2004).

26. Martinez-Garcia, E. *et al.* The MMSET histone methyl transferase switches global histone methylation and alters gene expression in t(4;14) multiple myeloma cells. *Blood* **117**, 211–20 (2011).

27. Popovic, R. *et al.* Histone Methyltransferase MMSET/NSD2 Alters EZH2 Binding and Reprograms the Myeloma Epigenome through Global and Focal Changes in H3K36 and H3K27 Methylation. *PLoS Genet.* **10**, e1004566 (2014).

28. Agarwal, P. *et al.* Genome-wide profiling of histone H3 lysine 27 and lysine 4 trimethylation in multiple myeloma reveals the importance of Polycomb gene targeting and highlights EZH2 as a potential therapeutic target. *Oncotarget* **7**, 6809–23 (2016).

29. Pichiorri, F. *et al.* MicroRNAs regulate critical genes associated with multiple myeloma pathogenesis. *Proc. Natl. Acad. Sci. U. S. A.* **105**, 12885–90 (2008).

30. Gutiérrez, N. C. *et al.* Deregulation of microRNA expression in the different genetic subtypes of multiple myeloma and correlation with gene expression profiling. *Leukemia* **24**, 629–637 (2010).

31. Smadja, N.-V. *et al.* Chromosomal analysis in multiple myeloma: cytogenetic evidence of two different diseases. *Leukemia* **12**, 960–969 (1998).

32. Anderson, K. C. & Carrasco, R. D. Pathogenesis of myeloma. *Annu. Rev. Pathol.* **6**, 249–74 (2011).

33. Chng, W. J. *et al.* Ploidy status rarely changes in myeloma patients at disease progression. *Leuk. Res.* **30**, 266–271 (2006).

34. Bergsagel, P. L. & Kuehl, W. M. Chromosome translocations in multiple myeloma. *Oncogene* **20**, 5611–5622 (2001).

35. Fonseca, R. *et al.* The recurrent IgH translocations are highly associated with nonhyperdiploid variant multiple myeloma. *Blood* **102**, 2562–7 (2003).

36. Gabrea, A., Bergsagel, P. L., Chesi, M., Shou, Y. & Kuehl, W. M. Insertion of Excised IgH Switch Sequences Causes Overexpression of Cyclin D1 in a Myeloma Tumor Cell. *Mol. Cell* **3**, 119–123 (1999).

37. John Shaughnessy Jr, Ana Gabrea, Ying Qi, Leslie Brents, Fenghaung Zhan, Erming Tian, Jeffrey Sawyer, Bart Barlogie, P. L. B. and M. K. Cyclin D3 at 6p21 is dysregulated by recurrent chromosomal translocations to immunoglobulin loci in multiple myeloma. *Blood* **91**, 3–21 (1998).

38. Marta Chesi, Elena Nardini, Robert S.C. Lim, Kerrington D. Smith, W. M. K. and P. L. B. The t(4;14) Translocation in Myeloma Dysregulates Both FGFR3and a Novel Gene, MMSET, Resulting in IgH/MMSET Hybrid Transcripts. *Blood* **92**, 3025–3034 (1998).

39. Marta Chesi, P. Leif Bergsagel, Oluwatoyin O. Shonukan, Maria Luisa Martelli, Leslie A. Brents, Theresa Chen, Evelin Schröck, T. R. and W. M. K. Frequent Dysregulation of the c-maf Proto-Oncogene at 16q23 by Translocation to an Ig Locus in Multiple Myeloma. *Blood* **91**, 4457–4463 (1998).

40. Hurt, E. M. *et al.* Overexpression of c-maf is a frequent oncogenic event in multiple myeloma that promotes proliferation and pathological interactions with bone marrow stroma. *Cancer Cell* **5**, 191–199 (2004).

41. Lohr, J. G. *et al.* Widespread genetic heterogeneity in multiple myeloma: Implications for targeted therapy. *Cancer Cell* **25**, 91–101 (2014).

42. Mithraprabhu, S. *et al.* Circulating tumour DNA analysis demonstrates spatial mutational heterogeneity that coincides with disease relapse in myeloma. *Leukemia* 1–36 (2016). doi:10.1038/leu.2016.366

43. Hideshima, T., Mitsiades, C., Tonon, G., Richardson, P. G. & Anderson, K. C. Understanding multiple myeloma pathogenesis in the bone marrow to identify new therapeutic targets. *Nat. Rev. Cancer* **7**, 585–598 (2007).

44. Basak, G. W., Srivastava, A. S., Malhotra, R. & Carrier, E. Multiple myeloma bone marrow niche. *Curr Pharm Biotechnol* **10**, 345–346 (2009).

45. Nishiuchi, R. *et al.* Ligand-binding specificities of laminin-binding integrins: A comprehensive survey of laminin–integrin interactions using recombinant α3β1, α6β1, α7β1 and α6β4 integrins. *Matrix Biol.* **25**, 189–197 (2006).

46. Ridley, R. *et al.* Expression of syndecan regulates human myeloma plasma cell adhesion to type I collagen. *Blood* **81**, (1993).

47. Aruffo, A., Stamenkovic, I., Melnick, M., Underhill, C. B. & Seed, B. CD44 is the principal cell surface receptor for hyaluronate. *Cell* **61**, 1303–1313 (1990).

48. Damiano, J. S., Cress, A. E., Hazlehurst, L. A., Shtil, A. A. & Dalton, W. S. Cell adhesion mediated drug resistance (CAM-DR): role of integrins and resistance to apoptosis in human myeloma cell lines. *Blood* **93**, 1658–67 (1999).

49. Hazlehurst, L. A., Damiano, J. S., Buyuksal, I., Pledger, W. J. & Dalton, W.

S. Adhesion to fibronectin via β1 integrins regulates p27 kip1 levels and contributes to cell adhesion mediated drug resistance (CAM-DR). *Oncogene* **19**, 4319–4327 (2000).

50. Landowski, T. H., Olashaw, N. E., Agrawal, D. & Dalton, W. S. Cell adhesion-mediated drug resistance (CAM-DR) is associated with activation of NF-κB (RelB/p50) in myeloma cells. *Oncogene* **22**, 2417–2421 (2003).

51. Degrassi, A. *et al.* In vitro culture of primary plasmacytomas requires stromal cell feeder layers. *Proc. Natl. Acad. Sci. U. S. A.* **90**, 2060–4 (1993).

52. Sanz-rodríguez, F. & Teixidó, J. VLA-4-Dependent Myeloma Cell Adhesion. *Leuk. Lymphoma* **41**, 239–245 (2001).

53. Masellis-Smith, A., Belch, A. R., Mant, M. J. & Pilarski, L. M. Adhesion of multiple myeloma peripheral blood B cells to bone marrow fibroblasts: a requirement for CD44 and alpha4beta7. *Cancer Res.* **57**, 930–6 (1997).

54. Faid, L. *et al.* Adhesive interactions between tumour cells and bone marrow stromal elements in human multiple myeloma. *Eur. J. Haematol.* **57**, 349–358 (2009).

55. Lokhorst, H. M. *et al.* Primary tumor cells of myeloma patients induce interleukin-6 secretion in long-term bone marrow cultures. *Blood* **84**, 2269–77 (1994).

56. Vincent, T. & Mechti, N. IL-6 regulates CD44 cell surface expression on human myeloma cells. *Leukemia* **18**, 967–975 (2004).

57. Lee, C. *et al.* TNF α mediated IL-6 secretion is regulated by JAK/STAT pathway but not by MEK phosphorylation and AKT phosphorylation in U266 multiple myeloma cells. *Biomed Res. Int.* **2013**, 580135 (2013).

58. Cook, G., Campbell, J. D., Carr, C. E., Boyd, K. S. & Franklin, I. M. Transforming growth factor beta from multiple myeloma cells inhibits

proliferation and IL-2 responsiveness in T lymphocytes. *J. Leukoc. Biol.* **66**, 981–988 (1999).

59. Bisping, G. *et al.* Paracrine interactions of basic fibroblast growth factor and interleukin-6 in multiple myeloma. *Blood* **101**, 2775–83 (2003).

60. Dankbar, B. *et al.* Vascular endothelial growth factor and interleukin-6 in paracrine tumor-stromal cell interactions in multiple myeloma. *Blood* **95**, 2630–6 (2000).

61. Melton, L. J., Kyle, R. A., Achenbach, S. J., Oberg, A. L. & Rajkumar, S. V. Fracture Risk With Multiple Myeloma: A Population-Based Study. *J. Bone Miner. Res.* **20**, 487–493 (2004).

62. Esteve, F. R. & Roodman, G. D. Pathophysiology of myeloma bone disease. *Best Pract. Res. Clin. Haematol.* **20**, 613–624 (2007).

63. Farrugia, A. N. *et al.* Receptor Activator of Nuclear Factor-kB Ligand Expression by Human Myeloma Cells Mediates Osteoclast Formation in Vitro and Correlates with Bone Destruction in Vivo. *CANCER Res.* **63**, 5438–5445 (2003).

64. Schmiedel, B. J. *et al.* RANKL expression, function, and therapeutic targeting in multiple myeloma and chronic lymphocytic leukemia. *Cancer Res.* **73**, 683–94 (2013).

65. Michigami, T. *et al.* Cell–cell contact between marrow stromal cells and myeloma cells via VCAM-1 and a4b1 -integrin enhances production of osteoclast-stimulating activity. *Neoplasia* **95**, 1953–1960 (2000).

66. Pearse, R. N. *et al.* Multiple myeloma disrupts the TRANCE/ osteoprotegerin cytokine axis to trigger bone destruction and promote tumor progression. *Proc. Natl. Acad. Sci. U. S. A.* **98**, 11581–6 (2001).

67. Kudo, O. *et al.* Interleukin-6 and interleukin-11 support human osteoclast formation by a RANKL-independent mechanism. *Bone* **32**, 1–7 (2003).

68. Kawano, M. *et al.* Autocrine generation and requirement of BSF-2/IL-6 for

human multiple myelomas. *Nature* **332**, 83–85 (1988).

69. Hata, H. *et al.* Interleukin-6 Gene Expression in Multiple Myeloma: A Characteristic of Immature Tumor Cells.

70. Portier, M. *et al.* Cytokine gene expression in human multiple myeloma. *Br. J. Haematol.* **85**, 514–20 (1993).

71. Frassanito, M. A., Cusmai, A., Iodice, G. & Dammacco, F. Autocrine interleukin-6 production and highly malignant multiple myeloma: relation with resistance to drug-induced apoptosis. *Blood* **97**, 483–489 (2001).

72. Reibnegger, G. *et al.* Predictive value of interleukin-6 and neopterin in patients with multiple myeloma. *Cancer Res.* **51**, 6250–3 (1991).

73. Pelliniemi, T. T. *et al.* Immunoreactive interleukin-6 and acute phase proteins as prognostic factors in multiple myeloma. Finnish Leukemia Group. *Blood* **85**, 765–71 (1995).

74. Levy, Y., Tsapis, A. & Brouet, J. C. Interleukin-6 antisense oligonucleotides inhibit the growth of human myeloma cell lines. *J. Clin. Invest.* **88**, 696–9 (1991).

75. Villunger, A. *et al.* Constituents of autocrine IL-6 loops in myeloma cell lines and their targeting for suppression of neoplastic growth by antibody strategies. *Int. J. Cancer* **65**, 498–505 (1996).

76. Sporeno, E. *et al.* Human interleukin-6 receptor super-antagonists with high potency and wide spectrum on multiple myeloma cells. *Blood* **87**, 4510–9 (1996).

77. Lichtenstein, A., Tu, Y., Fady, C., Vescio, R. & Berenson, J. Interleukin-6 Inhibits Apoptosis of Malignant Plasma Cells. *Cell. Immunol.* **162**, 248–255 (1995).

78. Hardin, J. *et al.* Interleukin-6 prevents dexamethasone-induced myeloma cell death. *Blood* **84**, 3063–70 (1994).

79. Ogata, A. *et al.* IL-6 triggers cell growth via the Ras-dependent mitogen-activated protein kinase cascade. *J. Immunol.* **159**, 2212–21 (1997).

80. Chauhan, D. *et al.* Cytochrome c-dependent and -independent induction of apoptosis in multiple myeloma cells. *J. Biol. Chem.* **272**, 29995–7 (1997).

81. Catlett-Falcone, R. *et al.* Constitutive activation of Stat3 signaling confers resistance to apoptosis in human U266 myeloma cells. *Immunity* **10**, 105–15 (1999).

82. Tu, Y., Gardner, A. & Lichtenstein, A. The phosphatidylinositol 3-kinase/AKT kinase pathway in multiple myeloma plasma cells: roles in cytokine-dependent survival and proliferative responses. *Cancer Res.* **60**, 6763–70 (2000).

83. Freund, G. G., Kulas, D. T. & Mooney, R. A. Insulin and IGF-1 increase mitogenesis and glucose metabolism in the multiple myeloma cell line, RPMI 8226. *J. Immunol.* **151**, 1811–20 (1993).

84. Jelinek, D. F., Witzig, T. E. & Arendt, B. K. A role for insulin-like growth factor in the regulation of IL-6-responsive human myeloma cell line growth. *J. Immunol.* **159**, 487–96 (1997).

85. Blank, N. *et al.* CD45 Tyrosine Phosphatase Controls Common -Chain Cytokine-Mediated STAT and Extracellular Signal-Related Kinase Phosphorylation in Activated Human Lymphoblasts: Inhibition of Proliferation Without Induction of Apoptosis. *J. Immunol.* **166**, 6034–6040 (2001).

86. Sprynski, A. C. *et al.* The role of IGF-1 as a major growth factor for myeloma cell lines and the prognostic relevance of the expression of its receptor. *Blood* **113**, 4614–26 (2009).

87. Tagoug, I., Sauty De Chalon, A. & Dumontet, C. Inhibition of IGF-1 Signalling Enhances the Apoptotic Effect of AS602868, an IKK2 Inhibitor, in Multiple Myeloma Cell Lines. *PLoS One* **6**, e22641 (2011).

88. Laron, Z. Insulin-like growth factor 1 (IGF-1): a growth hormone. *Mol. Pathol.* **54**, 311–6 (2001).

89. Ge, N. L. & Rudikoff, S. Insulin-like growth factor I is a dual effector of multiple myeloma cell growth. *Blood* **96**, 2856–61 (2000).

90. Mitsiades, C. S. *et al.* Activation of NF-κB and upregulation of intracellular anti-apoptotic proteins via the IGF-1/Akt signaling in human multiple myeloma cells: therapeutic implications. *Oncogene* **21**, 5673–5683 (2002).

91. Mitsiades, C. S. *et al.* TRAIL/Apo2L ligand selectively induces apoptosis and overcomes drug resistance in multiple myeloma: therapeutic applications. *Blood* **98**, 795–804 (2001).

92. Brenne, A.-T. *et al.* Interleukin-21 is a growth and survival factor for human myeloma cells. *Blood* **99**, 3756–62 (2002).

93. Tinhofer, I., Marschitz, I., Henn, T., Egle, A. & Greil, R. Expression of functional interleukin-15 receptor and autocrine production of interleukin-15 as mechanisms of tumor propagation in multiple myeloma. *Blood* **95**, 610–8 (2000).

94. Gu, Z. J. *et al.* Interleukin-10 is a growth factor for human myeloma cells by induction of an oncostatin M autocrine loop. *Blood* **88**, 3972–86 (1996).

95. Lu, Z. Y. *et al.* Interleukin-10 is a proliferation factor but not a differentiation factor for human myeloma cells. *Blood* **85**, 2521–7 (1995).

96. Derksen, P. W. B. *et al.* Illegitimate WNT signaling promotes proliferation of multiple myeloma cells. *Proc. Natl. Acad. Sci. U. S. A.* **101**, 6122–7 (2004).

97. Nefedova, Y., Sullivan, D. M., Bolick, S. C., Dalton, W. S. & Gabrilovich, D. I. Inhibition of Notch signaling induces apoptosis of myeloma cells and enhances sensitivity to chemotherapy. *Blood* **111**, 2220–9 (2008).

98. Nefedova, Y., Cheng, P., Alsina, M., Dalton, W. S. & Gabrilovich, D. I.

Involvement of Notch-1 signaling in bone marrow stroma-mediated de novo drug resistance of myeloma and other malignant lymphoid cell lines. *Blood* **103**, 3503–10 (2004).

99. Houde, C. *et al.* Overexpression of the NOTCH ligand JAG2 in malignant plasma cells from multiple myeloma patients and cell lines. *Blood* **104**, 3697–3704 (2004).

100. Muguruma, Y. *et al.* Jagged1-induced Notch activation contributes to the acquisition of bortezomib resistance in myeloma cells. *Blood Cancer J.* **7**, 650 (2017).

101. Jundt, F. *et al.* Jagged1-induced Notch signaling drives proliferation of multiple myeloma cells. *Blood* **103**, 3511–3515 (2004).

102. Podar, K. *et al.* Vascular endothelial growth factor triggers signaling cascades mediating multiple myeloma cell growth and migration. *Blood* **98**, 428–436 (2001).

103. Colla, S. *et al.* Do human myeloma cells directly produce basic FGF? *Blood* **102**, 3071–2; author reply 3072-3 (2003).

104. McMahon, G. VEGF receptor signaling in tumor angiogenesis. *Oncologist* **5 Suppl 1**, 3–10 (2000).

105. Carmeliet, P. VEGF as a Key Mediator of Angiogenesis in Cancer. *Oncology* **69**, 4–10 (2005).

106. Vacca, A. *et al.* Bone marrow neovascularization, plasma cell angiogenic potential, and matrix metalloproteinase-2 secretion parallel progression of human multiple myeloma. *Blood* **93**, 3064–73 (1999).

107. Vacca, A. *et al.* Bone marrow angiogenesis and progression in multiple myeloma. *Br. J. Haematol.* **87**, 503–8 (1994).

108. Rawstron, a C. *et al.* Circulating plasma cells in multiple myeloma: characterization and correlation with disease stage. *Br. J. Haematol.* **97**, 46–55 (1997).

109. Rawstron, A. *et al.* Distribution of myeloma plasma cells in peripheral blood and bone marrow correlates with CD56 expression. *Br. J. Haematol.* **104**, 138–143 (1999).

110. Fidler, I. J. The pathogenesis of cancer metastasis: The 'seed and soil' hypothesis revisited. *Nat. Rev. Cancer* **3**, 453–458 (2003).

111. Lambert, A. W., Pattabiraman, D. R. & Weinberg, R. A. Emerging Biological Principles of Metastasis. *Cell* **168**, 670–691 (2017).

112. Thiery, J. P., Acloque, H., Huang, R. Y. J. & Nieto, M. A. Epithelial-Mesenchymal Transitions in Development and Disease. *Cell* **139**, 871–890 (2009).

113. Lamouille, S., Xu, J. & Derynck, R. Molecular mechanisms of epithelial–mesenchymal transition. *Nat. Rev. Mol. Cell Biol.* **15**, 178–196 (2014).

114. Cano, a *et al.* The transcription factor snail controls epithelial-mesenchymal transitions by repressing E-cadherin expression. *Nat. Cell Biol.* **2**, 76–83 (2000).

115. De Craene, B. *et al.* The transcription factor snail induces tumor cell invasion through modulation of the epithelial cell differentiation program. *Cancer Res.* **65**, 6237–6244 (2005).

116. Pećina-Slaus, N. Tumor suppressor gene E-cadherin and its role in normal and malignant cells. *Cancer Cell Int.* **3**, 17 (2003).

117. Wheelock, M. J., Maeda, M., Shintani, Y., Johnson, K. R. & Fukumoto, Y. Cadherin switching. *J. Cell Sci.* **121**, 727–735 (2008).

118. Groen, R. W. J. *et al.* N-cadherin-mediated interaction with multiple myeloma cells inhibits osteoblast differentiation. *Haematologica* **96**, 1653–1661 (2011).

119. Dring, A. M. *et al.* A global expression-based analysis of the consequences of the t(4;14) translocation in myeloma. *Clin. Cancer Res.* **10**, 5692–5701 (2004).

120. Mrozik, K. M., Man, C., Hewett, D., Annie, W. S. & Blaschuk, O. W. Therapeutic targeting of N-cadherin is an effective treatment for multiple myeloma. *Br. J. Haematol.* **171**, 387–399 (2015).

121. Yang, M.-H. & Wu, K.-J. TWIST activation by hypoxia inducible factor-1 (HIF-1): Implications in metastasis and development. *Cell Cycle* **7**, 2090–2096 (2008).

122. Azab, A. K. *et al.* Hypoxia promotes dissemination of multiple myeloma through acquisition of epithelial to mesenchymal transition-like features. *Blood* **119**, 5782–5794 (2012).

123. Petit, I. *et al.* G-CSF induces stem cell mobilization by decreasing bone marrow SDF-1 and up-regulating CXCR4. *Nat. Immunol.* **3**, 687–694 (2002).

124. Paiva, B. *et al.* Detailed characterization of multiple myeloma circulating tumor cells shows unique phenotypic, cytogenetic, functional, and circadian distribution profile. *Blood* **122**, 3591–3598 (2013).

125. GS, N. *et al.* Circulating plasma cells detected by flow cytometry as a predictor of survival in 302 patients with newly diagnosed multiple myeloma. *Blood* **106**, 2276–2279 (2005).

126. Witzig, T. E. *et al.* Prognostic Value of Circulating Plasma Cells in Monoclonal Gammopathy of Undetermined Significance. *J. Clin. Oncol.* **23**, 5668–5674 (2005).

127. Bianchi, G. *et al.* High levels of peripheral blood circulating plasma cells as a specific risk factor for progression of smoldering multiple myeloma. *Leukemia* **27**, 680–685 (2013).

128. Alici, E., Konstantinidis, K. V., Aints, A., Dilber, M. S. & Abedi-Valugerdi, M. Visualization of 5T33 myeloma cells in the C57BL/KaLwRij mouse: establishment of a new syngeneic murine model of multiple myeloma. *Exp. Hematol.* **32**, 1064–1072 (2004).

129. Vanderkerken, K. *et al.* Selective initial in vivo homing pattern of 5T2 multiple myeloma cells in the C57BL/KalwRij mouse. *Br. J. Cancer* **82**, 953–959 (2000).

130. Selvaggi, G. & Scagliotti, G. V. Management of bone metastases in cancer: A review. *Crit. Rev. Oncol. Hematol.* **56**, 365–378 (2005).

131. Macedo, F. *et al.* Bone Metastases: An Overview. *Oncol. Rev.* **11**, 321 (2017).

132. Picker, L. J. & Butcher, E. C. Physiological and molecular mechanisms of lymphocyte homing. *Annu. Rev. Immunol* **10**, 561–91 (1992).

133. Nabeshima, K., Inoue, T., Shimao, Y. & Sameshima, T. Matrix metalloproteinases in tumor invasion: Role for cell migration. *Pathol. Int.* **52**, 255–264 (2002).

134. Riet, I. Van, Vanderkerken, K., De Greef, C. & Camp, B. Van. Homing behaviour of the malignant cell clone in multiple myeloma Differentiation and homing of normal B cells. *Med. Oncol.* **15**, 154–164 (1998).

135. Parmo-Cabañas, M. *et al.* Integrin α4β1 involvement in stromal cell-derived factor-1α-promoted myeloma cell transendothelial migration and adhesion: Role of cAMP and the actin cytoskeleton in adhesion. *Exp. Cell Res.* **294**, 571–580 (2004).

136. Makrynikola, V., Bianchi, A., Bradstock, K., Gottlieb, D. & Hewson, J. Migration of acute lymphoblastic leukemia cells into human bone marrow stroma. *Leukemia* **8**, 1734–43 (1994).

137. Miyake, K., Hasunuma, Y., Yagita, H. & Kimoto, M. Requirement for VLA-4 and VLA-5 integrins in lymphoma cells binding to and migration beneath stromal cells in culture. *J. Cell Biol.* **119**, 653–62 (1992).

138. Dufour, A., Zucker, S., Sampson, N. S., Kuscu, C. & Cao, J. Role of matrix metalloproteinase-9 dimers in cell migration: design of inhibitory peptides. *J. Biol. Chem.* **285**, 35944–56 (2010).

139. Möller, C., Strömberg, T., Juremalm, M., Nilsson, K. & Nilsson, G. Expression and function of chemokine receptors in human multiple myeloma. *Leukemia* **17**, 203–210 (2003).

140. Vande Broek, I. *et al.* Chemokine receptor CCR2 is expressed by human multiple myeloma cells and mediates migration to bone marrow stromal cell-produced monocyte chemotactic proteins MCP-1, -2 and -3. *Br. J. Cancer* **88**, 855–62 (2003).

141. Vande Broek, I. *et al.* Clinical significance of chemokine receptor (CCR1, CCR2 and CXCR4) expression in human myeloma cells: the association with disease activity and survival. *Haematologica* **91**, 200–6 (2006).

142. Menu, E. *et al.* Role of CCR1 and CCR5 in homing and growth of multiple myeloma and in the development of osteolytic lesions: a study in the 5TMM model. *Clin. Exp. Metastasis* **23**, 291–300 (2006).

143. Pellegrino, A. *et al.* CXCR3-binding chemokines in multiple myeloma. *Cancer Lett.* **207**, 221–227 (2004).

144. Arendt, B. K. *et al.* Interleukin 6 induces monocyte chemoattractant protein-1 expression in myeloma cells. *Leukemia* **16**, 2142–2147 (2002).

145. Barillé, S. *et al.* Metalloproteinases in multiple myeloma: production of matrix metalloproteinase-9 (MMP-9), activation of proMMP-2, and induction of MMP-1 by myeloma cells. *Blood* **90**, 1649–55 (1997).

146. Vande Broek, I. *et al.* Bone marrow endothelial cells increase the invasiveness of human multiple myeloma cells through upregulation of MMP-9: evidence for a role of hepatocyte growth factor. *Leukemia* **18**, 976–982 (2004).

147. Van Valckenborgh, E. *et al.* Upregulation of matrix metalloproteinase-9 in murine 5T33 multiple myeloma cells by interaction with bone marrow endothelial cells. *Int. J. Cancer* **101**, 512–518 (2002).

148. Alsayed, Y. *et al.* Mechanisms of regulation of CXCR4/SDF-1 (CXCL12)

dependent migration and homing in Multiple Myeloma. *Blood* **109**, 2708–2718 (2006).

149. Azab, A. K. *et al.* CXCR4 inhibitor AMD3100 disrupts the interaction of multiple myeloma cells with the bone marrow microenvironment and enhances their sensitivity to therapy. *Blood* **113**, 4341–4351 (2009).

150. De Luca, A. *et al.* Src and CXCR4 are involved in the invasiveness of breast cancer cells with acquired resistance to lapatinib. *Cell Cycle* **13**, 148–156 (2014).

151. Kucia, M. *et al.* CXCR4-SDF-1 signalling, locomotion, chemotaxis and adhesion. *J. Mol. Histol.* **35**, 233–245 (2004).

152. Nagasawa, T., Kikutani, H. & Kishimoto, T. Molecular Cloning and Structure of a Pre-B-Cell Growth-Stimulating Factor. *Proceedings of the National Academy of Sciences of the United States of America* **91**, 2305–2309

153. Hideshima, T. *et al.* The biological sequelae of stromal cell-derived factor-1alpha in multiple myeloma. *Mol. Cancer Ther.* **1**, 539–544 (2002).

154. Sanz-Rodriguez, F., Hidalgo, A. & Teixido, J. Chemokine stromal cell-derived factor-1 alpha modulates VLA-4 integrin-mediated multiple myeloma cell adhesion to CS-1/ fibronectin and VCAM-1. *Blood* **97**, 346–352 (2001).

155. Parmo-Cabañas, M. *et al.* Role of metalloproteinases MMP-9 and MT1-MMP in CXCL12-promoted myeloma cell invasion across basement membranes. *J. Pathol.* **208**, 108–118 (2006).

156. Dar, A. *et al.* Chemokine receptor CXCR4–dependent internalization and resecretion of functional chemokine SDF-1 by bone marrow endothelial and stromal cells. *Nat. Immunol.* **6**, 1038–1046 (2005).

157. Nguyen, D. H. & Taub, D. CXCR4 function requires membrane cholesterol: implications for HIV infection. *J. Immunol.* **168**, 4121–6

(2002).

158. Tomlinson, R. Multiple myeloma: Updated approach to management in 2018. *Aust. J. Gen. Pract.* **47**, 526–529 (2018).

159. San Miguel, J. F. *et al.* Persistent Overall Survival Benefit and No Increased Risk of Second Malignancies With Bortezomib-Melphalan-Prednisone Versus Melphalan-Prednisone in Patients With Previously Untreated Multiple Myeloma. *J. Clin. Oncol.* **31**, 448–455 (2013).

160. Benboubker, L. *et al.* Lenalidomide and dexamethasone in transplant-ineligible patients with myeloma. *N. Engl. J. Med.* **371**, 906–17 (2014).

161. Rajkumar, S. V. & Kumar, S. Multiple Myeloma: Diagnosis and Treatment. *Mayo Clin. Proc.* **91**, 101–19 (2016).

162. Obeng, E. A. *et al.* Proteasome inhibitors induce a terminal unfolded protein response in multiple myeloma cells. *Blood* **107**, 4907–4916 (2006).

163. Giuliani, N. *et al.* The proteasome inhibitor bortezomib affects osteoblast differentiation in vitro and in vivo in multiple myeloma patients. *Blood* **110**, 334–8 (2007).

164. von Metzler, I. *et al.* Bortezomib inhibits human osteoclastogenesis. *Leukemia* **21**, 2025–2034 (2007).

165. Roussel, M. *et al.* Front-line transplantation program with lenalidomide, bortezomib, and dexamethasone combination as induction and consolidation followed by lenalidomide maintenance in patients with multiple myeloma: a phase II study by the Intergroupe Francophone du Myélome. *J. Clin. Oncol.* **32**, 2712–7 (2014).

166. Anderson, K. C. Progress and paradigms in multiple myeloma. *Clin. Cancer Res.* **22**, 5419–5427 (2016).

167. Siegel, D. S. *et al.* A phase 2 study of single-agent carfilzomib (PX-171-003-A1) in patients with relapsed and refractory multiple myeloma. *Blood*

120, 2817–25 (2012).

168. Mateos, M.-V. *et al.* Carfilzomib in relapsed or refractory multiple myeloma patients with early or late relapse following prior therapy: A subgroup analysis of the randomized phase 3 ASPIRE and ENDEAVOR trials. *Hematol. Oncol.* **36**, 463–470 (2018).

169. Scalzulli, E., Grammatico, S., Vozella, F. & Petrucci, M. T. Proteasome inhibitors for the treatment of multiple myeloma. *Expert Opin. Pharmacother.* **19**, 375–386 (2018).

170. Moncada, B., Baranda, M. L., González-Amaro, R., Urbina, R. & Loredo, C. E. Thalidomide--effect on T cell subsets as a possible mechanism of action. *Int. J. Lepr. Other Mycobact. Dis.* **53**, 201–5 (1985).

171. Moreira, A. L. *et al.* Thalidomide exerts its inhibitory action on tumor necrosis factor alpha by enhancing mRNA degradation. *J. Exp. Med.* **177**, 1675–80 (1993).

172. Singhal, S. *et al.* Antitumor Activity of Thalidomide in Refractory Multiple Myeloma. *N. Engl. J. Med.* **341**, 1565–1571 (1999).

173. Barlogie, B. *et al.* Extended survival in advanced and refractory multiple myeloma after single-agent thalidomide: identification of prognostic factors in a phase 2 study of 169 patients. *Blood* **98**, 492–4 (2001).

174. Cibeira, M. T. *et al.* Long-term results of thalidomide in refractory and relapsed multiple myeloma with emphasis on response duration. *Eur. J. Haematol.* **77**, 486–92 (2006).

175. Glasmacher, A. *et al.* A systematic review of phase-II trials of thalidomide monotherapy in patients with relapsed or refractory multiple myeloma. *Br. J. Haematol.* **132**, 584–593 (2006).

176. Kotla, V. *et al.* Mechanism of action of lenalidomide in hematological malignancies. *J. Hematol. Oncol.* **2**, 36 (2009).

177. Hideshima, T. *et al.* Thalidomide and its analogs overcome drug

resistance of human multiple myeloma cells to conventional therapy. *Blood* **96**, 2943–50 (2000).

178. Ito, T. *et al.* Identification of a Primary Target of Thalidomide Teratogenicity. *Science (80-.).* **327**, 1345–1350 (2010).

179. Mendy, D. *et al.* Cereblon is a direct protein target for immunomodulatory and antiproliferative activities of lenalidomide and pomalidomide. *Leukemia* **26**, 2326–35 (2012).

180. Zhu, Y. X., Kortuem, K. M. & Stewart, A. K. Molecular mechanism of action of immune-modulatory drugs thalidomide, lenalidomide and pomalidomide in multiple myeloma. *Leuk. Lymphoma* **54**, 683–687 (2013).

181. Zhu, Y. X. *et al.* Cereblon expression is required for the antimyeloma activity of lenalidomide and pomalidomide. *Blood* **118**, 4771–4779 (2011).

182. van der Veer, M. S. *et al.* The therapeutic human CD38 antibody daratumumab improves the anti-myeloma effect of newly emerging multi-drug therapies. *Blood Cancer J.* **1**, e41 (2011).

183. de Weers, M. *et al.* Daratumumab, a Novel Therapeutic Human CD38 Monoclonal Antibody, Induces Killing of Multiple Myeloma and Other Hematological Tumors. *J. Immunol.* **186**, 1840–1848 (2011).

184. Usmani, S. Z. *et al.* Clinical efficacy of daratumumab monotherapy in patients with heavily pretreated relapsed or refractory multiple myeloma. *Blood* **128**, 37–44 (2016).

185. Lonial, S. *et al.* Daratumumab monotherapy in patients with treatment-refractory multiple myeloma (SIRIUS): an open-label, randomised, phase 2 trial. *Lancet (London, England)* **387**, 1551–60 (2016).

186. Plesner, T. *et al.* Phase 1/2 study of daratumumab, lenalidomide, and dexamethasone for relapsed multiple myeloma. *Blood* **128**, 1821–1828 (2016).

187. Mateos, M.-V. *et al.* Daratumumab plus Bortezomib, Melphalan, and Prednisone for Untreated Myeloma. *N. Engl. J. Med.* **378**, 518–528 (2018).

188. Dimopoulos, M. A. *et al.* Daratumumab plus lenalidomide and dexamethasone *versus* lenalidomide and dexamethasone in relapsed or refractory multiple myeloma: updated analysis of POLLUX. *Haematologica* **103**, 2088–2096 (2018).

189. Dimopoulos, M. A. *et al.* Elotuzumab plus Pomalidomide and Dexamethasone for Multiple Myeloma. *N. Engl. J. Med.* **379**, 1811–1822 (2018).

190. Dimopoulos, M. A. *et al.* Elotuzumab plus lenalidomide and dexamethasone in relapsed/refractory multiple myeloma: Extended 4-year follow-up and analysis of relative progression-free survival from the randomized ELOQUENT-2 trial. *Cancer* **124**, 4032–4043 (2018).

191. Baz, R. *et al.* Combination of rituximab and oral melphalan and prednisone in newly diagnosed multiple myeloma. *Leuk. Lymphoma* **48**, 2338–44 (2007).

192. Hansson, M. *et al.* A Phase I Dose-Escalation Study of Antibody BI-505 in Relapsed/Refractory Multiple Myeloma. *Clin. Cancer Res.* **21**, 2730–2736 (2015).

193. Kelly, K. R. *et al.* Indatuximab Ravtansine (BT062) in Combination with Low-Dose Dexamethasone and Lenalidomide or Pomalidomide: Clinical Activity in Patients with Relapsed / Refractory Multiple Myeloma. *Blood* **128**, (2016).

194. Jones, D. R. & Raison, R. L. Preclinical and clinical development of an anti-kappa free light chain mAb for multiple myeloma. *Mol. Immunol.* **67**, 89–94 (2015).

195. Mitsiades, N. *et al.* Molecular sequelae of histone deacetylase inhibition in human malignant B cells. *Blood* **101**, 4055–4062 (2003).

196. Nanavati, C. & Mager, D. E. Sequential Exposure of Bortezomib and Vorinostat is Synergistic in Multiple Myeloma Cells. *Pharm. Res.* **34**, 668–679 (2017).

197. San-Miguel, J. F. *et al.* Panobinostat plus bortezomib and dexamethasone versus placebo plus bortezomib and dexamethasone in patients with relapsed or relapsed and refractory multiple myeloma: a multicentre, randomised, double-blind phase 3 trial. *Lancet Oncol.* **15**, 1195–1206 (2014).

198. Mitsiades, C. S. *et al.* Emerging treatments for multiple myeloma: beyond immunomodulatory drugs and bortezomib. *Semin. Hematol.* **46**, 166–75 (2009).

199. Annunziata, C. M. *et al.* A mechanistic rationale for MEK inhibitor therapy in myeloma based on blockade of MAF oncogene expression. *Blood* **117**, 2396–2404 (2011).

200. Thomas, M. L. The Leukocyte Common Antigen Family. *Annu. Rev. Immunol.* **7**, 339–369 (1989).

201. Tchilian, E. Z. *et al.* A deletion in the gene encoding the CD45 antigen in a patient with SCID. *J. Immunol.* **166**, 1308–13 (2001).

202. Cale, C. M. *et al.* Severe combined immunodeficiency with abnormalities in expression of the common leucocyte antigen, CD45. *Arch. Dis. Child.* **76**, 163–4 (1997).

203. Chatila, T. *et al.* Mutations in the tyrosine phosphatase CD45 gene in a child with severe combined immunodeficiency disease. *Nat. Med.* **6**, 343–345 (2000).

204. Porcu, M. *et al.* Mutation of the receptor tyrosine phosphatase PTPRC (CD45) in T-cell acute lymphoblastic leukemia. *Blood* **119**, (2012).

205. Streuli, M., Hall, L. R., Saga, Y., Schlossman, S. F. & Saito, H. Differential usage of three exons generates at least five different mRNAs encoding

human leukocyte common antigens. *J. Exp. Med.* **166**, 1548–1566 (1987).

206. Hall, L. R. & Schlossman, S. F. Complete exon-intron organization of the human leukocyte common antigen (CD45) gene. *J. Immunol.* **141**, 2781–2787 (1988).

207. Chang, H. L., Lefrancois, L., Zaroukian, M. H. & Esselman, W. J. Developmental expression of CD45 alternate exons in murine T cells. Evidence of additional alternate exon use. *J. Immunol.* **147**, 1687–93 (1991).

208. Virts E, Barritt D, R. W. Expression of CD45 isoforms lacking exons 7, 8 and 10. *Mol. Immunol.* **35**, 167–176 (1998).

209. Okumura, M. *et al.* Comparison of CD45 extracellular domain sequences from divergent vertebrate species suggests the conservation of three fibronectin type III domains. *J. Immunol.* **157**, 1569–75 (1996).

210. D'Oro, U., Sakaguchi, K., Appella, E. & Ashwell, J. D. Mutational analysis of Lck in CD45-negative T cells: dominant role of tyrosine 394 phosphorylation in kinase activity. *Mol. Cell. Biol.* **16**, 4996–5003 (1996).

211. Desai, D. M., Sap, J., Schlessinger, J. & Weiss, A. Ligand-mediated negative regulation of a chimeric transmembrane receptor tyrosine phosphatase. *Cell* **73**, 541–554 (1993).

212. Desai, D. M., Sap, J., Silvennoinen, O., Schlessinger, J. & Weiss, A. The catalytic activity of the CD45 membrane- proximal phosphatase domain is required for TCR signaling and regulation. *EMBO J.* **13**, 4002–4010 (1994).

213. Felberg, J. & Pauline, J. Characterization of Recombinant CD45 Cytoplasmic Domain Proteins. *J. Biol. Chem.* **273**, 17839–17845 (1998).

214. Nam, H.-J., Poy, F., Saito, H. & Frederick, C. a. Structural basis for the function and regulation of the receptor protein tyrosine phosphatase

CD45. *J. Exp. Med.* **201**, 441–52 (2005).

215. Johnson, P., Ostergaard, H. L., Wasden, C. & Trowbridge, I. S. Mutational analysis of CD45-A leukocyte-specific Protein Tyrosine Phosphatase. *J. Biol. Chem.* **267**, 8035–8041 (1992).

216. Justement, L. B. The Role of CD45 in Signal Transduction. *Adv. Immunol.* **66**, (1997).

217. Hermiston, M. L., Xu, Z. & Weiss, A. CD45: A Critical Regulator of Signaling Thresholds in Immune Cells. *Annu. Rev. Immunol* **21**, 107–37 (2003).

218. Trowbridge, I. S. & Thomas, M. L. CD45: An Emerging Role as a Protein Tyrosine Phosphatase Required for Lymphocyte Activation and Development. *Annu. Rev. Immunol.* **12**, 85–116 (1994).

219. Barritt, L. C. & Turpen, J. B. Characterization of lineage restricted forms of a Xenopus CD45 homologue. *Dev. Comp. Immunol.* **19**, 525–36

220. Fujii, Y., Okumura, M., Inada, K., Nakahara, K. & Matsuda, H. CD45 isoform expression during T cell development in the thymus. *Eur. J. Immunol.* **22**, 1843–1850 (1992).

221. Fukuhara, K. *et al.* A study on CD45 isoform expression during T-cell development and selection events in the human thymus. *Hum. Immunol.* **63**, 394–404 (2002).

222. Hathcock, K. S., Hirano, H., Murakami, S., Hodes, R. J. & KAREN S. HATHCOCK,' HIROYUKI HIRANO, SHINYA MURAKAMI, A. R. J. H. CD45 expression by B cells. Expression of different CD45 isoforms by subpopulations of activated B cells. *J. Immunol.* **149**, 2286–94 (1996).

223. Byth, B. K. F. *et al.* CD45-Null Transgenic Mice Reveal a Positive Regulatory Role for CD45 in Early Thymocyte Development, in the Selection of CD4+CD8 + Thyrnocytes, and in B Cell Maturation. **183**, (1996).

224. Ogilvy, S. *et al.* Either of the CD45RB and CD45RO isoforms are effective in restoring T cell, but not B cell, development and function in CD45-null mice. *J. Immunol.* **171**, 1792–800 (2003).

225. June, C. H. *et al.* Inhibition of tyrosine phosphorylation prevents T-cell receptor-mediated signal transduction. *Proc. Natl. Acad. Sci. USA* **87**, 7722–7726 (1990).

226. Samelson, L. E., Phillips, a F., Luong, E. T. & Klausner, R. D. Association of the fyn protein-tyrosine kinase with the T-cell antigen receptor. *Proc. Natl. Acad. Sci. U. S. A.* **87**, 4358–4362 (1990).

227. Samelson, L. E., Patel, M. D., Weissman, a M., Harford, J. B. & Klausner, R. D. Antigen activation of murine T cells induces tyrosine phosphorylation of a polypeptide associated with the T cell antigen receptor. *Cell* **46**, 1083–90 (1986).

228. Rolli, V. *et al.* Amplification of B Cell Antigen Receptor Signaling by a Syk/ITAM Positive Feedback Loop. *Mol. Cell* **10**, 1057–1069 (2002).

229. Bunnell, S. C. *et al.* T cell receptor ligation induces the formation of dynamically regulated signaling assemblies. *J. Cell Biol.* **158**, 1263–1275 (2002).

230. Varma, R., Campi, G., Yokosuka, T., Saito, T. & Dustin, M. L. T Cell Receptor-Proximal Signals Are Sustained in Peripheral Microclusters and Terminated in the Central Supramolecular Activation Cluster. *Immunity* **25**, 117–127 (2006).

231. Douglass, A. D. & Vale, R. D. Single-molecule microscopy reveals plasma membrane microdomains created by protein-protein networks that exclude or trap signaling molecules in T cells. *Cell* **121**, 937–950 (2005).

232. Leupin, O., Zaru, R., Laroche, T., Muller, S. & Valitutti, S. Exclusion of CD45 from the T-cell receptor signaling area in antigen- stimulated T lymphocytes. *Curent Biol.* **10**, 277–280 (2000).

233. Roach, T. *et al.* CD45 regulates Src family member kinase activity associated with macrophage integrin-mediated adhesion. *Curr. Biol.* **7**, 408–417 (1997).

234. Shrivastava, P., Katagiri, T., Ogimoto, M., Mizuno, K. & Yakura, H. Dynamic regulation of Src-family kinases by CD45 in B cells. *Blood* **103**, 1425–1432 (2004).

235. Thomas, S. M. & Brugge, J. S. Cellular functions regulated by Src family kinases. *Annu. Rev. Cell Dev. Biol.* **13**, 513–609 (1997).

236. Okada, M. Regulation of the Src family kinases by Csk. *Int. J. Biol. Sci.* **8**, 1385–1397 (2012).

237. Roskoski, R. Src kinase regulation by phosphorylation and dephosphorylation. *Biochem. Biophys. Res. Commun.* **331**, 1–14 (2005).

238. Roskoski, R. Src protein-tyrosine kinase structure and regulation. *Biochem. Biophys. Res. Commun.* **324**, 1155–1164 (2004).

239. Xu, W., Doshi, A., Lei, M., Eck, M. J. & Harrison, S. C. Crystal structures of c-Src reveal features of its autoinhibitory mechanism. *Mol. Cell* **3**, 629–638 (1999).

240. Burns, C. M. *et al.* CD45 regulation of tyrosine phosphorylation and enzyme activity of src family kinases. *J. Biol. Chem.* **269**, 13594–13600 (1994).

241. Katagiri, T. *et al.* CD45 negatively regulates lyn activity by dephosphorylating both positive and negative regulatory tyrosine residues in immature B cells. *J. Immunol.* **163**, 1321–1326 (1999).

242. Irie-Sasaki, J. *et al.* CD45 is a JAK phosphatase and negatively regulates cytokine receptor signalling. *Nature* **409**, 349–354 (2001).

243. Papers, J. B. C. *et al.* CD45 controls interleukin-4-mediated IgE class switch recombination in human B cells through its function as a Janus kinase phosphatase. *J. Biol. Chem.* **277**, 28830–28835 (2002).

244. Radtke, S. *et al.* The Jak1 SH2 Domain Does Not Fulfill a Classical SH2 Function in Jak / STAT Signaling but Plays a Structural Role for Receptor Interaction and Up-regulation of Receptor Surface Expression. *J. Biol. Chem.* **280**, 25760–25768 (2005).

245. Lindauer, K., Loerting, T., Liedl, K. R. & Kroemer, R. T. Prediction of the structure of human Janus kinase 2 (JAK2) comprising the two carboxy-terminal domains reveals a mechanism for autoregulation. *Protein Eng. Des. Sel.* **14**, 27–37 (2001).

246. Saharinen, P. & Silvennoinen, O. The pseudokinase domain is required for suppression of basal activity of Jak2 and Jak3 tyrosine kinases and for cytokine-inducible activation of signal transduction. *J. Biol. Chem.* **277**, 47954–47963 (2002).

247. Saharinen P, Vihinen, M. & Silvennoinen, O. Autoinhibition of Jak2 Tyrosine Kinase Is Dependent on Specific Regions in Its Pseudokinase Domain. *Mol. Biol. Cell* **14**, 1448–1459 (2003).

248. Heim, M. H. The Jak-Stat Pathway: Cytokine Signalling from the Receptor to the Nucleus. *J. Recept. Signal Transduct.* **19**, 75–120 (1999).

249. Jatiani, S. S., Baker, S. J., Silverman, L. R. & Reddy, E. P. JAK/STAT Pathways in Cytokine Signaling and Myeloproliferative Disorders: Approaches for Targeted Therapies. *Genes Cancer* **1**, 979–993 (2010).

250. Rawlings, J. S., Kristin, M. & Harrison, D. A. The JAK/STAT signaling pathway. *J. Cell Sci.* **117**, 1281–1283 (2004).

251. Silva, C. M. Role of STATs as downstream signal transducers in Src family kinase-mediated tumorigenesis. *Oncogene* **23**, 8017–23 (2004).

252. Baker, S. J., Rane, S. G. & Reddy, E. P. Hematopoietic cytokine receptor signaling. *Oncogene* **26**, 6724–6737 (2007).

253. Shuai, K. & Liu, B. Regulation of JAK-STAT signalling in the immune system. *Nat. Rev. Immunol.* **3**, 900–911 (2003).

254. Ratei, R. *et al.* Immunophenotype and clinical characteristics of CD45-negative and CD45-positive childhood acute lymphoblastic leukemia. *Ann. Hematol.* **77**, 107–114 (1998).

255. Ozdemirli, M., Mankin, H. J., Aisenberg, A. C. & Harris, N. L. Hodgkin's disease presenting as a solitary bone tumor: A report of four cases and review of the literature. *Cancer* **77**, 79–88 (1996).

256. Ishikawa, H., Mahmoud, M. S., Fujii, R., Abroun, S. & Kawano, M. M. Proliferation of immature myeloma cells by interleukin-6 is associated with CD45 expression in human multiple myeloma. *Leuk Lymphoma* **39**, 51–55 (2000).

257. Tchilian, E. Z. & Beverley, P. C. L. Altered CD45 expression and disease. *Trends Immunol.* **27**, 146–153 (2006).

258. Schwinzer, R. *et al.* Enhanced frequency of a PTPRC (CD45) exon A mutation (77C-->G) in systemic sclerosis. *Genes Immun.* **4**, 168–9 (2003).

259. Vogel, A., Strassburg, C. P. & Manns, M. P. 77 C/G mutation in the tyrosine phosphatase CD45 gene and autoimmune hepatitis: evidence for a genetic link. *Genes Immun.* **4**, 79–81 (2003).

260. Dawes, R. *et al.* Altered CD45 expression in C77G carriers influences immune function and outcome of hepatitis C infection. *J. Med. Genet.* **43**, 678–84 (2006).

261. Landskron, J. *et al.* C77G in PTPRC (CD45) is no risk allele for ovarian cancer, but associated with less aggressive disease. *PLoS One* **12**, e0182030 (2017).

262. Wulf, G. G., Luo, K.-L., Goodell, M. A. & Brenner, M. K. Anti-CD45-mediated cytoreduction to facilitate allogeneic stem cell transplantation. *Blood* **101**, 2434–2439 (2003).

263. Zhang, Z. *et al.* Prolongation of xenograft survival using monoclonal

antibody CD45RB and cyclophosphamide in rat-to-mouse kidney and heart transplant models. *Transplantation* **69**, 1137–46 (2000).

264. Lazarovits, A. I. *et al.* Prevention and reversal of renal allograft rejection by antibody against CD45RB. *Nature* **380**, 717–20 (1996).

265. Townsend, K. P. *et al.* CD45 isoform RB as a molecular target to oppose lipopolysaccharide-induced microglial activation in mice. *Neurosci. Lett.* **362**, 26–30 (2004).

266. Tan, J., Town, T. & Mullan, M. CD45 inhibits CD40L-induced microglial activation via negative regulation of the Src/p44/42 MAPK pathway. *J. Biol. Chem.* **275**, 37224–31 (2000).

267. Matthews, D. C. *et al.* Marrow ablative and immunosuppressive effects of 131I-anti-CD45 antibody in congenic and H2-mismatched murine transplant models. *Blood* **93**, 737–45 (1999).

268. Matthews, D. C. *et al.* Phase I Study of 131I-Anti-CD45 Antibody Plus Cyclophosphamide and Total Body Irradiation for Advanced Acute Leukemia and Myelodysplastic Syndrome. *Blood* **94**, (1999).

269. Glatting, G. *et al.* Anti-CD45 monoclonal antibody YAML568: A promising radioimmunoconjugate for targeted therapy of acute leukemia. *J. Nucl. Med.* **47**, 1335–41 (2006).

270. Lee, K. & Burke, T. R. CD45 protein-tyrosine phosphatase inhibitor development. *Curr. Top. Med. Chem.* **3**, 797–807 (2003).

271. Stanford, S. M. & Bottini, N. Targeting Tyrosine Phosphatases: Time to End the Stigma. *Trends Pharmacol. Sci.* **38**, 524–540 (2017).

272. Perron, M. D. *et al.* Allosteric noncompetitive small molecule selective inhibitors of CD45 tyrosine phosphatase suppress T-cell receptor signals and inflammation in vivo. *Mol. Pharmacol.* **85**, 553–63 (2014).

273. Perron, M. & Saragovi, H. U. Inhibition of CD45 Phosphatase Activity Induces Cell Cycle Arrest and Apoptosis of CD45+ Lymphoid Tumors Ex

Vivo and In Vivo. *Mol. Pharmacol.* **93**, 575–580 (2018).

274. Pellat-Deceunynck, C. & Bataille, R. Normal and malignant human plasma cells: Proliferation, differentiation, and expansions in relation to CD45 expression. *Blood Cells, Mol. Dis.* **32**, 293–301 (2004).

275. Jackson, N. *et al.* An analysis of myeloma plasma cell phenotype using antibodies defined at the IIIrd International Workshop on Human Leucocyte Differentiation Antigens. *Clin. Exp. Immunol.* **72**, 351–6 (1988).

276. Schneider, U., Van Lessen, A., Huhn, D. & Serke, S. Two subsets of peripheral blood plasma cells defined by differential expression of CD45 antigen. *Br. J. Haematol.* **97**, 56–64 (1997).

277. Mahmoud, M. S., Ishikawa, H., Fujii, R. & Kawano, M. M. Induction of CD45 expression and proliferation in U-266 myeloma cell line by interleukin-6. *Blood* **92**, 3887–97 (1998).

278. Descamps, G. *et al.* The magnitude of Akt/phosphatidylinositol 3'-kinase proliferating signaling is related to CD45 expression in human myeloma cells. *J. Immunol.* **173**, 4953–9 (2004).

279. Huntington, N. D., Xu, Y., Nutt, S. L. & Tarlinton, D. M. A requirement for CD45 distinguishes Ly49D-mediated cytokine and chemokine production from killing in primary natural killer cells. *J. Exp. Med.* **201**, 1421–33 (2005).

280. Venot, C. *et al.* CD45neg but Not CD45pos Human Myeloma Cells Are Sensitive to the Inhibition of IGF-1 Signaling by a Murine Anti-IGF-1R Monoclonal Antibody, mAVE1642. *J. Immunol.* **177**, 4218–4223 (2014).

281. Ramakrishnan, V. *et al.* TG101209, a novel JAK2 inhibitor, has significant in vitro activity in multiple myeloma and displays preferential cytotoxicity for CD45+ myeloma cells. *Am. J. Hematol.* **85**, 675–686 (2010).

282. Schopf, F. H., Biebl, M. M. & Buchner, J. The HSP90 chaperone machinery. *Nat. Rev. Mol. Cell Biol.* **18**, 345–360 (2017).

283. Giulino-Roth, L. *et al.* Inhibition of Hsp90 Suppresses PI3K/AKT/mTOR Signaling and Has Antitumor Activity in Burkitt Lymphoma. *Mol. Cancer Ther.* **16**, 1779–1790 (2017).

284. Schoof, N., von Bonin, F., Trümper, L. & Kube, D. HSP90 is essential for Jak-STAT signaling in classical Hodgkin lymphoma cells. *Cell Commun. Signal.* **7**, 17 (2009).

285. Lin, H. *et al.* An activated JAK/STAT3 pathway and CD45 expression are associated with sensitivity to Hsp90 inhibitors in multiple myeloma. *Exp. Cell Res.* **319**, 600–611 (2013).

286. Asosingh, K. *et al.* In vivo homing and differentiation characteristics of mature (CD45−) and immature (CD45+) 5T multiple myeloma cells. *Exp. Hematol.* **29**, 77–84 (2001).

287. Asosingh, K. *et al.* Mechanisms involved in the differential bone marrow homing of CD45 subsets in 5T murine models of myeloma. *Clin. Exp. Metastasis* **19**, 583–591 (2002).

288. Kollet, O. *et al.* CD45 regulates retention, motility, and numbers of hematopoietic progenitors, and affects osteoclast remodeling of metaphyseal trabecules. *J. Exp. Med.* **205**, 2381–2395 (2008).

289. Lai, J. C. Y., Wlodarska, M., Liu, D. J., Abraham, N. & Johnson, P. CD45 regulates migration, proliferation, and progression of double negative 1 thymocytes. *J. Immunol.* **185**, 2059–70 (2010).

290. St-Pierre, J., Ostergaard, H. L., St-Pierre, J. & Ostergaard, H. L. A role for the protein tyrosine phosphatase CD45 in macrophage adhesion through the regulation of paxillin degradation. *PLoS One* **8**, e71531 (2013).

291. Zhao, M., Finlay, D., Zharkikh, I. & Vuori, K. Novel role of Src in priming Pyk2 phosphorylation. *PLoS One* **11**, 1–14 (2016).

292. Playford, M. P. & Schaller, M. D. The interplay between Src and integrins in normal and tumor biology. *Oncogene* **23**, 7928–7946 (2004).

293. Li, R., Wong, N., Jabali, M. D. & Johnson, P. CD44-initiated Cell Spreading Induces Pyk2 Phosphorylation, Is Mediated by Src Family Kinases, and Is Negatively Regulated by CD45. *J. Biol. Chem.* **276**, 28767–28773 (2001).

294. Wong, N. K. Y., Lai, J. C. Y., Maeshima, N. & Johnson, P. CD44-mediated elongated T cell spreading requires Pyk2 activation by Src family kinases, extracellular calcium, phospholipase C and phosphatidylinositol-3 kinase. *Cell. Signal.* **23**, 812–819 (2011).

295. Ishikawa, H. *et al.* Requirements of src family kinase activity associated with CD45 for myeloma cell proliferation by interleukin-6. *Blood* **99**, 2172–2178 (2002).

296. Asosingh, K., De Raeve, H., Van Riet, I., Van Camp, B. & Vanderkerken, K. Multiple myeloma tumor progression in the 5T2MM murine model is a multistage and dynamic process of differentiation, proliferation, invasion, and apoptosis. *Blood* **101**, 3136–41 (2003).

297. Kumar, S., Rajkumar, S. V, Kimlinger, T., Greipp, P. R. & Witzig, T. E. CD45 expression by bone marrow plasma cells in multiple myeloma: clinical and biological correlations. *Leukemia* **19**, 1466–1470 (2005).

298. P Moreau, N Robillard, H Avet-Loiseau, D Pineau, N Morineau, N Milpied, JL Harousseau, R. B. Patients with CD45 negative multiple myeloma receiving high-dose therapy have a shorter survival than those with CD45 positive multiple myeloma. *Haematologica* **89**, 1–5 (2004).

299. Gonsalves, W. I. *et al.* The prognostic significance of CD45 expression by clonal bone marrow plasma cells in patients with newly diagnosed multiple myeloma. *Leuk. Res.* **44**, 32–39 (2016).

300. Guo, J. *et al.* The prognostic impact of multiparameter flow cytometry immunophenotyping and cytogenetic aberrancies in patients with multiple myeloma. *Hematology* **21**, 152–161 (2016).

301. Sonneveld, P. *et al.* Treatment of multiple myeloma with high-risk

cytogenetics: A consensus of the International Myeloma Working Group. *Blood* **127**, 2955–2962 (2016).

302. Sanjana, N. E., Shalem, O. & Zhang, F. Improved vectors and genome-wide libraries for CRISPR screening. *Nat. Methods* **11**, 783–784 (2014).

303. J, J. *et al.* Genome-Scale CRISPR-Cas9 Knockout Screening in Human Cells. *Science (80-.).* **343**, 84–88 (2014).

304. Anders, S., Pyl, P. T. & Huber, W. HTSeq--a Python framework to work with high-throughput sequencing data. *Bioinformatics* **31**, 166–169 (2015).

305. Robinson, M. D., McCarthy, D. J. & Smyth, G. K. edgeR: a Bioconductor package for differential expression analysis of digital gene expression data. *Bioinformatics* **26**, 139–140 (2010).

306. Huang, D. W., Sherman, B. T. & Lempicki, R. A. Systematic and integrative analysis of large gene lists using DAVID bioinformatics resources. *Nat. Protoc.* **4**, 44–57 (2009).

307. Huang, D. W., Sherman, B. T. & Lempicki, R. A. Bioinformatics enrichment tools: paths toward the comprehensive functional analysis of large gene lists. *Nucleic Acids Res.* **37**, 1–13 (2009).

308. Saint-paul, L. *et al.* CD45 phosphatase is crucial for human and murine acute myeloid leukemia maintenance through its localization in lipid rafts. **7**,

309. Jansen, R., Embden, J. D. A. van, Gaastra, W. & Schouls, L. M. Identification of genes that are associated with DNA repeats in prokaryotes. *Mol. Microbiol.* **43**, 1565–1575 (2002).

310. Mojica, F. J. M., Díez-Villaseñor, C., García-Martínez, J. & Soria, E. Intervening sequences of regularly spaced prokaryotic repeats derive from foreign genetic elements. *J. Mol. Evol.* **60**, 174–82 (2005).

311. Makarova, K. S. *et al.* An updated evolutionary classification of CRISPR–

Cas systems. *Nat. Rev. Microbiol.* **13**, 722–736 (2015).

312. Lander, E. S. The Heroes of CRISPR. *Cell* **164**, 18–28 (2016).

313. Joung, J. K. & Sander, J. D. TALENs: a widely applicable technology for targeted genome editing. *Nat. Rev. Mol. Cell Biol.* **14**, 49–55 (2012).

314. Urnov, F. D., Rebar, E. J., Holmes, M. C., Zhang, H. S. & Gregory, P. D. Genome editing with engineered zinc finger nucleases. *Nat. Rev. Genet.* **11**, 636–646 (2010).

315. Sander, J. D. & Joung, J. K. CRISPR-Cas systems for editing, regulating and targeting genomes. *Nat. Biotechnol.* **32**, 347–55 (2014).

316. Gundry, M. C. *et al.* Highly Efficient Genome Editing of Murine and Human Hematopoietic Progenitor Cells by CRISPR/Cas9. *Cell Rep* **17**, 1453–1461 (2016).

317. Heckl, D. *et al.* Generation of mouse models of myeloid malignancy with combinatorial genetic lesions using CRISPR-Cas9 genome editing. *Nat. Biotechnol.* **32**, 941–6 (2014).

318. Mandal, P. K. *et al.* Efficient Ablation of Genes in Human Hematopoietic Stem and Effector Cells using CRISPR/Cas9. *Cell Stem Cell* **15**, 643–652 (2014).

319. Jiang, W., Bikard, D., Cox, D., Zhang, F. & Marraffini, L. A. RNA-guided editing of bacterial genomes using CRISPR-Cas systems. *Nat. Biotechnol.* **31**, 233–239 (2013).

320. Lieber, M. R. The Mechanism of Double-Strand DNA Break Repair by the Nonhomologous DNA End-Joining Pathway. *Annu. Rev. Biochem.* **79**, 181–211 (2010).

321. Li, X. & Heyer, W.-D. Homologous recombination in DNA repair and DNA damage tolerance. *Cell Res.* **18**, 99–113 (2008).

322. Bae, S., Park, J. & Kim, J.-S. Cas-OFFinder: a fast and versatile algorithm

that searches for potential off-target sites of Cas9 RNA-guided endonucleases. *Bioinformatics* **30**, 1473–1475 (2014).

323. Dehairs, J., Talebi, A., Cherifi, Y. & Swinnen, J. V. CRISP-ID: decoding CRISPR mediated indels by Sanger sequencing. *Sci. Rep.* **6**, 28973 (2016).

324. Manier, S. *et al.* Genomic complexity of multiple myeloma and its clinical implications. *Nat. Rev. Clin. Oncol.* **14**, 100–113 (2017).

325. Durand, S. & Cimarelli, A. The inside out of lentiviral vectors. *Viruses* **3**, 132–59 (2011).

326. Karousis, E. D., Nasif, S. & Mühlemann, O. Nonsense-mediated mRNA decay: novel mechanistic insights and biological impact. *Wiley Interdiscip. Rev. RNA* **7**, 661–682 (2016).

327. Desai, D. M., Sap, J., Silvennoinen, O., Schlessinger, J. & Weiss, A. The catalytic activity of the CD45 membrane-proximal phosphatase domain is required for TCR signaling and regulation. *EMBO J.* **13**, 4002–10 (1994).

328. Cao, J. *et al.* An easy and efficient inducible CRISPR/Cas9 platform with improved specificity for multiple gene targeting. *Nucleic Acids Res.* **44**, (2016).

329. Chen, S., Lee, B., Lee, A. Y.-F., Modzelewski, A. J. & He, L. Highly Efficient Mouse Genome Editing by CRISPR Ribonucleoprotein Electroporation of Zygotes. *J. Biol. Chem.* **291**, 14457–14467 (2016).

330. Zuris, J. A. *et al.* Cationic lipid-mediated delivery of proteins enables efficient protein-based genome editing in vitro and in vivo. *Nat. Biotechnol.* **33**, 73–80 (2015).

331. Matsui, W. *et al.* Characterization of clonogenic multiple myeloma cells. *Blood* **103**, 2332–6 (2004).

332. Kukreja, A. *et al.* Enhancement of clonogenicity of human multiple myeloma by dendritic cells. *J. Exp. Med.* **203**, 1859–1865 (2006).

333. He, C. & Klionsky, D. J. Regulation mechanisms and signaling pathways of autophagy. *Annu. Rev. Genet.* **43**, 67–93 (2009).

334. Mauthe, M. *et al.* Chloroquine inhibits autophagic flux by decreasing autophagosome-lysosome fusion. *Autophagy* **14**, 1435–1455 (2018).

335. Penninger, J. M., Irie-Sasaki, J., Sasaki, T. & Oliveira-dos-Santos, a J. CD45: new jobs for an old acquaintance. *Nat. Immunol.* **2**, 389–396 (2001).

336. Eagle, H. Nutrition Needs of Mammalian Cells in Tissue Culture. *Science (80-.).* **122**, 501–504 (1955).

337. Altman, B. J., Stine, Z. E. & Dang, C. V. From Krebs to clinic: glutamine metabolism to cancer therapy. *Nat. Rev. Cancer* **16**, 619–34 (2016).

338. Martinez-Outschoorn, U. E., Peiris-Pagés, M., Pestell, R. G., Sotgia, F. & Lisanti, M. P. Cancer metabolism: a therapeutic perspective. *Nat. Rev. Clin. Oncol.* **14**, 11–31 (2017).

339. Bolzoni, M. *et al.* Dependence on glutamine uptake and glutamine addiction characterize myeloma cells: A new attractive target. *Blood* **128**, 667–679 (2016).

340. Effenberger, M. *et al.* Glutaminase inhibition in multiple myeloma induces apoptosis via MYC degradation. *Oncotarget* **8**, 85858–85867 (2017).

341. Bajpai, R. *et al.* Targeting glutamine metabolism in multiple myeloma enhances BIM binding to BCL-2 eliciting synthetic lethality to venetoclax. *Oncogene* **35**, 3955–3964 (2016).

342. Mizushima, N. & Komatsu, M. Autophagy: renovation of cells and tissues. *Cell* **147**, 728–41 (2011).

343. Galluzzi, L. *et al.* Autophagy in malignant transformation and cancer progression. *EMBO J.* **34**, 856–880 (2015).

344. Savvidou, I., Khong, T. T. & Spencer, A. The Role of Autophagy in

Multiple Myeloma Progression. *Blood* **130**, (2017).

345. Johnsen, H. E. *et al.* The myeloma stem cell concept, revisited: from phenomenology to operational terms. *Haematologica* 1451–1459 (2016). doi:10.3324/haematol.2015.138826

346. Kim, D., Park, C. Y., Medeiros, B. C. & Weissman, I. L. CD19- CD45low/-CD38high/CD138+ plasma cells enrich for human tumorigenic myeloma cells. *Leukemia* **26**, 2530–2537 (2012).

347. Lin, C., Khong, T. T., Mithraprabhu, S. & Spencer, A. CD45-Ve but Not CD45+Ve U266 Myeloma Cells Demonstrate an Active Epithelial to Mesenchymal Transition (EMT) Transcriptional Programme. *Blood* **120**, (2012).

348. Irby, R. B. & Yeatman, T. J. Role of Src expression and activation in human cancer. *Oncogene* **19**, 5636–5642 (2000).

349. Mashimo, K. *et al.* RANKL-induced c-Src activation contributes to conventional anti-cancer drug resistance and dasatinib overcomes this resistance in RANK-expressing multiple myeloma cells. *Clin. Exp. Med.* (2018). doi:10.1007/s10238-018-0531-4

350. Heusschen, R. *et al.* SRC kinase inhibition with saracatinib limits the development of osteolytic bone disease in multiple myeloma. *Oncotarget* **7**, 30712–29 (2016).

351. Dai, Y. *et al.* Disruption of Src function potentiates Chk1-inhibitor – induced apoptosis in human multiple myeloma cells in vitro and in vivo. **117**, 1947–1958 (2016).

352. Chauhan, D. *et al.* RAFTK/PYK2-dependent and -independent apoptosis in multiple myeloma cells. *Oncogene* **18**, 6733–6740 (1999).

353. Zhang, Y. *et al.* Pyk2 promotes tumor progression in multiple myeloma. *Blood* **124**, 2675–2687 (2015).

354. Meads, M. B. *et al.* Targeting PYK2 mediates microenvironment-specific

cell death in multiple myeloma. *Oncogene* **35**, 2723–2734 (2016).

355. Bolós, V., Gasent, J. M., López-Tarruella, S. & Grande, E. The dual kinase complex FAK-src as a promising therapeutic target in cancer. *Onco. Targets. Ther.* **3**, 83–97 (2010).

356. Hughes, C. S., Postovit, L. M. & Lajoie, G. A. Matrigel: A complex protein mixture required for optimal growth of cell culture. *Proteomics* **10**, 1886–1890 (2010).

357. Springer, T. A. Traffic signals for lymphocyte recirculation and leukocyte emigration: the multistep paradigm. *Cell* **76**, 301–14 (1994).

358. Ueda, Y. *et al.* Mst1 regulates integrin-dependent thymocyte trafficking and antigen recognition in the thymus. *Nat. Commun.* **3**, 1098 (2012).

359. Mullooly, M., McGowan, P. M., Crown, J. & Duffy, M. J. The ADAMs family of proteases as targets for the treatment of cancer. *Cancer Biol. Ther.* **17**, 870–880 (2016).

360. Duffy, M. J., McKiernan, E., O'Donovan, N. & McGowan, P. M. The role of ADAMs in disease pathophysiology. *Clin. Chim. Acta* **403**, 31–36 (2009).

361. Konopleva, M. Y. & Jordan, C. T. Leukemia Stem Cells and Microenvironment: Biology and Therapeutic Targeting. *J. Clin. Oncol.* **29**, 591–599 (2011).

362. Burger, J. A. & Peled, A. CXCR4 antagonists: targeting the microenvironment in leukemia and other cancers. *Leukemia* **23**, 43–52 (2009).

363. Crazzolara, R. *et al.* High expression of the chemokine receptor CXCR4 predicts extramedullary organ infiltration in childhood acute lymphoblastic leukaemia. *Br. J. Haematol.* **115**, 545–553 (2001).

364. Roccaro, A. M. *et al.* CXCR4 regulates extra-medullary myeloma through epithelial-mesenchymal-transition-like transcriptional activation. *Cell Rep.* **12**, 622–635 (2015).

365. Vandyke, K. *et al.* HIF-2α promotes dissemination of plasma cells in multiple myeloma by regulating CXCL12/CXCR4 and CCR1. *Cancer Res.* **77**, 5452–5463 (2017).

366. Parsons, J. T., Martin, K. H., Slack, J. K., Taylor, J. M. & Weed, S. A. Focal adhesion kinase: a regulator of focal adhesion dynamics and cell movement. *Oncogene* **19**, 5606–5613 (2000).

367. Tornillo, G. *et al.* Dual Mechanisms of LYN Kinase Dysregulation Drive Aggressive Behavior in Breast Cancer Cells. *Cell Rep.* **25**, 3674-3692.e10 (2018).

368. Yadav, V. & Denning, M. F. Fyn is induced by Ras/PI3K/Akt signaling and is required for enhanced invasion/migration. *Mol. Carcinog.* **50**, 346–52 (2011).

369. Cavalloni, G. *et al.* Antitumor activity of Src inhibitor saracatinib (AZD-0530) in preclinical models of biliary tract carcinomas. *Mol. Cancer Ther.* **11**, 1528–38 (2012).

370. Nam, H.-J. *et al.* Antitumor Activity of Saracatinib (AZD0530), a c-Src/Abl Kinase Inhibitor, Alone or in Combination with Chemotherapeutic Agents in Gastric Cancer. *Mol. Cancer Ther.* **12**, 16–26 (2013).

371. Chang, Y. M. *et al.* Src family kinase oncogenic potential and pathways in prostate cancer as revealed by AZD0530. *Oncogene* **27**, 6365–6375 (2008).

372. Amano, O., Mizobe, K., Bando, Y. & Sakiyama, K. Anatomy and histology of rodent and human major salivary glands: -overview of the Japan salivary gland society-sponsored workshop-. *Acta Histochem. Cytochem.* **45**, 241–50 (2012).

373. Cannon, B. & Nedergaard, J. Brown adipose tissue: function and physiological significance. *Physiol. Rev.* **84**, 277–359 (2004).

374. Harsha, H. C. & Pandey, A. Phosphoproteomics in cancer. *Mol. Oncol.* **4**,

482–495 (2010).

375. Lietha, D. *et al.* Structural basis for the autoinhibition of focal adhesion kinase. *Cell* **129**, 1177–87 (2007).

376. Meenderink, L. M. *et al.* P130Cas Src-Binding and Substrate Domains Have Distinct Roles in Sustaining Focal Adhesion Disassembly and Promoting Cell Migration. *PLoS One* **5**, e13412 (2010).

377. Westhoff, M. A., Serrels, B., Fincham, V. J., Frame, M. C. & Carragher, N. O. Src-Mediated Phosphorylation of Focal Adhesion Kinase Couples Actin and Adhesion Dynamics to Survival Signaling. *Mol Cell Biol* **24**, 8113–8133 (2004).

378. Mitra, S. K., Hanson, D. A. & Schlaepfer, D. D. Focal adhesion kinase: In command and control of cell motility. *Nat. Rev. Mol. Cell Biol.* **6**, 56–68 (2005).

379. Hsia, D. A. *et al.* Differential regulation of cell motility and invasion by FAK. *J. Cell Biol.* **160**, 753–67 (2003).

380. Brábek, J. *et al.* CAS promotes invasiveness of Src-transformed cells. *Oncogene* **23**, 7406–7415 (2004).

381. Turner, C. E. Paxillin and focal adhesion signalling. *Nat. Cell Biol.* **2**, E231–E236 (2000).

382. Wu, P. *et al.* The impact of extramedullary disease at presentation on the outcome of myeloma. *Leuk. Lymphoma* **50**, 230–235 (2009).

383. Varettoni, M. *et al.* Incidence, presenting features and outcome of extramedullary disease in multiple myeloma: A longitudinal study on 1003 consecutive patients. *Ann. Oncol.* **21**, 325–330 (2010).

384. Tembhare, P., Yuan, C., Korde, N., Maric, I. & Landgren, O. Antigenic drift in relapsed extramedullary multiple myeloma: plasma cells without CD38 expression. *Leuk. Lymphoma* **53**, 721–4 (2012).

385. Avigdor, A., Raanani, P., Levi, I., Hardan, I. & Ben-Bassat, I. Extramedullary Progression Despite a Good Response in the Bone Marrow in Patients Treated with Thalidomide for Multiple Myeloma. *Leuk. Lymphoma* **42**, 683–687 (2001).

386. Rosiñol, L. *et al.* Extramedullary multiple myeloma escapes the effect of thalidomide. *Haematologica* **89**, 832–6 (2004).

387. Laura, R. *et al.* Bortezomib: an effective agent in extramedullary disease in multiple myeloma. *Eur. J. Haematol.* **76**, 405–408 (2006).

388. Raanani, P., Shpilberg, O. & Ben-Bassat, I. Extramedullary disease and targeted therapies for hematological malignancies--is the association real? *Ann. Oncol.* **18**, 7–12 (2006).

APPENDICES

Appendix 1: CD45 expression in HMCLs

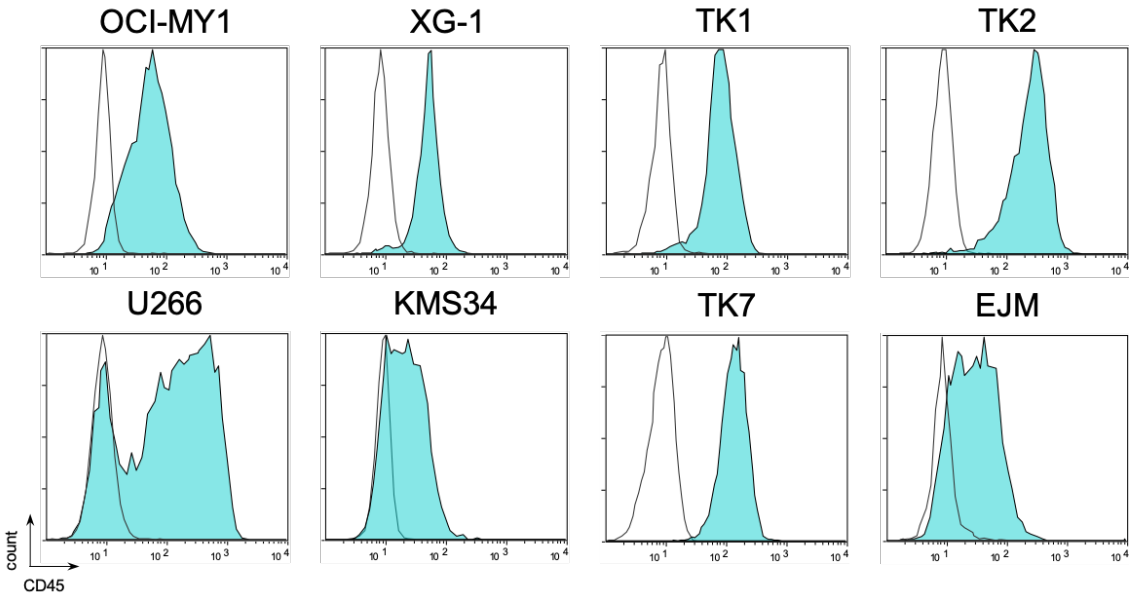

Appendix 1 CD45 expression in HMCLs. CD45 expression (blue histograms) of OCI-MY1, XG-1, TK1, TK2, U266, KMS34, TK7 and EJM was analysed by FACS. Isotype control is represented by an open black histogram.

Appendix 2: Sequences of $CD45^{KO}$ cells

OCI-MY1 A11

Sequence_1:

ATTTACAAGCTGAGGTCCTTGTTAGGGCAGTAAAGCACAGATAATTACGAAAAAAATGATATGGAGGCACCTAATGTGTTTTTTCTT
TTTCATGTTTTTTGGGGATATTTGGTTAGTTGATTTGATATTTTGGCATTTGCATTAATGTAGTTTTATTTATTCTGGAAAAATAAC
ACTCAATGTTCTATTTTCTTTTAGATGAAAAATATGCAAACATCACTGTGGATTACTTATATAACAAGGAAACTAAATTATTTACAGC
AAAGCTAAATGTTAATGAGAATGTGGAATGTGGAAACAATACTTGCACAAACAATGAGGTGCATAACCTTACAGAATGTAAAAATGC
GTCTGTTTCCATATCTCATAATTCATGTACTGCTCCTGATAAGACATTAATATTAGATGTGCCCAGCTTCTAGAAATCAATTTATTAC
TTCTAATAAATAAATAAAAACAACACACCTCTGTGGGGGGTGGTGTTCACCGGTCGCAGCAGGCAACTCTGCCTGATAAAACAAGA
CTGGATGAAAAAGAGGGTTCCTTCGTAGACAAACTGGAAGGAATCAACCTTGTCTGCCTGTACTCCAACCTAATAAATAGATGGAA
GATACAAACTAAGTCCTGTCCTGACCTGACCATACCATCTCAATTCAACTCAACTATCCTT

Sequence_2:

ATTTACAAGCTGAGGTCCTTGTTAGGGCAGTAAAGCACAGATAATTACGAAAAAAATGATATGGAGGCACCTAATGTGTTTTTTCTT
TTTCATGTTTTTTGGGGATATTTGGTTAGTTGATTTGATATTTTGGCATTTGCATTAATGTAGTTTTATTTATTCTGGAAAAATAAC
ACTCAATGTTCTATTTTCTTTTAGATGAAAAATATGCAAACATCACTGTGGATTACTTATATAACAAGGAAACTAAATTATTTACAGC
AAAGCTAAATGTTAATGAGAATGTGGAATGTGGAAACAATACTTGCACAAACAATGAGGTGCATAACCTTACAGAATGTAAAAATGC
GTCTGTTTCCATATCTCATAATTCATGTACTGCTCCTGATAAGACATTAATATTAGATGTGCTCACCTTCTAGAAATCAATTTATTAC
TTCTAATAAATAAATAAAAACAACACACTTTTGTGGGGGGTGTTGTTCACCGGTCGCAGGAGGCTACTCTGCCTGAAGAAACAAGA
CTGGATGAAAAAGAGCGTTGCTTCGGAGACAAACTGGATGGAATCATCCTTGTCTGACTTTACTCCAACCTAATTAATAGATGGAA
GATCAAAACAAAGTCCTGTCCTGTCCTGACCATACCATCTCAATTCAACTCAACTATCCTT

Sequence_3:

ATTTACAAGCTGAGGTCCTTGTTACCGTTGTAAAGCACAGATAATTACGAAAAAAATGATATGGAGGCACCTAATGTGTTTTTTCTT
TTTCATGTTTTTTGGGGATATTTGGTTAGTTGATTTGATATTTTGGCATTTGCATTAATGTAGTTTTATTTATTCTGGAAAAATAAC
ACTCAATGTTCTATTTTCTTTTAGATGAAAAATATGCAAACATCACTGTGGATTACTTATATAACAAGGAAACTAAATTATTTACAGC
AAAGCTAAATGTTAATGAGAATGTGGAATGTGGAAACAATACTTGCACAAACAATGAGGTGCATAACCTTACAGAATGTAAAAATGC
GTCTGTTTCCATATCTCATAATTCATGTACTGCTCCTGATAAGACATTAATATTAGATGTGCAAATAAGGAAATTAATATCAACTTTT
ATTTAATAAAATTTTTCTAAAAGTAGTAGAGTTTGTGGTGCGCCCTCGTCTAGTGATACTAGCGCGGTAGTGGTGGGCAGAGATCA
GGTGCTGGGGGGTAAAAAAATCTTCCTAGCCGAGAAGGGTGGTAGTGTCCTGGCTGTTGCTCAACAACGCAAAGGAATTGATAGC
TGGGGTGTTACAATTAATGCTCTGGTCATAACATACAAATTCAACTCAACTCAACTTACTTT

OCI-MY1 C9

Sequence_1:

TTTACAAGCTGAGGTCCTTGTTAGGGCAGTAAAGCACAGATAATTACGAAAAAAATGATATGGAGGCACCTAATGTGTTTTTTCTTT
TTCATGTTTTTTGGGGATATTTGGTTAGTTGATTTGATATTTTGGCATTTGCATTAATGTAGTTTTATTTATTCTGGAAAAATAACA
CTCAATGTTCTATTTTCTTTTAGATGAAAAATATGCAAACATCACTGTGGATTACTTATATAACAAGGAAACTAAATTATTTACAGCA
AAGCTAAATGTTAATGAGAATGTGGAATGTGGAAACAATACTTGCACAAACAATGAGGTGCATAACCTTACAGAATGTAAAAATGC
GTCTGTTTCCATATCTCATAATTCATGTACTGCTCCTGATAAGACATTAATATTAGATGTGCCCACCAGGTAAATATCAATTTATTTC
TTTTAATAAATTTATAAAAACAGTACACTTTTGTGTGTGGTGTTCTCCAGTGGTCACAGGAGCTAGTCTGGTGAGAGAACAGGGCT
GAGGGAAAGGAAATTCCTTGGAAACAAGTGGGTGAACTTTCTGCTGTCTTAACCAAGTAAAAATGATAGAGTCAAATAAGCCTTCT
GTTTACATCCATTAATCACCACTTCTACTTATTTAACAGGGAGATGTTTATGTGCAC

OCI-MY1 3C9

Sequence_1:
AGCTGAGGTCCTTGTTAGGGCAGTAAAGCACAGATAATTACGAAAAAAAATGATATGGAGGCACCTAATGTGTTTTTTCTTTTTCATG
TTTTTTGGGGATATTTGGTTAGTTGATTTGATATTTTGGCATTTGCATTAATGTAGTTTTATTTATTCTGGAAAAATAACACTCAAT
GTTCTATTTTCTTTTAGATGAAAAATATGCAAACATCACTGTGGATTACTTATATAACAAGGAAACTAAATTATTTACAGCAAAGCTA
AATGTTAATGAGAATGTGGAATGTGGAAACAATACTTGCACAAACAATGAGGTGCATAACCTTACAGAATGTAAAAATGCGTCTGTT
TCCATATCTCATAATTCATGTACTGCTCCTGATAAAACATTAATATTAAATGTGCCCACCATGTAAATATCAGTTTATTTCTTTTAAT
AAATTTATAAAAACAGTACACTTTTGTGTGTGGTGTTCTCCAGTGGTCACAAGAGCTAGTCTGGTGAGAGAACAGGGCTGAGGGAA
AGGAAATTCCTTGGAAACAAGTGGCTGAACTTTCTGCTGTCTTAACCAAGTAAAAATGATATAGTCAAATAAACCTTCTGTTTACAT
CCATTAATCACCACTTCTACTTATTTAACAGGGAAATGTTTATTAGCACTAA

Sequence_2:
AGCTGAGGTCCTTGTTAGGGCAGTAAAGCACAGATAATTACGAAAAAAAATGATATGGAGGCACCTAATGTGTTTTTTCTTTTTCATG
TTTTTTGGGGATATTTGGTTAGTTGATTTGATATTTTGGCATTTGCATTAATGTAGTTTTATTTATTCTGGAAAAATAACACTCAAT
GTTCTATTTTCTTTTAGATGAAAAATATGCAAACATCACTGTGGATTACTTATATAACAAGGAAACTAAATTATTTACAGCAAAGCTA
AATGTTAATGAGAATGTGGAATGTGGAAACAATACTTGCACAAACAATGAGGTGCATAACCTTACAGAATGTAAAAATGCGTCTGTT
TCCATATCTCATAATTCATGTACTGCTCCTGATAAAACATTAATATTAAATGTGCCCACCATGTAAATATCAGTTTATTTCTTTTAAT
AAATTTATAAAAACAGTACACTTTTGTGTGTGGTGTTCTCCATTGGTCACAAGACCTAGTCTGGTGAGAGAACAGGCCTGACGGAA
AGGAAATTCCTTGGAAACAAGTGGCTGAACTTTCTGCTGTCTTAACCAAGTAAAAATGATATAGTCAAATAAACCTTCTGTTTACAT
CCATTAATCACCACTTCTACTTATTTAACATGGAATCGTTTATGAGCACTAA

Sequence_3:
AGCTGAGGTCCTTGTTAGGCCATTATAGCACAGATAATTACGAAAAAAAATGATATGGAGGCACCTAATGTGTTTTTTCTTTTTCATG
TTTTTTGGGGATATTTGGTTAGTTGATTTGATATTTTGGCATTTGCATTAATGTAGTTTTATTTATTCTGGAAAAATAAGACTCAAT
GTTCTATTTTCTTTTAGATGAAAAATATGCAAACATCACTGTGGATTACTTATATAACAAGGAAACTAAATTATTTACAGCAAAGCTA
AATGTTAATGAGAATGTGGAATGTGGAAACAATACTTGCACAAACAATGAGGTGCATAACCTTACAGAATGTAAAAATGCGTCTGTT
TCCATATCTCATAATTCATGTACTGCTCCTGATTTGATAAATTTATAAGAACAGTACACTTGTGTGTGTGGTATTCTCCAGTGGTCA
CAGGATCATAAAATGGTGACAGATTTGGGTGTAGGGAACGGAAATGCTCTGGGAAAATAGTCTGAACTTTCTGCCGGTTTAATCAA
GTAAAAATGATAGAGTCAAATAAGCGTTCTGTTTACGTCCTTTAATCACCACTTCTACTTATGTAACAGGGAGGTGTTTAGGTGCAC
TAAATATAGTTTATCCTGCTAAGTGATTGTCCGCAGCGTTTCTTATGCACTTA

OCI-MY1 D8

Sequence_1:
GCTGAGGTCCTTGTTAGGGCATTAAAGCACAGATAATTACGAAAAAAAATGATATGGAGGCACCTAATGTGTTTTTTCTTTTTCATGT
TTTTTGGGGATATTTGGTTAGTTGATTTGATATTTTGGCATTTGCATTAATGTAGTTTTATTTATTCTGGAAAAATAACACTCAATG
TTCTATTTTCTTTTAGATGAAAAATATGCAAACATCACTGTGGATTACTTATATAACAAGGAAACTAAATTATTTACAGCAAAGCTAA
ATGTTAATGAGAATGTGGAATGTGGAAACAATACTTGCACAAACAATGAGGTGCATAACCTTACAGAATGTAAAAATGCGTCTGTTT
CCATATCTCATAATTCATGTACTGCTCCTGATAAGACATTAATATTAGATGTGCCCACCAGGTAAATATCATTTTATTTCTTTTAATA
AATTTATAAAAACAGTACACTTTTGTGTGTGGTGTTCTCCAGTGGTCACAGGATCTACTCTGGTGAGAGAACAGGGCTGAGGGAAA
AGAAATTCCTTGGAAACAAGTGGGAGAACTTTCTGCTGTCTTAACCAAGTAAAAATGATAGAGTCAAATAACCCTTCTGTTTACATC
CATTACTCACCACTTCTACTTATTTAACAGGGAGATGTTTATGTGCACTAAATA

Sequence_2:
GCTGAGGTCCTTGTTAGGGCAGTAAAGCACAGATAATTACGAAAAAAAATGATATGGAGGCACCTAATGTGTTTTTTCTTTTTCATGT
TTTTTGGGGATATTTGGTTAGTTGATTTGATATTTTGGCATTTGCATTAATGTAGTTTTATTTATTCTGGAAAAATAACACTCAATG
TTCTATTTTCTTTTAGATGAAAAATATGCAAACATCACTGTGGATTACTTATATAACAAGGAAACTAAATTATTTACAGCAAAGCTAA

ATGTTAATGAGAATGTGGAATGTGGAAACAATACTTGCACAAACAATGAGGTGCATAACCTTACAGAATGTAAAAATGCGTCTGTTT
CCATATCTCATAATTCATGTACTGCTCCTGATAAGACATTAATATTAGATGTGCACCAGGTAAATATCAATATATTTCTTTTAATAAA
TTTATAAAAACAGTACACTTTTGTGTGTGGTGTTCTCCAGTGGGCACAGGAGCGAGTGTGGTGAGAGAACAGGGCTGAGGGAAAG
GGAATTCCTTGGAAACAAGTGGGTGTACTTTCTGCTGTCTTAACCAAGTAAAAATGATATAGTCAAATAAGCGTTCTGTTTACATCC
ATTAATAACCACTTCTACTTATTTAACAGGGAAATGTTTATGTGCACTAAATATA

OCI-MY1 E8

Sequence_1:

AGGTCCTTGTTAGCCCTTTAAAGCACAGATAATTACGAAAAAAATGATATGGAGGCACCTAATGTGTTTTTTCTTTTTCATGTTTTT
TGGGGATATTTGGTTAGTTGATTTGATATTTTGGCATTTGCATTAATGTAGTTTTATTTATTCTGGAAAAATAACACTCAATGTTCT
ATTTTCTTTTAGATGAAAAATATGCAAACATCACTGTGGATTACTTATATAACAAGGAAACTAAATTATTTACAGCAAAGCTAAATGT
TAATGAGAATGTGGAATGTGGAAACAATACTTGCACAAACAATGAGGTGCATAACCTTACAGAATGTAAAAATGCGTCTGTTTCCAT
ATCTCATAATTCATGTACTGCTCCTGATAAGACATTAATATTAGATGTGCCCACCAGGTAAATATCATTTTATTTCTTTTAATAAATT
TATAAAAACAGTACACTTTTGTGTGTGGTGTTCTCCAGTGGTCACAAGATCTACTCTGGAGAGAAAACAGGGCTGAGGGAAAGGAA
ATTCCTTGAAAACAAGTGGGAGAACTTTCTGCTGTCTTAACCAAATAAAAATGATAGAGTCAAATAACCCTTCTGTTTACATCCATT
AATCACCACTTCTACTTATTTAACAGGGAGATGTTTATGTGCACTAAATA

Sequence_2:

AGGTCCTTGTTAACCCATTAAAGCACAGATAATTACGAAAAAAATGATATGGAGGCACCTAATGTGTTTTTTCTTTTTCATGTTTTT
TGGGGATATTTGGTTAGTTGATTTGATATTTTGGCATTTGCATTAATGTAGTTTTATTTATTCTGGAAAAATAACACTCAATGTTCT
ATTTTCTTTTAGATGAAAAATATGCAAACATCACTGTGGATTACTTATATAACAAGGAAACTAAATTATTTACAGCAAAGCTAAATGT
TAATGAGAATGTGGAATGTGGAAACAATACTTGCACAAACAATGAGGTGCATAACCTTACAGAATGTAAAAATGCGTCTGTTTCCAT
ATCTCATAATTCATGTACTGCTCCTGATAAGACATTAATATTAGATGTGCCCCCCAGGTAAATATAATTTTATTTCTTTTAATAAATT
TATAAAAACAATACACTTTTGTGTGTGGTGTTCTCCAGTGGTCACAAGAGCTACTCTGGAGAGAAAACAGGGCTGAGGGAAAGGAA
ATTCCTTGAAAACAAGTGGGAGAACTTTCTGCTGTCTTACAAAAGTAAAAATGATAGAGTCAAATAACCCTTCTGTTTACATCCTTT
AATCACCACTTCTACTTATTTAACAGGGATATGTTTATGTGCTCTAAATA

Sequence_3:

GGATGTAAGTTACGGGCGTTTTTGACACATAATTACGAACAAAGGGAAATAGAGGCAACCCTTGTGTTTTTTCTTTTTCATGTTTTT
TGGGGATATTTGGTTAGTTGATTTGATATTTAGCTCTTTGCATTAATGTAGTTTTATTTATTCTGGAAAAATAAGACTCAATGTTCT
ATTTTCTTTTAGATGAAAAATATGCAAACATCGCTGTGGATTACTTATATAACAAGGAAACTAAATTATTTACAGCAAAGCTAAATGT
TAATGAGAATGTGGAATGTGGAAACAATACTTGCACAAACAATGAGGTGCATAACCTTACAGAATGTAAAAATGCGTCTGTTTCCAT
ATCTCATAATTCATGTACTGCTCCTGATAATACATTAATATTAGATGTGCACGAGGTAAATATCATTATATTTCTTTTAATAAATTTA
TAAAAACAGTTCACTTTTGTGAGTGGGGATCTCCACTGGGCACAGGGGCCAGTGTGGTGTGAGAGCAGGGCTGAGAGAAAGGAAA
TTCCTTGGAGACAAGTGGGTGTACTTTCTGCTGTCTTAACTTTTTTAAAATGATATAGACAAATAAGCGTTCTGTTTACATCCCTCA
ATCACCACTTCTACTTATTTAACAGGGAAAAGTTTATGTGCACCAAATATA

XG-1 D5

Sequence_1:

TACAAGCTGAGGTCCTTGTTAGGGCAGTAAAGCACAGATAATTACGAAAAAAATGATATGGAGGCACCTAATGTGTTTTTTCTTTTT
CATGTTTTTTGGGGATATTTGGTTAGTTGATTTGATATTTTGGCATTTGCATTAATGTAGTTTTATTTATTCTGGAAAAATAACACT
CAATGTTCTATTTTCTTTTAGATGAAAAATATGCAAACATCACTGTGGATTACTTATATAACAAGGAAACTAAATTATTTACAGCAAA
GCTAAATGTTAATGAGAATGTGGAATGTGGAAACAATACTTGCACAAACAATGAGGTGCATAACCTTACAGAATGTAAAAATGCGTC
TGTTTCCATATCTCATAATTCATGTACTGCTCCTGATAAGACATTAATATTAGATGTGCCCACCATGTAAATATCTTTATATTTCTTA
AAATATATTTATAAAAACAGTACACTTGTGTGTGTGGTGCTCTCCAGTGGTCACAAGAGCGACTCTGGAGAGAGAACGAGGCAGAG
GAAAAGGATAGTCCGTGAACACGTGTGCGTGCTCTTTCCGCTGTCATACCCAAGTAAAAGTGATAGAGTCAAATACCCCTTCTGTTC

ACATCTAATAATCACCACTTATACATATTTCACAGGGATATGTTTATGTGCTCTAAA

Sequence_2:
TACAAGCTGAGGTCCTTGTTAGGGCAGTAAAGCACAGATAATTACGAAAAAAAATGATATGGAGGCACCTAATGTGTTTTTTCTTTTT
CATGTTTTTTGGGGATATTTGGTTAGTTGATTTGATATTTTGGCATTTGCATTAATGTAGTTTTATTTATTCTGGAAAAATAACACT
CAATGTTCTATTTTCTTTTAGATGAAAAATATGCAAACATCACTGTGGATTACTTATATAACAAGGAAACTAAATTATTTACAGCAAA
GCTAAATGTTAATGAGAATGTGGAATGTGGAAACAATACTTGCACAAACAATGAGGTGCATAACCTTACAGAATGTAAAAATGCGTC
TGTTTCCATATCTCATAATTCATGTACTGCTCCTGATAAGACATTAATATTAGATGTGCCCCCCATGTAAATCTCTTTCTATTTCTTA
AAATATATTTATAAAAAGCATACGCTTGTGTGTGTGGTGTTCGCCCGCGGGCACGAGCTAGGGTGTGGAGAGAGAACGAGGCAGA
GGAAAGTCATATCATTTGAAAACGTGAGGGTACTGTTTCCGCTGTCATCTCCAAGTAAAAGTGACAGACTCATATTCGGCTTGTGTA
CACCACTCATAACCTCCACTTATACATCTTTCACAGGGATATGTATATGCGCTCTAAA

Sequence_3:
TACAAGCTGAGGTCCTTGTTAGGGCAGTAAAGCACAGATAATTACGAAAAAAAATGATATGGAGGCACCTAATGTGTTTTTTCTTTTT
CATGTTTTTTGGGGATATTTGGTTAGTTGATTTGATATTTTGGCATTTGCATTAATGTAGTTTTATTTATTCTGGAAAAATAACACT
CAATGTTCTATTTTCTTTTAGATGAAAAATATGCAAACATCACTGTGGATTACTTATATAACAAGGAAACTAAATTATTTACAGCAAA
GCTAAATGTTAATGAGAATGTGGAATGTGGAAACAATACTTGCACAAACAATGAGGTGCATAACCTTACAGAATGTAAAAATGCGTC
TGTTTCCATATCTCATAATTCATGTACTGCTCCTGATAAGACATTAATATTAGACACCAAGTAAGGAACTATTAAAATTTTTCACTAT
TTATAATTATACAGTCCATTCTTTTGTTTGGGGGGCGCCATCCATTAGACAAACTGGTCTTTTGAGAGTGCAAACCTAGCTGTGGG
AGAGTAACATCGTAACAGATGGAAGGATTATAATCCGGTTGACCCTAGAACGTATGATTAAGAGAGATAAGCCAGATTTCTACATCT
ATTCACTTCCCACCCCACCTCCTTTTTTAGAAGGTATAGGTGTGCGCGAACAATAGA

XG-1 F5

Sequence_1:
TTACAAGCTGAGGTCCTTGTTAGGGCAGTAAAGCACAGATAATTACGAAAAAAAATGATATGGAGGCACCTAATGTGTTTTTTCTTTT
TCATGTTTTTTGGGGATATTTGGTTAGTTGATTTGATATTTTGGCATTTGCATTAATGTAGTTTTATTTATTCTGGAAAAATAACAC
TCAATGTTCTATTTTCTTTTAGATGAAAAATATGCAAACATCACTGTGGATTACTTATATAACAAGGAAACTAAATTATTTACAGCAA
AGCTAAATGTTAATGAGAATGTGGAATGTGGAAACAATACTTGCACAAACAATGAGGTGCATAACCTTACAGAATGTAAAAATGCGT
CTGTTTCCATATCTCATAATTCATGTACTGCTCCTGATAAGACATTAATATTAGAGGTAAATATCAATTTATTTCTTTTAATAAATTT
ATAAAAACAGTACACTTTTGTGTGTGGTGTTCTCCAGTGGTCACAGGAGCTAGTCTGGTGAGAGAACAGGGCTGACGGAAAGGAAA
TTCCTTGGAAACAAGTGGGTGAACTTTCTGCTGTCTTAACCAAGTAAAAATGATAGAGTCAAATAAGCCTTCTGTTTACATCCATTA
ATCACCACTTCTACTTATTTAACAGGGAGATGTTTATGTGCACTAAATATAG

Sequence_2:
TTACAAGCTGAGGTCCTTGTTAGGGCAGTAAAGCACAGATAATTACGAAAAAAAATGATATGGAGGCACCTAATGTGTTTTTTCTTTT
TCATGTTTTTTGGGGATATTTGGTTAGTTGATTTGATATTTTGGCATTTGCATTAATGTAGTTTTATTTATTCTGGAAAAATAACAC
TCAATGTTCTATTTTCTTTTAGATGAAAAATATGCAAACATCACTGTGGATTACTTATATAACAAGGAAACTAAATTATTTACAGCAA
AGCTAAATGTTAATGAGAATGTGGAATGTGGAAACAATACTTGCACAAACAATGAGGTGCATAACCTTACAGAATGTAAAAATGCGT
CTGTTTCCATATCTCATAATTCATGTACTGCTCCTGATAAGACATTAATATTAGAGGTGCACCAGGTAAATATCAATTTATTTCTTTT
AATAAATTTATAAAAACAGTACACTTTTGTGTGTGGTGTTCTCCAGTGGTCACAGGAGCTAGTCTGGTGAGAGAACAGGGCTGAGG
GAAAGGAAATTCCTTGGAAACAAGTGGGTGAACTTTCTGCTGTCTTAACCAAGTAAAAATGATAGAGTCAAATAAGCCTTCTGTTTA
CATCCATTAATCACCACTTCTACTTATTTAACAGGGAGATGTTTATGTGCAC

Sequence_3:
TTACAAGCTGAGGTCCTTGTTAGGGCAGTAAAGCACAGATAATTACGAAAAAAAATGATATGGAGGCACCTAATGTGTTTTTTCTTTT
TCATGTTTTTTGGGGATATTTGGTTAGTTGATTTGATATTTTGGCATTTGCATTAATGTAGTTTTATTTATTCTGGAAAAATAACAC
TCAATGTTCTATTTTCTTTTAGATGAAAAATATGCAAACATCACTGTGGATTACTTATATAACAAGGAAACTAAATTATTTACAGCAA
AGCTAAATGTTAATGAGAATGTGGAATGTGGAAACAATACTTGCACAAACAATGAGGTGCATAACCTTACAGAATGTAAAAATGCGT

CTGTTTCCATATCTCATAATTCATGTACTGCTCCTGATAAGACATTAATATTAGATGTGCCCACCAGGTAAATATCAATTTATTTCTT
TTAATAAATTTATAAAAACAGTACACTTTTGTGTGTGGTGTTCTCCAGTGGTCACAGGAGCTAGTCTGGTGAGAGAACAGGGCTGA
GGGAAAGGAAATTCCTTGGAAACAAGTGGGTGAACTTTCTGCTGTCTTAACCAAGTAAAAATGATAGAGTCAAATAAGCCTTCTGT
TTACATCCATTAATCACCACTTCTACTTATTTAACAGGGAGATGTTTATGTGC

TK2 C2

Sequence_1:
TTTACAAGCTGAGGTCCTTGTTAGGGCAGTAAAGCACAGATAATTACGAAAAAAAATGATATGGAGGCACCTAATGTGTTTTTTCTTT
TTCATGTTTTTTGGGGATATTTGGTTAGTTGATTTGATATTTTGGCATTTGCATTAATGTAGTTTTATTTATTCTGGAAAAATAACA
CTCAATGTTCTATTTTCTTTTAGATGAAAAATATGCAAACATCACTGTGGATTACTTATATAACAAGGAAACTAAATTATTTACAGCA
AAGCTAAATGTTAATGAGAATGTGGAATGTGGAAACAATACTTGCACAAACAATGAGGTGCATAACCTTACAGAATGTAAAAATGC
GTCTGTTTCCATATCTCATAATTCATGTACTGCTCCTGATAAGACATTAATATTAGATGTGCACCAGGTAAATATCAATTTATTTCTT
TTAATAAATTTATAAAAACAGTACACTTTTGTGTGTGGTGTTCTCCAGTGGTCACAGGAGCTAGTCTGGTGAGAGAACAGGGCTGA
GGGAAAGGAAATTCCTTGGAAACAAGTGGGTGAACTTTCTGCTGTCTTAACCAAGTAAAAATGATAGAGTCAAATAAGCCTTCTGT
TTACATCCATTAATCACCACTTCTACTTATTTAACAGGGAGATGTTTATGTGCA

TK2 G3

Sequence_1:
TTTACAAGCTGAGGTCCTTGTTAGGGCAGTAAAGCACAGATAATTACGAAAAAAAATGATATGGAGGCACCTAATGTGTTTTTTCTTT
TTCATGTTTTTTGGGGATATTTGGTTAGTTGATTTGATATTTTGGCATTTGCATTAATGTAGTTTTATTTATTCTGGAAAAATAACA
CTCAATGTTCTATTTTCTTTTAGATGAAAAATATGCAAACATCACTGTGGATTACTTATATAACAAGGAAACTAAATTATTTACAGCA
AAGCTAAATGTTAATGAGAATGTGGAATGTGGAAACAATACTTGCACAAACAATGAGGTGCATAACCTTACAGAATGTAAAAATGC
GTCTGTTTCCATATCTCATAATTCATGTACTGCTCCTGATAAGACATTAATATTAGATGTGCACCAGGTAAATATCAATTTATTTCTT
TTAATAAATTTATAAAAACAGTACACTTTTGTGTGTGGTGTTCTCCAGTGGTCACAGGAGCTAGTCTGGTGAGAGAACAGGGCTGA
GGGAAAGGAAATTCCTTGGAAACAAGTGGGTGAACTTTCTGCTGTCTTAACCAAGTAAAAATGATAGAGTCAAATAAGCCTTCTGT
TTACATCCATTAATCACCACTTCTACTTATTTAACAGGGAGATGTTTATGTGCAC

U266 B4

>equence_1:
CAGTAAAGCACAGATAATTTACGAAAAAAATGATATGGAGGCACCTAATGTGTTTTTTCTTTTTCATGTTTTTTGGGGATATTTGGT
TAGTTGATTTGATATTTTGGCATTTGCATTAATGTAGTTTTATTTATTCTGGAAAAATAACACTCAATGTTCTATTTTCTTTTAGATG
AAAAATATGCAAACATCACTGTGGATTACTTATATAACAAGGAAACTAAATTATTTACAGCAAAGCTAAATGTTAATGAGAATGTGG
AATGTGGAAACAATACTTGCACAAACAATGAGGTGCATAACCTTACAGAATGTAAAAATGCGTCTGTTTCCATATCTCATAATTCAT
GTACTGCTCCTGATAAGACATTAATATTAGATGTGCCCAGTAAGTATCTATTTATTTCTTTCATTAAATTTATTTATACAATCCATTT
TTGTTTGTGTGGGTCGCTCTTGATTGCTCGAACGAGCCAGTCGGGAGAAAAAGCCTGACGGAAGGAAAATACCTTGCATGCAAATG
AGTGAATTATCTTCCGTCTGACTTAACTAAATATAAAAGATACAATCAAACCTTCCGTTTGTTTCCATCAATCACCCCCTCTTTCTAT

Sequence_2:
CAGTAAAGCACAGATAATTTACGAAAAAAATGATATGGAGGCACCTAATGTGTTTTTTCTTTTTCATGTTTTTTGGGGATATTTGGT
TAGTTGATTTGATATTTTGGCATTTGCATTAATGTAGTTTTATTTATTCTGGAAAAATAACACTCAATGTTCTATTTTCTTTTAGATG
AAAAATATGCAAACATCACTGTGGATTACTTATATAACAAGGAAACTAAATTATTTACAGCAAAGCTAAATGTTAATGAGAATGTGG
AATGTGGAAACAATACTTGCACAAACAATGAGGTGCATAACCTTACAGAATGTAAAAATGCGTCTGTTTCCATATCTCATAATTCAT
GTACTGCTCCTGATAAGACATTAATATTAGATGTGCCCAGTAAGTATCTATTTATTTCTTTTATTAAATTTATTTATAAAATCAGTTT
TTGTTTGTGTTGGTCGCTCTTGATCGCTCGAGCGAGCCAGTCGGGAGAAAAAGCCTGACGGAAGGAAAATACATTGGATGGAAAT
GAGTGAATTATCTTCCTGCTGACTTAATTAAGTATAAAAGAGTCAATCAAACCTGCCGTTTGCTTCCATCAATCACCCACTATTTCTA

Sequence_3:
GATTAAATCACAGATAATTCACGAAAAAAATGATATAGAGGCACCTAATGTGTTTTTTCTTTTTCATGTTTTTTGGGGATATTTGGT
TAGTTGATTTGATATTTTGCCCTTTGCATTACTGTAGTTTTATTTATTCTGGAAAAATAAGACTCAATGTTCTATTTTCTTTTATATG
AAAAATATGCAAACATCACTGTGGATTACTTATATAACAAGGAAACTAAATTATTTACAGCAAAGCTAAATGTTAATGAGAATGTGG
AATGTGGAAACAATACTTGCACAAACAATGAGGTGCATAACCTTACAAAATGTAAAAATGCGTCTGTTTCCATATCTCATAATTCAT
GTACTGCTCCTGATAAAACATTAATATTAAATGTGCCAGCCAGATAAAAATCAATTTATTTATATTAATAAATAAAAAGAGAATTCAC
ACTTGTGTGGATTGTTTCAGCCGGGAGAGACCGTACTTTGGTTAGTGAGCGGAGAGGGGTGAGAGGAAGGTATTTCTTAAAAAGC
AGGTGGGCGTACTGTTCCCTTTACCAAGCAATAAAGATTGAAGGAGATAAGTAACCTTTCTAAATACCTTCATTAATATTCTCACTT
AC

U266 F9

Sequence_1:
ATATAAATTTACAAGCTGAGGTCCTTGTTAGGGCAGTAAAGCACAGATAATTACGAAAAAAAATGATATGGAGGCACCTAATGTGTTT
TTTCTTTTTCATGTTTTTTGGGGATATTTGGTTAGTTGATTTGATATTTTGGCATTTGCATTAATGTAGTTTTATTTATTCTGGAAA
AATAACACTCAATGTTCTATTTTCTTTTAGATGAAAAATATGCAAACATCACTGTGGATTACTTATATAACAAGGAAACTAAATTATT
TACAGCAAAGCTAAATGTTAATGAGAATGTGGAATGTGGAAACAATACTTGCACAAACAATGAGGTGCATAACCTTACAGAATGTAA
AAATGCGTCTGTTTCCATATCTCATAATTCATGTACTGCTCCTGATAAGACATTAATATTAGATGTGCCCGCCGGGTAAATATTATT
TTATTTCTTTAAAAAAATTTATAAAATGTTAATTTTTTTGAATAAGGAGTTCTCCATTGATGCCAGTGCCTAATCAGGTGAGAAAACA
GGCCTGAGGCAAAGGAAATTCCTTGAAAAAAAATGGCTTAACTTGCCGCCGTATCATCTATTTAAAAATTATCTATGCAATAAACCC
TTAAGTTTGACCCCATTATTCACAATTTTATTTTATTTAATAGGAAAAAATTTATGGGCCTCAAAAACA

Sequence_2:GTAGAAGTGGTCGATCAGGGATGTATGTTAAGGGCTTATTTCACACATAATTACGAACAAAGGGAAATAGAGGCAAC
TAATGTGTTTTTTCTTTTTCATGATTTTTGGGGATATTTGGTTAGTTGATTTCAAAATTAGCTCCTGGGATTACTGTAGTTCACCTC
ACTCTGGAAAGTACTGTTTTTATGTTCTATTTTCTTTTATATGAAAAATATGCAAACGTCGGGGTGTATTACTTATATAACAAGGAA
ACTAAATTATTTACAGCAAAGCTAAATGTTAATGAGAATGTGGAATGTGCAAACAATACTTGCACAAACAATGAGGTGCATAACCTT
ACAGAATGTAAAAATGCCTCAGTATCCTTATCTCATAATTCATGTACTGCTCCTGATAAGACATTAATATTAAATGTGCCCAACATGT
GAATATCTATTTACTTCTTTTAATAAAATTATTGAAACAGTACACTTTTGTGTGTGGTGTTCTCCAGTAGTCACAAGAGCTAGTCTG
GTGAGAGAACAAGGCTGATGGAAAAGAAATTCCATGGAAACAAGTGAGTGAACGTTCTGCTGTCTTAATCTAGTCAAAATGATAGA
GTCTTATAAGCCCTCTGATTACATCCATTAATCAACACTTCTACTTAAATAACAAGGAGATGTTTATGTGCACTCAATATA

Appendix 3: List of differentially expressed genes in $CD45^{KO}$ OCI-MY1 (clone C9).

Gene name	Gene type	log_2 FC	P-Value	FDR
AC079466.1	lincRNA	-9.4961006	5.83E-53	7.47E-49
IGHG1	IG C gene	-7.3673767	4.82E-43	3.09E-39
COX7B2	protein coding	-10.747476	2.85E-36	1.22E-32
CDKN1A	protein coding	-4.9905568	1.67E-27	5.34E-24
PARVB	protein coding	-5.7536118	2.22E-27	5.70E-24
ASS1	protein coding	-4.3199638	3.53E-23	6.45E-20
PREX1	protein coding	-4.0711544	1.56E-21	2.22E-18
PRKCB	protein coding	-4.5914307	2.20E-21	2.82E-18
PTPRC	protein coding	-4.0381255	7.02E-21	8.18E-18
BCAR3	protein coding	-3.9086815	2.36E-18	2.02E-15
CTD-2328D6.1	pseudogene	-3.6137459	2.44E-17	1.65E-14
SMOC1	protein coding	3.60853837	1.09E-16	6.10E-14
DPYSL3	protein coding	-3.5803185	1.95E-15	7.80E-13
PAX5	protein coding	-3.5523699	2.23E-15	8.64E-13
DDIT4	protein coding	-3.1649703	1.50E-14	5.05E-12
MT-ND5	protein coding	-3.0970415	3.04E-14	9.73E-12
HBE1	protein coding	-3.4154668	5.21E-14	1.63E-11
MT-CYB	protein coding	-2.820473	2.13E-12	5.94E-10
RRP9	protein coding	-2.812247	4.16E-12	1.09E-09
AFAP1L2	protein coding	-2.7830539	5.25E-12	1.27E-09
DUSP9	protein coding	-2.854508	1.36E-11	3.16E-09
MARCKS	protein coding	2.73990889	1.43E-11	3.27E-09
LCN9	protein coding	-3.0081558	3.21E-11	6.97E-09
RP11-25K19.1	antisense	-2.8568393	3.30E-11	7.05E-09
DACH1	protein coding	2.644203	1.09E-10	2.15E-08
CXCR4	protein coding	2.57947421	1.31E-10	2.54E-08
EMP2	protein coding	-2.532156	4.21E-10	7.81E-08
ZBTB7C	protein coding	-2.5350338	4.99E-10	9.00E-08
SNCB	protein coding	-2.7076456	9.35E-10	1.54E-07
DUSP4	protein coding	-2.4441419	1.11E-09	1.72E-07
FZD8	protein coding	-2.4907083	1.22E-09	1.85E-07
RRP1	protein coding	-2.3710253	2.32E-09	3.38E-07

ADAM19	protein coding	-2.3507335	3.82E-09	5.26E-07
EMP1	protein coding	-2.4379772	6.84E-09	8.76E-07
CYTH4	protein coding	-2.3107251	7.13E-09	8.87E-07
PYROXD2	protein coding	-2.4224082	7.62E-09	9.39E-07
DKK1	protein coding	-2.3690341	1.36E-08	1.63E-06
MT1F	protein coding	-2.4308888	3.80E-08	4.17E-06
ID1	protein coding	2.18045893	5.20E-08	5.55E-06
PLAUR	protein coding	-2.0584741	1.71E-07	1.64E-05
SLC47A1	protein coding	-2.1814987	1.88E-07	1.75E-05
MCOLN2	protein coding	2.12675178	1.90E-07	1.75E-05
STC2	protein coding	-2.0108433	2.48E-07	2.26E-05
HID1	protein coding	-2.0519979	3.02E-07	2.69E-05
MT-ND6	protein coding	-1.9949894	4.37E-07	3.78E-05
ST14	protein coding	-2.0791689	4.73E-07	4.07E-05
CCND1	protein coding	-2.0887813	5.10E-07	4.33E-05
LRP5	protein coding	-1.9614653	6.59E-07	5.41E-05
TGFBR3L	protein coding	-1.9367857	1.10E-06	8.67E-05
AC098973.2	lincRNA	2.10176907	1.47E-06	0.00011492
DUSP5	protein coding	-1.8549706	1.65E-06	0.00012706
FAM30A	lincRNA	-1.8490805	1.75E-06	0.00013322
SLC12A8	protein coding	-1.9169339	1.99E-06	0.00014824
HBEGF	protein coding	-1.9094934	2.00E-06	0.00014833
DNAJC5B	protein coding	1.90979989	2.07E-06	0.00015249
FAM167A	protein coding	-1.8505984	2.12E-06	0.00015421
OAS3	protein coding	-1.9030334	2.14E-06	0.00015506
DOC2A	protein coding	-2.0014019	2.51E-06	0.00017558
SFXN3	protein coding	-1.8520462	2.84E-06	0.00019695
IGFBP4	protein coding	1.89770567	3.22E-06	0.00021828
RHOBTB1	protein coding	1.8423978	3.24E-06	0.00021862
ITGAL	protein coding	-1.7899081	3.95E-06	0.00025403
ADM2	protein coding	-1.7741139	4.56E-06	0.00028942
ABCG2	protein coding	1.83337152	4.84E-06	0.00030543
ADAP1	protein coding	-1.8065079	4.98E-06	0.00031222
SNX24	protein coding	1.84325234	6.46E-06	0.00039415
MIR99AHG	lincRNA	-1.8880755	7.02E-06	0.00042607
BMF	protein coding	-1.7343543	7.33E-06	0.00043908
TMEM145	protein coding	-1.8218835	8.48E-06	0.00050047
MTUS1	protein coding	1.77325416	1.07E-05	0.00061611
GATM	protein coding	-1.7288318	1.17E-05	0.00066712

TMEM156	protein coding	-1.8019034	1.32E-05	0.00074659
CDA	protein coding	-1.7670881	1.51E-05	0.00083505
KLHL23	protein coding	1.77055218	1.54E-05	0.00084954
DENND5A	protein coding	1.70825516	1.68E-05	0.00091799
TRAT1	protein coding	1.79756894	1.82E-05	0.0009883
CAMK4	protein coding	1.69874361	2.17E-05	0.00115551
IDUA	protein coding	-1.7323452	2.23E-05	0.00117862
AC011515.2	unprocessed pseudogene	-1.8693455	2.48E-05	0.00129726
MME	protein coding	1.72141987	2.82E-05	0.00145648
P4HA1	protein coding	-1.6038636	3.13E-05	0.0016067
HIST1H2BJ	protein coding	1.60037848	3.34E-05	0.0016985
IER5L	protein coding	-1.6189798	3.42E-05	0.00173328
CCPG1	protein coding	-1.6005165	3.55E-05	0.00178845
AGPAT3	protein coding	-1.5990877	3.91E-05	0.00195154
METRNL	protein coding	-1.5952639	3.95E-05	0.00196357
SYP	protein coding	-1.6441187	4.36E-05	0.0021239
CTD-2575K13.6	Transcribed Unprocessed pseudogene	-1.8432677	4.87E-05	0.0023294
SLC22A18	protein coding	-1.586011	5.12E-05	0.00242879
SESN2	protein coding	-1.5532596	5.14E-05	0.0024295
PODXL2	protein coding	-1.6000714	5.23E-05	0.00245764
CHAC1	protein coding	-1.5651507	5.24E-05	0.00245764
P3H3	protein coding	-1.5834333	5.57E-05	0.00259333
HIST1H2BO	protein coding	1.64763304	5.66E-05	0.00263
LILRA2	protein coding	-1.5426709	6.33E-05	0.00289695
CDC42EP5	protein coding	-1.5830544	6.42E-05	0.00290374
RP5-1028K7.2	lincRNA	1.59076938	6.43E-05	0.00290374
STAT5A	protein coding	-1.5823739	6.79E-05	0.00303155
FHL1	protein coding	-1.5314009	7.10E-05	0.00316073
PIK3R3	protein coding	1.54768862	7.92E-05	0.00347394
JUN	protein coding	1.50912192	9.04E-05	0.00392718
NR1H2	protein coding	-1.483757	0.000107398	0.00458732
EPHB6	protein coding	-1.4959475	0.000118146	0.00499646
HERPUD1	protein coding	-1.4688022	0.000124585	0.00525143
RP11-449P1.1	lincRNA	1.67076142	0.00012593	0.00529073
FERMT2	protein coding	1.51403713	0.000141401	0.0058261
TRIB3	protein coding	-1.4476166	0.000155901	0.00632188

HIST1H2AG	protein coding	1.42201403	0.000209948	0.00809231
GPAT3	protein coding	-1.4315614	0.000211085	0.00809231
NOTUM	protein coding	-1.4147403	0.000260831	0.00974427
DEPTOR	protein coding	-1.4159951	0.000267413	0.00993226
COL9A2	protein coding	1.44942453	0.000278701	0.0102623
SEZ6L2	protein coding	-1.4035088	0.000282204	0.01036148
BCL2L11	protein coding	1.38949018	0.000292632	0.01071368
ZDHHC23	protein coding	1.40217572	0.00030535	0.01102183
PPP1R15A	protein coding	-1.3761609	0.000318034	0.01141536
TSC22D1	protein coding	1.40152442	0.000378	0.01338036
HLA-DRA	protein coding	1.35492513	0.000381895	0.01348101
MIR22HG	lincRNA	-1.4122272	0.000385501	0.01353077
LINC01055	lincRNA	1.44891945	0.000386473	0.01353077
SEPT3	protein coding	-1.3913487	0.000405993	0.01398311
PFKFB4	protein coding	-1.3943794	0.000406906	0.01398311
WISP1	protein coding	-1.3671093	0.000408724	0.01398311
HIST2H2BE	protein coding	1.36766595	0.000409214	0.01398311
FTSJ1	protein coding	-1.3568458	0.000411939	0.01403879
RPL13A	protein coding	-1.339583	0.000432025	0.01463102
RP11-114G22.1	lincRNA	1.49509877	0.000435858	0.01469758
CXXC4	protein coding	1.36921347	0.000441999	0.01486555
CASP7	protein coding	-1.3508989	0.000460658	0.01545253
KIF7	protein coding	1.35570654	0.000461982	0.0154565
C8orf46	protein coding	1.33462175	0.000472191	0.01575693
ADD2	protein coding	-1.3427263	0.000495363	0.0164445
CSGALNACT2	protein coding	-1.3415848	0.000510801	0.01686959
METTL7A	protein coding	1.32831812	0.000521266	0.01717097
NAPSA	protein coding	-1.3276341	0.000527892	0.01730029
DAAM1	protein coding	-1.3422494	0.000530817	0.01735175
PCBD1	protein coding	-1.3436207	0.000542969	0.01770383
SEMA3C	protein coding	-1.3340209	0.000570336	0.01845527
HIST1H4I	protein coding	1.33000297	0.000584835	0.01887675
HLA-F	protein coding	-1.3370559	0.000586716	0.01888988
PIP5KL1	protein coding	-1.3174379	0.00059313	0.01904855
MSI1	protein coding	-1.316403	0.000639429	0.02035251
HIST1H1C	protein coding	1.2901712	0.000697928	0.02178937
NXPH4	protein coding	-1.3020558	0.000699351	0.02178937
RGS10	protein coding	-1.2990791	0.000701807	0.02178937

MAN1C1	protein coding	-1.2886479	0.000737102	0.02270488
ID3	protein coding	1.28414452	0.000745956	0.0228401
GAS2L1	protein coding	1.289095	0.000754817	0.02302359
DENND6B	protein coding	-1.2904721	0.000793445	0.02403593
RP11-598F7.3	antisense	1.45919074	0.000815173	0.02457793
FLT3LG	protein coding	-1.3000786	0.000817322	0.02458491
CDH17	protein coding	1.28084427	0.000827616	0.02483622
NREP	protein coding	1.28334057	0.000832847	0.0249348
KIR3DX1	protein coding	-1.2852434	0.000851575	0.0254361
HES6	protein coding	1.26729607	0.000888816	0.02630321
EPHB2	protein coding	1.26635917	0.00089571	0.02638536
LINC01234	lincRNA	-1.294051	0.000906043	0.02656757
RP11-473I1.9	lincRNA	-1.2774631	0.000936423	0.02720934
PLD4	protein coding	1.25930391	0.000954752	0.02761668
ABTB1	protein coding	-1.2636812	0.001050258	0.02977435
EMC10	protein coding	-1.2457257	0.001067765	0.03020385
JOSD2	protein coding	-1.2499402	0.001076829	0.03039314
DPP4	protein coding	-1.2921735	0.001097736	0.03086649
RHOB	protein coding	-1.2408764	0.001098417	0.03086649
PLK2	protein coding	-1.3289669	0.001128308	0.03136845
TLE6	protein coding	-1.3217441	0.001129778	0.03136845
CTH	protein coding	-1.2495695	0.001142247	0.03147688
OPTN	protein coding	-1.2379271	0.001226914	0.03323822
DERL3	protein coding	-1.2300681	0.001240971	0.03351592
GRIK4	protein coding	-1.2367099	0.001290065	0.03458345
RABAC1	protein coding	-1.2225465	0.001321222	0.03512477
AF127936.5	lincRNA	1.28165812	0.001363068	0.03601311
RRBP1	protein coding	-1.2150064	0.001384669	0.03650853
LIPH	protein coding	-1.2307703	0.001456649	0.03809286
KCNK6	protein coding	-1.2172617	0.001473218	0.03836955
FAM43A	protein coding	-1.2255878	0.001494269	0.03883888
EGR1	protein coding	-1.2102391	0.001505735	0.03905768
FAM149A	protein coding	-1.2403485	0.001519473	0.03933439
GLUL	protein coding	1.20565061	0.001547099	0.03988839
EVI5L	protein coding	-1.2373466	0.001585136	0.04051013
MIR210HG	lincRNA	-1.2633426	0.001588298	0.04051013
CERS4	protein coding	-1.2624197	0.001593344	0.04051013
PIH1D1	protein coding	-1.1930716	0.001706594	0.04296326
RP11-473I1.9	3prime	-1.193661	0.00174033	0.04355583

	overlapping ncRNA			
HRH2	protein coding	-1.2254941	0.001785681	0.04443051
AC026806.2	lincRNA	-1.3405077	0.00179717	0.04447962
TDRKH	protein coding	1.20443046	0.001811593	0.04472784
HHLA2	protein coding	-1.1906112	0.001817303	0.04478254
KRT86	protein coding	-1.1885292	0.001836493	0.04508204
WASF1	protein coding	1.18756963	0.001893299	0.04637102
WIPI1	protein coding	-1.2069059	0.001896239	0.04637102
TMEM171	protein coding	1.21082002	0.001930336	0.04693609
FLNB	protein coding	1.1848075	0.001939568	0.04707126
HSPA2	protein coding	1.20855073	0.001947471	0.0471737
HIST1H2BC	protein coding	1.2803254	0.001951413	0.04718001